Formulation Insights Group
School of Pharmacy
University of Nottingham

The phase behaviour of xanthan based biopolymer mixtures

Matthew Boyd B.Pharm (Hons) MRPharmS

Thesis submitted to the University of Nottingham for the degree of Doctor of Philosophy

September 2005

Abstract

It was proposed that a phase separated system might be utilised to deliver a concentrated polysaccharide mucosal protective coating in gastro oesophageal reflux disease (GORD). In this context the phase behaviour of xanthan gum in combination with sodium alginate and other polymers was studied. Above a threshold concentration of alginate, aqueous mixtures of xanthan exhibited phase separation, resulting in loss of normal viscoelastic properties and the formation of a low viscosity system. The shape of the phase diagram showed behaviour typical of a segregative system, with the continuous phase composed exclusively of alginate and the disperse phase being rich in xanthan gum. Increasing alginate molecular weight reduced the threshold concentration for separation, as predicted by the Flory-Huggins theory, but changes in alginate mannuronate:guluronate ratio had no effect. Increasing ionic strength elevated the threshold concentration. Xanthan separation was elicited by other aqueous anionic polyelectrolytes, but not neutral water soluble polymers. Scleroglucan, another rigid-rod polysaccharide, was investigated as an alternative to xanthan but did not show similar separation behaviour, suggesting that the charge on the xanthan molecule is a necessary prerequisite. Reversal of phase separation by dilution across the phase boundary provided increases in viscosity. A 1% xanthan:2% alginate mixture doubled in viscosity whereas if diluted with simulated gastric fluid a seven-fold increase was seen, as a result of conversion to an alginic acid gel. This offers a mechanism for producing the desired viscosity barrier. Low viscosity polyelectrolytes, with concentrations close to the phase boundary yielded the greatest viscosity increases. In the phase separated system, the disperse phase exhibited an unusual strand-like morphology whose birefringence suggests a liquid crystalline structure. The variable size of the strands was explained in terms of kinetics of xanthan molecular aggregation in media of different viscosity.

Acknowledgements

I must first thank Reckitt Benckiser (Healthcare) UK Ltd and the BBSRC for their financial support of this project.

I shall be eternally grateful to both Dr Colin Melia and Professor John Mitchell my academic supervisors, for their help, guidance and wisdom during this project. Dr Melia was always there with a listening ear. His inspiration, patience and guidance have been a constant help throughout. I must also thank Professor John Mitchell who has introduced me to a whole new and interesting discipline of science and his help with the theoretical ideas associated with this project.

I must also express my gratitude to my industrial sponsors Professor Peter Dettmar, Dr Ian Jolliffe and Mr Frank Hampson, their guidance and input has been invaluable and our review meetings have always been highly productive, informative and challenging. The work of Professor Dettmar is a shining example of how industry and academia can work together to achieve a common goal. I should also like to thank Dr Vicki Strugala formerly at Reckitt Benckiser for her help with the Fluorescence work.

In the Division of Food Science at Sutton Bonington, there are a lot of great friends to thank, but I must make a special mention of Mr Phil Glover who managed to cope every time there was a knock at the door asking for more equipment or supplies; Mr Mike Chapman, who 20 minutes after being asked if something could be specially made not only said 'yes' but then produced the item and Dr Bill MacNaughton for his help with

the DSC work. I must also thank all my friends and colleagues for their support and help, but especially Guy, Jane, Abde, and Nameeta for their support and help.

In the School of Pharmacy I must thank Mrs Christine Grainger-Boultby for all her technical support during the project, and also her assistance in obtaining the SEM images. The support and friendship of the Formulation Insights Group has been outstanding. I thank Jon, Simon, Fog, Emma, Arthur and Barry for all their help but I must give special thanks to Gurjit for his help with the confocal work, and Craig for all his helpful discussions and support.

I must also thank my parents without whom I would not have come this far. Their love and support has been unfaltering throughout my education, even at the most stressful times. And finally I must thank Tina who has been with me throughout the ups and downs of my PhD. continually offering her love and support.

Table of contents

Table of figures

Chapter 1

Chapter 2

Chapter 3

Chapter 4

Chapter 5

Chapter 6

Table of tables

Chapter 1

Chapter 3

Chapter 5

Abbreviations and symbols

η^*	Complex viscosity
δ	Phase angle (delta)
σ	Shear stress
σ_y	Yield stress
σ^0	Stress amplitude
γ	Strain
$\dot{\gamma}$	Strain (shear) rate
γ^0	Strain amplitude
η	Viscosity (apparent)
η_0	Zero shear viscosity
η_∞	Infinite shear viscosity
λ	Lambda
Φ	Volume fraction
θ	The angle between molecule orientation and the director in a liquid crystal
χ	Interaction Parameter (Flory)
ρ	Density
ω	Frequency of oscillation
%	Percentage
Ba^{2+}	Barium ion
^oC	Degree centigrade
C^*	Critical concentration above which an anisotropic phase exists within an isotropic phase
C^{**}	Critical concentration above which a system is fully anisotropic
Ca^{2+}	Calcium ion

CFR	Code of Federal Regulations
CMC	Sodium carboxymethylcellulose
Cos	Cosine
CP 4/40	Cone & plate 4^{o}/40mm geometry
Da	Dalton
DMF	N,N-dimethylformamide
DSC	Differential scanning calorimeter
EDAC	1-ethyl-3-(3-dimethylaminopropyl) carbodiimide
EDTA	Ethylenediamine tetraacetic acid (Tetra sodium salt)
FDA	American Food & Drug Administration
g	Gram
ΔG	Change in Gibbs' free energy
G	Guluronate
GG	Sequences of polyguluronate
G^{*}	Complex modulus
G’	Elastic modulus
G”	Viscous modulus
GRAS	Generally regarded as safe
ΔH	Change in enthalpy
Hz	Hertz
k	Boltzmann constant
KCl	Potassium chloride
kDa	Kilodalton
keV	Kiloelectron volt
LBG	Locust bean gum
LMA	Low-methoxyl amidated (pectin)
LVR	Linear viscoelastic region
M	Mannuronate
mA	Milliamp
mg	Milligram
MG	Alternating sequences of mannuronate and guluronate
Mg^{2+}	Magnesium ion
$MgCl_2$	Magnesium chloride

min	Minute
ml	Millilitre
mm	Millimetre
MM	Sequences of polymannuronate
mPa.s	Millipascal second
Mw	Molecular weight
NaCl	Sodium chloride
NaOH	Sodium hydroxide
NRRL	Northern Regional Research Laboratories
nm	Nanometre
p	Axial ratio
Pa	Pascal
Pa.s	Pascal second
PAA	Polyacrylate sodium
q	Persistence length
r	The number of segments per molecule
rpm	Revolutions per minute
RVA	Rapid Visco Analyser
s	Second
s	Order parameter of a liquid crystal
ΔS	Change in entropy
SD	Standard deviation
SEM	Scanning electron microscopy
SGF	Simulated gastric fluid
Sin	Sine
Sr^{2+}	Strontium ion
T	Absolute temperature (Kelvin)
Tan	Tangent
USP	United States Pharmacopoeia
V^{*}	Critical volume fraction above which an anisotropic phase exists within an isotropic phase
V^{**}	Critical volume fraction above which a system is fully anisotropic

Definitions

Percentage All percentages quoted within this thesis are expressed on a weight basis.

Percentage dilution Percent dilution refers to the percentage of water added, by weight, to a given composition.

For example dilution of a 1% polysaccharide solution would be as follows:

% dilution	Mass of solution	Mass of diluent	Final concentration % w/w
0	100g	0	1%
10%	90g	10g	0.9%
20%	80g	20g	0.8%
30%	70g	30g	0.7%
50%	50g	50g	0.5%

Chapter 1

Introduction

1.1 Xanthan gum

Xanthan gum is a microbial exopolysaccharide produced by the naturally occurring bacterium *Xanthomonas campestris*. *X. campestris* was originally isolated from the cabbage plant, where it is responsible for black rot disease (Kennedy and Bradshaw 1984). It is a widely used biopolymer in the food and pharmaceutical industries and is often used for the purposes of thickening, suspending, stabilising and gelling (Sutherland 2001). Xanthan gum is also used in many other fields such as petroleum production, pipeline cleaning, enhanced oil recovery, textile printing and dyeing, ceramic glazes, slurry explosives and in cosmetics (Kang and Pettitt 1993). These applications will be discussed later on.

1.1.1 Origin

Since the original discovery of xanthan in the late 1950's and subsequent commercial production in the early 1960's there have been numerous studies to understand its functional and molecular properties (Kennedy and Bradshaw 1984; Kang and Pettitt

1993). The initial interest came from the Northern Regional Research Laboratories (NRRL, U.S. Department of Agriculture), where NRRL B-1459 was isolated as part of a wider screening program for new microbial polysaccharide entities. The NRRL were keen to find new functional polysaccharides to reduce supply and quality issues associated with seasonal, climatic, and skilled labour dependency of other plant sources. The US also had an overstock of corn starch, providing a plentiful supply of glucose for fermentation (Kennedy and Bradshaw 1984).

NRRL B-1459 became known as xanthan, and was shown to be a polysaccharide with three important properties (a) high viscosity at low concentration; (b) high pseudoplasticity; and (c) insensitivity to variation in salt concentration, pH and temperature (Jeanes, Pittsley et al. 1961; Morris 1977; Southwick, Jamieson et al. 1982). These features will be discussed in detail later on.

Xanthan is produced on an industrial scale by fermentation, in a well-aerated and principally carbohydrate medium containing other trace elements. It is precipitated from the fermentation broth using isopropyl alcohol, then dried and milled (Cottrell, Kang et al. 1980).

1.1.2 The structure of xanthan

1.1.2.a The primary structure

Xanthan consists of a pentasaccharide repeating subunit consisting of two D-glucopyranosyl units, two D-mannopyranosyl units and a D-glucopyranosyluronic acid unit as determined by methylation analysis and uronic acid degradation (Jansson, Kenne et al. 1975). The molecule has a (1 → 4) linked β -D-glucopyranosyl backbone, as is found in cellulose, but with a trisaccharide side chain attached to the O-3 position on alternate glucosyl units. The side chain is constructed such that the D-glucuronosyl unit is flanked by mannosyl units as shown in Figure 1.1 (Jansson, Kenne et al. 1975;

Melton, Mindt et al. 1976). Approximately half of the terminal D-mannosyl units have a pyruvic acid moiety bridging the O-4 and O-6 positions, the other D-mannosyl unit being substituted at the O-6 position with an acetal group (Kang and Pettitt 1993). As a consequence of glucuronic acid in the side chain, xanthan is available as a sodium, potassium or calcium salt (Cottrell, Kang et al. 1980). Xanthan has been estimated to have a molecular weight between 2 - 50 x 10^{-6} Da. This wide range of values is believed to arise from polymer chain association (Dintzis, Babcock et al. 1970).

1.1.2.b The secondary structure

Polysaccharides which display interesting solution properties, tend to form ordered structures in the aqueous environment (Kennedy and Bradshaw 1984). Rees (1972) made the first observations that xanthan existed in an ordered form using optical rotation. It was observed that with increasing temperature a sigmoidal change in optical rotation could be seen, suggesting a conformational change and order to disorder transition. Other studies using rheology, NMR relaxation, and circular dichroism all confirmed this initial theory (Holzwarth 1976; Morris, Rees et al. 1977; Milas and Rinaudo 1979). An increase in ionic strength has been shown to shift the transition point to higher temperatures, such that xanthan exists in the ordered form to temperatures above 100^{o}C (Morris 1977).

X-ray diffraction studies have shown the molecular conformation to be a right handed 5-fold helix, in which the tri-saccharide side chains align with the backbone providing rigidity to the helix (Moorhouse, Walkinshaw et al. 1977). Numerous studies have been performed to elicit the exact conformation of xanthan however there is still no unanimous consensus. Some studies suggest a single helix (Holzwarth 1976; Norton, Goodall et al. 1984) whilst others propose a double helix (Holzwarth and Prestridge 1977; Paradossi and Brant 1982; Sato, Norisuye et al. 1984; Gamini and Mandel 1994). Electron microscopy of xanthan has been performed by Stokke and co-workers to further understand the conformation however this provided evidence of both

conformations, making it difficult to generalise the secondary structure of xanthan (Stokke, Elgsaeter et al. 1986). Work by Young et al. was unable to distinguish between the single or double helix, but established that the helical ordered form is stabilized principally by hydrogen bonding (Young, Martino et al. 1994). Paoletti and co-workers (1983) have reported that the nature of the double helix is either side-by-side or intertwined but could not be determined. The model proposed by Norton et al. (1984) is shown in Figure 1.2.

The degree of acetylation and pyruvation is important for the stabilization of the ordered form (Gamini and Mandel 1994). It is known that the acetate groups tend to promote the formation of the ordered form through hydrogen bonding, in contrast to the pyruvate groups which favour the disordered form as a result of electrostatic repulsion (Pelletier, Viebke et al. 2001).

A significant number of polymers form random coils in solution. This is often referred to as the flexible chain model. In 1949 Kratky and Porod investigated an exception to this, the wormlike chain model. The details of the model are not essential here, however an important parameter used within it is known as q or the persistence length of the polymer chain. The importance of q is that it provides a description of chain stiffness and for flexible polysaccharides such as carboxymethylcellulose, q has been quoted of being between 8 and 30 nm. Xanthan however has values of q ranging from 100 - 300 nm indicating that the xanthan molecules form a long rigid rod in solution (Lapasin and Pricl 1999), however there have also been suggestions that xanthan can be classed as semi-rigid chain (Holzwarth 1981).

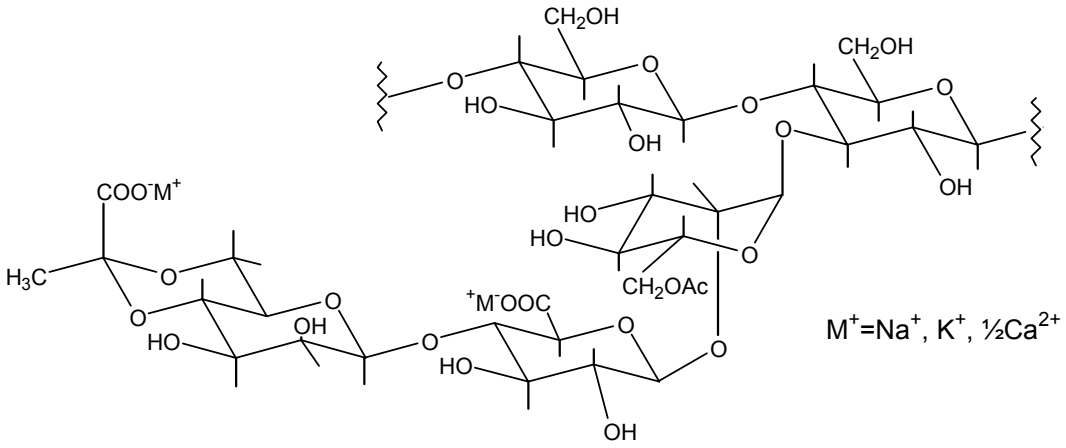

Figure 1.1. The primary structure of xanthan.
Xanthan is made from a cellulose backbone with a trisaccharide side chain on alternate glucose residues. The side chain is made from a glucuronic acid residue flanked by two mannose residues (Jansson, Kenne et al. 1975). The terminal mannose is approximately 50% pyruvated, the other mannose having an acetal group.

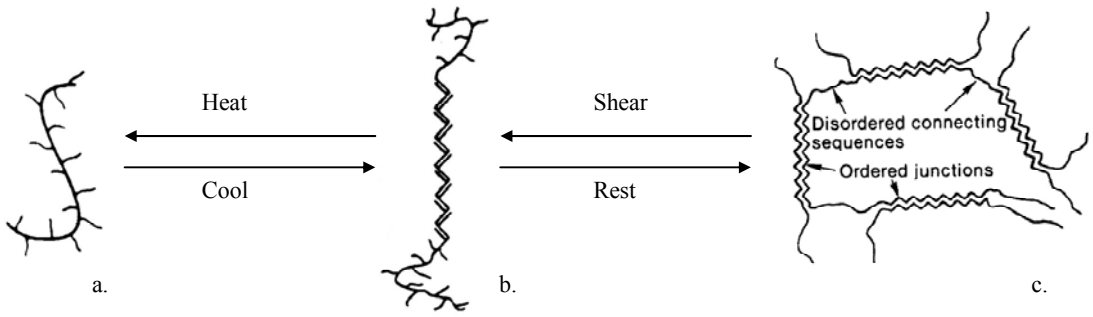

Figure 1.2. A diagrammatic representation of the order to disorder transitions in xanthan gum under the influences of temperature and shear.
The long range ordered network (c.) is converted to a local ordered system (b.) by shear and then to the random coil (a.) by heat. Adapted from (Norton, Goodall et al. 1984).

1.1.3 Solution properties

In an aqueous environment at low ionic strength, polyelectrolytes normally exist in a highly extended conformation and give rise to a high solution viscosity. Increasing temperature normally reduces the viscosity as a result of chain flexibility. Increasing ionic strength results in intramolecular charge screening, reducing the size of the polymer coil and resulting in a drop in the solution viscosity (Kennedy and Bradshaw 1984).

Xanthan is soluble in both hot and cold water (Garcia-Ochoa, Santos et al. 2000). It exhibits high viscosity at a low concentration and maintains its viscosity in high ionic environments, indicating a departure from the normal random coil conformation. In some cases solution viscosity may increase with ionic strength (Whitcomb 1978). Xanthan also maintains its viscosity in moderate ionic environments with increasing temperature. In low ionic environments there is an anomalous increase in viscosity with increasing temperature over a specific narrow range indicating a conformational change (Morris 1977) but in general xanthan viscosity is independent of salt concentration above 0.1% salt (Kang and Pettitt 1993). Under the influence of shear, xanthan is pseudoplastic and exhibits very low viscosity at high shear rates (Milas, Rinaudo et al. 1985). These solution properties are directly related to the xanthan behaviour in solution, in which the rod-like helical chains entangle to form a complex network. The weak aggregation of the network results in the pronounced pseudoplasticity, however the high low shear viscosity is a result of helix rigidity. The addition of electrolytes reduces electrostatic repulsion allowing the side chains to align with the helical backbone and further promoting the helical conformation (Kang and Pettitt 1993). The addition of divalent ions has been proposed to also improve coil-coil interactions by bridging carboxylate groups (Ross-Murphy, Morris et al. 1983). The temperature stability can be attributed to the stability of the helical conformation.

There has been much debate over whether xanthan exhibits a yield stress. Early work suggested this to be true (Whitcomb, Ek et al. 1977), however using modern instrumentation it is now believed not to be the case.

Xanthan, in the presence of salt is insensitive to pH over the range pH 2-10 (Sandford, Pittsley et al. 1977). Deacetylation tends to occur above pH 9, however this has little effect on the its solution properties (Kang and Pettitt 1993). At pH values below 3, deacetylation and depyruvation also occur, again having little effect on the solution properties (Callet, Milas et al. 1988; Garcia-Ochoa, Santos et al. 2000).

1.1.3.a Compatibility with other materials

Xanthan shows a remarkable level of compatibility with most substances. Xanthan is unaffected by enzymes such as protease, cellulase, hemicellulase, pectinase and amylase when in the ordered conformation, xanthan is however degraded by cellulase when promoted to the disordered form. Xanthan is also degraded by enzymes produced by some *Bacillus* species (Sutherland 1995).

Xanthan is compatible with monovalent and most divalent salts and the viscosity is maintained at high salt concentrations. Polyvalent salts however do show compatibility issues. Salts such as aluminum (III) sulphate and lead (II) nitrate can cause gelation and precipitation over a wide pH range and salts such as copper (II) chloride, barium (II) chloride and iron (II) sulphate are incompatible above pH 10 (Cottrell, Kang et al. 1980; Kang and Pettitt 1993).

Xanthan dissolves directly in strong acids including 5% sulphuric acid and 10% hydrochloric acid. It also dissolves in strong alkalis such as 5% sodium hydroxide to yield thickened solutions. All of these solutions have good stability over several months. Xanthan is also compatible with a number of organic solvents such as methanol, ethanol, isopropanol and acetone up to concentrations as high as 50%. At

concentrations higher than this gelation or precipitation occurs. Xanthan is however incompatible with peroxides (Challen 1993; Kang and Pettitt 1993).

Xanthan is also compatible with non-ionic surfactants up to concentrations of 20% and anionic surfactants up to 15%. At concentrations above these a salting out effect occurs (Cottrell, Kang et al. 1980).

1.1.4 Interactions with galactomannans

Xanthan is well known to interact with galactomannans such as locust bean (LBG, also known as carob) gum to yield a synergistic increase in viscosity at low concentrations and a thermo-reversible gel at higher concentrations (Maier, Anderson et al. 1993; Zhan, Ridout et al. 1993; Casas and Garcia-Ochoa 1999). Galactomannans are a group of polysaccharides that are composed of a mannose backbone with galactose substitutions unevenly distributed along the backbone, yielding unsubstituted 'smooth' regions and substituted 'hairy' regions (Dea, Morris et al. 1977). Locust bean gum typically has on average one galactose residue for every four mannose residues (Maier, Anderson et al. 1993).

Many studies have been undertaken to find optimal compositions for synergy and it was first suggested that the ratio of 1:3 xanthan:LBG was optimal (Dea and Morrison 1975) however others suggest a ratio of 1:1 using a wholly soluble grade of LBG to form the highest viscosity gel (Mannion, Melia et al. 1992). In reality the optimal ratio is likely to depend on the fraction of LBG that is soluble at the temperature of the experiment. Gel strength has been shown to be optimal with the deacetylated form of xanthan (Tako, Asato et al. 1984). It has been proposed that the gelation is a result of interaction of the helical regions of the xanthan molecule with the unsubstituted mannan backbone (Dea and Morris 1977).

The interaction between xanthan and galactomannans, especially locust bean gum, has been given particular interest as it offers a completely different functionality compared with that of the two components individually in solution (Rinaudo 2001).

1.1.5 Regulatory status

Xanthan gum was given the status GRAS (generally regarded as safe) in 1969 following extensive studies on oral consumption (21 CFR 172.695; Kang and Pettitt 1993).

1.1.6 Uses of xanthan gum

From the description of the properties described above the reader will appreciate that xanthan gum is a most useful hydrocolloid. Since its discovery it has found many uses some of which will be discussed below. A number of key food uses for xanthan are shown in Table 1.1, pharmaceutical and oil based uses in Table 1.2, and some miscellaneous uses in Table 1.3.

Application	Functionality Utilised	Reference
Dressings	Xanthan is used for its emulsion properties. Dressings are oil in water emulsions and the addition of xanthan can extend stability to greater than 1 year.	(Cottrell, Kang et al. 1980) (Kang and Pettitt 1993)
Dry mixes	Xanthan is used in dry mixes such as sauces to impart viscosity enhancement.	(Cottrell, Kang et al. 1980) (Kang and Pettitt 1993)
Syrups	Xanthan is used for its thickening properties and consistency. Xanthan also leaves a sheen on drying to increase appeal.	(Cottrell, Kang et al. 1980) (Kang and Pettitt 1993)
Dairy products	Xanthan and locust bean are used in combination to stabilize cottage cheeses and impart structure. They are also used in cheese spreads and other dairy products.	(Andrew 1977) (Kang and Pettitt 1993)
Baked goods	Xanthan is used in batters to improve processing in large scale manufacture. Xanthan is also used in dough as it improves freeze-thaw stability and improves moisture retention. It also improves mouthfeel.	(Cottrell, Kang et al. 1980) (Kang and Pettitt 1993)

Table 1.1. Some examples of food uses for xanthan gum.

Application	Functionality Utilised	Reference
Controlled release tablets	Xanthan can be used as a controlled release matrix tablet.	(Talukdar and Kinget 1995)
Liquid medicines	Xanthan can be used as a suspending agent for poorly soluble drugs. It can also stabilize emulsions and creams.	(Kang and Pettitt 1993)
Petroleum production and oil well drilling	The high viscosity properties at low shear rate assists with removal of bit cuttings and other debris removal. The low viscosity across jet nozzles allows improved strata penetration rates, lower viscosities at the drill bit.	(Eckel 1968) (MacWilliams, Rogers et al. 1973) (Carico 1976)
Workover and completion	Workover and completion fluids are essential for increasing oil productivity. Xanthan is useful as it provides excellent hole cleaning and suspension properties.	(Cottrell, Kang et al. 1980) (Kang and Pettitt 1993)
Fracturing	Xanthan is used in hydraulic fracturing to improve productivity of the well, by effecting deeper penetration of reservoir fractures. It is used as it makes an ideal suspending agent for the proppant, coupled with its insensitivity to temperature and salt.	(Cottrell, Kang et al. 1980) (Kang and Pettitt 1993)
Pipeline cleaning	Xanthan is able to remove rust, welding rod, welding slag and other debris from gas pipelines. As xanthan is toxicologically harmless it is safe for open sea disposal.	(Kang and Pettitt 1993)
Enhanced oil recovery	Xanthan is used in enhanced oil recovery as it reduces the mobility of water, and is therefore useful in polymer flooding.	(Sandvik and Maerker 1977) (Kang and Pettitt 1993)

Table 1.2. Some examples of pharmaceutical and oil industry applications for xanthan gum.

Application	Functionality Utilised	Reference
Textile printing	Xanthan is used for its thickening properties to prevent migration of dyes.	(Racciato 1976) (Cottrell, Kang et al. 1980)
Ceramic glazes	Xanthan is compatible with glaze components. It is able to control drying time and thereby reduced imperfections.	(Kang and Pettitt 1993)
Cleaners	Xanthan is stable with acid and alkali. Its pseudoplasticity also allow easy application and then retention.	(Kang and Pettitt 1993)
Slurry explosives	Xanthan is used to thicken nitrate based explosives as a result of its high compatibility with salts. This can be pumped into rock fissures or used in a canister form.	(Kang and Pettitt 1993)
Agriculture	Xanthan is used for suspension of chemicals and to prevent drift. It also promotes cling for greater duration of action. Xanthan is also used in liquid feeds for its suspending properties.	(Andrew 1977) (Cottrell, Kang et al. 1980)
Paints, Polishes and Inks	Xanthan is used for its thickening properties to prevent migration.	(Cottrell, Kang et al. 1980)

Table 1.3. Some miscellaneous uses for xanthan gum.

1.2 Sodium alginate

Alginates are derivatives of alginic acid and are sourced principally from the *Phaeophyceae* (brown seaweeds) which can contain anything between 18 to 40% expressed as alginic acid. The first substantial work within the alginate industry was by ECC Stanford in the 19th century and various companies have produced commercial alginate from as early as 1885. In the 1920's the Kelco company was the first company to commercially produce pure sodium alginate (Clare 1993). Alginates can also be produced from bacterial sources such as *Pseudomonas aeruginosa* and *Azobacter vinelandii* (Sutherland 1993; Draget, Skjåk-Bræk et al. 1997), however these are not in widespread use as a result of differences in properties and estimated production costs (Gacesa 1988; Clare 1993).

1.2.1 The structure of alginate

The alginate molecule is a linear chain comprised of two monomer units, β-D-mannuronopyranosyl and α-L-guluronopyranosyl (Rees and Samuel 1967). The structures are shown in Figure 1.3. The overall ratio and sequence of these monomeric units determines the properties of any given alginate. It is known that the monomers are arranged in a block fashion using any of the following combinations: -MM- (polymannuronate), -GG- (polyguluronate), and -MG- (alternating uronates) (Haug, Larsen et al. 1966; Clare 1993; Skaugrud, Hagen et al. 1999). The dissociation constant for alginates varies with composition as the pKa for mannuronic acid is 3.38, and 3.65 for guluronic acid.

The M block regions are linked in a $^4C_1$ conformation yielding a flat ribbon like conformation whereas the G blocks regions are linked in a $^1C_4$ conformation resulting in a more buckled ribbon. These are represented in Figure 1.4. Alginates high in G-blocks yield gels of higher strength in contrast to alginates contianing high amounts of M-blocks (Clare 1993).

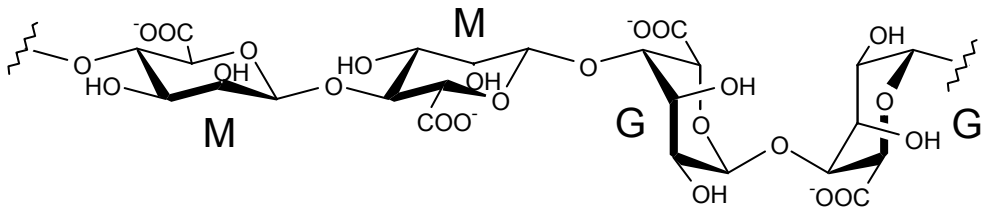

Figure 1.3. The basic repeating subunits of alginic acid. (M) β-D-mannuronic acid, (G) α-L-guluronic acid.
(adapted from Gacesa 1988)

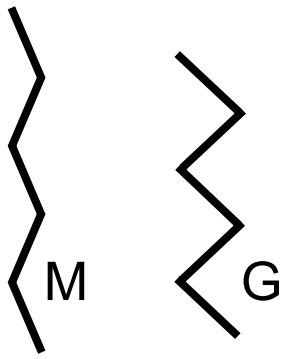

Figure 1.4. A diagrammatic representation of the conformation of (M) polymannuronate and (G) polyguluronate sequences.
The polymannuronate sequences show a conformation similar to a flat ribbon, whereas the polyguluronate sequences adopt a buckled ribbon conformation. Each line represents one sugar monomer.
(taken from Clare 1993)

The exact composition of each alginate is highly dependent on the species of seaweed from which it has been produced, and also the season, environmental conditions and the age of the plant (Skaugrud, Hagen et al. 1999; Anon. 2000). There can also be variation between different parts of the same plant.

The uronic acid distribution can be determined by high resolution nuclear magnetic resonance and the compositions of some typical examples are shown in Table 1.4.

Type of seaweed	% MM	% MG & % GM	% GG
Laminaria hyperborea (stem)	17	26	57
Laminaria hyperborea (leaf)	36	38	26
Laminaria digitata	43	32	25
Lessonia nigrescens	40	38	22
Lessonia trabeculata	56	26	18
Eclonia maxima	38	34	28
Macrocystis pyrifera	38	46	16
Ascoplhyllum nodosum	44	40	16
Laminaria japonica	48	36	16

Table 1.4. Examples of typical percentage compositions of block sequences of alginates produced from a number of different seaweeds as established by nuclear magnetic resonance.
MM-poly mannuronate; GG-polyguluronate; MG/GM-alternating mannuronate/guluronate. (Anon. 2000)

Bacterial alginates are initially synthesised as polymannuronate but are then modified by the bacterial C-5 epimerase enzymes to achieve the desired structures (Sutherland 1993). It is therefore possible to produce pure polymannuronate alginates, however complete enzymatic conversion to polyguluronate is not possible as the enzyme requires at least two adjacent mannuronate units to achieve conversion (Clare 1993). The production of C-5 epimerases by expression in *Escherichia coli* using recombinant DNA technology has greatly enhanced the possibilities of producing more custom designed alginates (Draget, Strand et al. 2000). C-5 epimerisation is not restricted to bacterial alginates, however for the purposes of research customised bacterial alginates are easier to produce and manipulate.

1.2.2 Solution properties

Alginic acid is insoluble whereas all monovalent salts of alginic acid are soluble. In contrast all divalent alginic acid salts except magnesium are insoluble. Alginates offer a wide range of rheological properties depending on viscosity grade and concentration. Solutions increase in viscosity with increasing concentration and molecular weight. Solutions of high viscosity exhibit shear thinning behaviour with increasing shear rate. Solution of low viscosity grades tend to behave in a more Newtonian-like fashion. Alginates are stable to pH variation over the range from pH 5 - 11 due to full ionization of the carboxylate groups. However below pH 4 the alginate converts to alginic acid and forms a viscous acid gel or precipitate depending on the rate of pH decrease (Draget, Skjåk-Bræk et al. 2006). A pronounced decrease in viscosity is seen with increasing temperature which is generally reversible, however prolonged heating can cause depolymerization, lowering viscosity (Clare 1993). As a general rule a $1^{o}C$ rise in temperature will cause a 2.5% decrease in alginate viscosity as a result of increased chain flexibility (Anon. 2000). The addition of salt reduces the viscosity of alginate mixtures (Cottrell and Kovacs 1980) as a result of carboxylate charge screening allowing the polymer chains to contract.

1.2.3 Gelation of alginate

1.2.3.a Ionic gelation

Alginates form gels with divalent ions and show a relative binding affinity in the order $Ba^{2+} > Sr^{2+} > Ca^{2+} >> Mg^{2+}$ (Smidsrød 1974; Morris 1990). Alginates that are high in GG blocks produce the strongest gels. This can be explained by the preferential binding within the hydrophilic pocket created within the polyguluronate chain. The addition of divalent ions forms diamond shaped arrangements with poly-guluronate sequences (Figure 1.5), and the crosslink between two polyguluronate chains results in gelation (Stokke, Smidsrød et al. 1991). This has become commonly termed as the *dimeric egg box model* and is illustrated in Figure 1.6 (Grant, Morris et al. 1973; Morris 1986; Smidsrød and Draget 1996). The buckled ribbon conformation of the GG blocks is optimal for Ca^{2+} binding, the conformation of the MM blocks and the MG blocks is less favourable and hence gel strength is lower (Clare 1993).

The preparation of calcium-alginate gels is achieved through two methods: diffusion or internal gelation (Imeson 1990). The diffusion method involves allowing a soluble calcium source such as calcium chloride to diffuse with time into a soluble alginate solution, for example by use of a dialysis membrane. Direct addition of a soluble calcium source to an alginate solution results in immediate gelation around the calcium source, and a highly inhomogeneous gelation occurs. An alternative method is to disperse an insoluble calcium salt such as calcium orthophosphate throughout the alginate solution and add a slow acidifier such as D-glucono-δ-lactone. The decrease in pH dissolves the calcium source and produces a homogenous calcium alginate gel.

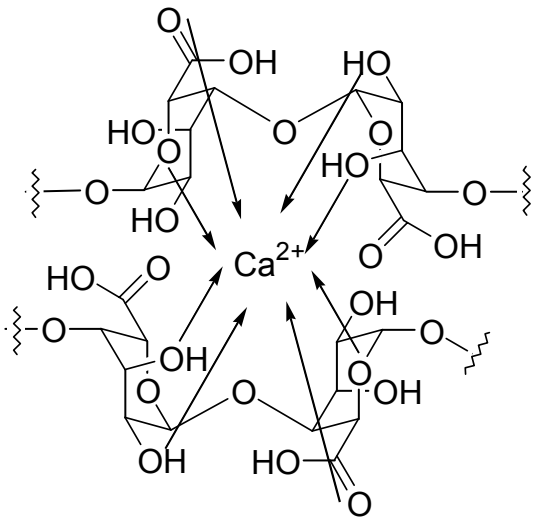

Figure 1.5. A diagram representing the proposed interaction between a calcium ion and segments of a polyguluronate chain to form a calcium-alginate gel.
(adapted from Smidsrød and Draget 1996)

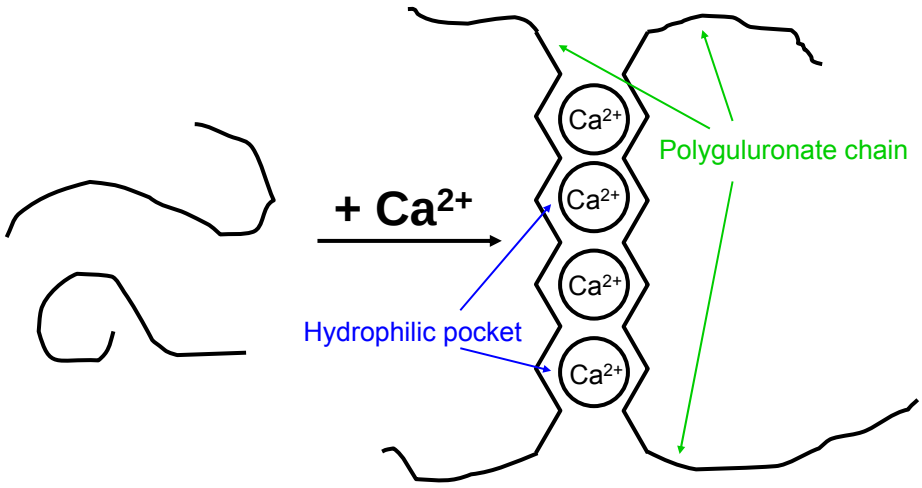

Figure 1.6. A diagrammatic representation interaction between polyguluronate sequences in alginate and calcium ions. Also known as the *dimeric egg box model*.
(adapted from Clare 1993; adapted from Draget, Skjåk-Bræk et al. 1994)

1.2.3.b Acid gelation

Alginate solutions form gels at pH values below the pKa of the uronide residues, which are often termed acid gels. These form as a result of intermolecular hydrogen bonding and the strengths of the gels are highly dependent on the chemical composition of the alginate used (Draget, Skjåk-Bræk et al. 2006). M rich and G rich form gels, whereas the weakest gels are formed by alginates with a random M:G sequence as a result of the lack of repeating structure.

1.2.4 The uses of alginate

Commercial alginates are available as a number of different forms including sodium, potassium and calcium salts. A propan-1,2-diol alginate is also available. All have regulatory approval under the European Union 'Miscellaneous Additive Directives'. Alginates have been given GRAS status by the American Food & Drug Administration (21 CFR 184.1724). The wide range of different applications for alginates with their functionality is illustrated in Table 1.5 and Table 1.6.

Application	Functionality Utilised	Reference
Tablet disintegrant	Rapid swelling enhances disintegration.	(McDowell 1977)
Modified release tablet	Swelling properties of alginate create a slow release matrix.	(Hodsdon 1995) (Tonnesen and Karlsen 2002)
Suspending agent	Thickening properties.	(McDowell 1977)
Alginate reflux formulation	Gelation by acid and calcium to form a raft on the stomach contents.	(Mandel, Daggy et al. 2000)
Wound management	Gelation and ability to absorb water. Alginates also have cellular effects.	(Schultz, Sibbald et al. 2003) (British National Formulary 2005)
Micro-encapsulation	Encapsulation of Islet cells to prevent rejection in Type I diabetes.	(Soon-Shiong 1999)
Tissue engineering	Calcium gels make suitable materials for cellular scaffolds.	(Kuo and Ma 2001) (Marijnissen, van Osch et al. 2002)
Dental impressions	Gelation produces accurate dental impressions.	(McDowell 1977)

Table 1.5. Pharmaceutical uses of alginates.

Application	Functionality Utilised	Reference
Bakery creams	Provides a range of different textures through gelling and thickening providing good mouthfeel.	(Anon. 2000) (McDowell 1977)
Dressings and fruit juices	Emulsifying and stabilizing.	(Anon. 2000) (Clare 1993)
Fruit fillings	Gelling thickening and stabilizing.	(Anon. 2000) (McDowell 1977) (Cottrell and Kovacs 1980)
Ice creams	Stabilizing and prevention of crystal formation.	(Anon. 2000) (McDowell 1977)
Low fat spreads	Stabilising and good mouthfeel and flavour release characteristics.	(Anon. 2000)
Beers	Maintains foam levels.	(Anon. 2000) (Cottrell and Kovacs 1980)
Pet foods	Gelling of meat chunks.	(Anon. 2000)
Adhesives	Improves viscosity to assist application.	(Cottrell and Kovacs 1980)
Textiles	Viscosity control of spreading and surface penetration.	(Anon. 2000) (Clare 1993)
Food film coating	Calcium gelation on the surface provides protection against bacterial damage and dehydration.	(Clare 1993) (McDowell 1977)
Welding	Improve adhesion of welding flux.	(McDowell 1977)
Explosives	Gelation of materials.	(Cottrell and Kovacs 1980)

Table 1.6. Food and non-pharmaceutical uses of alginates.

1.3 Phase separation

Phase separation in polymeric systems is a common phenomenon, with miscibility being the exception rather than the rule (Albertsson 1986). Polymers tend to be of high molecular weight and as a result the overall entropy change on mixing is small. As a direct consequence of this, interactions between polymer segments become a dominant factor in determining whether or not separation occurs and in what form the separation will present itself.

If the interactions between two polymer entities are repulsive, then the polymers will separate into two phases in which one is rich in polymer 1 and the other rich in polymer 2. This type of separation is known as segregative phase separation or simple coacervation, although the latter nomenclature is not now commonly used (Bergfeldt, Piculell et al. 1996; Tolstoguzov 2003). This is the most common type of separation observed and examples include aqueous mixtures of polyethylene glycol and dextran, methylcellulose and dextran, and sodium carboxymethylcellulose with sodium dextran sulphate (Albertsson 1986; Piculell and Lindman 1992).

The second type of separation observed is where polymer segments have an attractive interaction. This can yield a two phase system in which one phase is rich in both polymers, and a polymer depleted phase is created essentially comprised of solvent. This type of separation is known as associative separation or complex coacervation and commonly arises from polymers with opposite charges (Tolstoguzov 2003). Associative separation occurs in mixtures of gelatin and gum arabic, when the mixture is at pH's below the isoelectric point of gelatin (Bungenberg de Jong 1949; Bungenberg de Jong 1949). This type of separation also occurs when interactions between the polymers and the solvent are poor (Bergfeldt, Piculell et al. 1996). In the intermediate case where separation occurs and one of the polymers distributes evenly between the phases, it is known as borderline separation. These three types of separation yield characteristic shapes on a ternary polymer:polymer:solvent phase diagram and these are illustrated in

Figure 1.7. The magnitude of the interaction(s) will strongly influence the concentration threshold above which separation will occur. In the case of mixtures containing more than two polymers multiple phases can form.

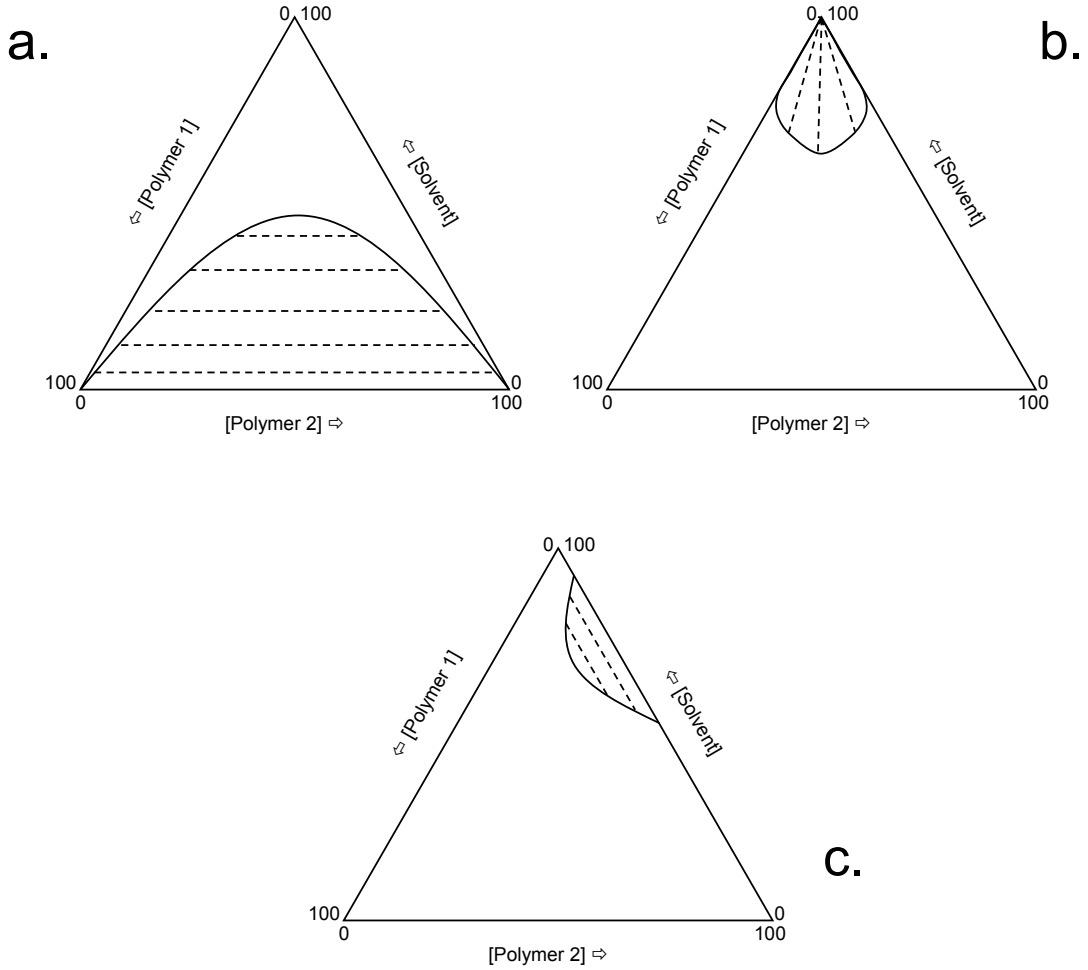

Figure 1.7. Schematic representations of the 3 different types of phase separation available to a ternary polymer/polymer/solvent mixture.
(Taken from Piculell, Bergfeldt et al. 1995; Bergfeldt, Piculell et al. 1996)
(a) shows a segregative separation where two phases form each one rich in one polymer. (b) shows an associative separation with one phase rich in both polymers, the other phase essentially composed of solvent. (c) shows a borderline separation where one polymer is distributed evenly between both phases. The solid line is the binodal line indicating the boundary between the 1 phase homogeneous region and the 2 phase separated region. The dashed lines indicate tie-lines, any mixture from on the tie line will separate into the 2 compositions where the tie line meets the binodal. Depending on the exact location on the tie line will dictate the relative phase volumes.

The thermodynamic theory underlying phase separation is discussed in chapter 6 within the context of the results presented, but a general overview is provided here, to introduce the reader to the types of phase separation issues that are important.

1.3.1 Factors affecting phase separation

Phase behaviour is dependent on a number of factors, one or more of which will influence partitioning into multiple phases.

1.3.1.a Polymer molecular weight

The molecular weight of the two polymer components can have a significant impact on phase separation. In general an increase in the molecular weight of either or both polymers will reduce the critical concentration required before separation occurs (Albertsson and Tjerneld 1994). The difference in molecular weight between polymers also has significant impact on the phase behaviour of a mixed system and the greater the difference the more asymmetric the binodal will appear (Albertsson 1986). Polydispersity in polymer samples is common. In practical terms this is generally shown by an area in which the binodal rests, rather than a clearly defined locus of points.

1.3.1.b Hydrophobicity of a polymer

Substitution of a polymer, in particular uncharged polymers, can impact on separation properties. For example a mixture of dextran and hydroxypropyl dextran becomes more incompatible with increasing hydroxypropyl (hydrophobic) content (Albertsson 1986). The degree of hydrophobicity, as a result of substitution level is also important in determining the polymers interaction with water. For example cellulose is insoluble in water as a result of its high level of intramolecular hydrogen bonding, substitution with

methoxyl groups, to form methylcellulose, reduces these hydrogen bonds promoting the interaction with water. The variance in polymer-solvent compatibility is often indicated on the phase diagram by an asymmetric shape with non-horizontal tie lines (Tompa 1956). Solvent compatibility can be a driving force for separation in its own right, even if the net polymer-polymer interaction is neutral or attractive (Piculell, Bergfeldt et al. 1995)

1.3.1.c Ionic environment

The ionic environment of a mixture often contributes to the phase behaviour of a mixed system. It is common for salts to partition equally between separating phases in order to maintain electrostatic and chemical potential neutrality (Albertsson 1995), however this is not always the case. In mixtures of polyelectrolytes, a raised ionic strength is able to screen electrostatic effects, and in the case of two similarly charged polyelectrolytes a reduction in the repulsion is possible, thereby reducing the likelihood of separation or raising the critical concentration threshold. In the case of a polyelectrolyte-uncharged polymer mixture the addition of salt reduces problems associated with electroneutrality and thereby encourages separation (Piculell, Bergfeldt et al. 1995).

1.3.1.d pH

The overall pH of a mixture may also have significant effects on separation behaviour. In the case of polyelectrolytes such as poly(acrylic acid), when the pH is above the pKa the carboxylate groups will be ionised in solution and the polymer will behave as a polyelectrolyte, whereas below the pKa the carboxyl groups will be unionized and the polymer will behave more as a neutral polymer. A good example of the consequences of changing pH is shown in a study by Bergfeldt and co-workers (1995) who investigated the phase behaviour of mixtures of poly(acrylic acid) and poly(styrene sulphonate) in 1M NaCl. They showed that that at high pH, where all of the acid residues are ionised, a

segregative separation was observed, whereas at low pH where poly(acrylic acid) was unionised an associative separation was observed.

1.4 Liquid crystals

Liquid crystals are a state of matter between liquids which have essentially no order and solid crystals which have a regular repeating construction (Collings 1990). A diagrammatic representation of the liquid crystalline order is shown in Figure 1.8. They are also commonly referred to as mesophases or anisotropic liquids (Lapasin and Pricl 1999). Liquid crystals can be formed from both polymers or monomers. They can be further subdivided into lyotropic liquid crystals which arise from solute/solvent interactions, and are therefore usually mixtures, and thermotropic liquid crystals which are as a result of heating a crystalline state above its melting point, so are usually single components (Lapasin and Pricl 1999). The central property of liquid crystals is anisotropy. This is commonly produced by alignment of rigid molecules, hence most liquid crystals are totally rigid in conformation or contain rigid parts.

Liquid crystals are defined by the degree of order within the system. In all liquid crystals, molecules have an average orientation parallel to an axis known as the director (Figure 1.9). The degree of order is defined by the order parameter, *s*, which is described in equation 1.1, where θ is the angle between the orientation of the molecule and the director (Wissbrun 1981). The function within the angled brackets is an averaged quantity across all molecules in a sample.

$$s = \frac{1}{2}\left(3\left\langle \cos^2\theta \right\rangle - 1\right) \tag{1.1}$$

It follows that when *s* equals 0 then there is no overall direction and the molecular arrangement is random which describes the isotropic system, when *s* is unity, perfect alignment of molecules with director exists. Typically, liquid crystals have values

between 0.3 and 0.9. In the case of thermotropic liquid crystals this value decreases as the temperature increases melting the liquid crystal (Collings 1990).

As the reader will appreciate, there are many different arrangements displaying order that can be formed. Some examples of the commonly occurring types of liquid crystals are shown in Figure 1.10. Nematic liquid crystals show no long range order, however all molecules tend to align in a preferred direction, although not perfectly. Cholesteric (also known as chiral nematic) liquid crystals also show no long range order and have molecular orientation. The principal difference is that the director changes in a helical orientation perpendicular to the plane of the directors. The most ordered liquid crystals are the smectic series (Lapasin and Pricl 1999). Molecules are arranged in clearly defined layers giving rise to long range positional ordering in a single dimension perpendicular to the plane however with each layer there may be variation in level of order and direction. Smectic A liquid crystals have equidistant planes where the director and the normal to the plane are aligned; smectic B liquid crystals also have this planar structure but also possess a second dimension, hexagonal arrangement. Smectic C also has a planar arrangement however the average director is inclined at an angle away from the normal to the plane (Collings 1990).

.

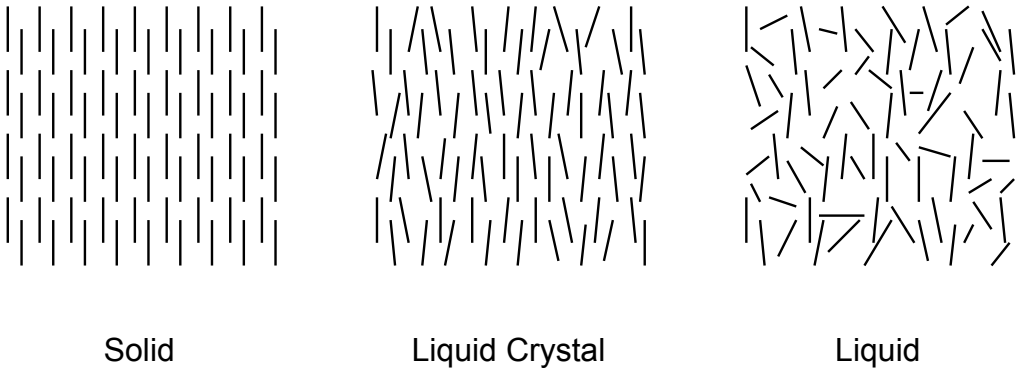

Figure 1.8. A diagrammatic representation showing the changes in molecular orientation across state changes from solid to liquid crystalline to the liquid state.
(adapted from Collings 1990)

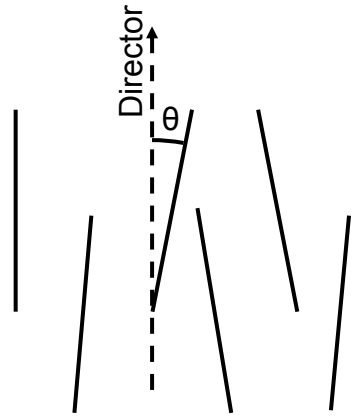

Figure 1.9. A pictorial description of the liquid crystal director.
(adapted from Collings 1990)

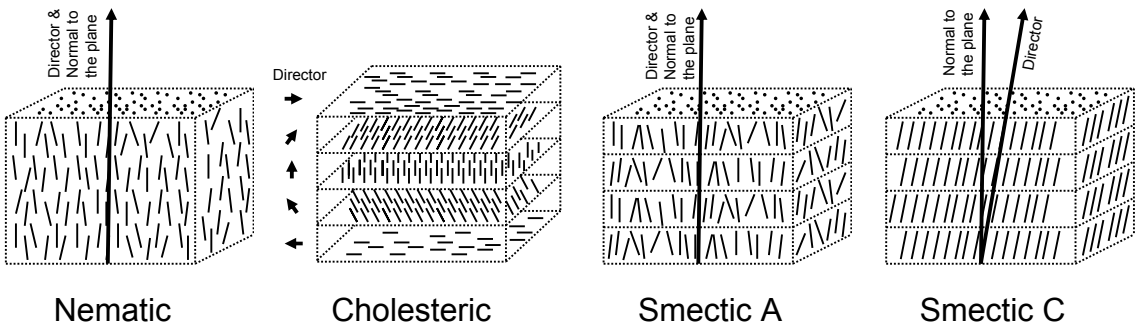

Figure 1.10. Diagrammatic representations of the molecular orientation of a selection of liquid crystal variants.
(adapted from Lapasin and Pricl 1999)

As mentioned previously liquid crystals tend to form from rigid or semi-rigid structures. These can be in the form of an interspersed rigid backbone structure, and are hence termed longitudinal liquid crystalline polymers, alternatively they can take the form of a flexible backbone with rigid side group entities and these are known as comb-like liquid crystalline polymers both of these types are known as segmented mesophases (Lapasin and Pricl 1999). Another group of mesophases are those made from polymers which are uniformly stiff or are semiflexible and are chemically homogenous on a scale significantly shorter than their persistence length. These are known as uniform mesophases and include polypeptides, aromatic polyamides and also some polysaccharides. Some polysaccharides which have been shown to give rise to liquid crystal formation include schizophyllan (Van, Norisuye et al. 1981; Sato and Teramoto 1996; Teramoto, Yoshiba et al. 2001), scleroglucan (Yanaki, Norisuye et al. 1984; Lee and Brant 1999) and xanthan gum (Jeanes 1973; Maret, Milas et al. 1981; Rinaudo and Milas 1982; Milas and Rinaudo 1983; Hatakeyama T., Nakamura K. et al. 1989; Sato, Kakihara et al. 1990; Sato, Kakihara et al. 1990; Sato and Teramoto 1991). Xanthan gum has been suggested to exhibit anisotropy at concentrations as low as 0.8% (Carnali 1991) or 0.7% (Allain, Lecourtier et al. 1988). Other biological substances that form liquid crystals include DNA (Livolant and Bouligand 1986; Merchant and Rill 1994; Merchant and Rill 1997) bile salts (Amenitsch, Edlund et al. 2003) and the tobacco mosaic virus (Sato and Teramoto 1991; Inatomi, Jinbo et al. 1992).

1.4.1 Properties of liquid crystals

1.4.1.a Optical effects

Liquid crystals are most commonly observed by the use of a light microscope fitted with crossed polarising lenses. In normal circumstances the use of crossed polarising lenses gives rise to a dark field with no light transmission. In the case of liquid crystals however this is not the case. When polarized light enters into an anisotropic crystal it is refracted into two light beams (Figure 1.11). Each beam becomes polarised with the vibrational directions perpendicular to each other and travel at different velocities. One of the rays travels through the crystal at the same velocity in every direction, this is known as the ordinary ray, the other ray travels with a velocity dependent on the propagation direction within the crystal. This is known as the extraordinary ray (Davidson and Abramowitz 2004). The only exception to this behaviour is where light enters along the optical axis, in this case the light behaves as if it were travelling through an isotropic sample. The difference in retardation between the ordinary and extraordinary rays is known as birefringence and is dependent on the sample thickness and the difference in refractive index. When the birefringent rays exit the sample they are still at right angles to the each other, the component vectors of the waves pass through the analyser and the light is repolarised. As a result of the retardation, interference (either constructive or destructive) occurs, and as a consequence some samples show a spectrum of colours.

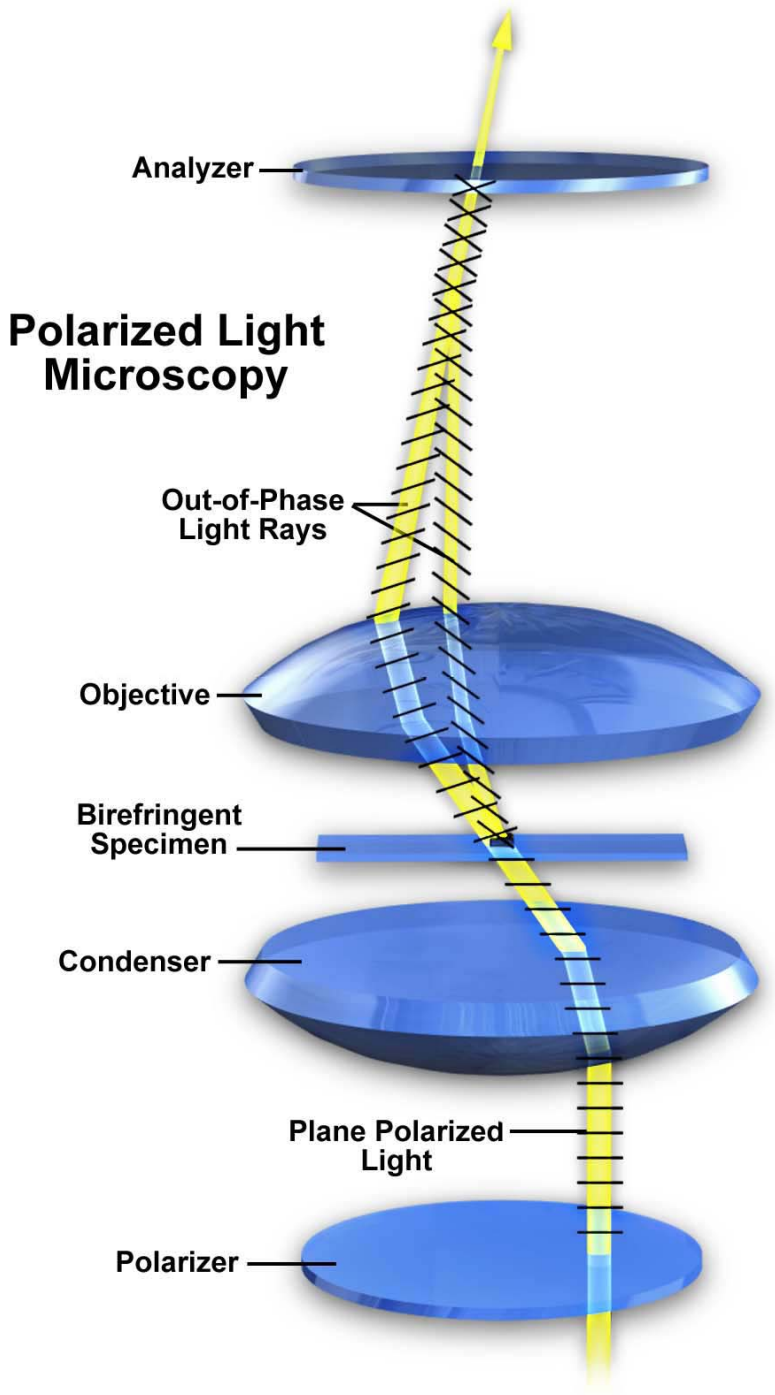

Figure 1.11. A schematic representation of a birefringent sample (e.g. a liquid crystal) between crossed polarising lenses.
As polarised light passes through the condenser it is concentrated onto the sample. On passing through the sample the light is double refracted into an ordinary and extraordinary ray, these rays travel at different velocities. As a result of this wave difference the waves interfere with each other either constructively or destructively, this often results in a range of colours being observed. (Taken from Davidson and Abramowitz 2004)

1.4.1.b Rheological effects

In all polymeric systems an initial increase in polymer concentration results in an increase in viscosity. For polymers that form liquid crystals, a point is reached where a further increase in concentration results in a decrease in viscosity (Onogi and Asada 1980; Wissbrun 1981; Sperling 2001). This viscosity drop is primarily as a result of liquid crystal formation where molecules become aligned and optically anisotropic. This alignment often reduces the viscosity to less than that of an equivalent random coil of the same molecular weight, as a result of the reduced number of entanglements. Xanthan has also been shown to exhibit this type of behaviour (Oertel and Kulicke 1991). The authors interpreted the viscosity changes in terms of the changes from a single phase, isotropic system to two phase mixed isotropic/anisotropic system, and then a single phase anisotropic system at high concentration (Figure 1.12). They interpreted the viscosity maximum as the inversion from anisotropic in isotropic, to isotropic in anisotropic in accordance with the work previously performed by Matheson (1980).

The maximum observed in viscosity has been shown in both continuous shear and dynamic oscillatory shear rheology where a maximum in both the elastic and viscous moduli are observed as a function of concentration (Lee and Brant 2002; Lee and Brant 2002)

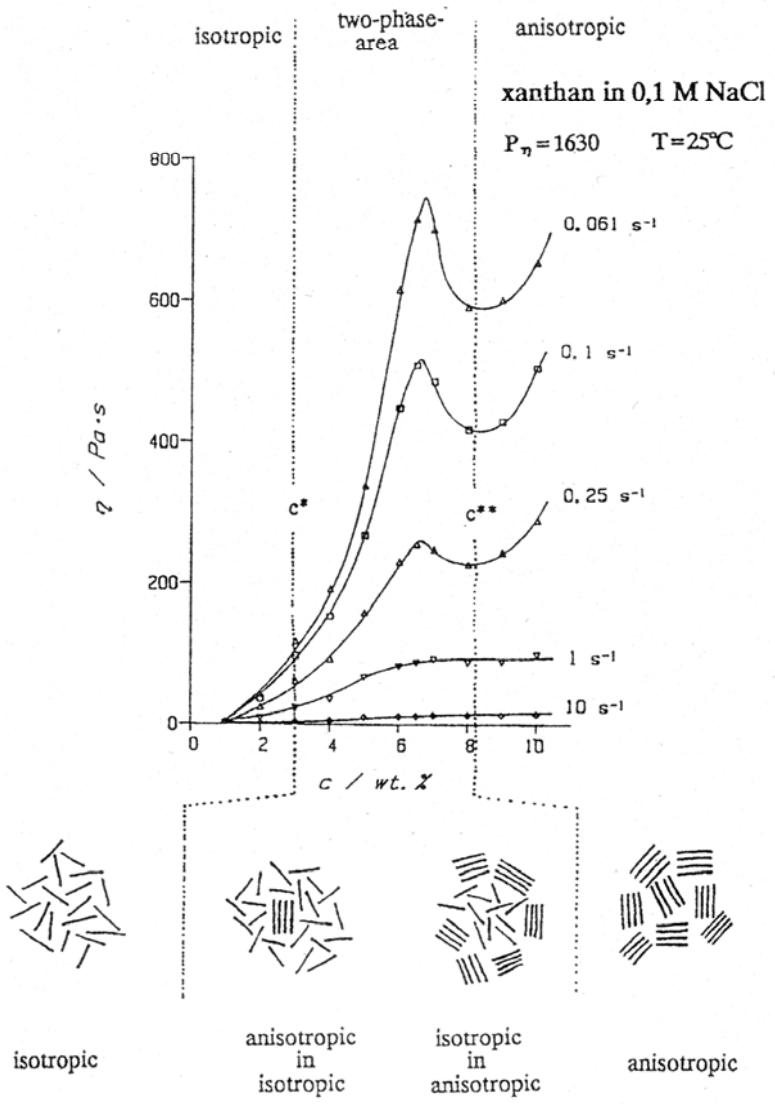

Figure 1.12. The viscosity of xanthan solutions as a function of concentration and shear rate.
(Taken from Oertel and Kulicke 1991)

1.5 Rheology

The term rheology is relatively recent and was first used in 1929 at the founding of the American Society of Rheology and was defined as *"the study of the deformation and flow of matter"* and is derived from the Greek word *Rheos* meaning 'stream' or 'anything flowing' and *ology* meaning study (Butterfield, Summers et al. 2003). The concepts behind rheology were however studied far earlier by Robert Hooke in 1678, who developed the *"True theory of elasticity"* and also Isaac Newton in 1687, who published work on steady shearing flow (Barnes, Hutton et al. 1989).

1.5.1 Shear stress and shear strain

Consider the application of lateral force **F** to the surface of a cube as shown in Figure 1.13. The force per unit of area **A** is known as the shear stress (σ) and is measured in Pascals (Pa). This shear stress causes a resulting deformation Δ and a shear strain (γ), which can be defined by:

$$\gamma = \frac{\Delta}{d} \tag{1.2}$$

where *d* is the distance between the top and bottom surfaces. As both Δ and *d* share the same units, strain is dimensionless. Where the body to which the force is applied is an elastic solid, the force will cause deformation, on removal of the force, the object will resume its original shape. Where the body is a viscous liquid the application of the force will result in flow of the liquid. The rate (velocity gradient) at which this liquid flows is known as the shear rate ($\dot{\gamma}$) and is defined by:

$$\dot{\gamma} = \frac{U}{d} \qquad \text{or} \qquad \dot{\gamma} = \frac{d\gamma}{dt} \tag{1.3}$$

where U is the relative velocity. Shear rate is measured in reciprocal seconds (s^{-1}) (Barnes, Hutton et al. 1989).

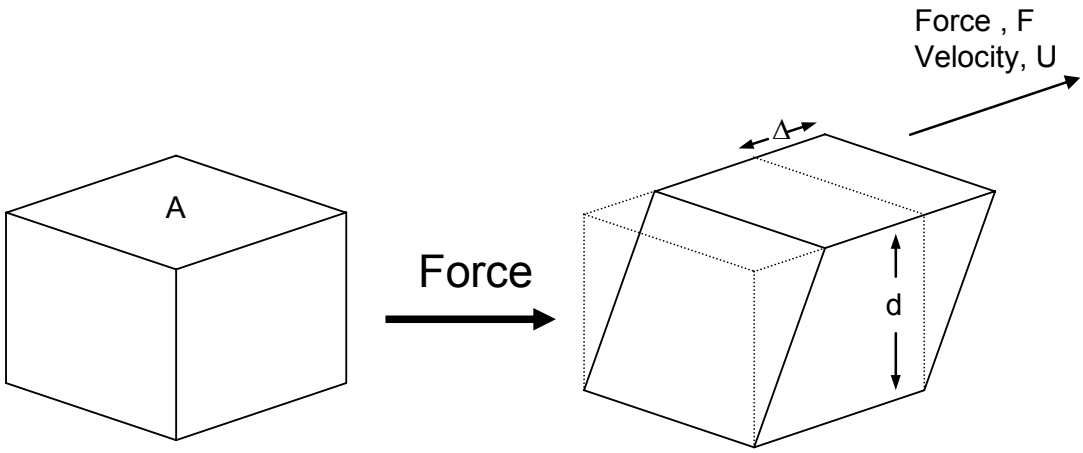

Figure 1.13. A diagrammatic representation of shear strain deformation.
The force **F** is applied to the body over a given area **A**. This results in a deformation **Δ.** (Adapted from Barnes, Hutton et al. 1989)

1.5.2 Viscometry

Shear stress (σ) is proportional to shear rate as indicated in equation 1.4. Thus as the force increases so does the velocity of the liquid. The constant of proportionality for this relationship is known as viscosity (η), a measure of flow properties, and is measured in Pascal seconds (Pa.s).

$$\sigma = \eta\dot{\gamma} \tag{1.4}$$

If the constant of proportionality viscosity, remains constant, the shear rate is directly proportional to the shear stress. This is known as Newtonian flow and is illustrated in Figure 1.14a. Fluids such as oils tend to exhibit Newtonian behaviour as a result of the presence of only short range interactions and the lack of entanglement networks.

Not all materials behave as Newtonian fluids. There are three other principal types of rheological behaviour which are illustrated in Figure 1.14. Figure 1.14b shows a material which exhibits pseudoplastic flow. In this type of material there is a significant decrease in viscosity with increasing shear rate. These type of materials tend to be polymeric in nature exhibiting high viscosity at low shear rates as a result of the disruption of long range entanglement networks or rod-like molecules when the viscosity decrease is due to rods becoming aligned reducing the resistance to flow. Xanthan gum is a typical example of a pseudoplastic material. Figure 1.14c shows plastic behaviour. In this case, the flow curve can look similar to pseudoplastic flow however, there is a threshold shear stress which must be overcome before the fluid will flow. The material can be reversibly deformed, however above the threshold (yield stress) the material starts to flow as a result of structure breakdown. Examples of such materials include emulsions such as mayonnaises (Tabilo-Munizaga and Barbosa-Canovas 2005) or highly concentrated suspensions (Aulton 1988; Lapasin and Pricl 1999). The last type of fluid behaviour is that shown in Figure 1.14d and is known as dilatant flow or shear thickening. In this type of fluid the viscosity increases with

increasing shear stress. This type of flow is far less common than the other three previously described and tends to occur in highly concentrated dispersions of small deflocculated particles. At low shear the particles are free to move, and exhibit low viscosity. At high shear the particles aggregate thereby increasing the resistance to flow and hence the viscosity increases (Barnes, Hutton et al. 1989). Apparent dilatancy can also be observed when laminar flow is superseded by turbulent flow, therefore care must be taken when interpreting flow data.

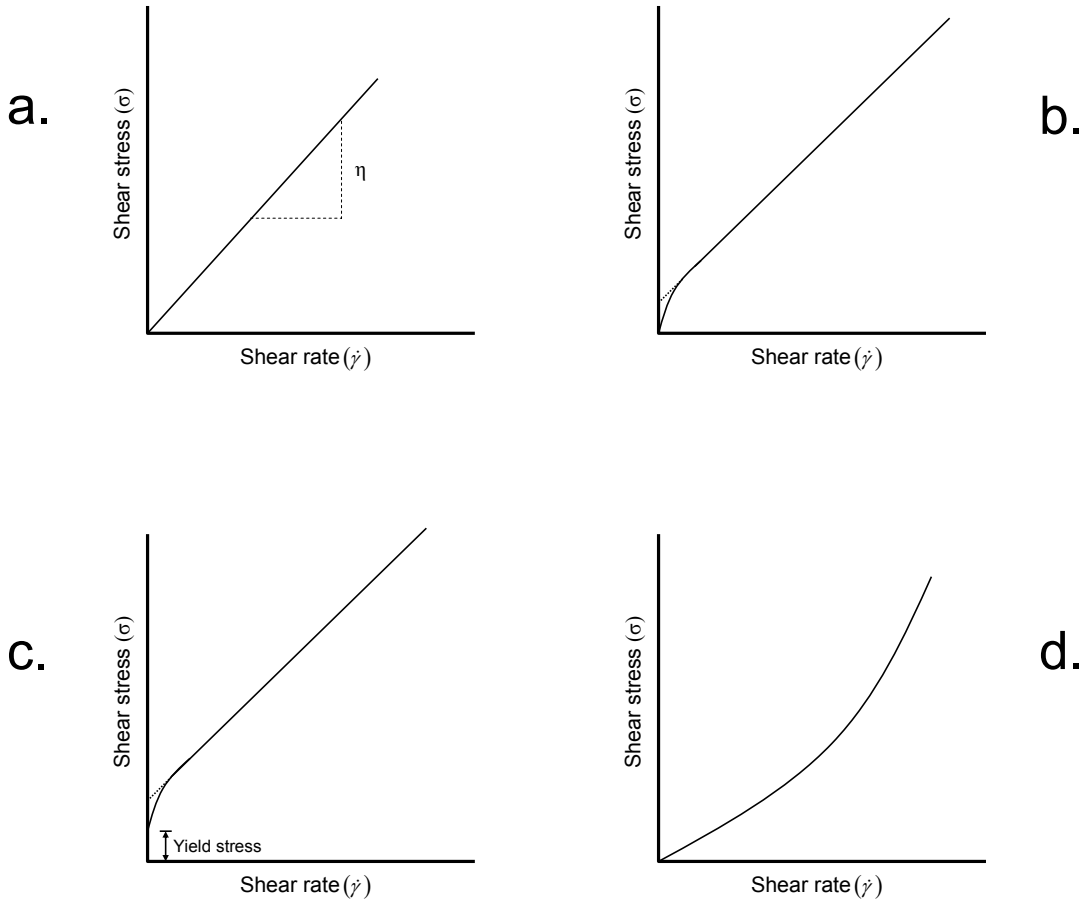

Figure 1.14. Diagrammatic representations of the four principal types of continuous shear behaviour exhibited by fluids.
(a) Newtonian behaviour, (b) pseudoplastic behaviour, (c) plastic behaviour and, (d) dilatant behaviour. (Aulton 1988; Florence and Attwood 1988; Barnes, Hutton et al. 1989)

To assist in describing fluid behaviour a number of models have been proposed to describe shear flow (Lapasin and Pricl 1999). The simplest model is the power-law model described by Ostwald and de Waele and is shown in equation 1.5 where K and n are constants.

$$\sigma = K\dot{\gamma}^n \tag{1.5}$$

The power law therefore states that for value of $n < 1$ the mixture shear thins, for values of $n > 1$ the fluid shear thickens. When n = 1 the fluid is Newtonian (cf. equation 1.4 which therefore makes $K = \eta$). The power law is simple and easy to apply and is often very useful in the middle shear rate region. Modern rheometers are able to obtain shear data over increasingly wide ranges, and often the power law becomes inadequate as viscosity often tends to asymptote to constant values as $\dot{\gamma} \longrightarrow 0$ (the zero-shear viscosity, η_0) and $\dot{\gamma} \longrightarrow \infty$ (the infinite shear viscosity, η_∞). To overcome these issues a number of models have been proposed such as the Cross model and the Carreau model. The Cross model is shown in equation 1.6 where λ describes the position of the power-law region on the shear rate scale.

$$\sigma = \eta_\infty \dot{\gamma} + \frac{(\eta_0 - \eta_\infty)\dot{\gamma}}{1 + (\lambda\dot{\gamma})^{1-n}} \tag{1.6}$$

In addition, the presence of a yield stress can also be a problem. Equations such as the Herschel-Bulkley equation (1.7) take this into account by adding a parameter to describe the yield stress, σ_y.

$$\sigma = \sigma_y + K\dot{\gamma}^n \tag{1.7}$$

1.5.3 Factors affecting viscosity

Whilst the characteristics of materials have a large impact on the type of flow behaviour, there are however other important factors which can affect the viscosity of a fluid.

1.5.3.a Concentration

With the exception of the liquid crystalline transition mentioned previously, increasing the concentration of a polymer component in a solution will increase the viscosity. At low concentrations, molecules are sufficiently far apart in solution that their coils do not overlap and viscosity is approximately linearly related to concentration ($\eta \propto c^{1}$). At a critical overlap concentration, known as c^*, coils overlap and molecules entangle (Sworn 2004). In this region $\eta \propto c^{3.5-4.0}$ (Lapasin and Pricl 1999).

1.5.3.b Temperature

Temperature can have pronounced effects on the viscosity of a fluid. Often with materials such as oils an elevated temperature will result in a significant decrease in viscosity as a result of intermolecular van der Waals bonds being reduced and hence raising molecular mobility. In the case of water a $1^{o}C$ rise will result in a 3% decrease in viscosity, therefore to achieve a level of 1% accuracy, temperature must be controlled to within $\pm 0.3^{o}C$. Polymers also exhibit similar temperature effects as elevated temperatures can break intermolecular bonds such as hydrogen bonds. There are also systems which can increase in viscosity with increasing temperature. These tend to be fluids that gel as a result of heat, examples include methylcellulose and hydroxypropylmethylcellulose (Haque and Morris 1993; Haque, Richardson et al. 1993) which are both generally liquid at room temperature but gel on heating.

1.5.3.c Shear rate

The effect of shear rate has been dealt with briefly when describing the types of flow behaviour. As a result of the different behaviour types shear rate can often play a significant role with both advantages and disadvantages. In the case of dilitant fluids an increase in the rate of flow will significantly enhance viscosity making pumping difficult. Pseudoplastic fluids such as xanthan show low viscosity at high shear rates making pumping easier.

Shear rate is different for different applications. Table 1.7 shows some examples of common applications and their relative shear rates. It follows that pseudoplastic materials make ideal suspending agents as they exhibit high viscosity at low shear rates, particularly producing suspensions in a high shear mixer is relatively easy as the viscosity is greatly reduced at high shear rates.

Situation	Typical shear rate range (s^{-1})	Application
Sedimentation of fine powders in a suspending liquid	10^{-6} - 10^{-4}	Medicines, paints
Leveling due to surface tension	10^{-2} - 10^{-1}	Paints, printing inks
Draining under gravity	10^{-1} - 10^{1}	Painting and coating. Toilet bleaches
Extruders	10^{0} - 10^{2}	Polymers
Chewing and swallowing	10^{1} -10^{2}	Foods
Dip coating	10^{1} -10^{2}	Paints, confectionary
Mixing and stirring	10^{1} -10^{3}	Manufacturing liquids
Pipe flow	10^{0} - 10^{3}	Pumping, blood flow
Spraying and brushing	10^{3} - 10^{4}	Spray-drying, painting, fuel atomization
Rubbing by hand	10^{4} -10^{5}	Application of creams and lotions to the skin
Milling pigments in fluid bases	10^{3} - 10^{5}	Paints, printing inks
High speed coating	10^{5} -10^{6}	Paper
Lubrication	10^{3} - 10^{7}	Gasoline engines

Table 1.7. Typical shear rates found in some common industrial settings.
(Barnes, Hutton et al. 1989)

1.5.4 Viscoelasticity

A viscoelastic material is a material that exhibits both viscous and elastic properties. There are two types of viscoelastic measurement that are generally performed: static tests and dynamic tests. Static tests include creep and stress relaxation, which are outside of the scope of this thesis. Only dynamic measurements will be discussed here.

1.5.5 Oscillation rheometry

In this type of measurement the sample is subjected to a sinusoidally oscillating stress, for example between a cone and plate geometry, and the resulting strain is observed (Figure 1.15). When the sample is perfectly elastic, the resulting strain is in phase with the stress, i.e. all of the energy applied to the sample is stored and returned on relaxation. If the resulting strain is $\pi/2$ radians (90^o) out of phase with the stress, the sample is a perfect viscous liquid, i.e. where all the energy supplied would be dissipated as heat (and/or sound). A viscoelastic substance shows behaviour midway between these two extremes. Where the ratio of stress to strain is a function of time and is unaffected by stress magnitude the behaviour is known as the linear viscoelastic region (Ferry 1980).

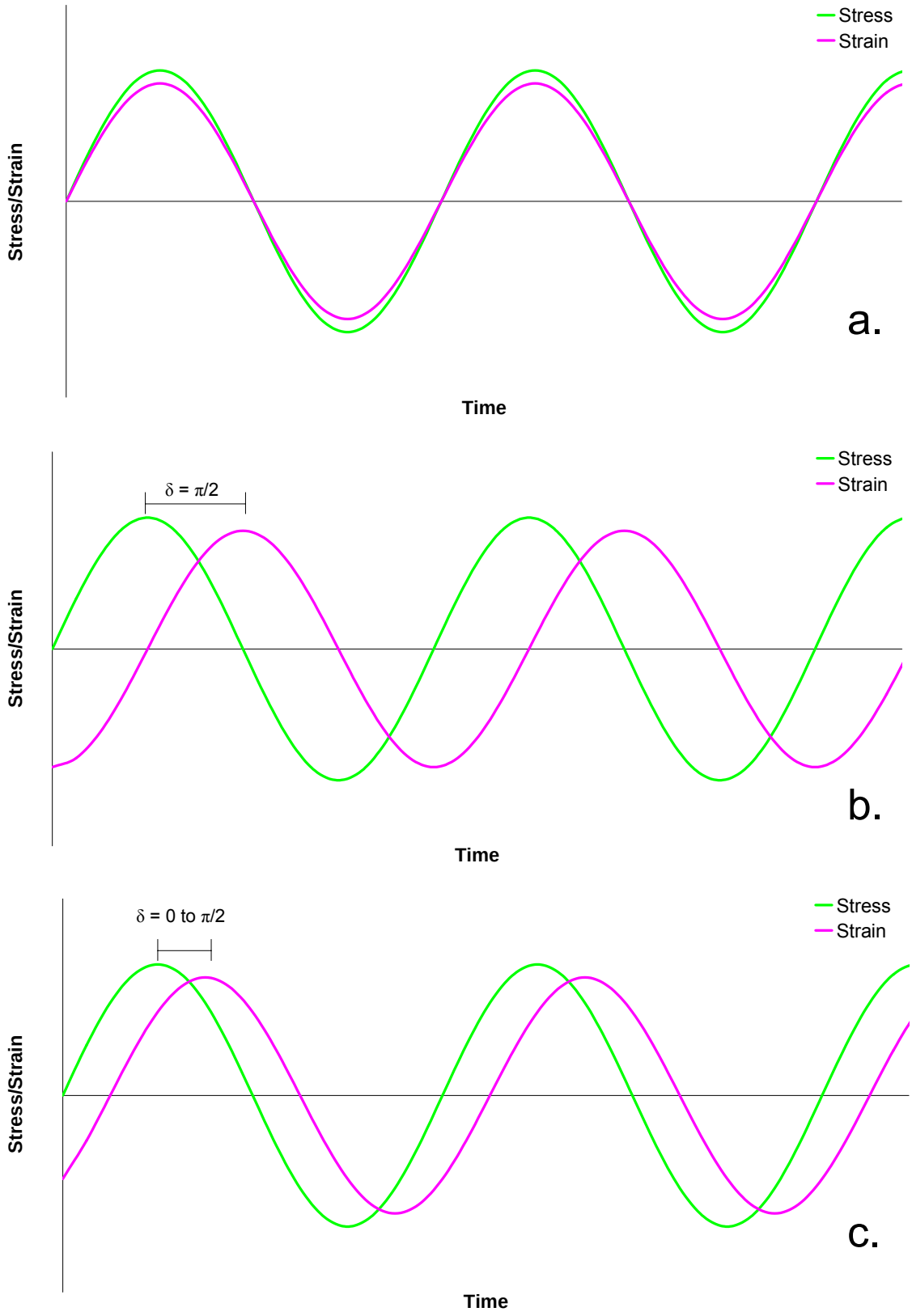

Figure 1.15. The relationship between stress and strain in different viscoelastic samples.
(a) a purely elastic sample, (b) a purely viscous sample and (c) a viscoelastic sample (Adapted from Barnes, Hutton et al. 1989).

Viscoelasticity, particularly linear viscoelasticity, can provide a useful insight in to the internal structure of a sample. It can be used as an analytical tool, and as a quality control measure of physical properties for industrially produced products (Barnes, Hutton et al. 1989).

There are a number of key parameters used to describe viscoelastic behaviour as the result of the dynamic experiment (Ferry 1980). These are the complex modulus (G^*) which is derived from the relative ratios of stress (σ^0) and strain amplitude (γ^0) (Equation 1.8), the elastic modulus (also known as storage modulus or G'), the viscous modulus (also known the loss modulus or G") and the phase angle (also known as δ).

$$G^* = \frac{\sigma^0}{\gamma^0} \tag{1.8}$$

G' is defined as the stress in phase with the strain divided by the strain during sinusoidal oscillation and gives a measure of how much of the energy applied to the system is stored. G" is defined as the stress out of phase with the strain divided by the strain and gives a measure of how much energy is dissipated. δ is the angle by which the stress is out of phase with the strain. These parameters are related to the complex modulus and phase angle through equations 1.9 and 1.10.

$$G' = G^* \cos\delta \tag{1.9}$$

$$G'' = G^* \sin\delta \tag{1.10}$$

The tangent of the phase angle δ, is the ratio of G" to G' (Equation 1.11). Values of tan delta below unity indicate G' dominance and hence the structure is elastic dominant, values greater than unity indicate G" is dominant and the system is dominated by viscous properties.

$$\frac{G''}{G'} = \tan\delta \tag{1.11}$$

The complex modulus is related to the storage and loss moduli by equation 1.12

$$\left|G^*\right| = \sqrt{G'^2 + G''^2} \tag{1.12}$$

The final parameter to mention is the complex viscosity (η^*). This is defined as the complex modulus divided by the frequency of oscillation ω, and is shown in equation 1.13.

$$\eta^* = \frac{G^*}{\omega} \tag{1.13}$$

In isotropic polymer solutions it is common to observe that the continuous and oscillatory shear show similar behaviour. This relationship is known as the Cox-Merz rule. This rule is only true of isotropic solutions; in the presence of aggregation and in systems forming polymer liquid crystals the quantities become considerably different, with weak gel-like substances often showing values of $\eta^*(\omega) > \eta(\gamma)$. The Cox-Merz rule can therefore be utilised as a method for distinguishing between structured fluids and ordinary polymer solutions (Lapasin and Pricl 1999).

As previously alluded to, for the equations to be valid, measurements must be performed such that the stress and strain are proportional and thus the ratio remains unchanged (Ross-Murphy 1988). This region is known as the Linear Viscoelastic Region (LVR). In simple terms it means this is the region where the stress supplied to the sample is insufficient to damage the internal structure of the sample. The LVR can be obtained by making small oscillations about a fixed origin of a rotational geometry such as a cone and plate. With each oscillation, the strain moved increases in a forced harmonic motion within the set parameters (Figure 1.16). From this, a graph of G' and G" can be plotted against either stress or strain. A diagrammatic version is shown in

Figure 1.17. For small stresses and strains G' and G" remain constant, indicating no variation in the ratio of stress to strain, this is the LVR. Beyond the LVR the value of G' and G" generally decrease and the linearity is no longer present. The equations are invalid outside of the LVR so care must be taken to ensure all samples are measured within it (Barnes, Hutton et al. 1989).

A value of stress and strain is chosen from the amplitude sweep sufficiently far from the upper non-linear region to ensure valid results. This fixed value is then used to apply a frequency sweep in which small deformation oscillations are again applied to the sample; however instead of varying strain amplitude, the frequency of the oscillations is varied (Figure 1.18). Measurements of this type give a viscoelastic spectrum.

Some examples of viscoelastic spectra are shown in Figure 1.19. In the dilute solution (5% dextran) there is a pronounced frequency dependence; however at all frequencies G" is greater than G' indicating viscous dominated properties. In the gel (1% agar) G' is greater than G" at all frequencies and the moduli are essentially frequency independent. The behaviour of a concentrated solution is between these two extremes. There is noticeable frequency dependence; at low frequencies G" > G' indicating viscous properties, whereas at high frequencies G' > G" more akin to an elastic system (Morris 1984; Ross-Murphy 1988).

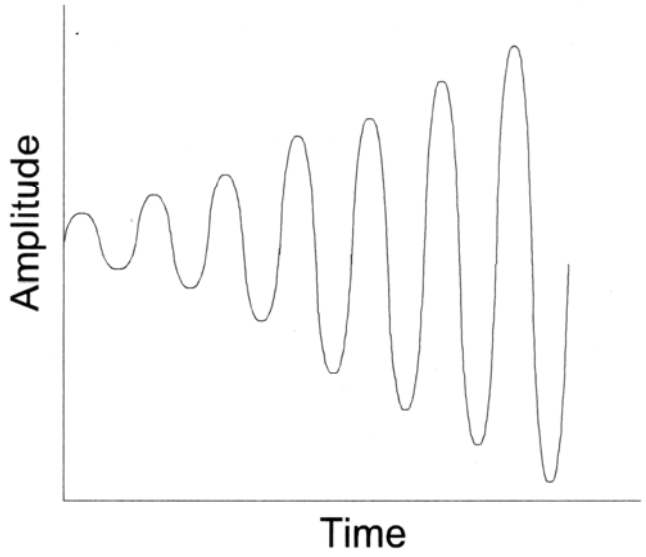

Figure 1.16. A diagrammatic representation of how an amplitude sweep is applied to a sample as a function of time.
The amplitude sweep applied is from low strain amplitudes to high. (Taken from Steffe 1996)

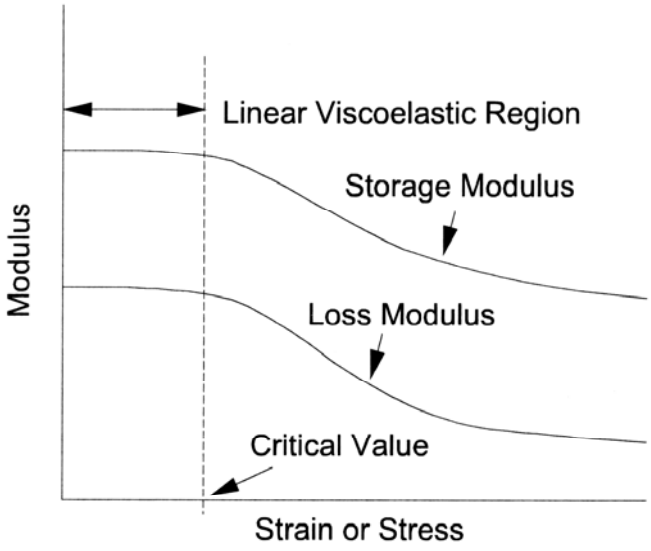

Figure 1.17. A diagrammatic representation of the results obtained from an amplitude sweep performed on an elastic dominated sample.
The linear viscoelastic region is the area in which the viscoelastic moduli are independent of stress and strain, and the sample is undamaged by the effect of oscillation. (Taken from Steffe 1996)

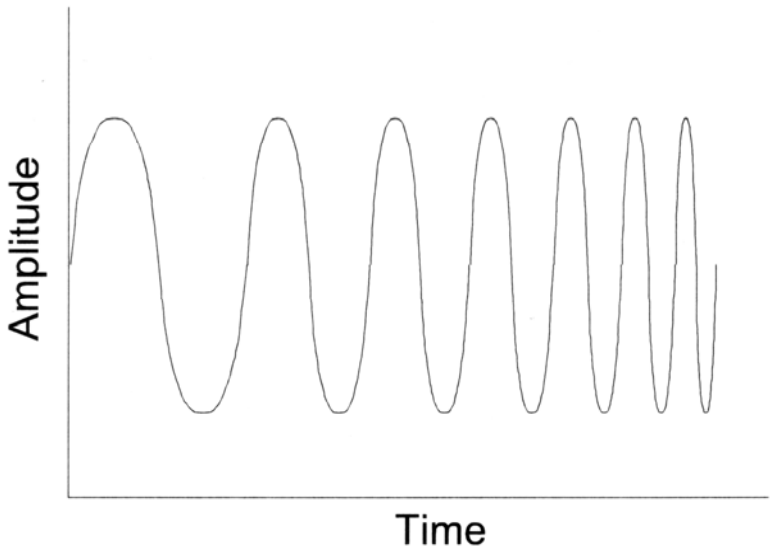

Figure 1.18. A diagrammatic representation of how a frequency sweep is applied to a sample as a function of time.
Frequency ramp applied is from a low frequency of oscillation to a high frequency. (Taken from Steffe 1996)

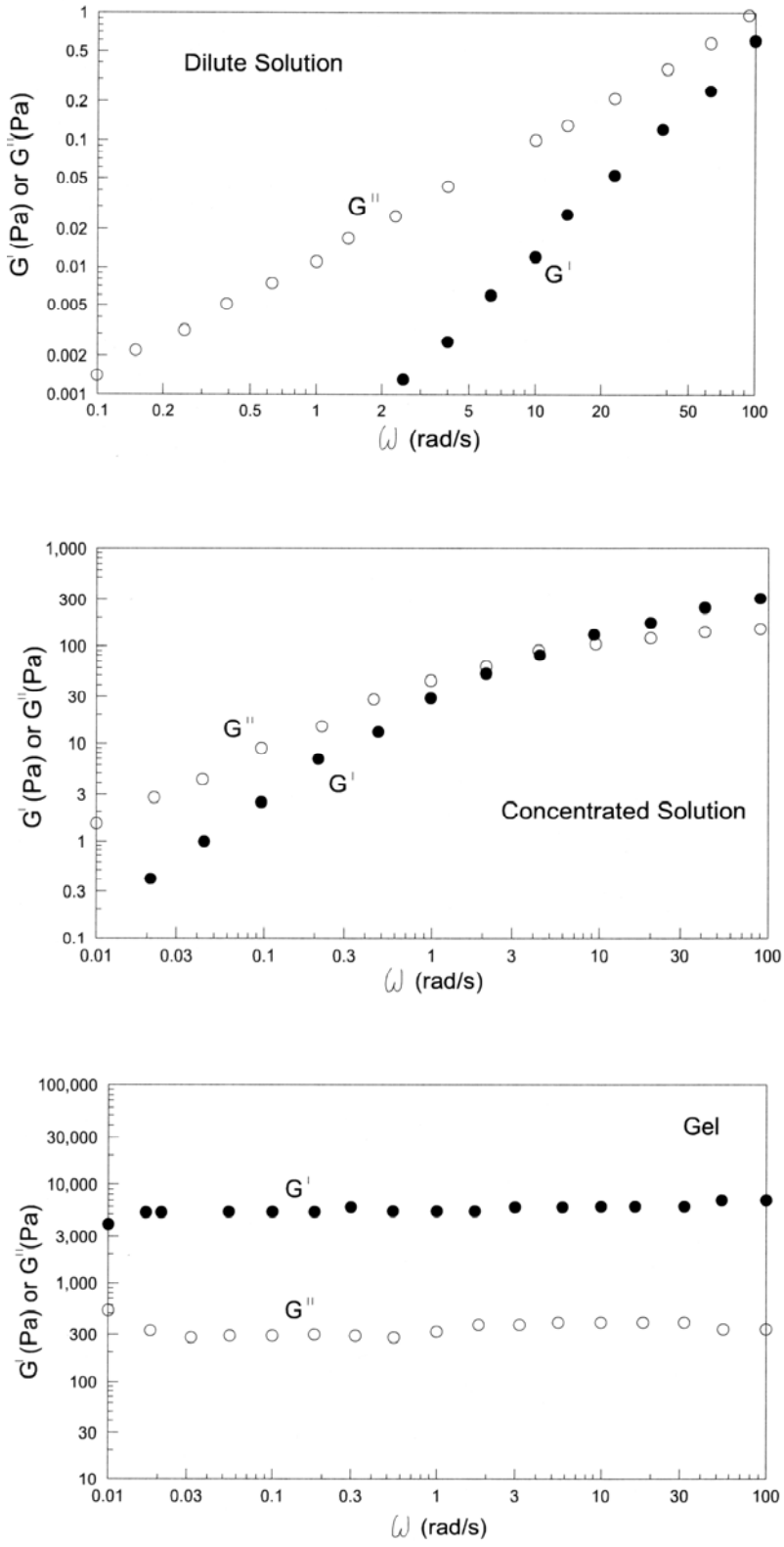

Figure 1.19. Examples of different types of mechanical spectra.
(a) 5% dextran solution (dilute solution), (b) 5% λ-carrageenan (concentrated solution) and (c) 1% agar (a gel). (Taken from Steffe 1996)

Xanthan shows interesting viscoelastic properties that do not fall in to the idealised spectra presented above. In dilute solution (< 0.3%) xanthan shows viscoelastic properties with G' greater than G" at low frequencies, both increase significantly as a function of frequency, with G" being significantly great than G' at high frequencies (> 1 $rad.s^{-1}$). Despite the significant increase both moduli remain at value below 0.1 Pa even at high frequencies (Cuvelier and Launay 1986). At higher concentrations (> 0.5%) the properties of xanthan are significantly different. G' is greater than G" across a wide range of frequencies (10^{-2} - 10^{2} $rad.s^{-1}$) and these increase in a frequency dependent fashion with the ratio of G' to G" remaining constant (Lim, Uhl et al. 1984; Cuvelier and Launay 1986; Richardson and Ross-Murphy 1987). This behaviour has been described as the formation of a 'weak gel' where small strain amplitudes provide gel-like properties whilst retaining the ability to flow with fracture (Ross-Murphy, Morris et al. 1983; Morris 1984; Richardson and Ross-Murphy 1987; Ross-Murphy 1995).

The correlation between $\eta^*(\omega)$ and $\eta(\gamma)$ for 1% xanthan has also been studied. There is significant deviation between the two curves with $\eta^*(\omega) > \eta(\gamma)$ indicating a failure of the Cox-Merz rule further suggesting a weak gel-like behaviour (Richardson and Ross-Murphy 1987; Ross-Murphy 1995).

1.6 Oesophageal drug delivery

Traditionally drug delivery to the oesophagus has concentrated on physical barriers to protect against gastric refluxate, or the local delivery of drugs for the treatments of cancers and fungal infections. The approaches to achieving localized delivery have generally involved the lodging of tablets or capsules in the oesophagus often resulting in localized damage (Batchelor 2005).

1.6.1 The anatomy and physiology of the oesophagus

The oesophagus is a muscular tube that is approximately 25 cm in length and 2 cm in diameter (Waugh and Grant 2001). It connects the pharynx to the stomach and its role is the transport of food and liquid from the mouth to the stomach (Figure 1.20). The oesophagus has 3 anatomical regions. The upper region is 4 - 6 cm in length and is made from striated muscle. It has a sphincter at the top known as the upper oesophageal sphincter which is closed except for swallowing and the expulsion of air. The middle section is 12 -14 cm in length and is constructed from smooth muscle. The lower section forms the lower 3 - 4 cm of the oesophagus and contains the lower oesophageal sphincter (Pope 1997) (also known as the cardiac and gastro-oesophageal sphincter, Figure 1.21). This lower sphincter is responsible for ensuring that the contents of the stomach remain in the stomach during digestion and preventing reflux. The oesophagus is principally lined with stratified epithelium which is relatively impermeable. It is protected by this epithelium and also saliva and mucin from the mouth, lubricating the passage of food and reducing abrasion. At the lower end of the oesophagus the oesophageal epithelia changes to stomach epithelia which are covered with protective mucus to protect against local acid (Batchelor 2005).

Transit time through the oesophagus of a healthy individual is typically 10 to 14 seconds.

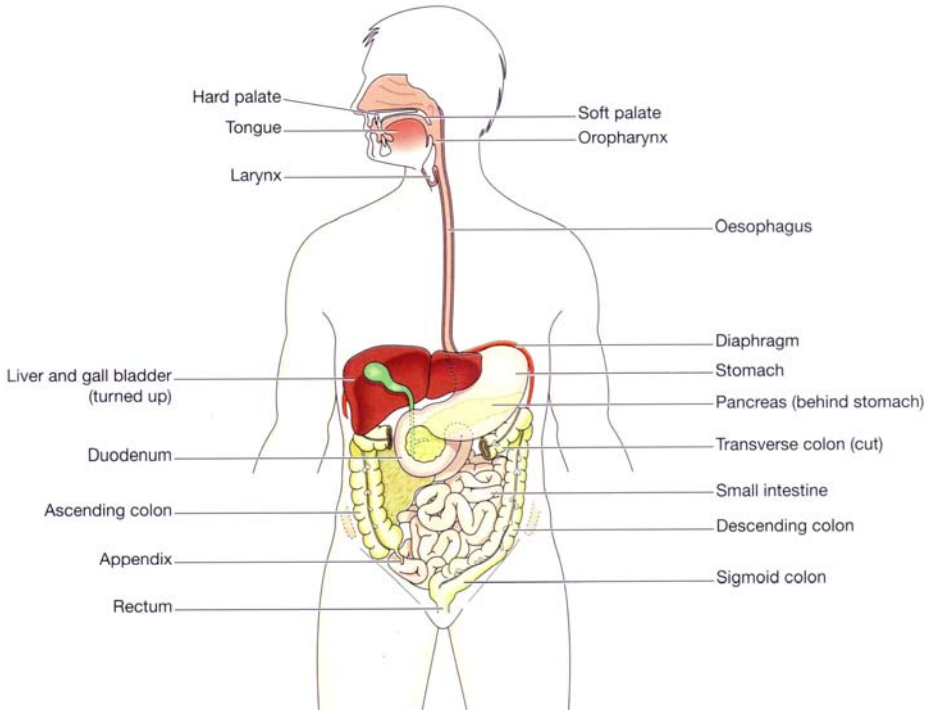

Figure 1.20. The anatomy of the human gastrointestinal (GI) tract.
(Taken from Waugh and Grant 2001)

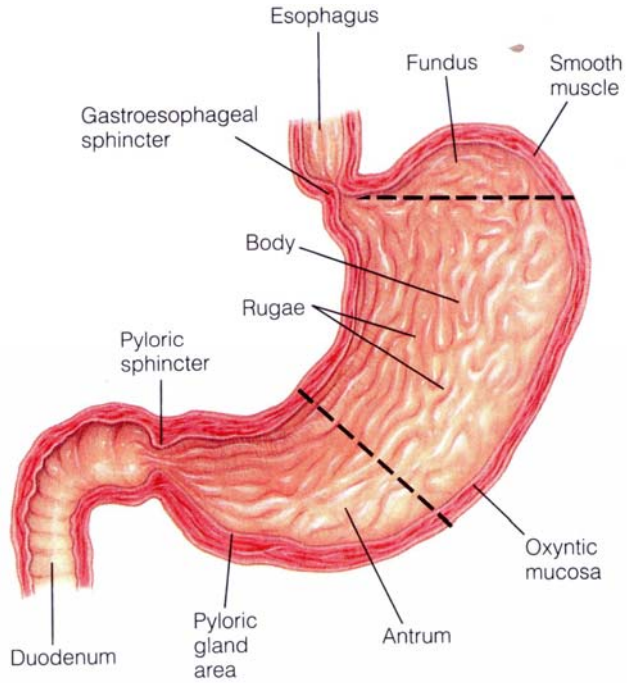

Figure 1.21. The anatomy of the lower oesophagus and the stomach.
(Taken from Sherwood 1993)

1.6.2 Diseases of the oesophagus

There are five principal conditions affecting the oesophagus, Achalasia, Gastro-oesophageal reflux disease, Barrett's oesophagus, Oesophageal adenocarcinoma and Infections.

1.6.2.a Achalasia

Achalasia is a disorder of the lower oesophageal sphincter and is typically nervous in origin. On swallowing instead of relaxing as normal it closes more vigorously. As a consequence the food is greatly delayed from transferring into the stomach leading to significant distension, and in severe cases pneumonia as a result of aspirated food (Sherwood 1993).

1.6.2.b Gastro-oesophageal reflux disease

Gastro-oesophageal reflux disease, also known as GORD, arises from the opposite of achalasia, reduced lower sphincter tone. (It should be noted by the reader that often GORD is referred to as GERD as American English drops the initial 'O' from oesophagus.) Reflux is a normal physiological event that occurs in everyone; however there is wide variation of opinion on its frequency. It was reported by Nandurkar and Talley (2000) that 44% of the USA report clinical symptoms on a monthly basis, whereas Locke, Talley et al (1997) reported that 40% of an American population experience heartburn at least once in a 12 month period. Symptoms of GORD include heartburn and regurgitation, however there are a number of allied symptoms such as asthma, wheezing, chronic cough, hoarseness and laryngitis which have all been shown to have links with reflux (DiPalma 2001). GORD is associated with a number of risk factors including poor diet, cigarette smoking, alcohol ingestion, obesity and prolonged

use of non-steroidal anti-inflammatory drugs (NSAIDS) (Locke, Talley et al. 1999), all of which increase the frequency and severity of symptoms.

In addition to the acidic nature of a reflux event other damaging agents are also subject to reflux and include pepsin, bile and other pancreatic proteins. There have been a number of studies into the effects of pepsins and there is considerable evidence to suggest that the pepsin component of the refluxate is responsible for a significant amount of the damage associated with reflux (Castell, Murray et al. 2004). Current therapies rely on both pharmacological and physical methods and are detailed in Table 1.8

1.6.2.c Barrett's oesophagus and oesophageal adenocarcinoma

Barrett's oesophagus is a condition where the normal squamous epithelial lining of the oesophagus is replaced by columnar epithelial cells similar to gastric epithelium. There is a strong link between the presence of GORD and Barrett's oesophagus, however the exact link is still under much debate (Fitzgerald 2005) but is likely to be a result of damage induced by acid and pepsin.

Barrett's oesophagus is an important disease at it has been shown to be a precursor for oesophageal adenocarcinoma (Fléjou 2005) which is a highly lethal carcinoma with only a 10% survival rate at 5 years (Lagergren 2005).

1.6.2.d Infections

Infections of the oesophagus are generally associated with patients who are immunocompromised such as those with HIV or undergoing cancer chemotherapy. A number of agents are available to treat these conditions; however they have limited efficacy as a result of the low permeability of the oesophagus and their low systemic availability (Batchelor 2005).

Method	Category	Examples	Method of action
Physical	Rafting agent	Alginate based medicines including: Gaviscon™ Gastrocote™ Peptac™ Rennie Duo™	Alginate products form a raft on the surface of the stomach contents as a result of the liberation of carbon dioxide from the sodium bicarbonate and alginate cross liking from the calcium carbonate. This provides a physical barrier to the reflux episode. (Mandel, Daggy et al. 2000; Marciani, Little et al. 2002)
	Coating agent	Sucraflate (Antepsin™)	It is an aluminium salt of sulphated sucrose and is believed to bind preferentially to ulcers providing a protective layer. (Potts, Wilson et al. 2000)
Pharmacological	Antacids	Magnesium Trisilicate mixture Aluminium hydroxide	Provide short-term neutralization of stomach acid (British National Formulary 2005)
	H_2-Antagonists	Cimetidine (Tagamet™) Ranitidine (Zantac™) Famotidine (Pepcid™)	Block the histamine H_2 receptor on the acid producing parietal cells of the stomach, reducing acid secretion. (Vivian and Thompson 2000; British National Formulary 2005)
	Proton Pump Inhibitors (PPI's)	Omeprazole (Losec™) Esomeprazole (Nexium™) Lansoprazole (Zoton™) Pantoprazole (Protium™) Rabeprazole (Pariet™)	PPI's block the proton pump on the parietal cell which secretes hydrogen ions into the stomach contents thereby blocking acid secretion. PPI's can inhibit gastric secretion for up to 72 hours following a single dose. (Vivian and Thompson 2000; British National Formulary 2005)

Table 1.8. Treatment methods for gastro-oesophageal reflux disease (GORD).

1.7 Aims and objectives

GORD has been discussed. An alternative strategy to the current rafting agents would be a barrier on the oesophagus such that irrespective of the number or force of the reflux episodes, the oesophagus would remain protected. There has been a significant interest in this approach in recent years, however work has concentrated on the use of aqueous solutions of alginate (Batchelor, Banning et al. 2002; Batchelor, Dettmar et al. 2004; Tang, Dettmar et al. 2005; Tang, Dettmar et al. 2005; Tang, Dettmar et al. 2005) or suspensions of alginate within a water miscible vehicle (Richardson, Dettmar et al. 2004; Richardson, Dettmar et al. 2005).

It is proposed that xanthan gum could be used as a basis for this barrier formulation in combination with sodium alginate. By understanding the solution properties and phase behaviour of xanthan based biopolymer mixtures, it is hoped that modulation of these properties could be utilised in such a way that there might be controlled delivery to the desired site of action and an increase in the level of sodium alginate retention and also the thickness and quality of the barrier.

1.7.1 Principal aims

The principal aims of this project are:

1. To characterise the phase behaviour of biopolymer mixtures containing xanthan gum and sodium alginate.

2. To further understand the attributes associated with the phase behaviour of xanthan and alginate by the use of alternative biopolymers.

3. To investigate the use of xanthan based mixtures as a potential system for delivering high concentrations of polysaccharide, which could ultimately be used as an oesophageal barrier.

1.8 Thesis organisation

The following diagram illustrates the organization of this thesis

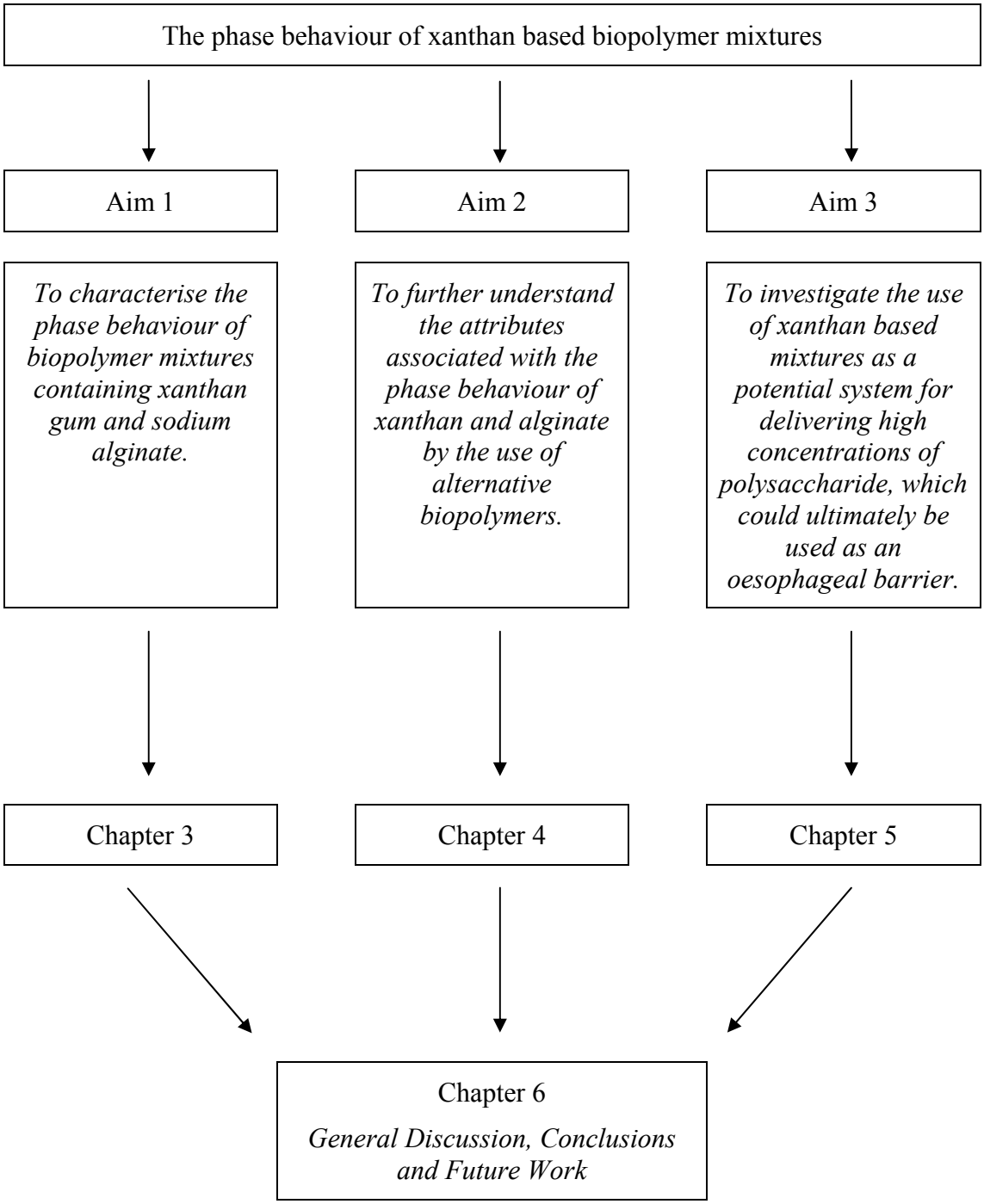

Chapter 2

Materials and methods

2.1 Materials

Details of the materials used in this study are included in the appendix 1.

2.2 Methods

2.2.1 Moisture determination

2.2.1.a Polysaccharides

It is well known that in their natural state polysaccharide samples contain significant moisture. As humidity change may cause fluctuations, and in order to prepare solutions on a dry weight basis, moisture contents were determined at intervals throughout the project. The ambient moisture content of the samples were determined in triplicate

using an MB45 moisture analyser balance (Ohaus, Leicester, UK). Samples (500 – 600 mg) were heated on disposable aluminium sample pans from ambient to 105^{o}C using a linear temperature ramp over 5 minutes and held at this temperature until there was less than a 1 mg change over 2 minutes. The endpoint was automatically determined by the apparatus. As a result of the lower moisture content of the methylcellulose samples, the heating ramp was reduced to 3 minutes to allow the sample to reach 105^{o}C before the endpoint was determined.

2.2.1.b Polyacrylate sodium

Polyacrylate samples were supplied as concentrated solutions and as the vapour of polyacrylate sodium (PAA) can be a respiratory system irritant, moisture determination using a moisture analyser was therefore unsuitable. These solutions were dried *in vacuo* over phosphorous pentoxide at room temperature until constant weight was achieved.

2.2.2 Preparation of stock solutions

As a result of the highly viscous nature of concentrated polysaccharide systems, all samples were prepared on a weight basis.

Solutions were prepared by dispersion of the polysaccharides in water down the side of a vortex created by an Ika-werke (Staufen, Germany) Eurostar 'Digital' overhead stirrer (Eurostar 'Power control visc' for high viscosity solutions) with a Jiffy® mixer blade. The Jiffy® blades were chosen as a result of their unique design which creates optimal mixing conditions without creating splashing or introducing air. The dispersions were then stirred at various speeds and lengths of time to assist hydration. Xanthan was dispersed at 1000rpm for 45 minutes; alginate was dispersed at 500rpm for 20 minutes. Other polysaccharides are discussed in their corresponding sections.

2.2.2.a Preparation of mixtures

Mixtures were prepared by combining the stock solutions, adding water as necessary and stirring at 1000rpm for 5 minutes. The mixtures were stored in the fridge overnight at 4^{o}C prior to any testing.

Where a series of mixtures contained an added excipient, this was added to the xanthan stock phase at the time of dispersion.

2.2.2.b Preparation of simulated gastric fluid

Simulated Gastric Fluid (SGF) without the inclusion of the enzyme component was prepared in accordance with the United States Pharmacopoeia (2005). Each litre of SGF contains 2g of sodium chloride and 7.0ml of concentrated hydrochloric acid (ACS grade).

2.2.3 Rheology

All rheological measurements were performed on a CVOR (Bohlin Instruments, Cirencester UK) digitally controlled stress rheometer. Unless otherwise stated rheological measurements were performed at 25 ± 0.1^{o}C. Temperature was controlled by a circulating water jacket system attached to a KTB 30 (Bohlin Instruments) water circulator.

2.2.3.a Sample loading

All samples were studied using a cone and plate (4^{o}/40mm) geometry with a 150µm gap. A new sample was used for each test run which had not been subject to any other

testing. To minimise any shear effects, samples were loaded carefully using a plastic spoon. Any excess sample was removed using a spatula to ensure accurate measurements (Figure 2.1). For measurements conducted above 25^{o}C a plastic cover with a solvent trap was fitted to the rheometer to prevent solvent evaporation and edge effects.

2.2.3.b Continuous shear rheology

Continuous shear measurements were performed to establish the effects of increasing shear on viscosity. Shear rates in the range of 0.01 - 1000s^{-1} were studied with an equilibrium period at each given shear rate of 30s where no data was collected followed by a measurement period of 30s. These parameters allowed the sample to reach steady state prior to measurements being taken to ensure good reproducibility.

2.2.3.c Dynamic oscillatory rheology - Amplitude sweep

An amplitude sweep was performed for each sample to establish the linear viscoelastic region. Samples were subjected to a stress sweep from 0.1 Pa to 5 Pa using a logarithmic scale generated by the instrument software.

2.2.3.d Dynamic oscillatory rheology - Frequency sweep

Frequency sweeps were performed from 0.1 - 3 Hz using 20 points on a logarithmic scale using a strain and stress value within the middle of the linear viscoelastic region obtained from the amplitude sweep (Figure 2.2). All measurements were performed in triplicate.

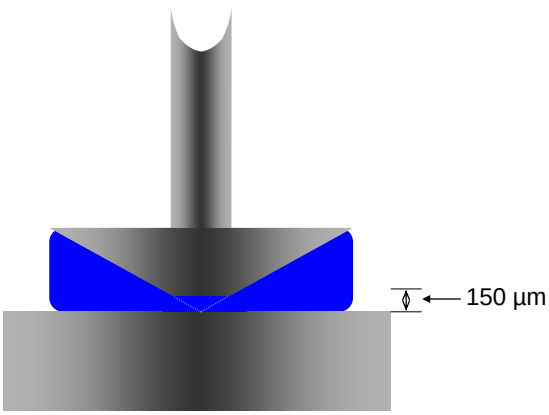

Figure 2.1. A cross section through a cone and plate (4°/40mm) geometry showing how a sample should be loaded.

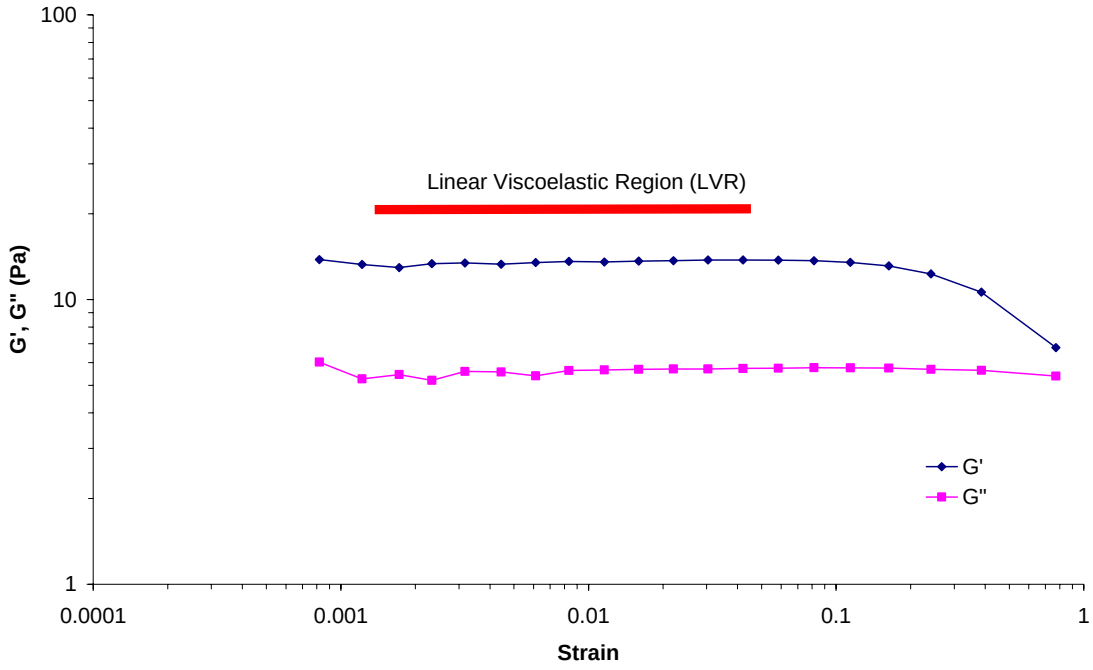

Figure 2.2 A typical example of a dynamic oscillatory amplitude sweep.
The sample tested was a mixture of 1% xanthan and 1.2% alginate.

2.2.4 Polyelectrolyte titration

Phase diagrams were established using a polyelectrolyte titration method. The Mütek PCD 03 (Carisbrooke Instruments, Woking, UK) apparatus measures streaming potential and neutralises the potential by titration against a counter charged polyelectrolyte which interacts in a stoichiometric ratio (Vernhet, Pellerin et al. 1996).

Stock solutions of xanthan, alginate and carboxymethylcellulose (0.1%) were prepared as previously described. From these a series of dilute solutions were prepared and used to calibrate the poly(diallyldimethyl ammonium chloride) (poly DADMAC, 0.001N) titration reagent. 10.00g aliquots of the polysaccharide solutions were titrated using an automatic Titrino (Metrohm, Buckingham, UK) device, against the poly DADMAC reagent in 0.1 ml additions every 10 seconds until the streaming potential was neutralised. The Mütek software calculated the point of zero charge. All readings were performed in triplicate using water as a reference.

Mixtures of xanthan (1%) and alginate (2% - 10%) or CMC (2% - 5%) were prepared as previously described. 12.00g aliquots were centrifuged (MSE Multex, 4000 rpm, 1 hour), and the supernatants weighed and analysed for moisture content as previously described. The supernatants were then diluted to contain approximately 0.01% dry polysaccharide mass, and analysed for charge. All readings were performed in triplicate.

2.2.5 Rapid Visco Analyser

The Rapid Visco Analyser (RVA, Newport Scientific) is an instrument normally associated with starch pasting experiments. The instrument consists of a thermal control enclosure into which a sample canister can be placed and a plastic paddle inserted. The paddle is designed to both measure the viscosity of the medium, and to also mix the

contents enabling process effects to be monitored. In this study the RVA is used to monitor the effects of dilution of systems with water and also the effects of temperature.

Each paddle used was zeroed using the RVA software prior to use, to reduce inter-paddle variation. 30.0g of sample was placed in the disposable metal canister, the paddle carefully inserted and transferred to the RVA. The viscosity of the sample was established at 4 second intervals at 200 rpm over a 10 minutes period. All samples were subject to a 30s equilibration period and experiments were conducted at 25 ± 0.5^{o}C unless otherwise stated.

Dilution was studied by adding the requisite amount of mixture to the sample canister followed by the appropriate amount of diluent, with care being taken not to effect mixing during the addition. In all cases the total weight of the mixture plus diluent was kept constant at 30.0g.

2.2.6 Microscopy

Samples were mounted on a standard glass microscope slide with a coverslip, and examined between crossed polarising lenses using a Leitz Diaplan microscope. The samples were viewed through a x1.25 magnification changer with a Leitz Wetzlar PL Fluotar 10/0.30 Phaco 1 objective lens. The images were recorded using a Nikon Coolpix 990 digital camera with an MDC lens fitting (0.82 – 0.29x) at maximum optical telephoto. The image scale was calibrated using a glass mounted graticule (1mm, 0.01 divisions; Graticules Ltd, Tonbridge, Kent, UK) slide at the same settings by image analysis software (Image Pro Plus v.4.1, Media Cybernetics).

Chapter 3

The solution properties of mixtures of xanthan gum and sodium alginate

3.1 Introduction

The scientific literature relating to xanthan gum and sodium alginate has been described in chapter 1. It is interesting to note that although both of these hydrocolloids have found extensive uses in their own right, there is very little reported use in combination. No recorded studies were found in the mainstream scientific literature.

3.2 Aims

This chapter will examine the physical properties of aqueous mixtures of xanthan and alginate. It will specifically examine:

1. The consequences of mixing xanthan gum with sodium alginate.
2. The phase behaviour of xanthan/alginate mixtures.
3. The effects of adding ionic species into these mixtures.
4. The effects of adding non-ionic species.

3.3 Materials and methods

3.3.1 Materials

The details of all the materials used are listed in Appendix 1

3.3.2 Preparation of concentrated polysaccharide solutions

Solutions were prepared by dispersion of the requisite amount of powder in water. A large surface area vortex was created using an Ika-Werke Eurostar Digital (Staufen, Germany) overhead stirrer using a Jiffy™ stirrer blade. The powder was added down the side of the created vortex. Xanthan gum was dispersed at 1000 rpm for 45 minutes, sodium alginate at 500 rpm for 20 minutes

All powders were analysed for moisture content as described in section 2.2.1, and weighings were made on a dry weight basis. Unless otherwise stated, the sodium alginate used for the experiments was Protanal® LFR5/60 (35kDa, 64% Guluronate).

3.3.3 Preparation of mixtures

Mixtures were prepared by the combination of concentrated stock solutions, adding water as necessary to achieve the desired concentrations. These were then stirred at 1000 rpm for 5 minutes to effect mixing. All mixtures were allowed to stand overnight at 4^{o}C prior to testing.

3.3.4 Centrifugation of samples to analyse separate phase components

Centrifugation was employed to separate the individual phases within the mixture to allow analysis, as these can show widely differing properties.

100g of sample was centrifuged in an MSE Multex (Beckenham, Kent, UK) centrifuge at 4000rpm for 1 hour. The supernatant was decanted taking care not to disturb the lower phase. The remaining lower phase was centrifuged for a further hour and any additional supernatant decanted.

3.3.5 Rheological analysis - Viscometry

The continuous shear properties of hydrocolloid mixtures were measured using a 4^{o}/40mm cone and plate geometry on a CVOR digital controlled stress rheometer (Bohlin Instruments, Cirencester UK). Samples were thermally equilibrated at 25 ± 0.1^{o}C for 1 minute and then analysed at a number of defined shear rates. Each shear rate was subject to an equilibration delay time of 30 seconds (no measurement taken by the instrument) followed by an integration time of 30 seconds.

Where samples were monitored over an extended time period a fresh sample was used for each measurement. The samples were stored at 4^{o}C between readings.

3.3.6 Rheological analysis – Dynamic oscillation

Viscoelastic properties were analysed as described in section 2.2.3 using a 4^{o}/40mm cone and plate geometry at 25 ± 0.1^{o}C.

3.3.7 Differential scanning calorimetry (DSC)

Experiments were undertaken using a Seteram Micro-DSC III (Caluire, France). 600mg of test sample was placed into a sealed DSC pan and measured against 600mg of water in a sealed reference pan. Samples were cooled from ambient to 5^{o}C then heated at 1^{o}C/minute to 90^{o}C. The samples were then cooled back to 25^{o}C at the same rate.

3.3.8 Fluorescent labelling of hydrocolloids

Confocal laser scanning microscopy was used to establish the spatial distribution of the biopolymers in solution. The fluorescent tagging was achieved by covalently linking a fluorescein derivative, fluoresceinamine (Mw = 347) using a test method supplied by Reckitt Benckiser (Healthcare) UK Ltd. (Strugala 2003). This method yields a theoretical substitution level of 1 labelled carboxylate group to every 250 carboxylate groups available.

A stock solution of fluoresceinamine was prepared by dissolving 35.43mg of fluoresceinamine in 1ml of N,N-dimethylformamide (DMF). This was stored at 4^{o}C until used.

1g of hydrocolloid was dissolved using an overhead stirrer in 200ml (300ml for xanthan gum) of deionised water until dissolved. The pH (Inolab pH level 1 meter, WTW Wissenschaftlich-Technische Werkstätten GmbH, Weilheim Germany) was noted and then adjusted to 4.75 using 0.1M HCl or 0.01M NaOH. 100mg of 1-ethyl-3-(3-dimethylaminopropyl) carbodiimide (EDAC) was added followed by 200µl fluoresceinamine (5-aminofluorescein) stock solution. The solution was stirred on ice for 30 minutes the pH then readjusted to 4.75 and a further 100mg of EDAC added. After further 30 minutes stirring the solution was readjusted to pH 4.75 and left to stir on ice for 6 hours. The solution was stored overnight in the fridge.

The following day the solution was readjusted to the originally recorded pH, placed in dialysis sacks (Mw cut off 12-14 kDa) and dialysed against deionised water until no absorbance was seen at λ-max (490nm) in the dialysate.

The labeled biopolymers were frozen to -80^{o}C and freeze dried using a Super Modulyo (BOC Edwards, Crawley UK) freeze dryer until no further ice formation was observed in the collection area (3 - 4 days). Throughout the drying process the freeze drying chamber was enshrouded in a heavy duty black plastic bag to protect the labeled biopolymers from light. The dried biopolymers were then placed in an airtight container and kept in the fridge until required.

3.3.9 Confocal microscopy

Concentrated stock solutions of 2% xanthan, 8% alginate, 2% fluorescently tagged xanthan (as described in section 3.3.7) and 2% fluorescently tagged alginate were prepared using the dispersion technique described in section 2.2.2. Two fluorescent mixtures were prepared by combining appropriate amounts of the concentrated biopolymer solutions. The fluorescent xanthan mixture was prepared to contain 0.1% fluorescently labeled xanthan, 0.9% unlabelled xanthan and 4% unlabelled sodium alginate. The fluorescent alginate mixture contained 1% unlabelled xanthan gum, 0.1% labeled alginate and 3.9% unlabelled alginate. Both mixtures were fully stirred at 1000 rpm for 5 minutes.

Fluorescence images were obtained using a BioRad MRC-600 confocal microscope (BioRad, Hemel Hempstead, UK) equipped with a 15 mW Krypton Argon laser and a Nikon Optiphot upright microscope. Images were acquired at Ex488/Em510 nm using a BHS filter block. Black level was standardised at a pixel intensity of 5 (on a scale of 0-255) and the gain was set to provide an image as bright as possible without saturation. Confocal aperture was set at 2 and the objective used was a Plan 4/0.13NA air lens (Nikon, UK).

3.4 Results and discussion

3.4.1 Viscometric characterisation of xanthan and alginate solutions

The relationship between apparent viscosity and shear rate for a 1% xanthan gum solution, a 5% sodium alginate LFR 5/60 solution and a 1% xanthan gum:5% sodium alginate mixture is shown in Figure 3.1. The pseudoplastic behaviour typical of xanthan solutions was clearly seen, whereas the sodium alginate solution exhibited the marked insensitivity to shear rate indicative of Newtonian behaviour which is unusual as alginates have been reported to exhibit moderate pseudoplasticity (Clare 1993). Newtonian behaviour is most probably as a result of the low molecular weight of the alginate used (35 kDa). The mixture showed a viscosity profile midway between that of the two components. This would suggest the properties of the mixture are as a result of a mutual dilution effect.

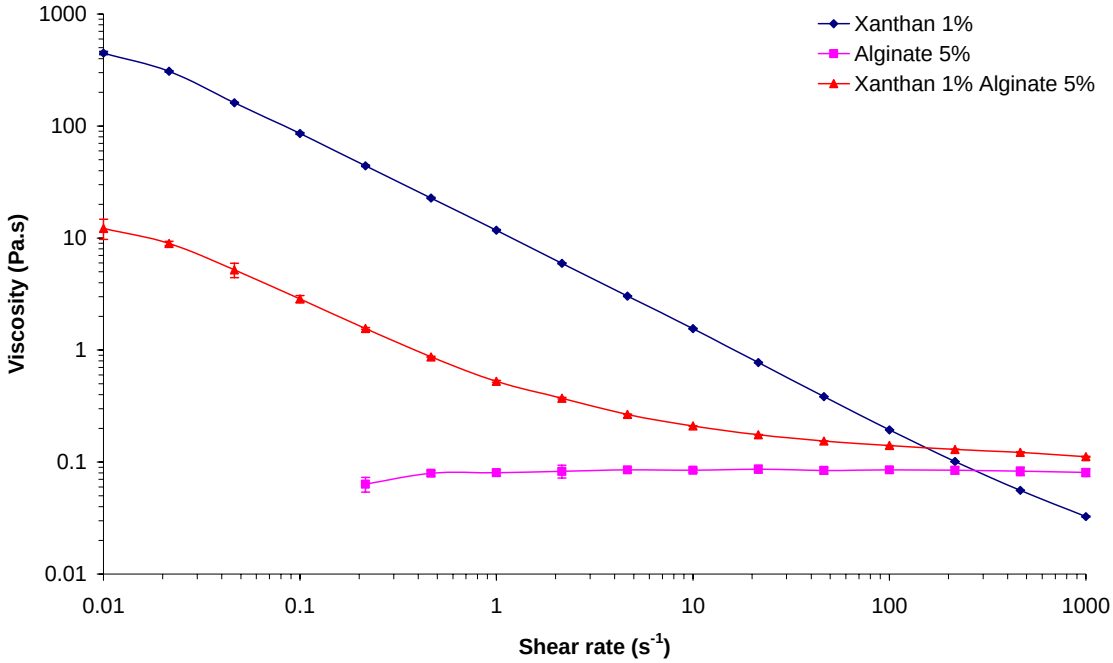

Figure 3.1. Continuous shear viscosity profiles of a mixture of 1% xanthan and 5% sodium alginate LFR 5/60 in comparison with the individual components.
Geometry CP 4°/40mm. 25 ± 0.1°C. Delay time and integration time at each shear rate were 30s each. Mean ± SD, n=3

3.4.2 Viscometric characterisation of xanthan gum and sodium alginate mixtures

Figure 3.2 shows the viscosity profiles of mixtures containing 1% xanthan gum with a range of sodium alginate concentrations from 0 to 5%. At alginate concentrations up to 1%, the behaviour was substantially xanthan-like, but between 2% and 5% alginate a different viscometric profile was seen. At low shear rates viscosity was substantially reduced, whereas at high shear rates viscosity appeared to increase with increasing alginate concentration. The 1.5% alginate solution exhibited intermediate behaviour.

The low ($0.1s^{-1}$) and high ($1000s^{-1}$) shear viscosities of the mixtures are shown in Figure 3.3a and Figure 3.3b respectively. Figure 3.3a shows that at low concentrations of alginate (<1%) there was little change in viscosity whereas between 1% and 2% there was a marked drop in viscosity of almost two orders of magnitude. Thereafter the viscosity remained at a low level. Conversely Figure 3.3b shows there was a steady increase in viscosity with increasing alginate concentration.

Figure 3.2 and Figure 3.3a would suggest that a specific event occurs within the range of 1% to 2% added alginate. In contrast to this, Figure 3.3b might suggest that there is an additive effect.

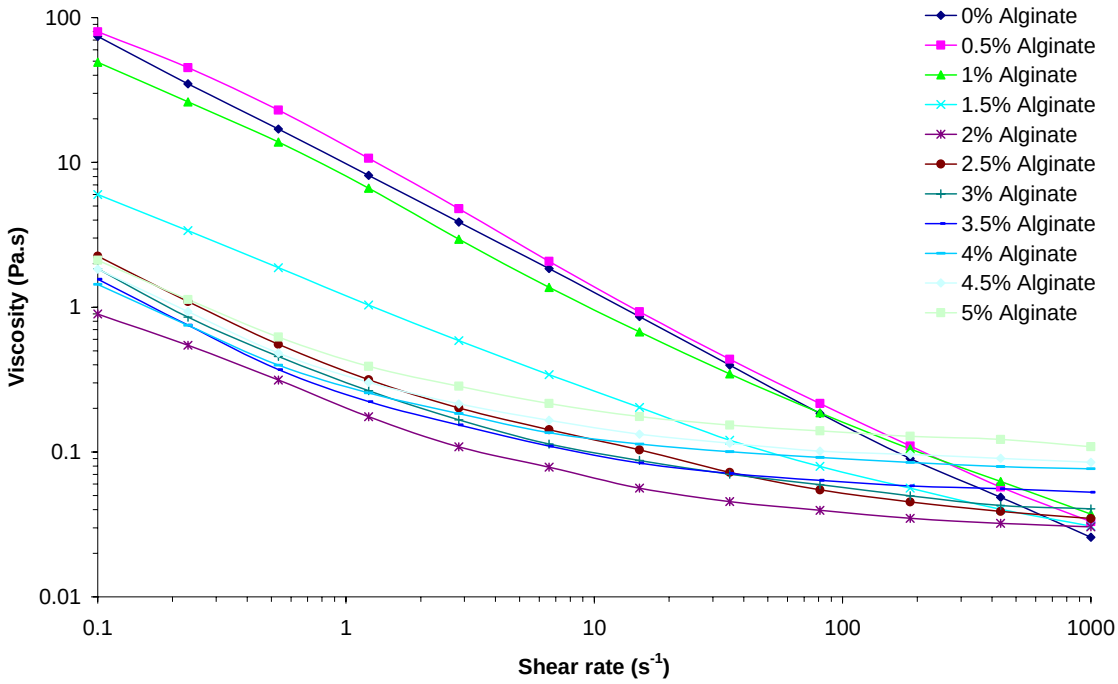

Figure 3.2. Continuous shear viscosity profiles of mixtures containing 1% xanthan with varying concentrations of alginate.
Geometry CP 4°/40mm. 25 ± 0.1°C. Delay time and integration time at each shear rate were 30s each. Mean ± SD, n=3

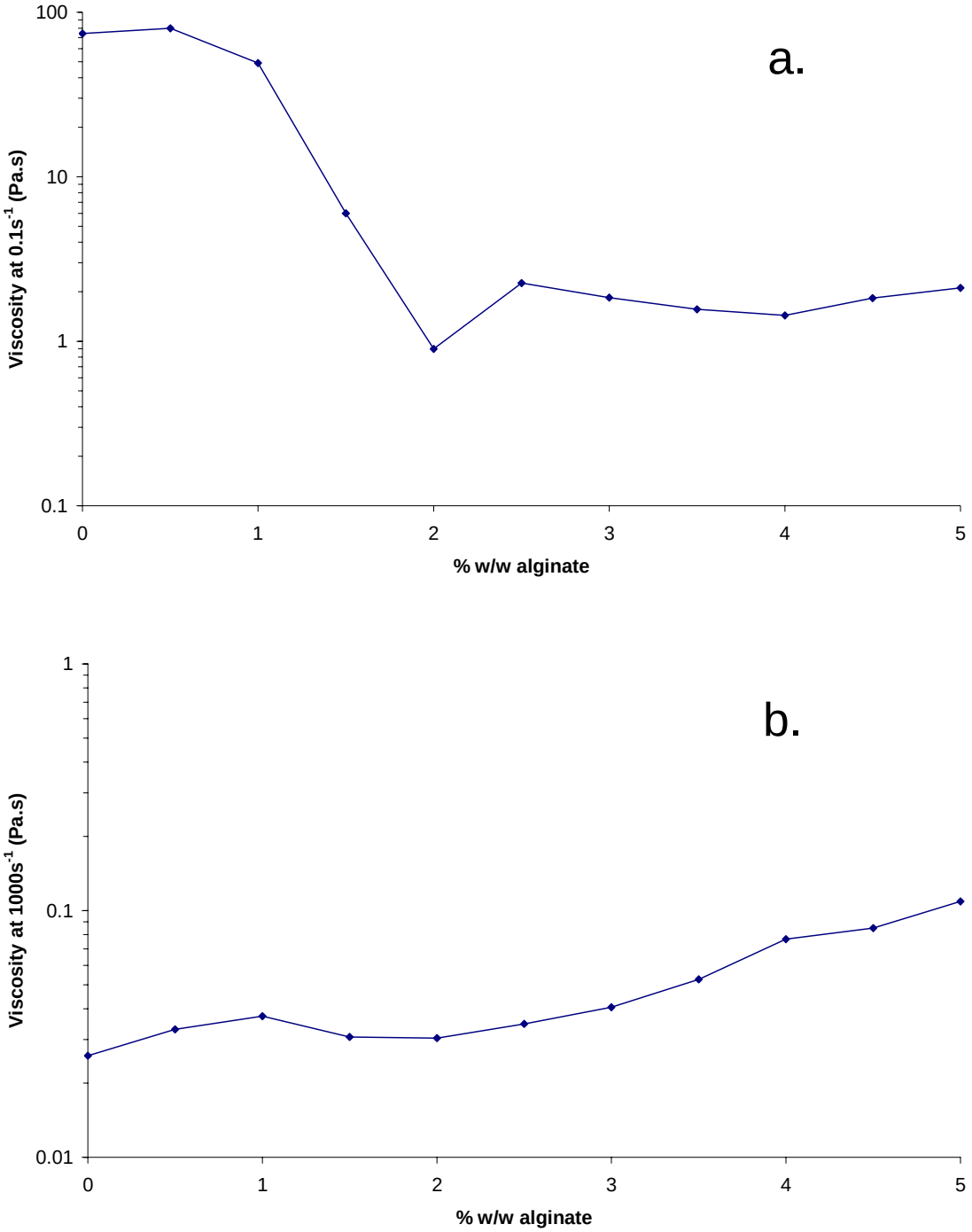

Figure 3.3. The continuous shear viscosity of mixtures containing 1% xanthan and various concentrations of alginate at (a) low ($0.1s^{-1}$) and (b) high ($1000s^{-1}$) shear rate.
Geometry CP 4^{o}/40mm. 25 ± 0.1^{o}C. Delay time and integration time at each shear rate were 30s each. Mean ± SD, n=3

3.4.3 Viscoelastic characterisation of xanthan gum and sodium alginate mixtures

Whilst all measurements provide valuable data with respect to changes in solution properties, the rheological technique of dynamic oscillatory shear rheology can provide information about how energy from small oscillations applied to sample is recovered or dissipated, and hence provide information with respect to the internal structure of samples.

The viscoelastic properties of mixtures of 1% xanthan with 0 – 5% sodium alginate were measured. Figure 3.4 shows the elastic modulus (G') values of the mixtures with respect to frequency. Addition of 0.5% alginate had little effect on G' whereas amounts of 1% or greater resulted in a reduction in G' values almost to zero.

Figure 3.5 shows the different values of G' at a single frequency (1.02 Hz), for ease of comparison. This figure shows a marked similarity to Figure 3.3a. At low concentrations of added alginate (<0.5%) there was little change in G'. The addition of 0.5% - 1.5% showed a dramatic reduction in G' values to less than 10% of that with no alginate present. Higher concentrations of alginate (>2%) did not alter the value of G' further.

The viscoelastic profiles of a 1% xanthan solution and a mixture of 1% xanthan and 5% alginate are shown in Figure 3.6. In the case of 1% xanthan gum the values of G' are significantly greater than G" at all frequencies examined, and both parameters increase proportionally with frequency; behaviour indicative of a weak-gel like system (Ross-Murphy 1995). However in the xanthan gum:sodium alginate mixture G' was greater than G" at the lower frequencies whereas above 0.35 Hz the mixture was G" dominant. Values of both G' and G" are reduced by almost two orders of magnitude in the mixture to values indicating essentially non-viscous properties. A solution of 5% sodium

alginate was also tested but values of G' and G" were too small for the instrument to measure.

This data strongly supports the previous finding that a dramatic change occurs when alginate content is increased above a threshold concentration, and this is clearly not a simple averaging effect (of the viscosity of xanthan and the viscosity of alginate), as a more gradual change would be observed. Mixtures containing high concentrations of alginate appear to show weak viscoelastic properties similar to that of alginate solutions.

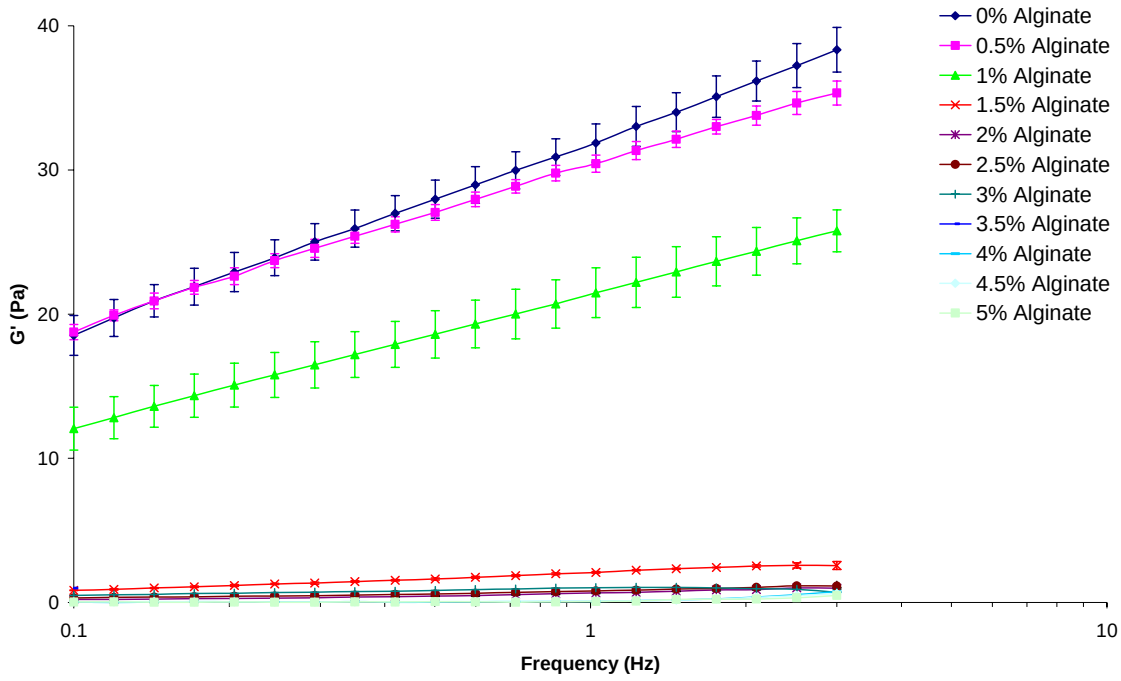

Figure 3.4. The elastic modulus of mixtures containing 1% xanthan gum and varying amounts of sodium alginate LFR 5/60.
Geometry CP 4°/40mm. 25 ± 0.1°C. Mean ± SD, n=3

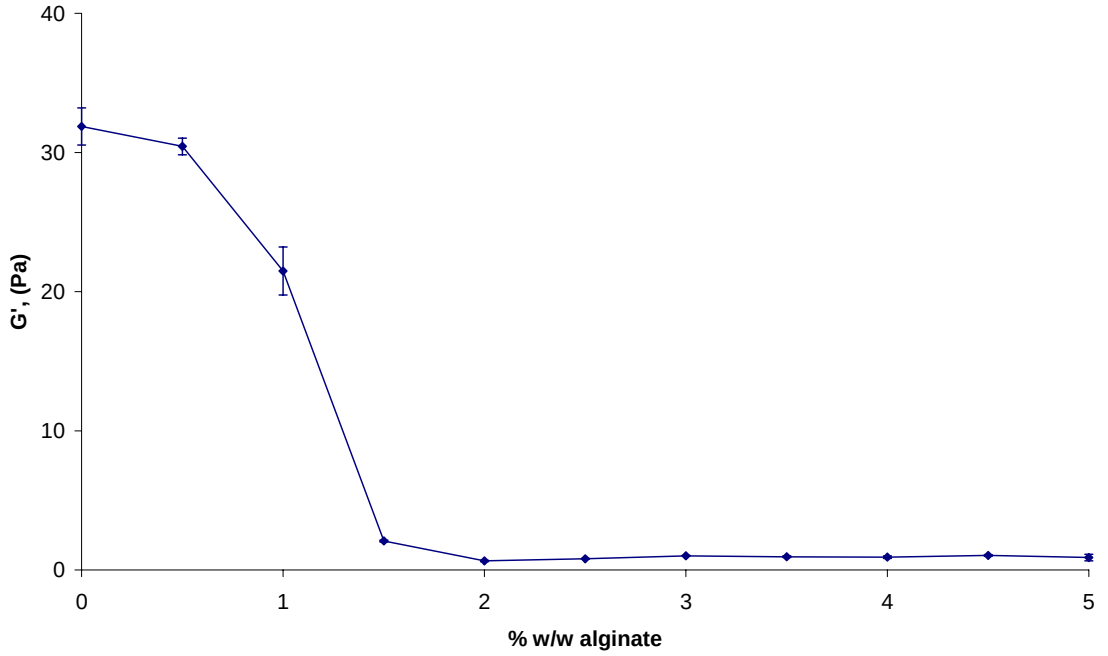

Figure 3.5. The elastic modulus of mixtures containing 1% xanthan gum and varying amounts of sodium alginate LFR 5/60 at a single frequency.
Geometry CP 4°/40mm. 25 ± 0.1°C. Frequency 1.02Hz Mean ± SD, n=3

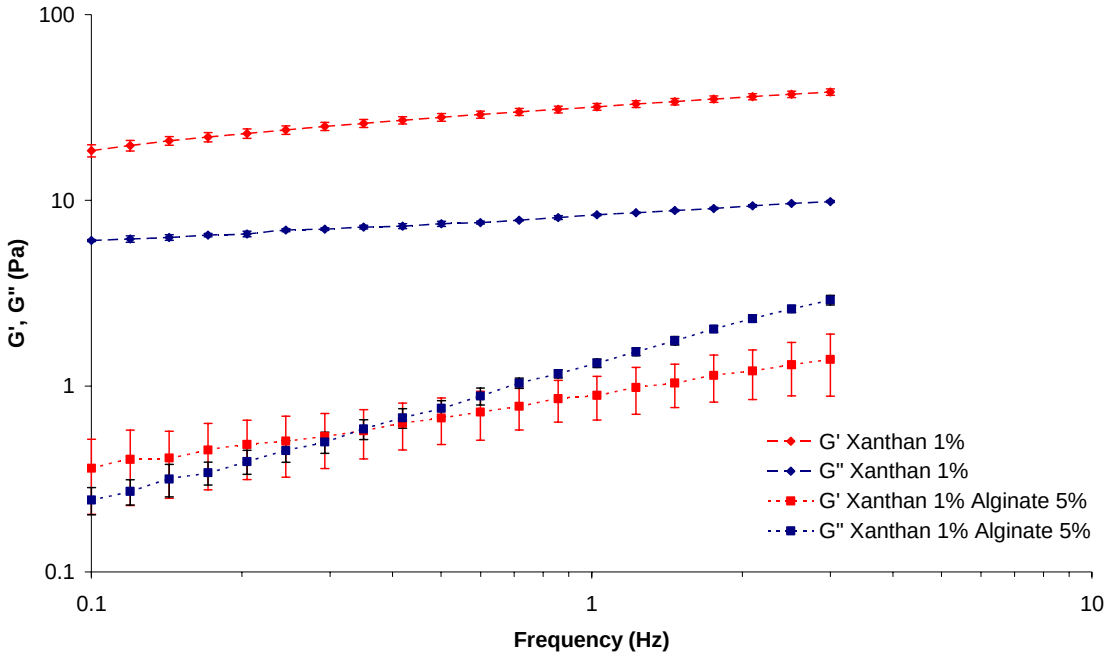

Figure 3.6. The viscoelastic properties of a 1% xanthan solution and a mixture containing 1% xanthan with 5% alginate.
Geometry CP 4°/40mm. 25 ± 0.1°C. Mean ± SD, n=3

3.4.4 Microscopy of mixtures of xanthan and alginate

Light microscopy is often employed in mixed systems to investigate phase behaviour most notably in emulsion systems. Figure 3.7 shows crossed polarised, light microscopy images of a 1% xanthan gum solution, a 5% sodium alginate solution, and a 1% xanthan:5% alginate mixture. The individual hydrocolloid solutions showed a dark image with no light transmission whereas images of the mixture showed birefringent white strand-like mesophases on a dark background. The strands varied in size and appeared to be 4-20μm in width.

The presence of these strand-like structures showed that the sample was heterogeneous and similar effects have been observed in high concentration xanthan systems. The low viscosity and existence of these mesophases suggest that in the mixture, the xanthan is being concentrated in these strand-like areas.

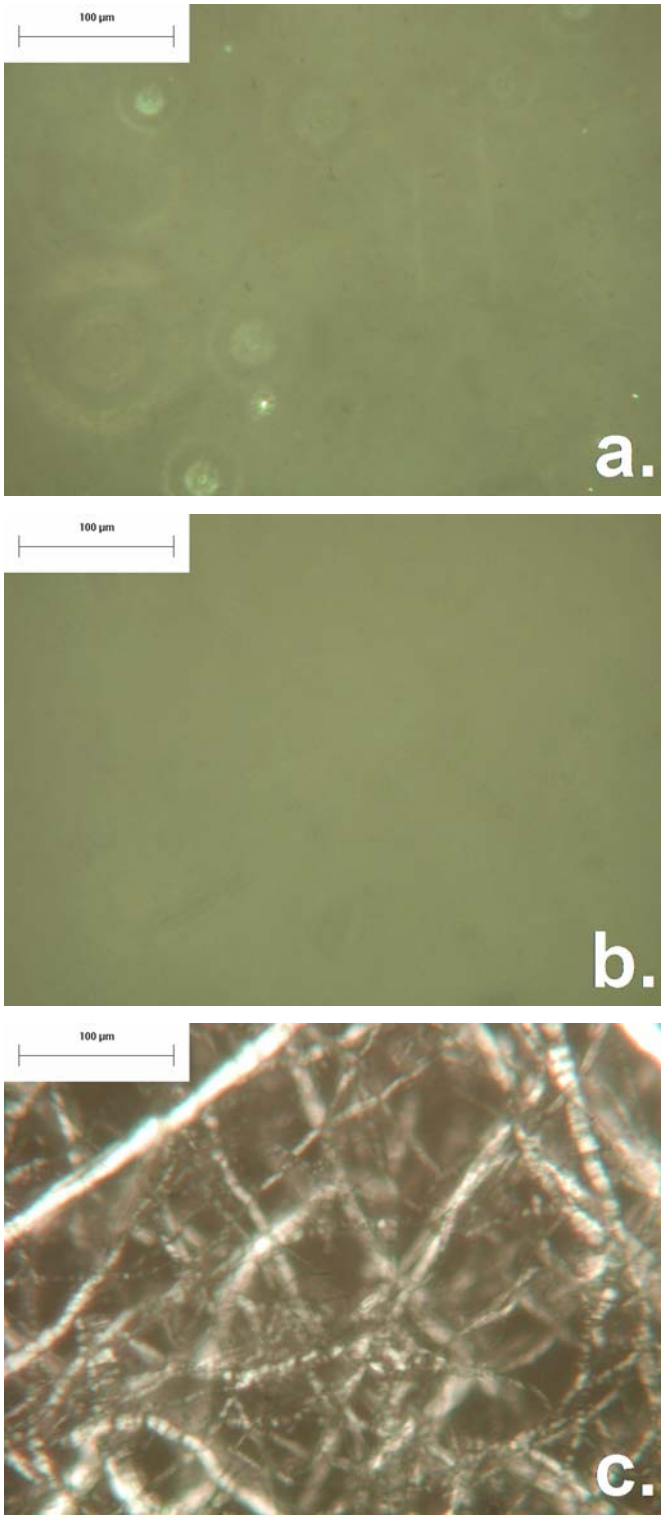

Figure 3.7. Light microscope images viewed between crossed polarizing lenses of a sample of (a) 1% xanthan, (b) 5% alginate and (c) a mixture containing 1% xanthan with 5% alginate.

3.4.5 Centrifugation of mixtures of xanthan and alginate

Figure 3.8 shows centrifuge tubes containing 1% xanthan gum, 5% sodium alginate and a mixture of 1% xanthan gum and 5% sodium alginate after centrifugation at 4000 rpm for 1 hour. The xanthan and alginate solutions were unaffected, but the mixture clearly separated into two distinct phases. The upper phase appeared to have a slight brown tint similar to that of the 5% sodium alginate solution suggesting the presence of alginate in the upper phase. Figure 3.9 shows images of the individual phases under crossed polarised light. Only the lower phase showed a significant degree of birefringence.

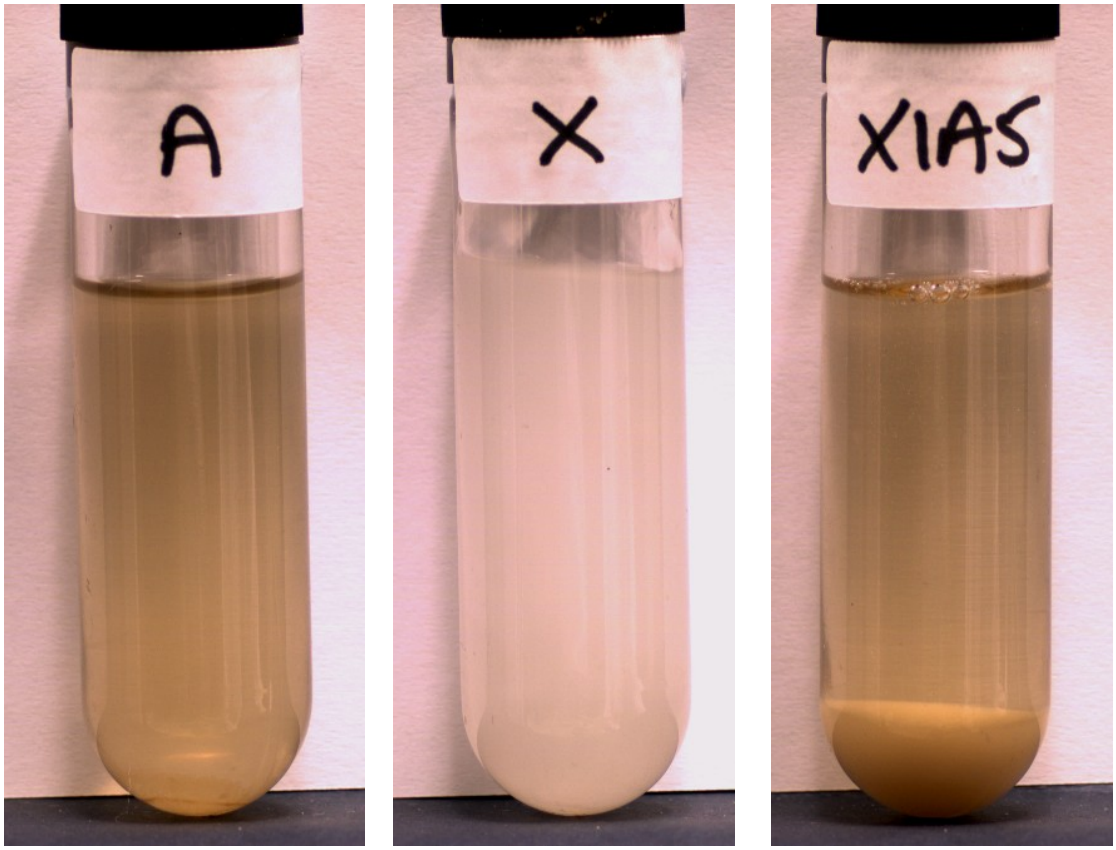

Figure 3.8. Tubes containing (A) 5% alginate, (X) 1% xanthan and a (X1A5) 1% xanthan:5% alginate mixture after centrifugation for 1 hour at 4000rpm.

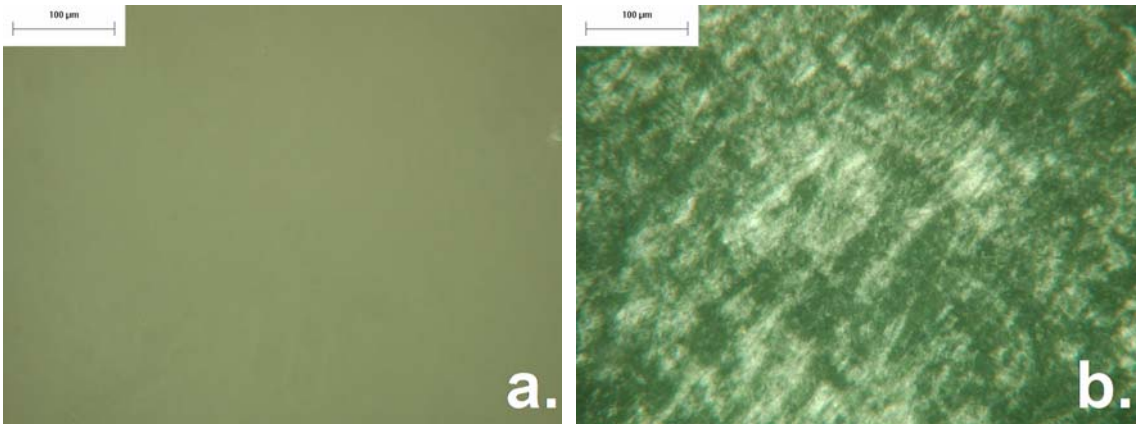

Figure 3.9. Crossed polarized light images of the (a) upper supernatant phase and (b) the lower phase extracted from the centrifuged sample of 1% xanthan and 5% alginate shown above.

3.4.6 The rheological properties of the individual phases

A mixture of 1% xanthan gum and 5% sodium alginate was centrifuged as described in section 3.3.4. Continuous shear and viscoelastic measurements were made on each of the phases.

The continuous shear profiles of the upper and lower phases of the centrifuged mixture with respect to the shear profiles of the individual biopolymers and the uncentrifuged mixture are shown in Figure 3.10. The upper phase showed Newtonian behaviour similar to that of the 5% alginate solution. The lower phase showed high viscosity at low shear rates and marked pseudoplasticity and was similar in appearance to that of 1% xanthan, with the exception that at all shear rates the viscosity was an order of magnitude higher.

The similarity in behaviour of the upper phase to that of the alginate solution suggests that the upper phase is predominantly composed of alginate. Likewise the viscosity profile of lower phase showed marked similarity to that of xanthan and suggests that the lower phase is predominantly xanthan. The magnitude of the viscosities at each shear rate are notably greater for the lower phase when compared with that of the 1% xanthan solution, and it is possible that the xanthan in the lower phase is concentrated to greater than 1%.

The viscoelastic properties of the lower phase in comparison with xanthan and the xanthan and alginate mixture are shown in Figure 3.11. The upper phase had no measurable viscoelastic properties, and therefore is not included. The behaviour of the lower phase parallels that of 1% xanthan with G' being greater than G" at all frequencies and both moduli showing a slight frequency dependence. The magnitude of the values for G' and G" were significantly higher for the lower phase, and would suggest that the lower phase is principally composed of a higher concentration of xanthan.

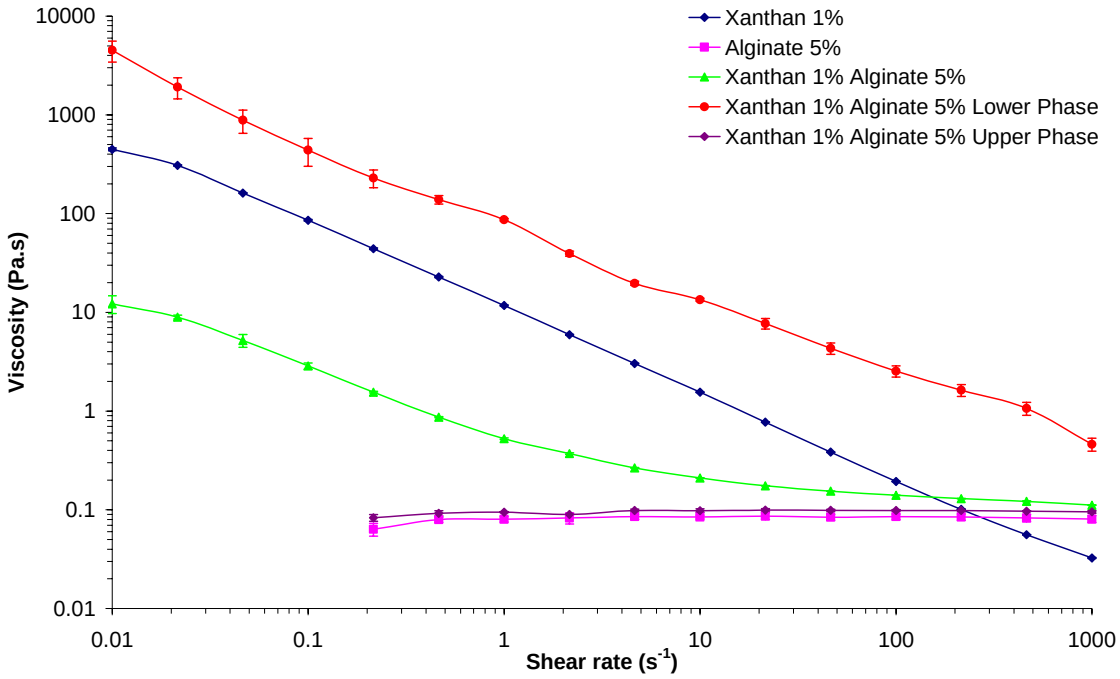

Figure 3.10. The continuous shear viscosity profiles of a mixture of 1% xanthan and 5% alginate, before and after centrifugation and decantation relative to the individual biopolymer solutions.
The individual phases were measured by separating the phases following centrifugation. Geometry CP 4°/40mm. 25 ± 0.1°C. Mean ± SD, n=3.

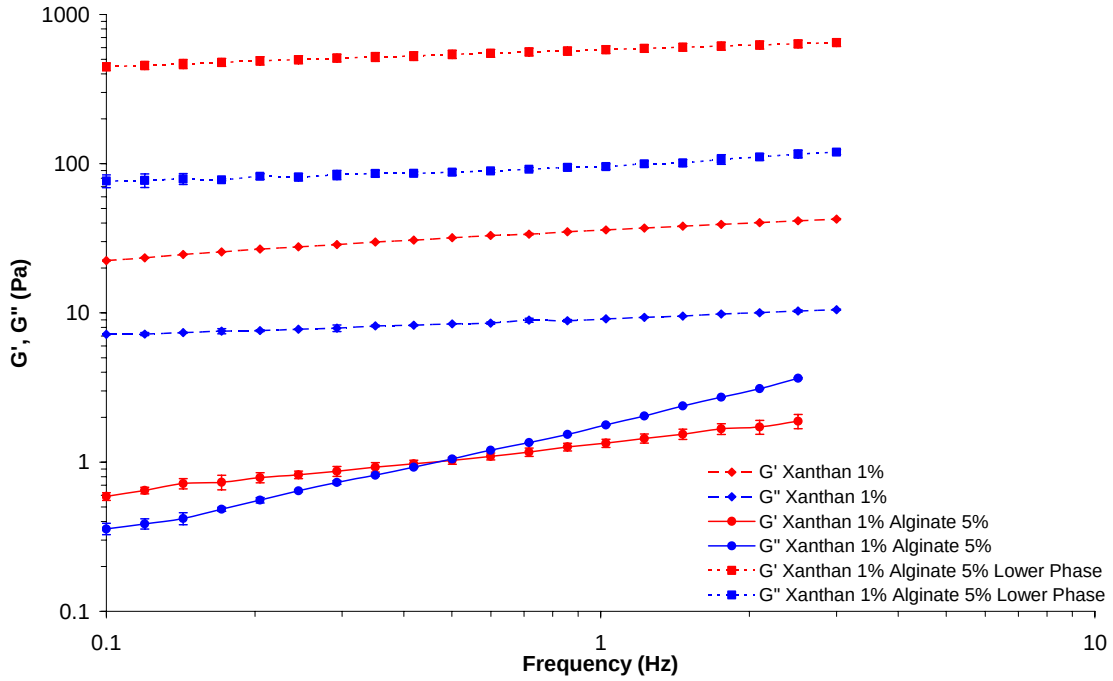

Figure 3.11. The viscoelastic profile a mixture of 1% xanthan and 5% alginate before and after centrifugation and decantation relative to the individual biopolymer solutions.
The individual phases were measured by separating the phases following centrifugation. 5% alginate and the upper phase of the mixture are not shown as they do not have any measurable viscoelastic properties. Geometry CP 4°/40mm. 25 ± 0.1°C. Frequency 1.02Hz Mean ± SD, n=3.

3.4.7 The effect of varying xanthan and alginate concentration in the xanthan/alginate mixtures

Previous experiments have shown that at 5% sodium alginate, mixtures of xanthan gum and sodium alginate undergo phase separation. This section examines more closely the effect of sodium alginate and xanthan gum concentration on the phase separation phenomenon.

Figure 3.12 shows the changing viscoelastic properties of mixtures of 1% xanthan gum and sodium alginate with respect to sodium alginate concentration. Low concentrations (<0.75%) had little effect, with G' remaining greater than G". Increasing sodium alginate concentrations from 0.75% to 1.5% resulted in a marked decrease in G' and G", with values falling almost to zero. Higher concentrations of alginate elicited little further change.

The corresponding crossed polarized microscopy images from these samples are shown in Figure 3.13. The images of 1% xanthan and 1% xanthan:1% alginate mixture showed no birefringence. Increasing alginate concentration to 1.2% revealed indistinct areas of birefringence, whereas at 1.4% evidence of structure began to emerge. At 2% alginate clear strand-like structures were observed at the 5% alginate concentration.

These figures show that as the viscoelastic properties of the mixtures start to decrease, the birefringent areas emerge, and this suggests that the strand appearance is linked to the observed changes in rheological properties.

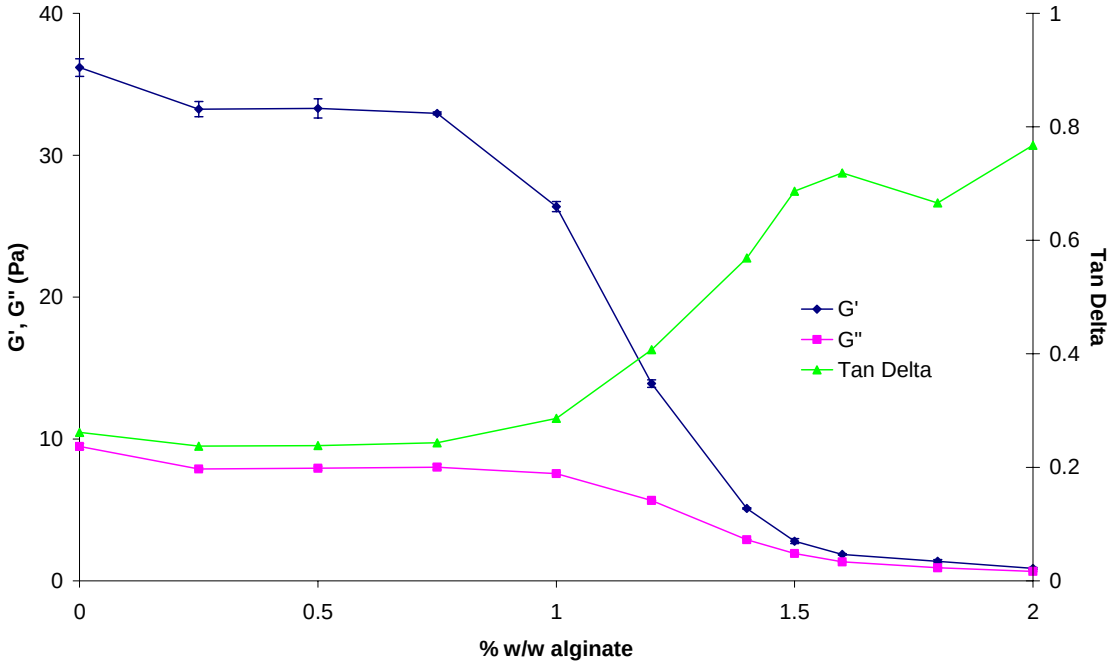

Figure 3.12. The viscoelastic profile of mixtures of 1% xanthan with varying concentrations of alginate.
Geometry CP 4°/40mm. 25 ± 0.1°C. Frequency 1.02Hz Mean ± SD, n=3.

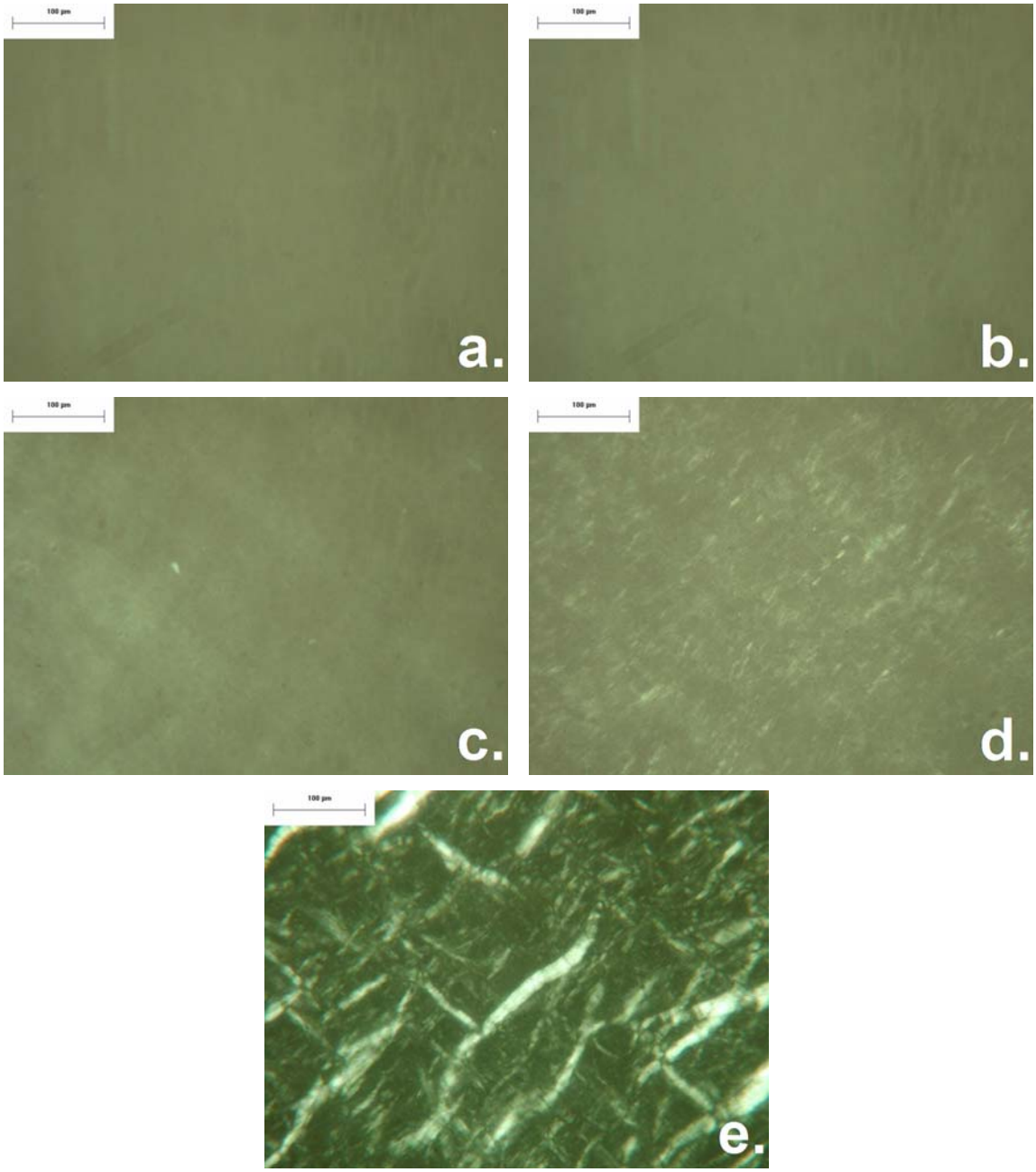

Figure 3.13. Microscope images taken of samples between crossed polarizing lenses of mixtures of 1% xanthan gum and varying amounts of sodium alginate.
(a) 1% Xanthan, (b) 1% xanthan 1% alginate, (c) 1% xanthan 1.2% alginate, (d) 1% xanthan 1.4% alginate, (e) 1% xanthan 2% alginate.

Figure 3.14 shows the viscoelastic profiles of mixtures containing 0.5% xanthan gum and 0 - 2% sodium alginate. The graph was similar in shape to that shown in Figure 3.12 with the mixtures containing 1% xanthan. G' is greater than G", and values remain unchanged until a concentration of 1% alginate was reached after which there was a significant decrease in both G' and G". At concentrations of alginate greater than 1.5% the viscoelastic properties reached values below the limits measurable by the instrument.

The viscoelastic profile for mixtures containing 2% xanthan gum is shown in Figure 3.15. The shape exhibited is similar to that shown in Figure 3.12, and showed the decrease in G' with increasing alginate concentration but with a gradual change in G' and G" over a wider range of alginate concentrations between 0.25% and 2%.

Figure 3.12, Figure 3.14 and Figure 3.15 have shown that separation occurs over a range of xanthan concentrations which may be as a result of polysaccharide polydispersity (Albertsson 1986).

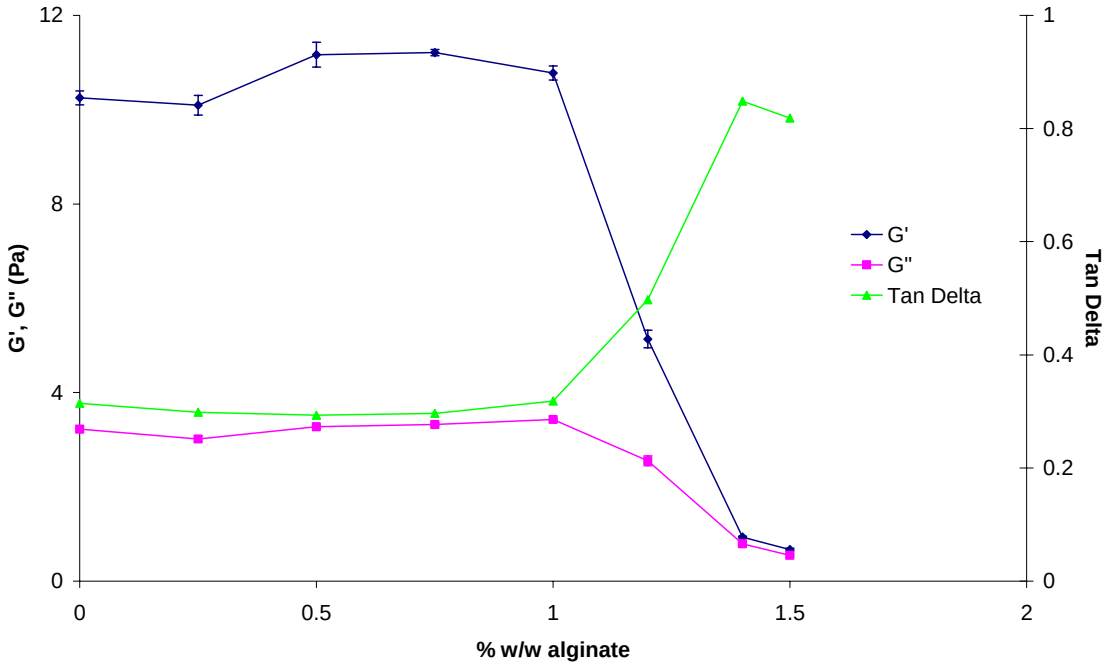

Figure 3.14.The viscoelastic profile of mixtures of 0.5% xanthan with varying concentrations of alginate.
Geometry CP 4°/40mm. 25 ± 0.1°C. Frequency 1.02Hz Mean ± SD, n=3.

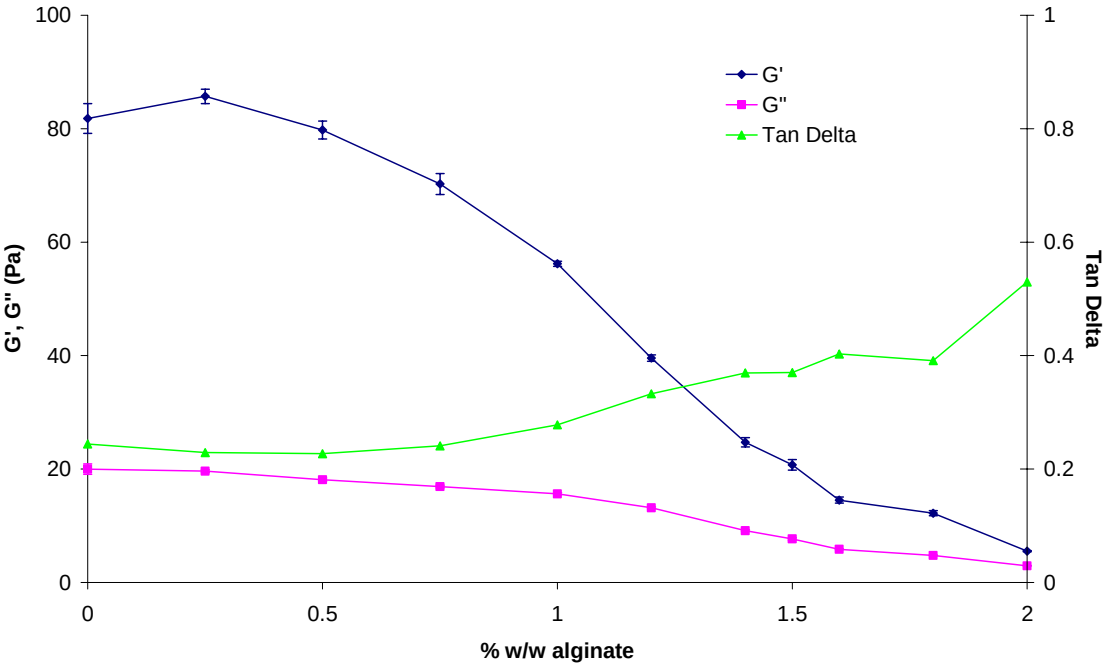

Figure 3.15.The viscoelastic profile of mixtures of 2% xanthan with varying concentrations of alginate.
Geometry CP 4°/40mm. 25 ± 0.1°C. Frequency 1.02Hz Mean ± SD, n=3.

3.4.8 Establishment of a phase diagram for mixtures of xanthan and alginate

Phase diagrams provide key information with respect to understanding how a separating system functions and how changes to the system may affect the separation phenomena. The phase diagram for xanthan gum/sodium alginate mixtures was established using a polyelectrolyte titration method. The Mütek PCD03 particle charge determination apparatus has historically been used in the paper industry for measuring surface charge, but recently has been used for the analysis of hydrocolloids in solution (Vernhet, Pellerin et al. 1996), in which one charged polymer is titrated against another oppositely charged polymer in a stoichiometric ratio.

The standard curves for the titration of Poly DADMAC against xanthan gum and sodium alginate are shown in Figure 3.16. Both curves show good linearity. The slopes show that the charge ratio (number of charges per sugar residue) xanthan:alginate is approximately 1.5:5 by weight. This would be in agreement to the 50% level of pyruvation often quoted as being typical for xanthan gum (Kang and Pettitt 1993).

Using the charge ratio obtained from the standard curves, and the mass of dry matter in a given sample, it is possible to obtain equations 3.1 and 3.2 respectively, where V is the volume of titrant required to neutralise the charge; X is the mass of xanthan in the sample; A is the mass of alginate in the sample; T is the total dry polysaccharide mass in the sample.

$$V = 1.463X + 5.095A \tag{3.1}$$

$$T = X + A \tag{3.2}$$

Substituting equation 3.2 into 3.1 gives one unknown and therefore allows the mass of either or both of the polysaccharides to be found.

The ternary phase diagram for xanthan, alginate and water constructed from values obtained from the polyelectrolyte titration method is shown in Figure 3.17. The dotted line represents an interpretation of where the binodal line might sit. The shape is indicative of a segregative separation system (Bergfeldt, Piculell et al. 1996), however asymmetric in appearance. The phase diagram shows that there is no xanthan in the disperse phase, this reinforces the inferences from both the microscopy and the rheology of the individual phases. Likewise the lower phase is predominantly a highly concentrated xanthan phase which explains the extensive birefringence and pseudoplasticity observed.

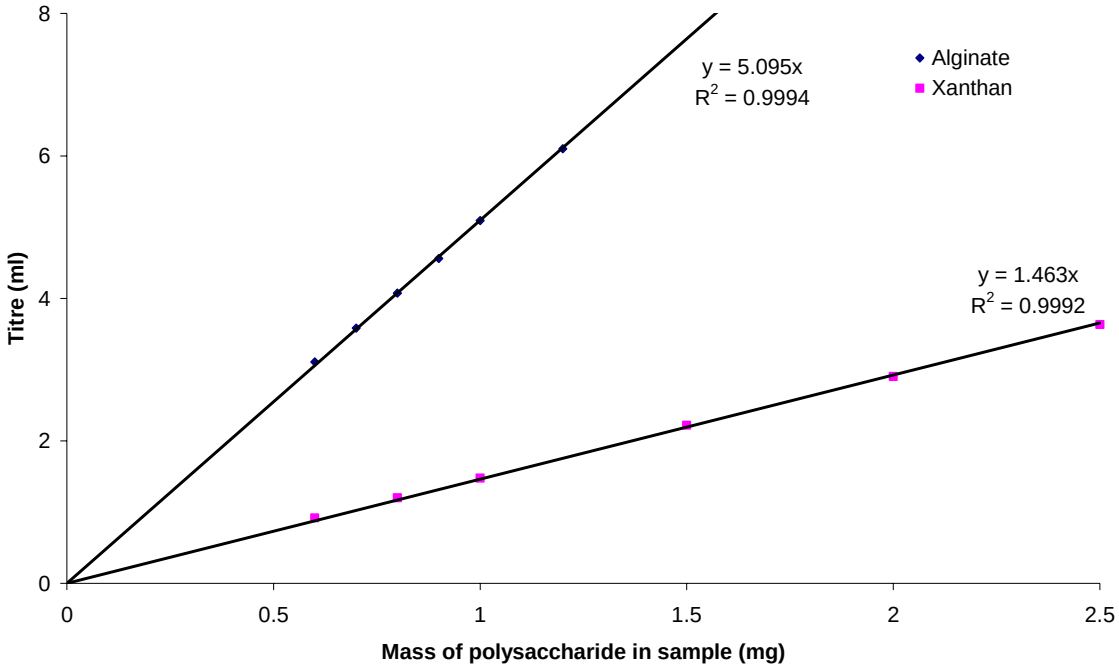

Figure 3.16. The polyelectrolyte titration standard curves for xanthan and alginate.
Biopolymers were titrated against Poly DADMAC, a counter charged polyelectrolyte to the point of zero streaming potential using the Mütek PCD03 particle charge detection equipment.

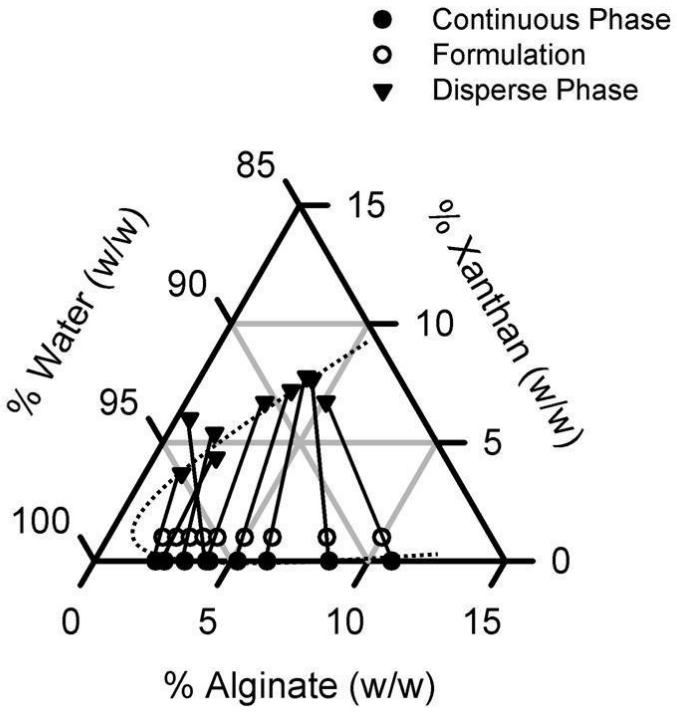

Figure 3.17. The phase composition diagram for xanthan and alginate in water.
The phase diagram was obtained by titration against poly DADMAC, a cationic polyelectrolyte, using the Mütek PCD03. The dotted line indicates an approximation of the binodal indicating the concentrations where phase separation occurs.

3.4.9 Fluorescence microscopy of xanthan/alginate mixtures

Fluorescence is very useful in determining the spatial distribution of components in a system as its sensitivity allows the detection of very small concentrations of dispersed components.

Figure 3.18 shows two confocal fluorescence microscope images of mixtures containing 1% xanthan gum with 4% alginate. Figure 3.18a shows a mixture where 0.1% of the alginate in the sample has been covalently labelled with fluoresceinamine. It shows widespread fluorescence throughout the sample (yellow), with a number of strand-like areas where the intensity of the fluorescence is reduced (darker red). Figure 3.18b shows a mixture where 0.1% of the xanthan in the sample has been covalently labelled with fluoresceinamine. This shows a predominantly dark image (black) with fluorescence highly concentrated in strand-like regions.

The fluorescently labelled alginate image suggests that alginate is distributed throughout the sample, but is less in the darker red regions. This could be as a result of a reduced amount of alginate being present in these areas, or there being no alginate, but with some signal arising from high intensity areas in front or behind the sample. This reduction in fluorescence, as opposed to absolute extinction, is in agreement with the phase diagram which suggests that whilst all of the xanthan moves into one phase, and the majority of alginate remains in the continuous phase, some residual alginate is left within the xanthan phase. The fluorescent xanthan image suggests that xanthan concentrates into the strand-like structures and is exclusively found in them, again in agreement with the phase diagram.

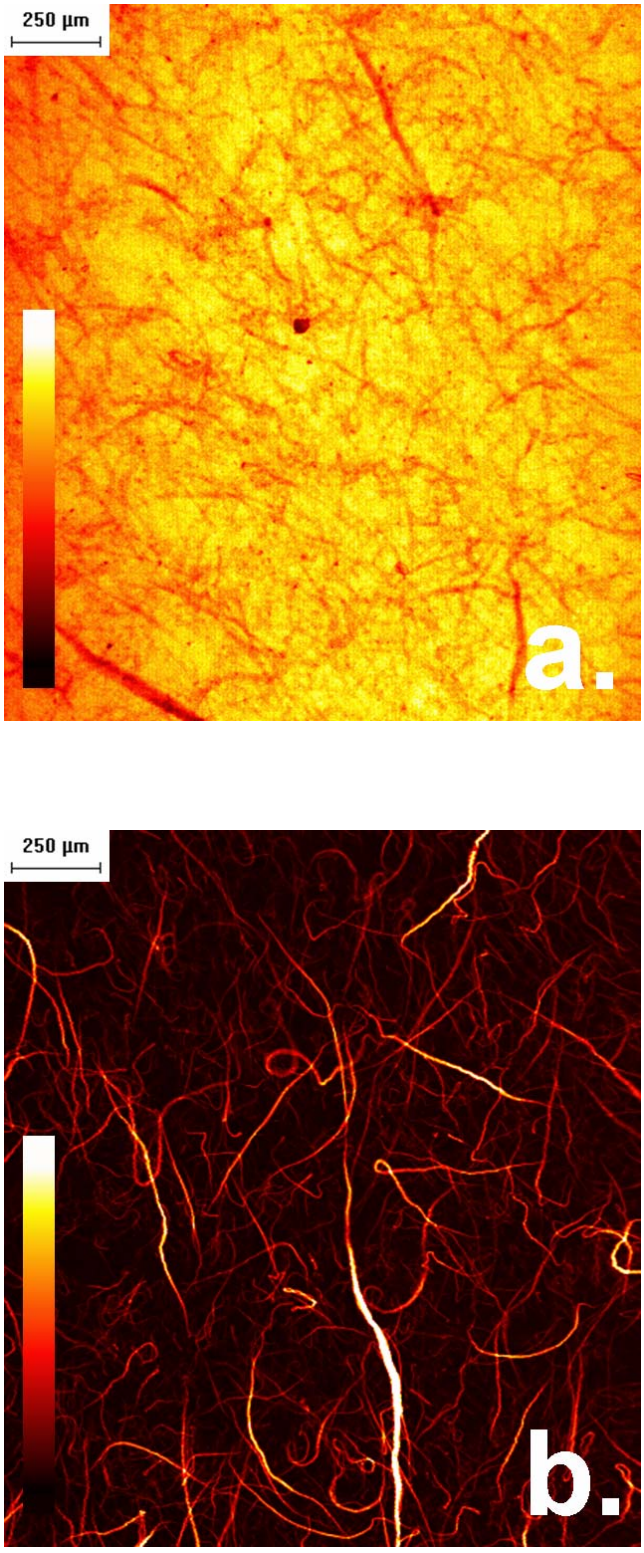

Figure 3.18. Confocal micrographs of 1% xanthan 4% alginate.
(a) shows a sample where 0.1% of the alginate in the mixture has been covalently labeled with fluoresceinamine, (b) shows a sample where 0.1% of the xanthan in the mixture has been covalently labeled with fluoresceinamine.

3.4.10 Differential scanning calorimetry of mixtures of xanthan and alginate

It is common for the addition of heat energy to a system to reverse phase separation in biopolymers and this may or may not be associated with structural changes on a molecular level (Sperling 2001). This section describes DSC experiments to examine if the phase separation previously observed was thermo-reversible, and what enthalpic changes were associated with this. Figure 3.19 shows DSC thermograms of 1% xanthan gum, 5% sodium alginate and a mixture of 1% xanthan with 5% alginate. 1% xanthan shows an endothermic event between 60^{o}C and 80^{o}C in both the heating and cooling curves, whereas the traces for both 5% sodium alginate and the xanthan/alginate mixture show no thermal events in the temperature range studied.

The thermal event on the trace for 1% xanthan gum corresponds to the order-disorder transition previously described in chapter 1 for xanthan gum (Norton, Goodall et al. 1984). The shift in transition from the generally quoted range of 35^{o}C to 60^{o}C (Norton, Goodall et al. 1984) to the observed transition between 60^{o}C and 80^{o}C suggests that the xanthan sample used in this study may contain a residual amount of salt (Morris 1977; Kitamura, Kuge et al. 1990). Sodium alginate is not known to undergo any thermal transitions as alginate forms non-specific entanglement networks, therefore the lack of thermal events in 5% sodium alginate trace is not unexpected. The DSC trace for the mixture also showed no thermal event, and this would suggest that within the temperature range studied, separation is not reversible by thermal methods. It would also suggest that the xanthan within the sample had been affected by the addition of alginate such that either the ordered form had been destroyed removing the order-disorder transition, or the order-disorder transition had been moved to a temperature outside of the range studied. As salt is know to raise the order-disorder transition temperature of xanthan, and the level of sodium added from the 5% alginate is high, it is far more probable that the latter is correct.

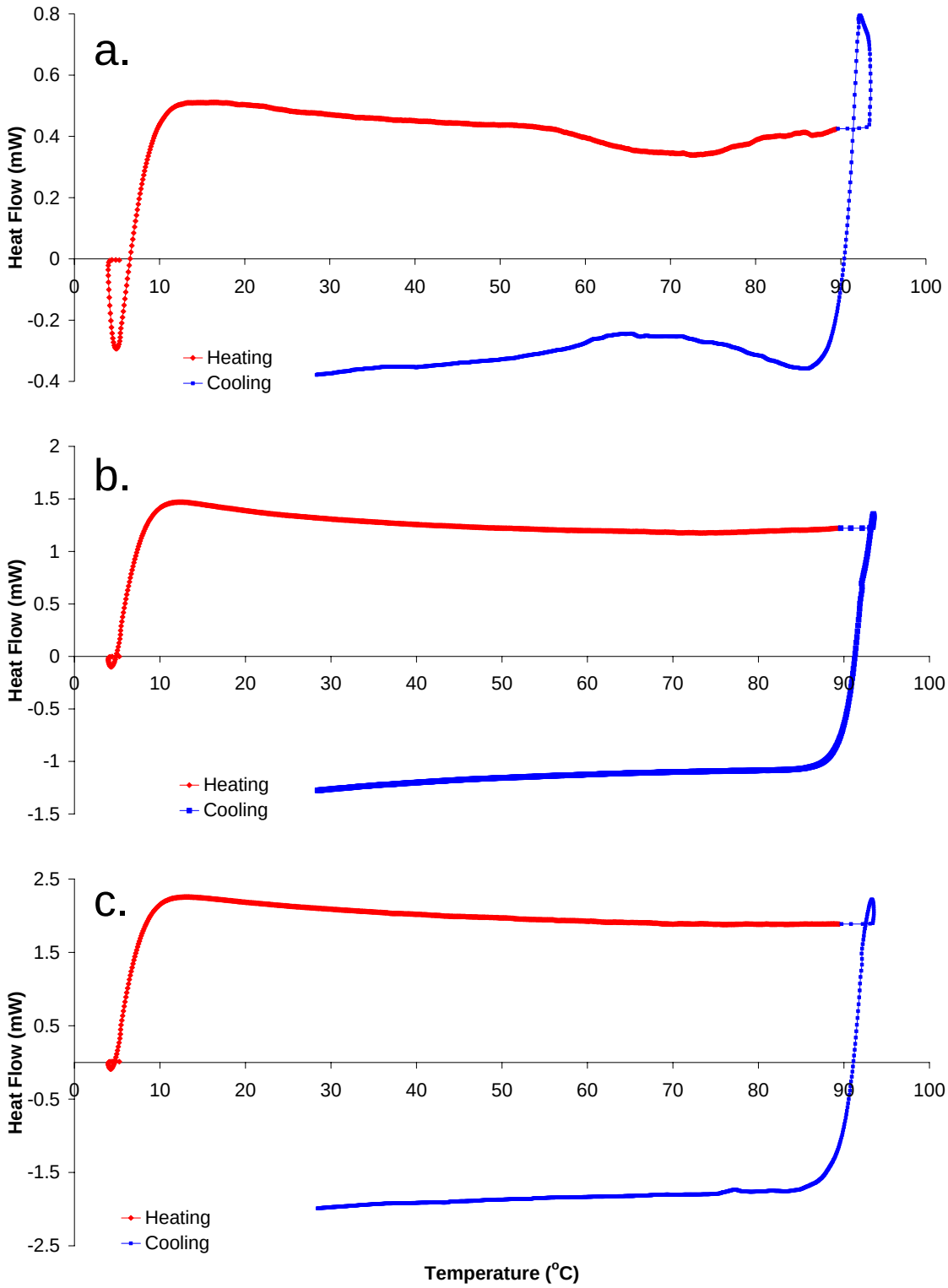

Figure 3.19. A DSC thermogram of a sample of (a) 1% xanthan, (b) 5% alginate and (c) a mixture 1% xanthan and 5% alginate.
Samples were cooled from ambient to 5°C then heated from 5°C to 90°C and then cooled to 25°C at a rate of 1°C/min.

3.4.11 The effects of adding ionic species to mixtures of xanthan and alginate

The use of ionic species in foods and pharmaceutical formulations is universal, and can have a significant impact on biopolymer solution properties. The following section investigates the effect of adding salts to the xanthan/alginate mixtures.

3.4.11.a The effects of monovalent salts

The effects of monovalent salts on the rheological properties of mixtures containing 1% xanthan are shown with respect to alginate concentration in Figure 3.20. To make the data comparable, cationic charge equivalence by weight was used. 0.638% potassium chloride (KCl) is cationic charge equivalent by weight to 0.5% sodium chloride (NaCl). The addition of salts shifted the curve such that a higher concentration of alginate was required to produce the dramatic reduction in G' shown previously. In the case of 0.5% NaCl or 0.638% KCl the concentration of alginate required to elicit separation was shifted from the 1 - 1.5% to 2.5% - 3%. Likewise the addition of 1% NaCl or 1.276% KCl shifted the concentration of alginate required to 3 - 3.5%. Figure 3.20 shows that irrespective of which monovalent salt was used there was little difference in the alginate concentration required.

The effects of adding salt to alginate is well known, with high concentrations often causing precipitation (McDowell 1977). The effect of salt on xanthan viscosity is also known, with viscosity generally increasing with the addition of salt up to 0.05% and thereafter remaining unchanged up to 1% (Kang and Pettitt 1993). Figure 3.21 examines the effect on viscoelasticity of adding sodium chloride to 1% xanthan gum to see if high concentrations of salt could induce a salting out effect, and whether this may be a mechanism for driving phase separation. It was observed that with increasing salt concentration G' also increased at all frequencies. The increase in G' would suggest that the weak gel-like properties of xanthan are enhanced by the addition of salt and that

salting out does not occur. This therefore suggests that the separation observed is not driven by a salting out effect as a result of the sodium alginate counter ions.

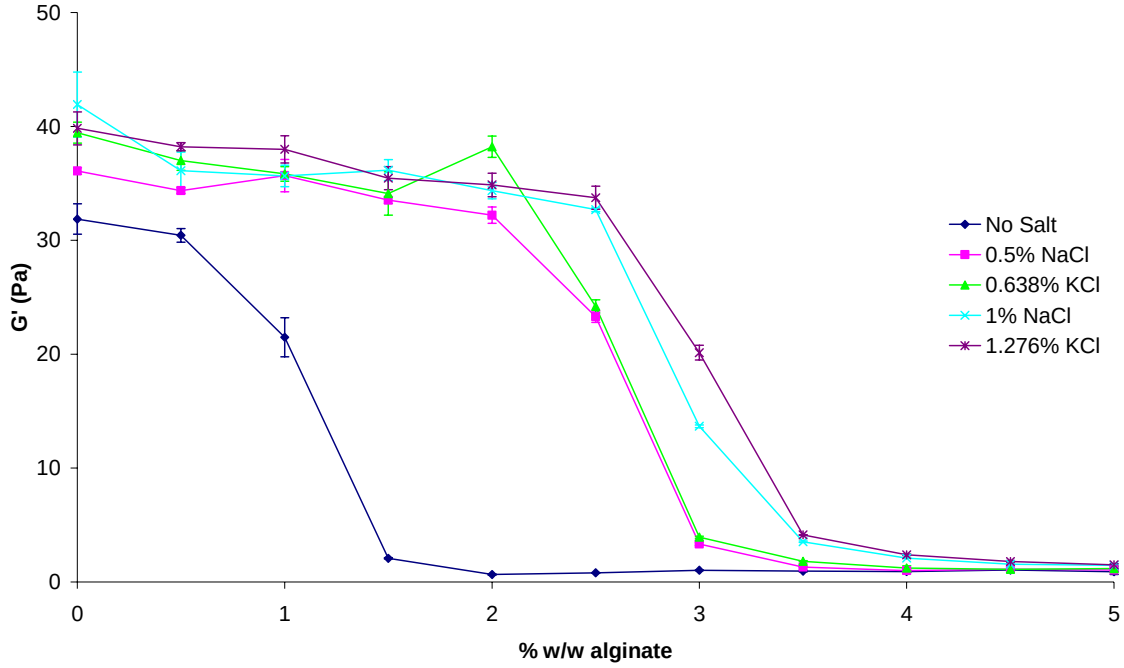

Figure 3.20. The effect on viscoelasticity of adding alginate to 1% xanthan in the presence or absence of either sodium or potassium chloride.
0.638% Potassium Chloride (KCl) is cationic charge equivalent by weight to 0.5% sodium chloride (NaCl). Geometry CP 4°/40mm. 25 ± 0.1°C. Frequency 1.02Hz Mean ± SD, n=3.

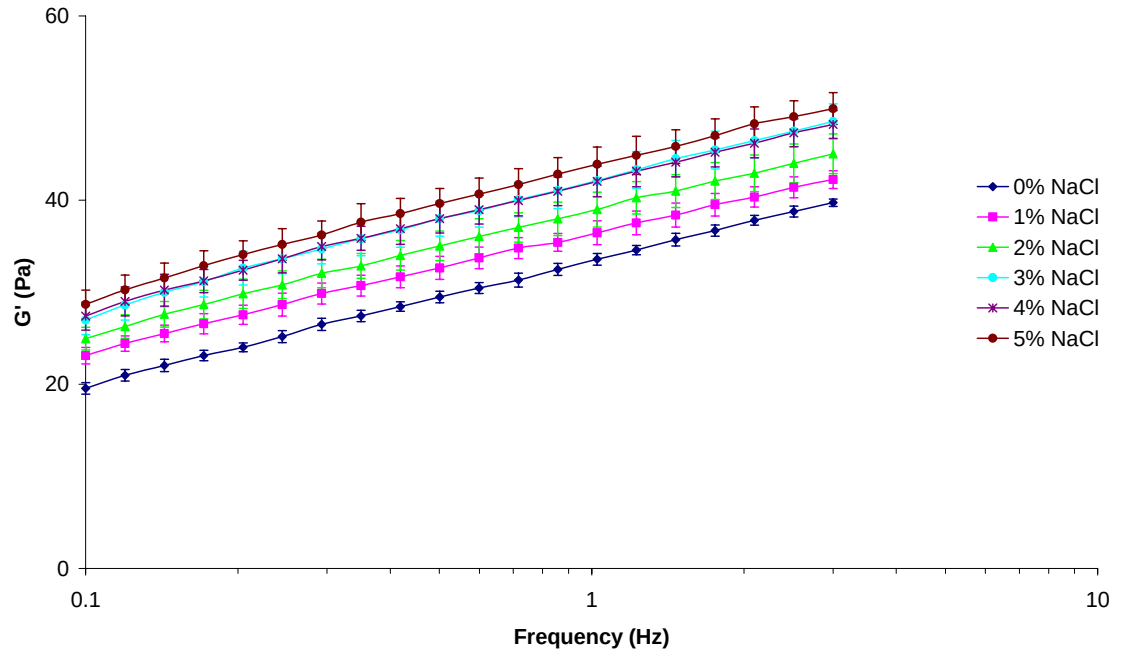

Figure 3.21. The effect of adding sodium chloride (NaCl) on the elastic modulus of 1% xanthan gum.
Geometry CP 4°/40mm. 25 ± 0.1°C. Mean ± SD, n=3.

3.4.11.b The effects of a divalent salt

Investigating the effect of divalent ions is more complicated as it is well documented in the scientific literature that calcium, strontium and barium produce ionic alginate gels. This makes calcium an unsuitable choice to investigate whether divalent ions have a similar effect to monovalent ions. Magnesium ions however are known not to cause this gelation effect (Smidsrød 1974). The effect of magnesium ions on the phase separation behaviour is shown in Figure 3.22. It shows the effect of adding sodium alginate to 1% xanthan gum in the presence of 0.771% magnesium chloride (cationic charge equivalent to 1% NaCl by weight). The profile is significantly different to that seen in the absence of ions. It can be seen that in mixtures containing up to 1% alginate there was a slight decrease in G'. The addition of alginate from 1% up to 3% showed a general increase in G'. This was followed by a decrease in G' between 3% and 4% alginate, and then a further increase from 4% to 5% alginate. The samples were viewed between crossed polarising lenses where it could be seen that at concentrations of 4% and above, strands similar to those observed previously were seen.

The viscoelastic profiles of a 1% xanthan gum solution, a 5% alginate solution, and a mixture of 1% xanthan with 5% alginate all containing 0.771% $MgCl_2$ are shown in Figure 3.23. The 1% xanthan solution exhibited the weak gel-like profile seen previously. The values of G' and G" are the same and would suggest that the magnesium chloride had little effect on the xanthan component. G' is greater than G" at all frequencies in the mixture with the values being higher than either of the individual biopolymer components. The 5% alginate solution showed a similar profile to that of the mixture but at lower moduli values, this is in contrast to the alginate solution with no magnesium chloride present, where no viscoelastic moduli could be measured. Investigating this further Figure 3.24 shows the effect of adding increasing concentrations of magnesium chloride to a solution of 5% sodium alginate. Below 0.7% magnesium chloride, no measurable viscoelastic properties were detected. However above 0.7%, G' and G" rapidly increased with a corresponding decrease in tan delta. The increase in G' reaches a maximum at 1.3% added magnesium chloride. This

suggests that the addition of magnesium chloride has a gelation-type effect on alginate, which is subject to a threshold concentration.

The microscopy images suggest that magnesium has a similar effect to that of monovalent salts by increasing the concentration of alginate required to cause separation with xanthan. It would be inappropriate to quantitatively state at which concentration onset of separation took place as the gelation effects observed with the magnesium chloride would probably have retarded the formation of strands by increasing the viscosity of the overall mixture.

The gelation-like effects observed would suggest that the magnesium ions create a very weak cross linked matrix in contrast to calcium salts which gel alginate at low concentration.

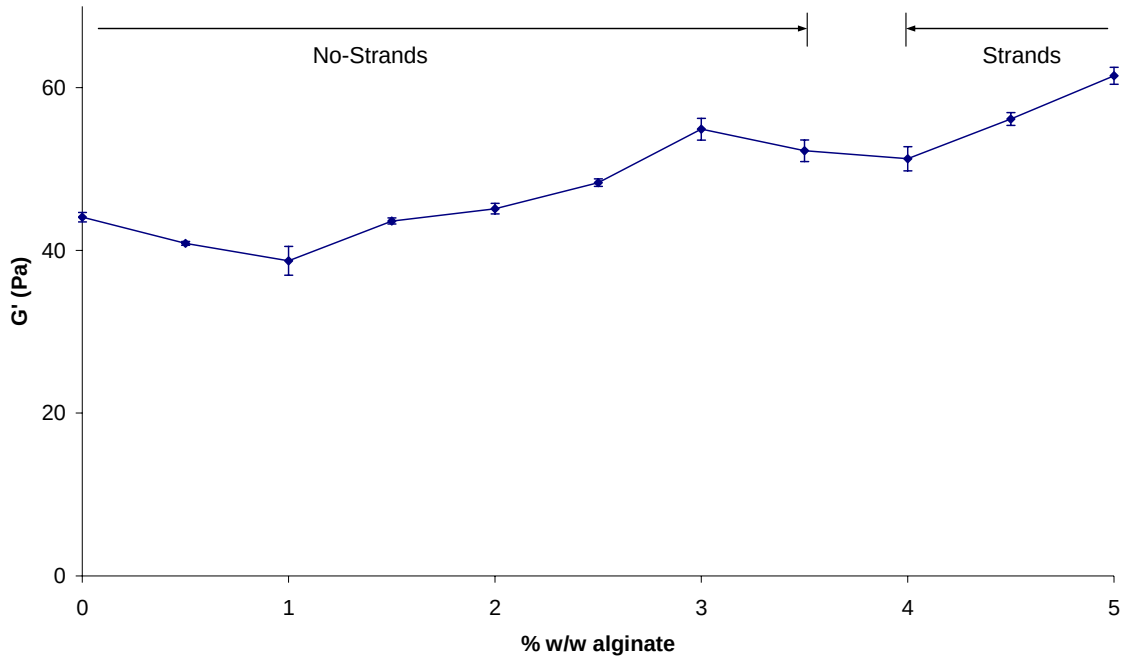

Figure 3.22. The effect on viscoelasticity of adding alginate to 1% xanthan in the presence of magnesium chloride.
Each mixture contains 0.771% $MgCl_2$ (which is cationic charge equivalent to 1% NaCl by weight). The strand-like appearance that has been observed with previously separated mixtures is indicated at the top of the graph. Geometry CP 4°/40mm. 25 ± 0.1°C. Frequency 1.02Hz Mean ± SD, n=3.

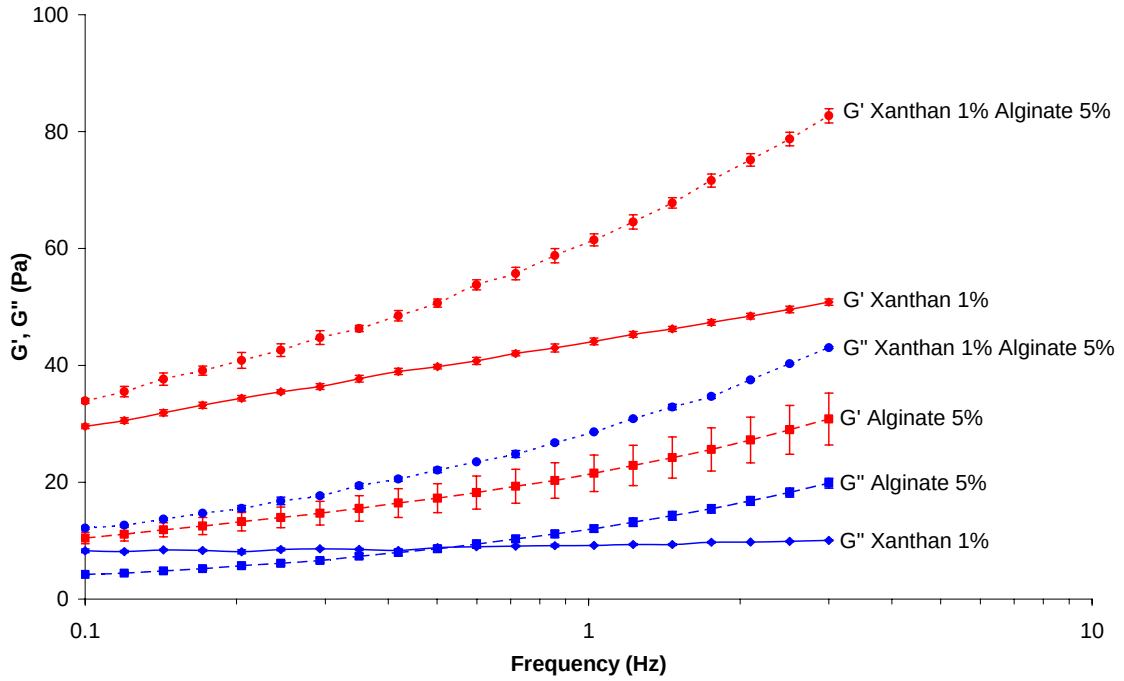

Figure 3.23. The viscoelastic properties of 1% xanthan, 5% alginate and a mixture containing both biopolymers. All of the samples also contain 0.771% $MgCl_2$.
Geometry CP 4°/40mm. 25 ± 0.1°C. Mean ± SD, n=3

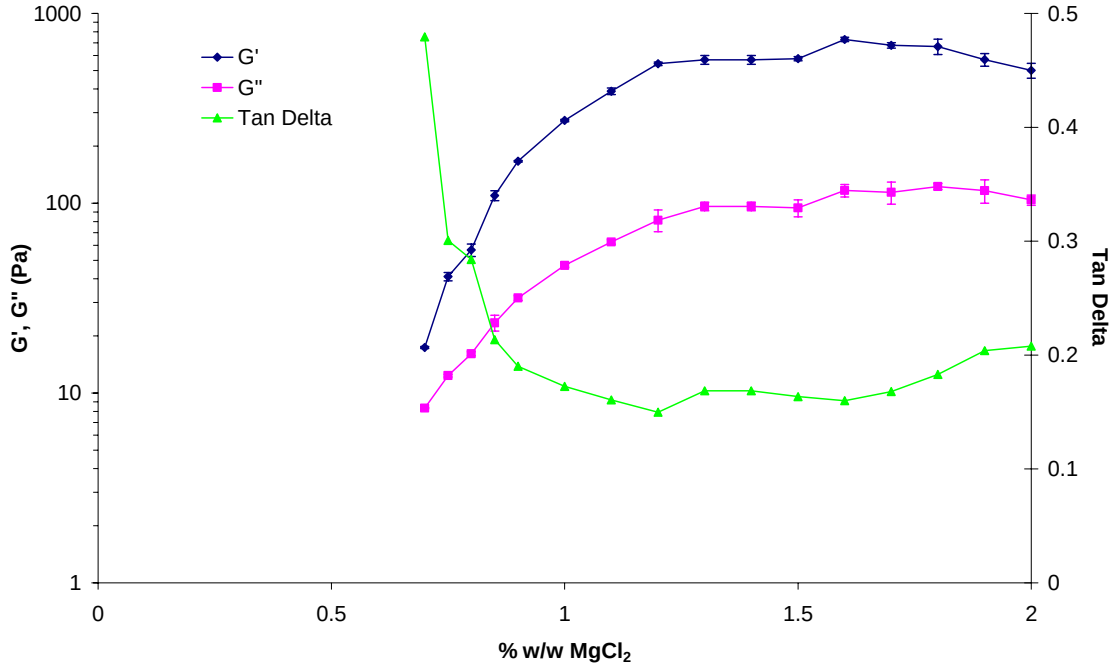

Figure 3.24. The viscoelastic properties of 5% alginate solutions containing varying concentrations of $MgCl_2$.
Geometry CP 4°/40mm. 25 ± 0.1°C. Frequency 1.02Hz. Mean ± SD, n=3

3.4.12 The effects of varying the molecular weight and primary structure of the alginate used in the mixtures

The previous section has demonstrated how mixtures of xanthan gum and sodium alginate undergo phase separation. This section looks at the effects of varying the molecular weight of the sodium alginate and the effect of using a guluronate (G), or mannuronate dominant (M) sodium alginate on the separation properties of the mixtures. A summary of the range of sodium alginate used is provided in Table 3.1.

The effects of adding differing molecular weight sodium alginates to 1% xanthan gum is shown in Figure 3.25. The addition of the 75 kDa alginate shifted the typical decrease in G' to between 0.5% and 1% added alginate. The addition of the other alginates shifted the decrease to between 0% and 0.5%. In the mixtures containing the 35kDa and 75 kDa alginates, G' remained constant after the dramatic decrease. The 221 kDa and 404.4 kDa alginate samples however showed a steady increase in G' following the massive decrease in G'. Figure 3.26 looks at two pairs of alginates with similar molecular weights but differing M:G ratios. For each of the pairs M:G ratio appears to elicit little difference in effect.

Figure 3.27 looks in greater detail at the rheological changes at low concentrations of alginate with respect to molecular weight. The 35 kDa alginate showed a significant decrease in G' between 0.75% and 1.5% added alginate. The 75 kDa alginate showed a significant decrease in G' between 0.5% and 1%, the 221kDa alginate between 0.1% and 0.6% and the 404.4 kDa alginate between 0.05% and 0.45% alginate. This clearly shows that with increasing molecular weight, the concentration of alginate required to elicit separation is decreased. Figure 3.28 examines more closely the effects of M:G ratio. As in Figure 3.26, it would appear that M:G ratio has little effect on the concentration of alginate required to elicit separation. This would suggest that whilst changes in molecular weight have pronounced effects in the phase separation, molecular conformation does not.

Figure 3.29 shows images of the mixtures containing 1% xanthan with each of the different alginates (at their highest concentration) used in Figure 3.27 and Figure 3.28. The image containing the 75 kDa alginate showed very similar morphology to that of the mixture containing the 35kDa alginate with large well defined strand-like structures. The images of xanthan with the other four alginates (c-f) showed less well defined morphology, whilst still retaining the birefringence previously seen.

Figure 3.30 shows complex viscosity values (1.02 Hz, 25^{o}C) of the mixtures used in Figure 3.29. The complex viscosity of the 35 kDa alginate was low. The 75 kDa alginate exhibited a viscosity which was approximately double that of the 35 kDa alginate. The other four alginate mixtures show a similar complex viscosity, approximately an order of magnitude greater than that of the 35 kDa alginate.

The effects of increasing the molecular weight have been demonstrated above. To examine if low molecular entities would behave in a similar manner an oligo-alginate was mixed with xanthan. Figure 3.31 shows the effect of adding an oligo-alginate to 1% xanthan. This alginate has a typical residue length of 7 monomer units (Mw = 1550 Da). The addition of 9% of the oligo-alginate had no significant effect on the G' value, but addition of 9% - 14% showed a decrease in G' similar to that shown previously with the other alginates. G' values reach a similarly low level at 15% to that seen with 5% sodium alginate LFR 5/60 (35 kDa).

Sodium Alginate Grade	Molecular weight (weight average Mw)	Composition	
		% Guluronate	% Mannuronate
Protanal® LFR 5/60	35 000	64%	36%
Protanal® LF10L	75 000	45%	55%
Protanal® LF120L	221 000	44%	56%
Protanal® SF120	195 000	69%	31%
Protanal® SF200	411 600	69%	31%
Protanal® H120L	404 400	46%	54%

Table 3.1. A summary of different sodium alginates used to study the effect of molecular weight and mannuronate:guluronate ratio on xanthan:alginate phase separation.

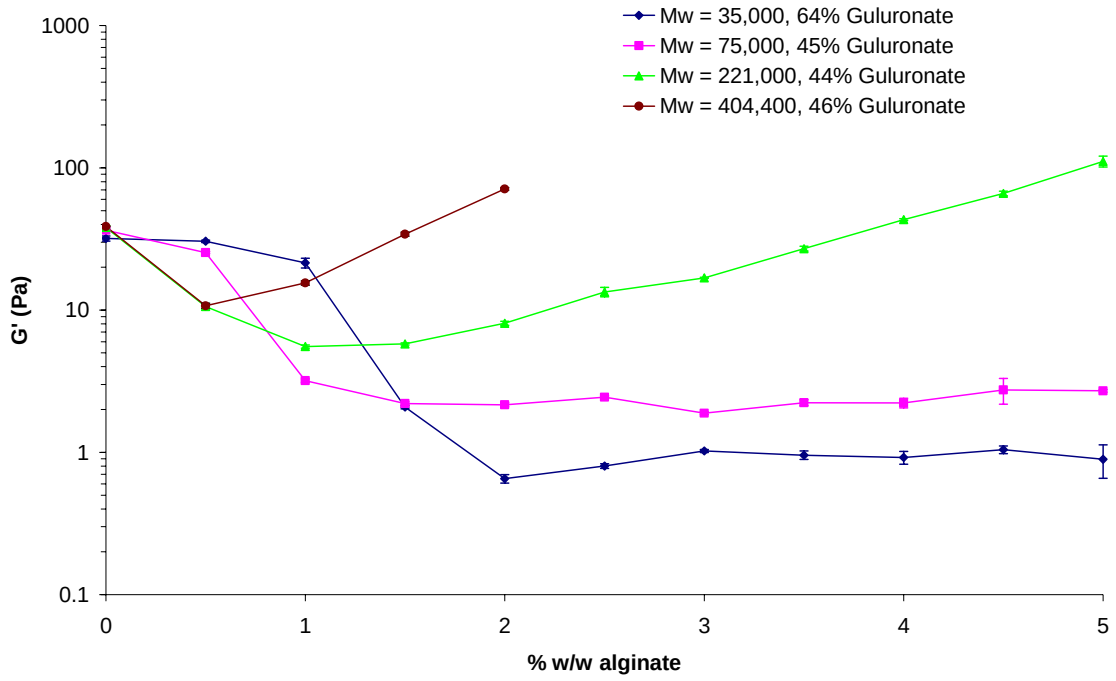

Figure 3.25. The effects on viscoelasticity of adding alginates of differing molecular weights to 1% xanthan gum.
Geometry CP 4°/40mm. 25 ± 0.1°C. Frequency 1.02Hz. Mean ± SD, n=3

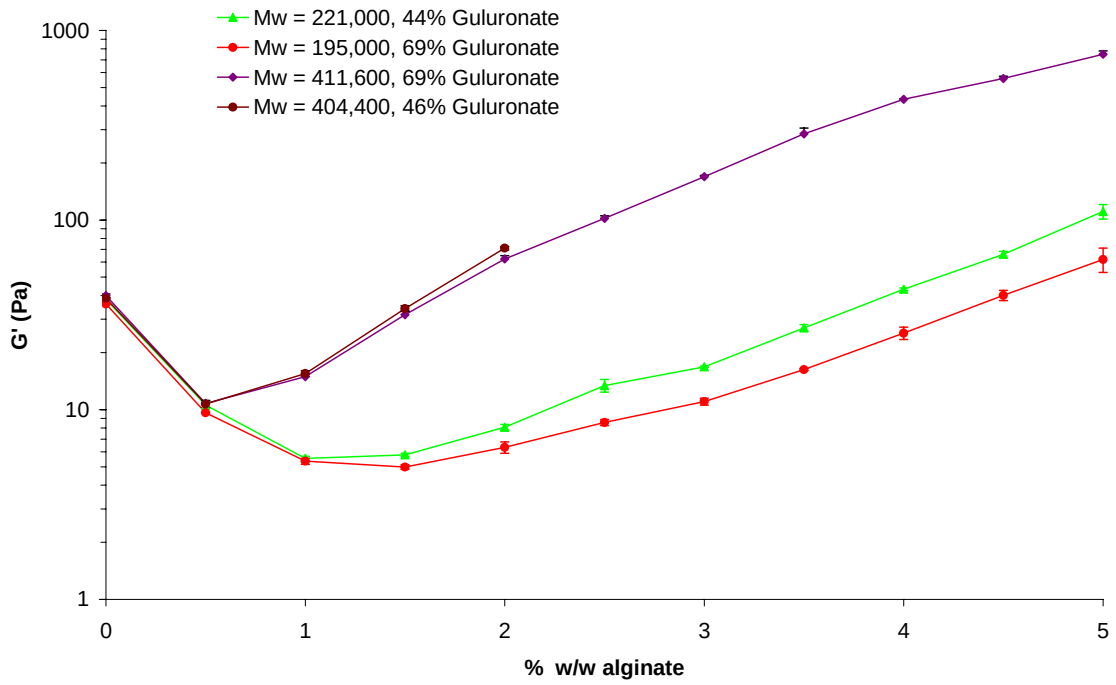

Figure 3.26. The effects on viscoelasticity of adding alginates of differing M:G ratios to 1% xanthan gum.
Geometry CP 4°/40mm. 25 ± 0.1°C. Frequency 1.02Hz. Mean ± SD, n=3

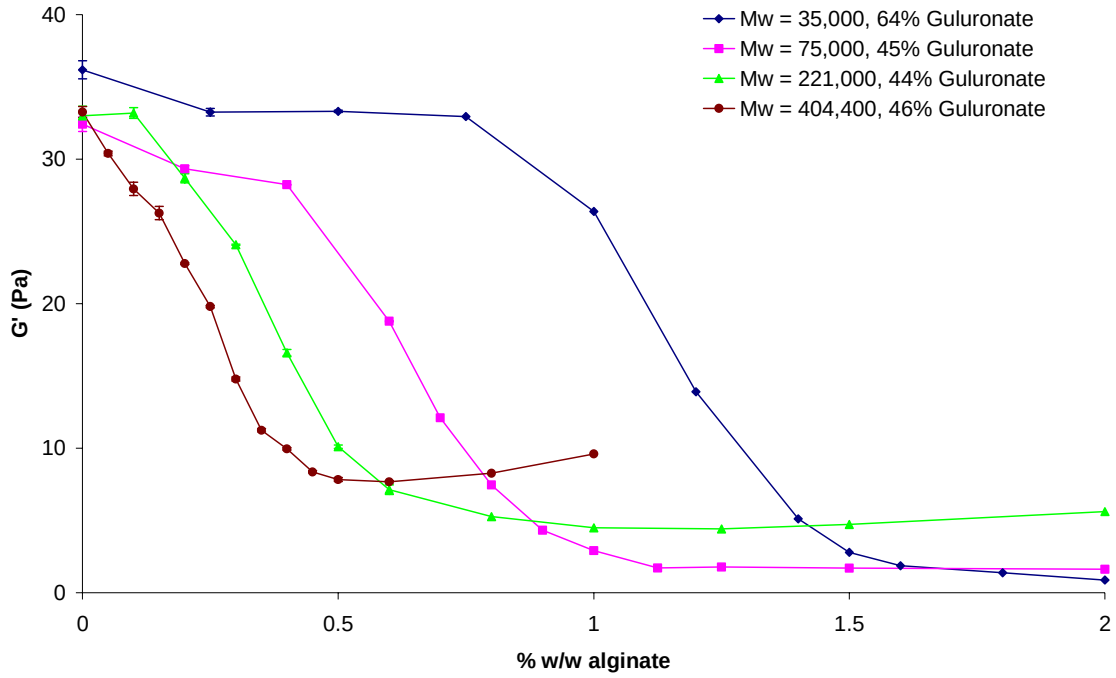

Figure 3.27. The effects on viscoelasticity of adding low amounts of sodium alginates with differing molecular weights to 1% xanthan gum.
Geometry CP 4°/40mm. 25 ± 0.1°C. Frequency 1.02Hz. Mean ± SD, n=3

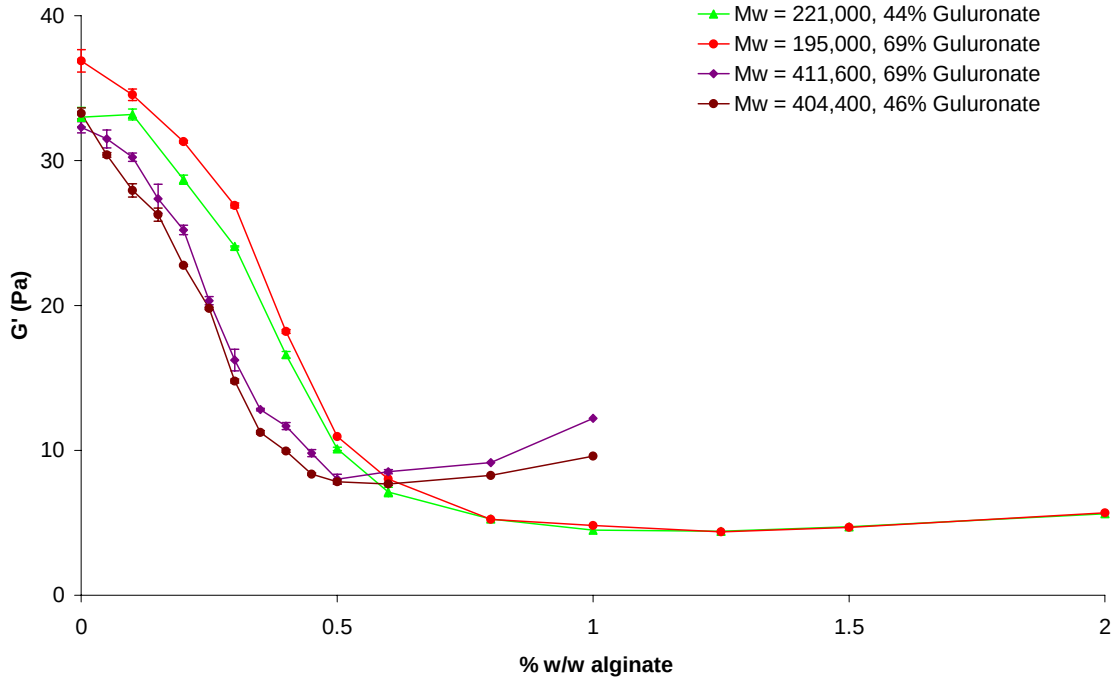

Figure 3.28. The effects on viscoelasticity of adding low amounts of sodium alginates with differing M:G ratios to 1% xanthan gum.
Geometry CP 4°/40mm. 25 ± 0.1°C. Frequency 1.02Hz. Mean ± SD, n=3

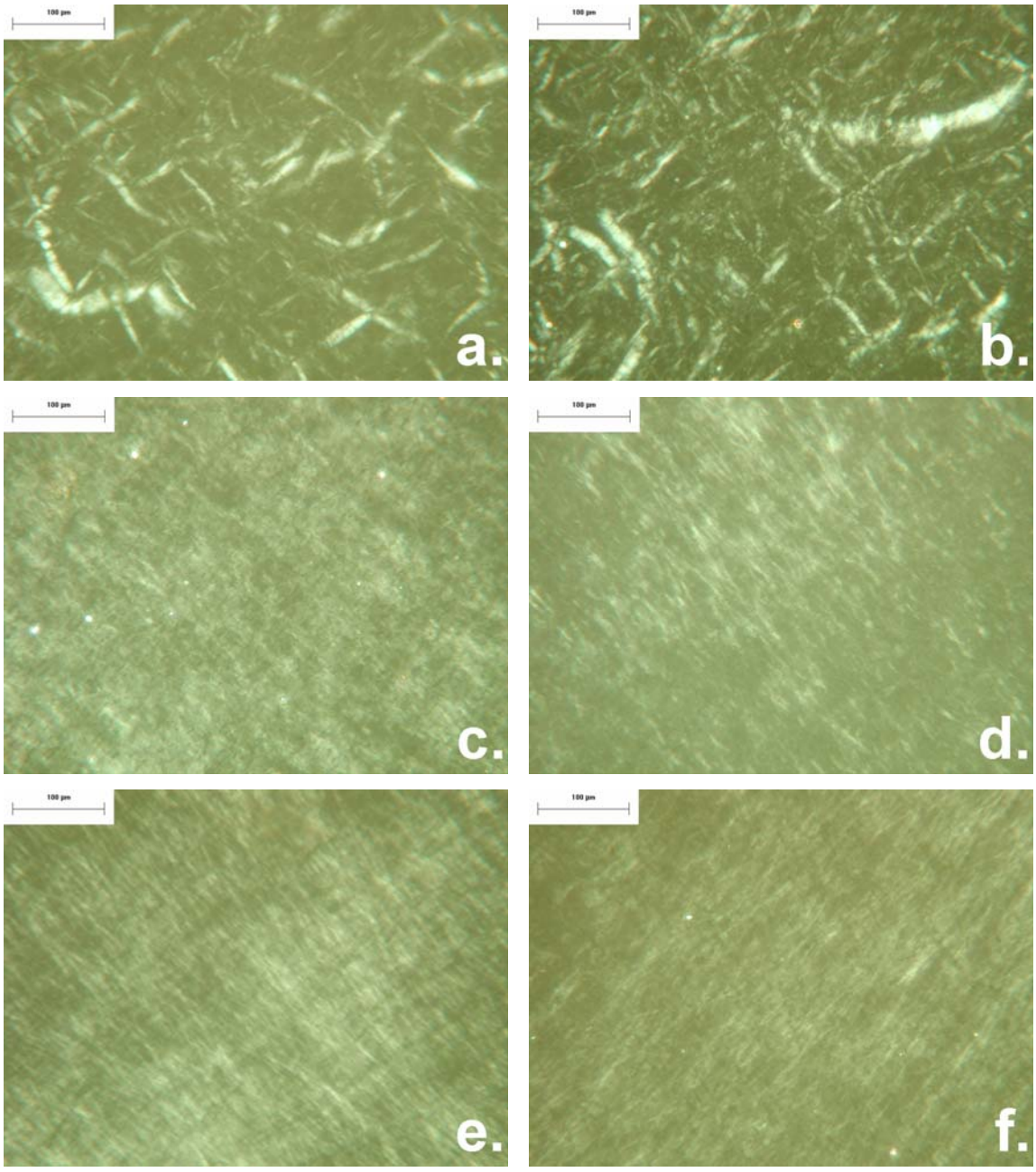

Figure 3.29. Crossed-polarized light micrographs of mixtures containing 1% xanthan and various different alginates.
(a) Mw = 35,000, 64% G; (b) Mw = 75,000, 45% G; (c) Mw = 221,000, 44% G; (d) Mw = 195,000, 69% G; (e) Mw = 411,600, 69% G; (f) Mw = 404,400 46% G. Images a - d contained 2% alginate, images e and f contained 1% alginate

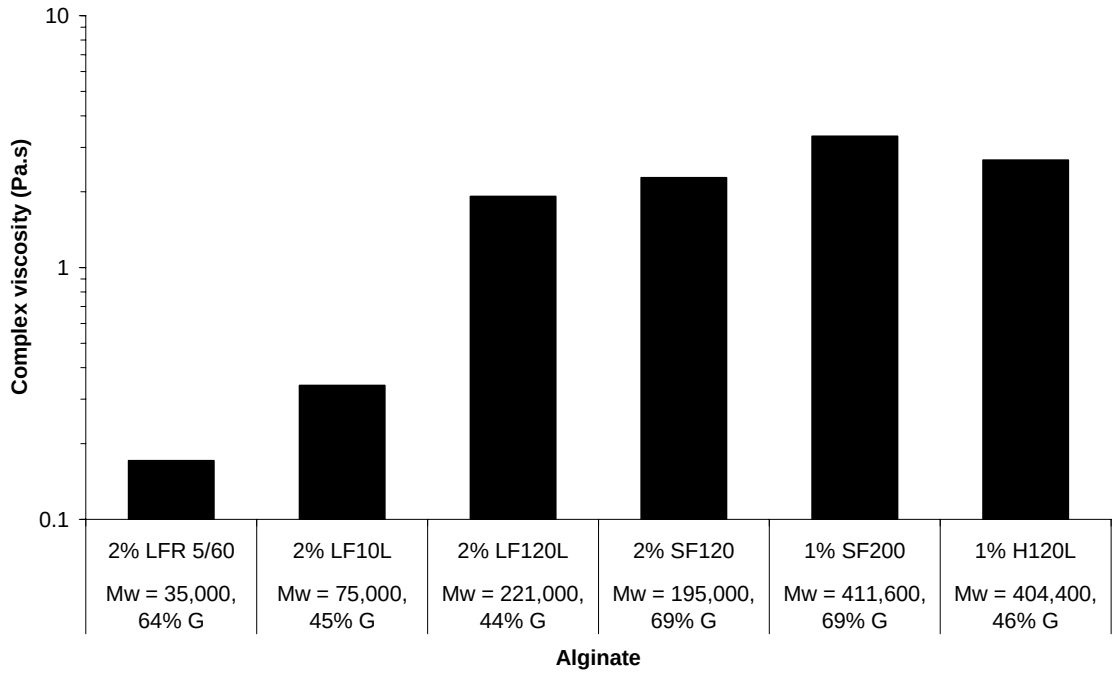

Figure 3.30. The complex viscosities of mixtures containing different molecular weight alginates.
All mixtures contain 1% xanthan and the concentration of each alginate indicated on the x-axis.
Geometry CP 4°/40mm. 25 ± 0.1°C. Frequency 1.02Hz. Mean ± SD, n=3

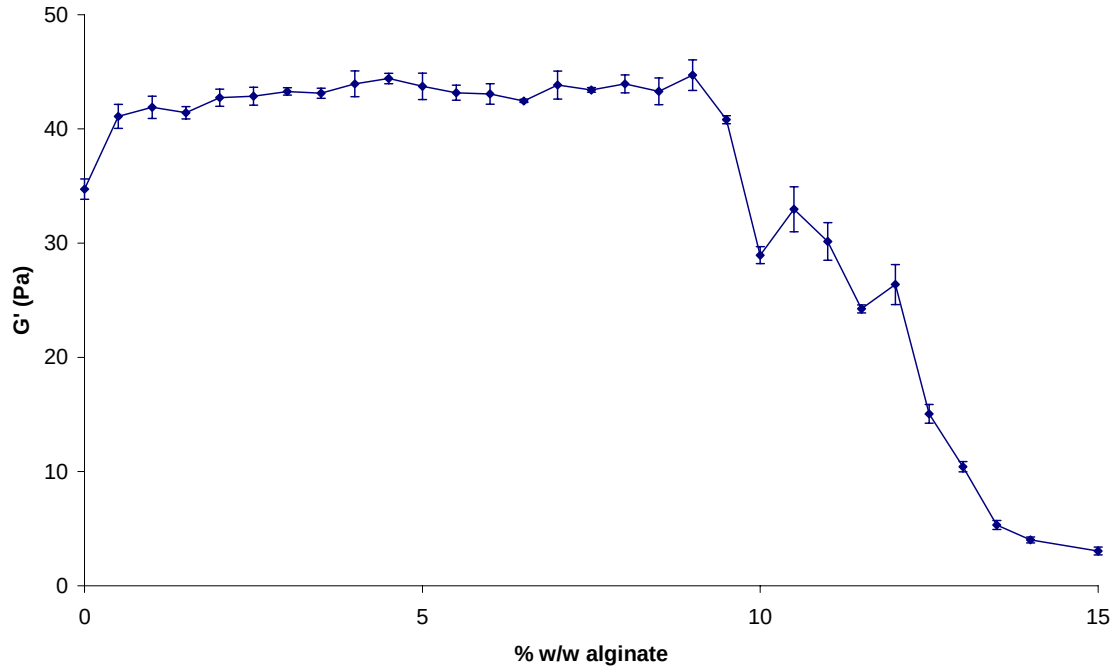

Figure 3.31. The effect on viscoelasticity of adding an oligo-alginate to 1% xanthan.
Mw = 1550 Da, 7 monomer residues
Geometry CP 4°/40mm. 25 ± 0.1°C. Frequency 1.02Hz. Mean ± SD, n=3

3.4.13 The effects of adding soluble non-ionic species to mixtures of xanthan and alginate

A wide variety of non-ionic materials are widely used in food and pharmaceutical products and this section examines the effects of adding certain non-ionic species (sucrose, sorbitol or glycerol) to mixtures of xanthan and alginate. Although components such as sucrose are often present in concentrations of up to 70% in foods, the concentration of 5% was chosen so that effects observed could be related to the non-ionic species being present, rather than there being a reduced amount of water present.

Figure 3.32 shows how adding these to mixtures of xanthan gum and sodium alginate LFR 5/60 slightly raises the values of G' at all values. This is most probably as a result of the slight increase in the concentration of xanthan due to the reduced water content. The position of the decrease in G' was unaffected by the addition of these non-ionic materials.

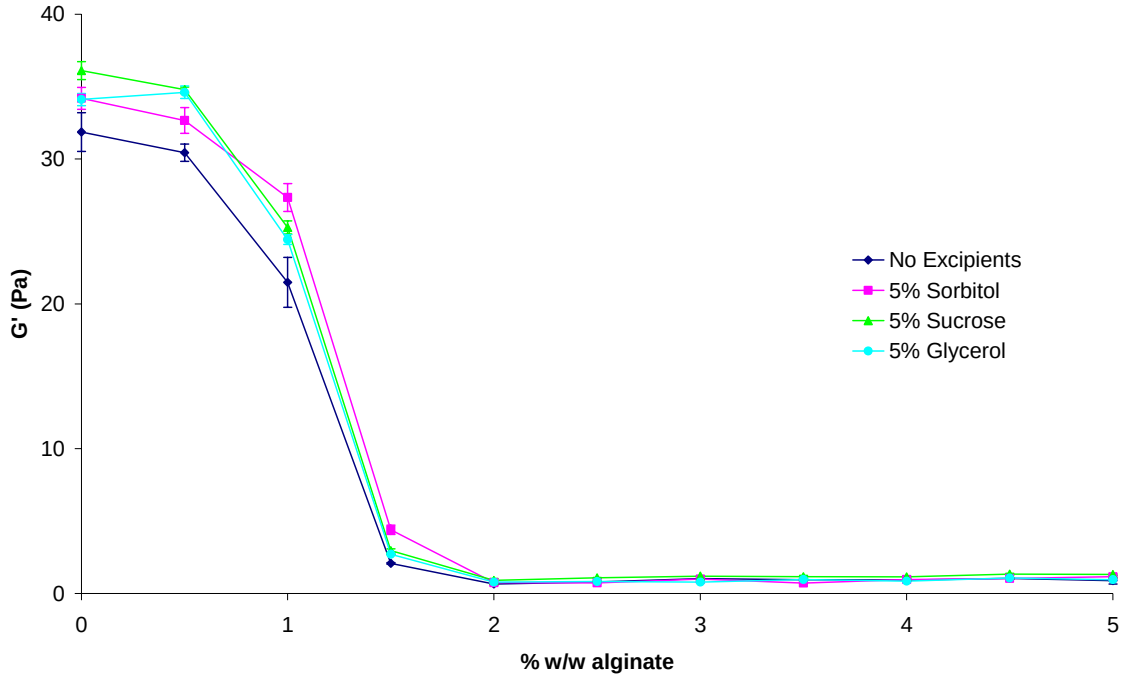

Figure 3.32. The effect on viscoelasticity of adding three common non ionic materials to mixtures of 1% xanthan and varying concentrations of sodium alginate.
Mean ± SD, n=3.

3.4.14 The effect of time on the rheological stability of the samples under study

The stability of samples is critical to the validity of data. This section investigates the effects of time on the rheological stability of a number of the samples under study. The time shown was started after the mixture has been completely mixed. Figure 3.33 shows that over the standard storage conditions employed (1 to 1.5 days) there was no significant variation in viscosity, suggesting that the samples were stable to degradation. The samples were prepared without antimicrobial agents and it was observed that after approximately 7 days that a green fungus was growing on the samples making their use inappropriate.

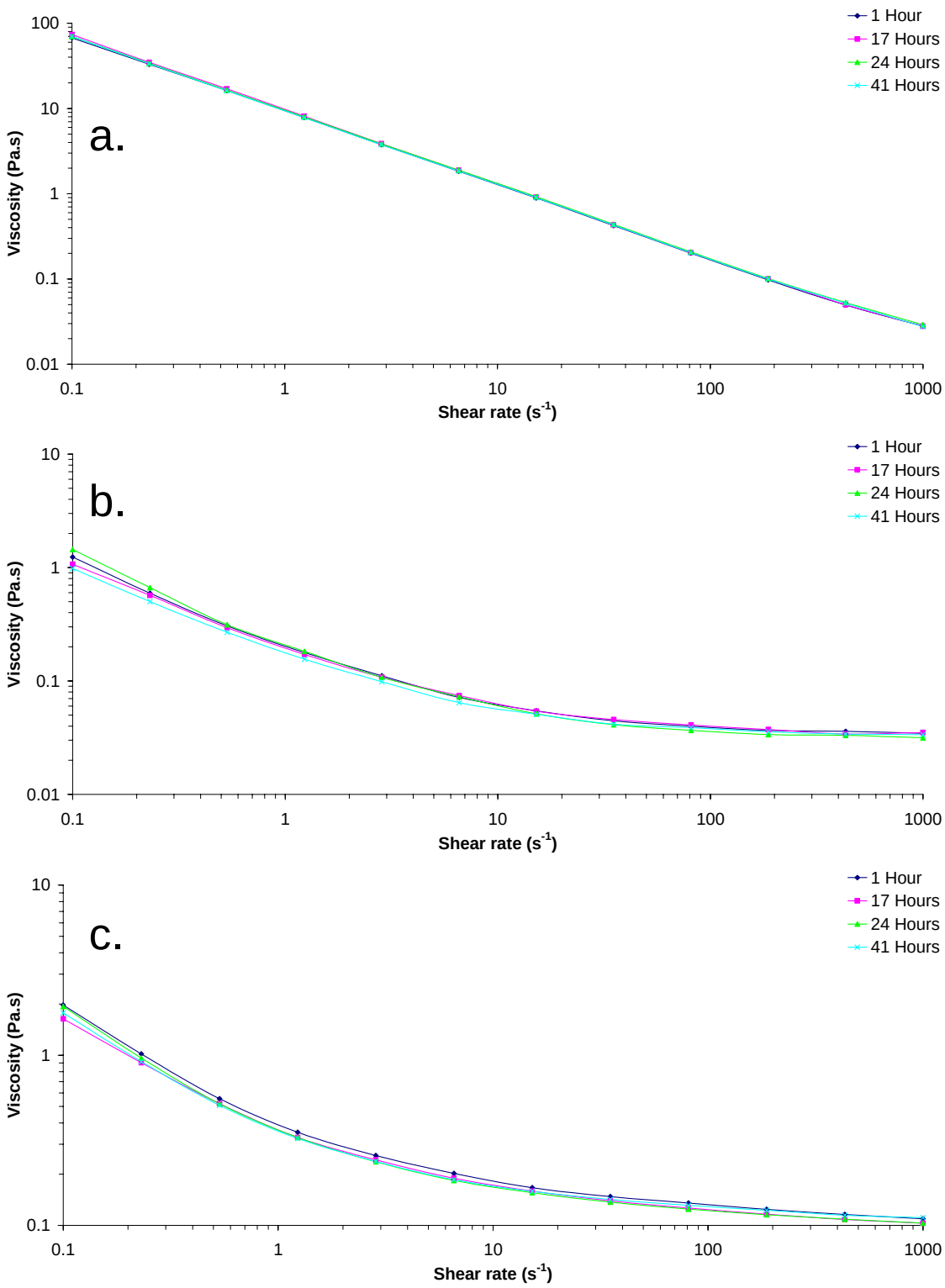

Figure 3.33. The viscosity profiles of samples of 1% xanthan gum with sodium alginate as a function of storage time.
(a) 0% alginate, (b), 2.5% alginate, (c) 5% alginate.
Geometry CP 4^{o}/40mm. 25 ± 0.1^{o}C. Delay time and integration time at each shear rate were 30s each.

3.5 Conclusion

The work presented in this chapter has clearly demonstrated that at sufficiently high biopolymer concentrations, mixtures composed of xanthan gum and sodium alginate phase separate. As a result of this separation, strand-like birefringent mesophases form, due to concentration of xanthan gum into the disperse phase. These strands lie within a continuous phase exclusively composed of sodium alginate. The effects of altering the molecular weight of the alginate used have been studied and shown that an alginate as low as 1.5 kDa can elicit separation. The molecular weight has also been shown to alter the concentration of alginate necessary to trigger separation, such that with increasing molecular weight less alginate is required.

The effects of additional ionic species within the mixture has been investigated and shown that in the presence of monovalent salts, the concentration of alginate required to cause separation is increased; however the choice of monovalent salt does not appear to be of much significance. A magnesium (divalent) salt has also been investigated and shown to shift the phase boundary. Non-ionic additives had no apparent effect on the separation properties.

Chapter 4

Attributes required for phase separation in xanthan mixtures – An extension to polymers other than sodium alginate

4.1 Introduction

In chapter 3 the properties of xanthan gum and sodium alginate mixtures were investigated. This chapter investigates if the phase separation phenomenon extends to similar hydrocolloids, and examines what structural features are required to achieve this.

4.1.1 Carboxymethylcellulose

Sodium carboxymethylcellulose (CMC) is a semi-synthetic polysaccharide produced by carboxymethyl etherification of cellulose. An idealised structure of carboxymethylcellulose (DS = 1.0) is given in Figure 4.1a (Karabinos and Hindert 1954) showing substitution via the C-6 carbon, substitution also occurs via the C-2 and C-3 positions. Along the repeating cellulose backbone, a number of carboxylate groups have been introduced to yield a linear, non-branched anionic polysaccharide. The

carboxymethyl substitution is usually non-uniform and is dependent on the processing conditions used during synthesis. The rheological properties of CMC reflect its random coil conformation in solution and again make it similar to alginate. CMC is commonly used in the paper industry, texture processing, detergents, drilling fluids and protective coatings (Ghannam and Esmail 1997; Anon. 1999) . A more purified form is used in food, pharmaceuticals and the cosmetic industry as a emulsion stabilizer, suspending agent, tablet excipient or as a viscosifier (Feddersen and Thorp 1993; Ghannam and Esmail 1997). CMC has GRAS status (21 CFR 182.1745) and is listed in UK foods as E466 (Food Standards Agency 2005).

CMC has been studied for its mucoadhesive properties to promote localized drug delivery (Rossi, Bonferoni et al. 1999).

4.1.2 Pectin

Pectins are polysaccharides extracted principally from citrus peel and apple pomace (Guo, Skinner et al. 1998). Pectins are comprised of a backbone of galacturonic acids which are partly methyl esterified and form 'smooth' regions (Figure 4.1b). Occasional insertions of alternating rhamnose and galacturonic acid residues may also be found in the backbone providing a kink in the conformation. Neutral side chain branches mainly comprised of arabinose and galactose can also be found attached to the alternating sequences, these areas form 'hairy' non-gelling regions. Pectins are classified as either high-methoxyl (>50%) or low methoxyl (<50%) according to their degree of substitution. Most commercial low methoxyl pectins are reacted with ammonia to yield low methoxyl-amidated (LMA) pectins (Thakur, Singh et al. 1997). High methoxyl pectins are commonly used in jams as they form gels at low pH and high solid content (typically sugar). Low methoxyl pectins gel in the presence of calcium ions (Sakai, Sakamoto et al. 1993), and the use of amidated LM pectins reduces the amount of calcium required for gelation (Rolin 1993). Pectin has GRAS status (21 CFR 184.1588) and is listed in UK foods as E440 (Food Standards Agency 2005). The use of LMA

pectin in this study provides a polysaccharide carrying a similar charge to alginate but with a semi-branched conformation.

The use of pectin in anti-reflux medicines has also been investigated (Sugden and Hutchinson 1995; Cox 1996; Cox 1996; Eccleston and Paterson 2003); however no pectin based product is currently available on the UK market.

4.1.3 Carrageenan

Carrageenans are a group of linear galactan polysaccharides obtained from *Rhodophyceae* (red algal seaweeds). In this study the λ sub-type is used as a result of its high solubility and absence of gelling properties (Therkelsen 1993). λ-carrageenan differs from alginate, pectin and CMC as the anionic side chains are sulphate groups (Figure 4.1c). Carrageenans are most commonly used in the dairy sector, and serve as stabilizers, viscosifiers and gelling agents. Carrageenans are also used in gelled water deserts, bakery and meat products. Carrageenans also have GRAS status (21 CFR 172.620) and are permitted for use in food as additive E407 (Food Standards Agency 2005). The use of carrageenan will help understand the necessity of charge and how the charge is provided.

4.1.4 Maltodextrin

To investigate the necessity of molecular charge for phase separation, two non-ionic polysaccharides were chosen; maltodextrin and methylcellulose. Maltodextrin is a hydrolysis product, made by the degradation of starch using acid or enzymes (Chronakis 1998). It is sometimes known as ‘glucose polymer’ as it is made exclusively from glucose (Figure 4.1d). The degree of hydrolysis is expressed by a value known as the Dextrose equivalent (DE) which refers to the number of grams of reducing sugar present in 100g of material. The maltodextrin used in this study has a DE of 18 and is often used as a binder and/or diluent in solid dosage forms and is used in liquid

formulations to increase viscosity and inhibit crystallization. Maltodextrins are easily dispersible and highly soluble with a neutral, non-sweet taste (Cerestar 2005). Maltodextrin also has GRAS status (21 CFR 184.1444).

4.1.5 Methylcellulose

Methylcellulose, is a linear semi-synthetic cellulose ether (Doelker 1993). The introduction of methoxyl groups increases the solubility of the cellulose molecule by reducing the propensity for intramolecular hydrogen bonding. Its structure is shown in Figure 4.1e. Methylcellulose solutions show thermal properties unlike many other hydrocolloids. Whereas certain polysaccharides gel when the temperature is lowered, and melt when heated, methylcellulose shows the reverse. Above a critical temperature it gels, and when it is returned to ambient temperatures it liquefies. It has been proposed by Haque and Morris (1993) that the methylcellulose exists in solution as aggregated bundles held together by sparingly or unsubstituted regions and by hydrophobic aggregation of denser methoxylated regions. The elevation of temperature causes these bundles to disaggregate exposing methyl groups, causing a large increase in volume with the formation of a water constrained cage-like structure, and ultimately a hydrophobically cross-linked network. The temperature at which this occurs is influenced by the degree of substitution (Li, Thangamathesvaran et al. 2001). Methylcellulose also has GRAS status (21 CFR 182.1480) and can be found on UK labels as E461 (Food Standards Agency 2005).

Methylcellulose has a wide number of uses in wallpaper adhesives, paints, fertilizers, gypsum plaster, and detergents. In food products it is used in dressings to stabilize emulsions and its unusual thermal gelation properties are used in fried foods and bakery products. Methylcellulose is also used extensively in the pharmaceutical industry in tablet coatings, for controlled drug release and in ophthalmic preparations (Grover 1993).

4.1.6 Sodium polyacrylate

To further examine the interaction of xanthan with anionic polymers, Polyacrylate sodium, the sodium salt of poly(acrylic acid) (PAA) was chosen as a model anionic non-polysaccharide polymer. PAA has a regular repeating sequence (Figure 4.1f) and carries approximately 2.3 times more charge per monomer unit than alginate when comparing the mass to charge ratio.

Despite the nature of PAA, it has found use in the food industry. The American Food & Drugs Administration (FDA) has allowed its restricted use in food and it is used to control mineral scale during the evaporation of beet sugar juice or cane sugar juice in the production of sugar. Its use is limited and is under strict control and must meet the specification of having a weight average molecular weight of 2,000 to 2,300; and a weight average molecular weight to number average molecular weight ratio of not more than 1.3 (21 CFR 173.73).

4.1.7 Scleroglucan

To investigate the characteristics of xanthan that may be significant in separation, the neutral polysaccharide scleroglucan was chosen as a substitute for xanthan. Scleroglucan is a β 1→3 glucan with similar properties to xanthan. Scleroglucan has a glucose backbone, with a single glucose residue on every third glucose of the backbone (Figure 4.1g) (Brigand 1993). Scleroglucan adopts a rod-like triple helical structure in solution, and shows marked pseudoplasticity under the effects of shear (Sutherland 1994). The rheological properties of scleroglucan are also highly resistant to temperature and pH, providing characteristics comparable with xanthan (Coviello, Palleschi et al. 2005). Scleroglucan, like xanthan, can form weak gels in solution (Grassi, Lapasin et al. 1996) and is also capable of forming liquid crystalline phases (Yanaki, Norisuye et al. 1984). The principal difference between xanthan and scleroglucan with respect to this study is that scleroglucan carries no charge.

An unusual property of scleroglucan is that it has been shown to possess some biological activity. It has been shown to reduce cholesterol in a scleroglucan supplemented diet (Halleck 1970; Halleck 1970) and also to have anti-tumour properties (Komatsu, Kikumoto et al. 1970; Singh and Whistler 1974; Whistler, Bushway et al. 1976).

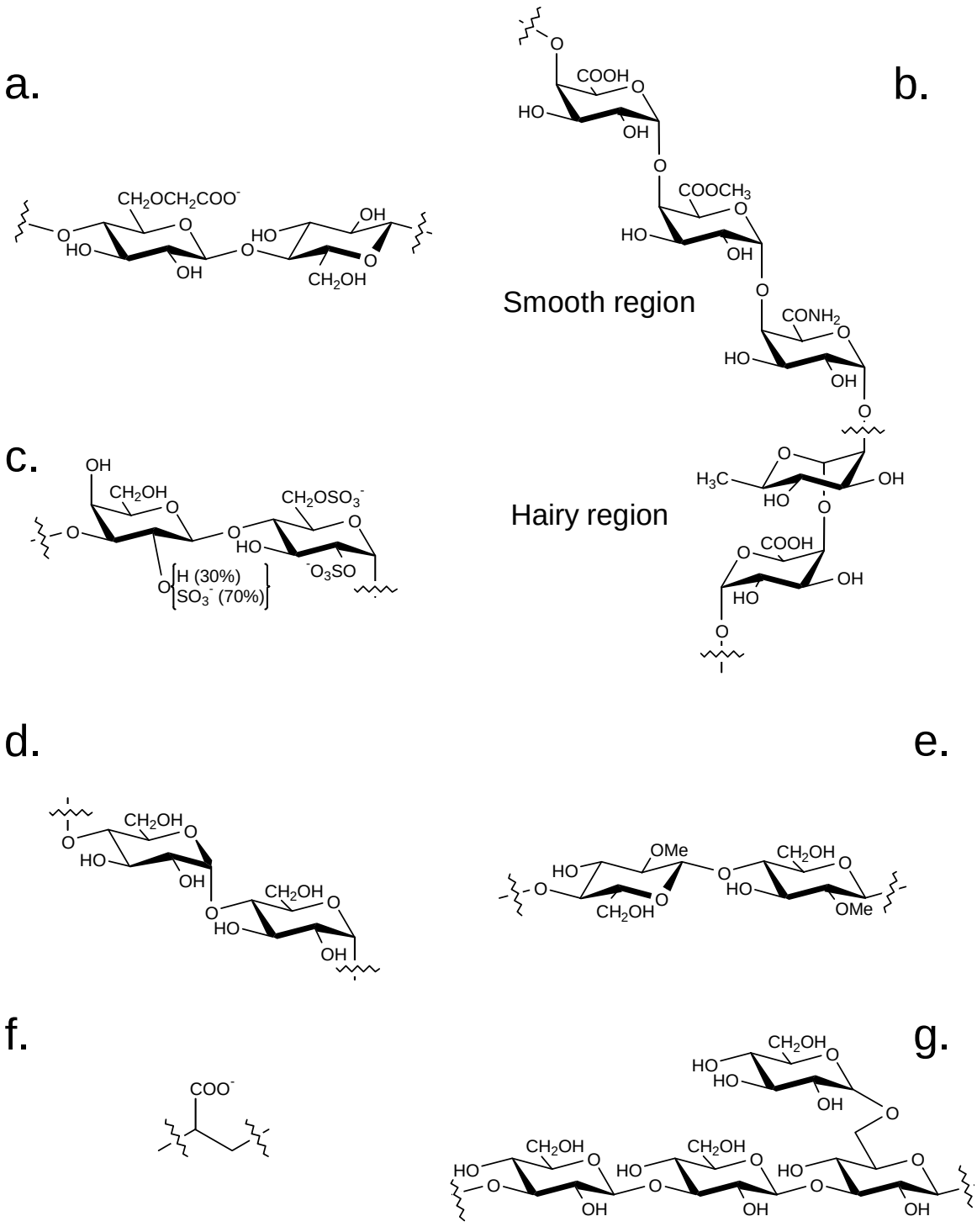

Figure 4.1. The monomeric subunits of the polymers used in this chapter.
(a) Carboxymethylcellulose; (b) pectin; (c) λ-carrageenan; (d) maltodextrin; (e) methylcellulose; (f) polyacrylic acid and (g) scleroglucan. The pectin shown shows the smooth and hairy regions, however the neutral side chains often found with the hairy regions have not been shown.

4.2 Aims

This chapter will examine the structural criteria required for the separation phenomena observed with mixtures of xanthan and alginate. It will specifically examine:

1. Whether this effect is exclusive to xanthan and alginate. Can one or both of the components be replaced?
2. The type of charge carried by the components and its necessity.
3. Is the polysaccharide nature of xanthan and alginate necessary, or can this be generalised further to include other polymeric systems?
4. Can the effect of alginate molecular weight be reproduced with other polymers?
5. Does the second component have to be a polymer?

These questions will be probed by using a number of different entities. The origin of separation properties is often complex and the use of different materials will provide an insight into the factors which may be necessary for separation.

The first and second aim will be investigated by studying a number of alternative polysaccharides including CMC which is structurally similar to alginate, pectin another carboxylated polysaccharide, carrageenan a sulphated polysaccharide, maltodextrin and methylcellulose both neutral polysaccharides and also scleroglucan, which is a stiff helical polysaccharide with many properties similar to xanthan. The third and fourth aims will be investigated by looking at mixtures composed of xanthan and sodium polyacrylate(s) as a model polymer. The fifth aim will be investigated by examining the effects of using Tetrasodium EDTA, a highly charged small molecule on solutions containing xanthan gum.

4.3 Materials and methods

4.3.1 Materials

The details of all the materials used are listed in Appendix 1

4.3.2 Preparation of concentrated polysaccharide solutions

Powders were analysed for moisture content as described in section 2.2.1, and weighings were adjusted to reflect the level of moisture present. Solutions were prepared by dispersion of the requisite amount of powder in water. A large surface area vortex was created using an Ika-Werke Eurostar Digital (Staufen, Germany) overhead stirrer using a Jiffy™ stirrer blade. The powder was added down the side of the created vortex. Solutions were then stirred until visually homogenous or in accordance with the suppliers directions (see individual polysaccharides).

4.3.2.a Carboxymethylcellulose

Carboxymethylcellulose was dispersed at room temperature for 20 minutes at 500 rpm.

4.3.2.b Pectin

Pectin (low methoxyl amidated type) was dispersed at 80^{o}C (Degussa Texturant Systems) in a specially constructed beaker enshrouded by a circulating water jacket (Figure 4.2) for 15 minutes at 500 rpm. The heat source was removed and the mixture was stirred at 50 rpm until cooled to room temperature.

4.3.2.c Carrageenan

Lambda carrageenan was dispersed at room temperature for 30 minutes at 1000 rpm.

4.3.2.d Maltodextrin

Maltodextrin was dispersed at room temperature for 20 minutes at 1000 rpm.

4.3.2.e Methylcellulose

Methylcellulose was dispersed in half of the requisite amount of water at 90^{o}C. This dispersion was then transferred to the fridge, and the remaining quantity of water (chilled to 4^{o}C) added (Colorcon 2002). The mixture was then stirred at 500 rpm for 10 minutes. The speed was the reduced to 50 rpm and left to stir overnight at 4^{o}C.

4.3.2.f Scleroglucan

Scleroglucan was dispersed at room temperature for 45 minutes at 1000 rpm.

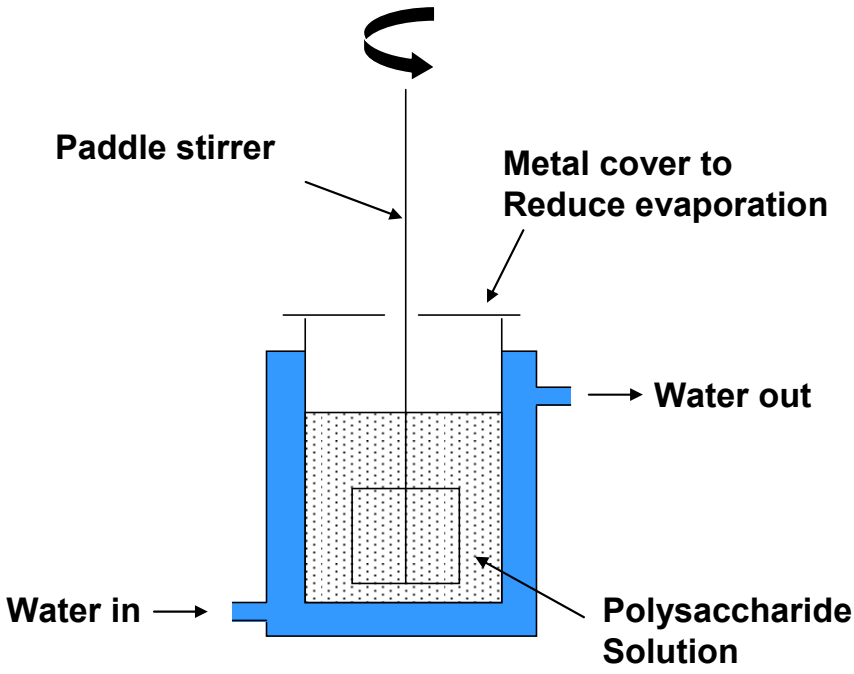

Figure 4.2. Water jacket system used for the dispersion of hydrocolloids at high temperature. Water was circulated through the jacketing system to allow the mixture inside to be dispersed at temperature greater than room temperature. The mixing vessel was covered with a metal lid to reduce water loss due to evaporation.

4.3.3 Preparation of concentrated sodium polyacrylate

Sodium polyacrylate samples were purchased as highly concentrated solutions. Using accurately determined moisture content values (method previously described in chapter 2), concentrated stock solutions were prepared by diluting with water and stirring at 500 rpm for 10 minutes.

4.3.4 Preparation of mixtures

Mixtures were prepared by the combination of concentrated stock solutions, adding water as necessary, to achieve the desired concentrations. These were then stirred at 1000 rpm for 5 minutes to effect mixing. In the case of the xanthan/methylcellulose mixtures, a speed of 500 rpm for 10 minutes was used to reduce frothing. All mixtures were allowed to stand overnight at 4^{o}C prior to testing.

4.3.5 Rheology

Viscoelastic properties were analysed as previously described in section 2.2.3 using a 4^{o}/40mm cone and plate geometry on a CVOR digital controlled stress rheometer (Bohlin Instruments, Cirencester UK). Each sample was thermally equilibrated to 25 ± 0.1^{o}C for a minimum of 60 seconds prior to testing. An amplitude sweep was performed for each individual mixture to ensure measurements were performed in the linear viscoelastic region.

4.3.6 Polyelectrolyte titration

The phase composition diagram for mixtures of xanthan gum and CMC in water was established using the polyelectrolyte titration method described in section 2.2.4. Standard curves for xanthan and CMC were prepared to establish the equation for calculating the phase compositions. The equations used were:

$$V = 1.343X + 3.684C \quad (4.1)$$

$$T = X + C \quad (4.2)$$

where V is the volume of titrant required to neutralise the charge; X is the mass of xanthan in the sample; C is the mass of CMC in the sample; T is the total dry polysaccharide mass in the sample.

4.3.7 Microscopy

Crossed polarised light microscope images were obtained using the method described in section 2.2.6 at room temperature.

4.3.8 Scanning electron microscopy (SEM)

A mixture containing 1% xanthan and 5% PAA (30 kDa) was prepared as described above. A drop of this solution was dropped on to an adhesive carbon SEM stub and allowed to air dry. The stub was sputter coated with a thin gold film using an SCD030 gold coater (Balzers Union, FL9496) for 4 minutes at 30 mA. These settings are known to provide a coating of approximately 25 nm which is suitable for SEM imaging. The gold coated sample was then imaged using an SEM 505 (Phillips, Holland) at 25.0 keV.

4.4 Results and discussion

4.4.1 Mixtures of carboxymethylcellulose and xanthan

The effect on viscoelastic properties of adding a low viscosity grade CMC to 1% xanthan gum as a function of concentration is shown in Figure 4.3. Low concentrations of CMC (0.5%) had little effect on the viscoelastic parameters. Further addition of CMC up to 1.125% showed a dramatic decrease in G', and to a lesser extent G", with a corresponding increase in tan delta suggesting a change from elastic like behaviour to more viscous behaviour. At high concentrations (>1.25%), G' and G" remained low. This would suggest that the addition of CMC above 0.5% causes the viscoelastic properties of xanthan to be diminished. This effect is similar to that previously observed with xanthan:alginate mixtures in section 3.4.3.

The viscoelastic changes with respect to frequency observed when 2% CMC was added to xanthan are shown in Figure 4.4. Xanthan is G' dominant at all frequencies and increases in a frequency dependent manner. The mixture shows small values for both G' and G" indicating essentially non-viscous properties. Figure 4.5 shows a crossed polarised light microscope image of the 1% xanthan:2% CMC mixture. Distinct birefringent regions can be observed indicating phase separation has occurred.

The phase composition diagram of xanthan:CMC mixtures (Figure 4.6) was obtained using the polyelectrolyte titration technique. It shows that the disperse phase composition is rich in xanthan gum whilst the continuous phase is solely composed of CMC. The shape of the binodal indicates that the separation is segregative in type and is asymmetrical. These results suggest that the separation observed for xanthan:alginate mixtures is not exclusive to alginate, but can also be extended to CMC.

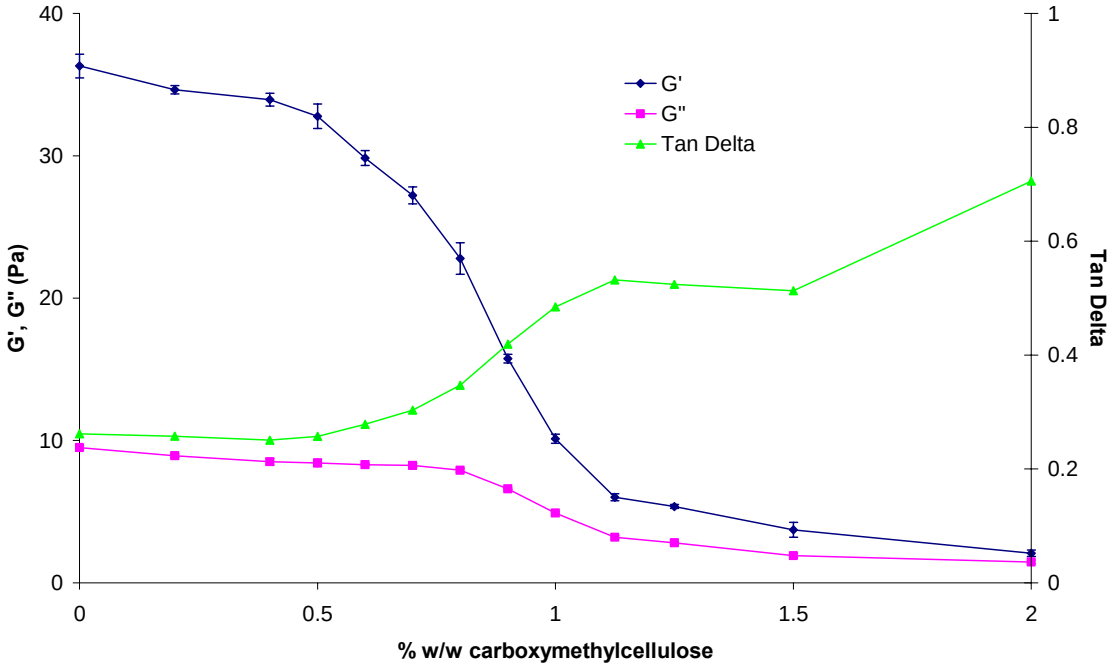

Figure 4.3. The effect of increasing concentrations of CMC on the viscoelastic properties of 1% xanthan gum.
See appendix 1 for details of the CMC used in this experiment.
Frequency = 1.02Hz Geometry = CP 4°/40mm. Temperature = 25 ± 0.1°C. Mean ± SD, n=3.

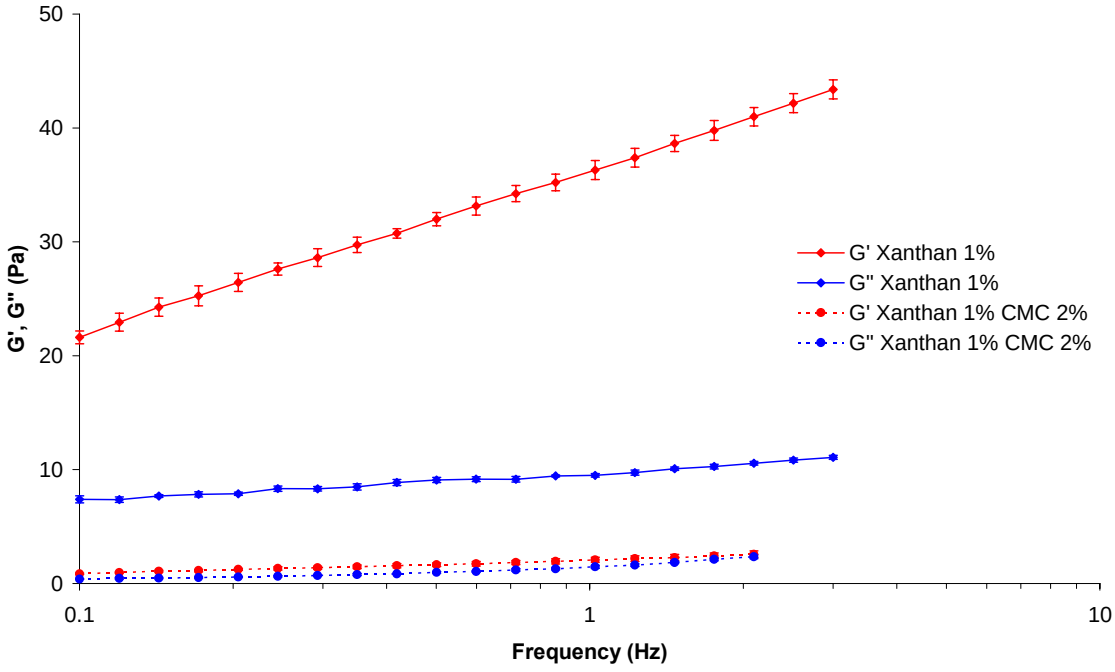

Figure 4.4. The effect of CMC on the overall viscoelastic properties of xanthan gum.
See appendix 1 for details of the CMC used in this experiment.
Geometry = CP 4°/40mm. Temperature = 25 ± 0.1°C. Mean ± SD, n=3.

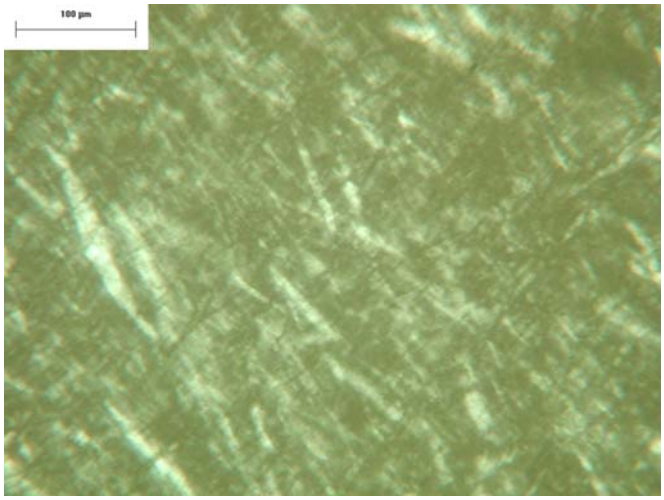

Figure 4.5. A light microscope image taken between crossed polarising lenses of a mixture of 2% CMC with 1% xanthan.

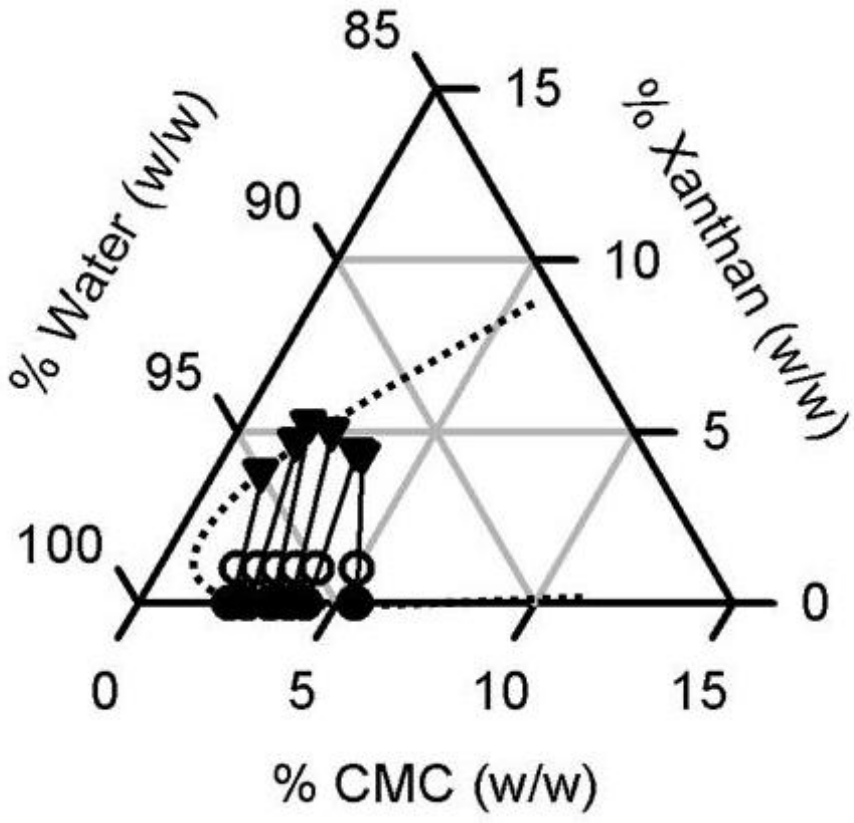

Figure 4.6. The ternary phase composition diagram for xanthan gum and sodium carboxymethylcellulose.
(O) Overall mixture composition; (▼) disperse phase; (●) Continuous phase.
The dotted line represents an approximation of the binodal indicating the concentrations where phase separation occurs.

4.4.2 Mixtures of LMA pectin and xanthan

Pectin is a branched carboxylated polysaccharide therefore making it structurally different from both alginate and CMC. The following experiments investigated if pectin has similar effects on xanthan to that of alginate and CMC.

Figure 4.7 and Figure 4.8 examine the effects of adding a low methoxyl amidated pectin to xanthan gum. Low concentrations of pectin (< 2%) caused an increase in the elastic modulus suggesting an additive effect between xanthan and pectin. Higher concentrations of pectin showed the decrease in G' and a corresponding increase in tan delta. This is similar to that previously observed in the xanthan:alginate mixtures suggesting a change from the weak gel-like properties of xanthan to a more viscous-like system. The image shown in Figure 4.9 shows birefringence, further suggesting that xanthan:pectin mixtures also phase separate.

This evidence would suggest that the separation phenomenon is not restricted to linear anionic polysaccharides, but can also be observed with branched polysaccharides.

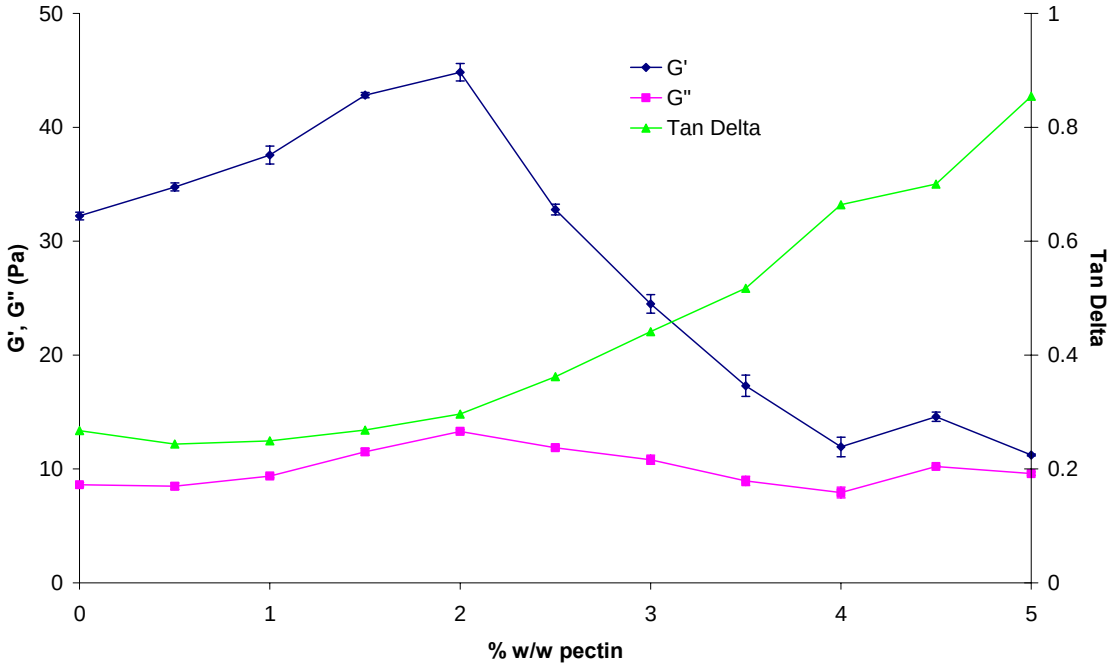

Figure 4.7. The effect of increasing concentrations of pectin on the viscoelastic properties of 1% xanthan gum.
The pectin used in this experiment was a low methoxyl amidated pectin.
Frequency = 1.02Hz Geometry = CP 4°/40mm. Temperature = 25 ± 0.1°C. Mean ± SD, n=3

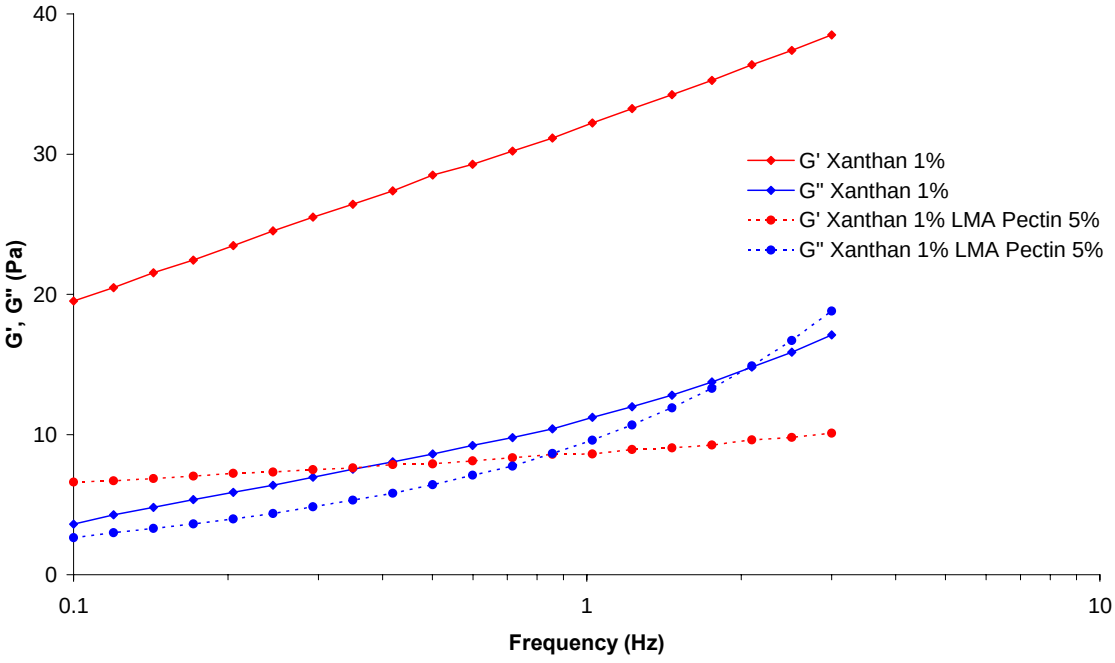

Figure 4.8. The effect of pectin on the overall viscoelastic properties of xanthan gum.
The pectin used in this experiment was a low methoxyl amidated pectin.
Geometry = CP 4°/40mm. Temperature = 25 ± 0.1°C. Mean ± SD, n=3..

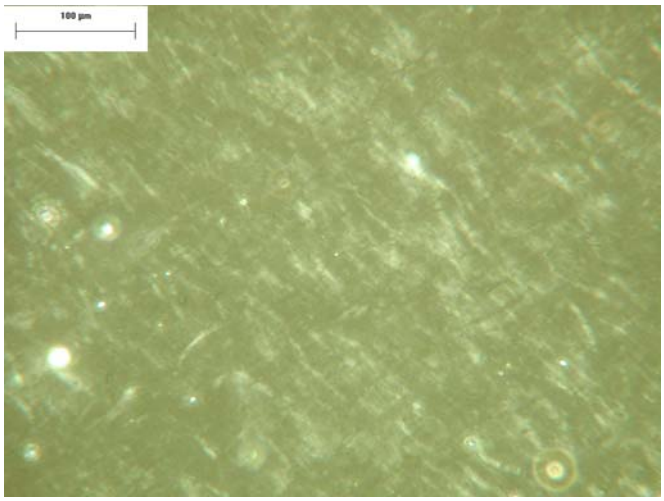

Figure 4.9. A light microscope image taken between crossed polarising lenses of a mixture of 5% LMA pectin with 1% xanthan.

4.4.3 Mixtures of λ-carrageenan and xanthan

Carrageenans are sulphated linear polysaccharides. A lambda type carrageenan was chosen for this experiment as it is non-gelling, unlike the other carrageenan subtypes. The use of carrageenans will establish whether or not the phase separation with xanthan is restricted to carboxylated polysaccharides, or whether other anionic moieties are sufficient.

Figure 4.10 and Figure 4.11 show the effects of adding a lambda carrageenan to xanthan gum. Low concentrations (< 0.75%) of carrageenan caused a decrease in the viscoelastic parameters. This is similar to that previously observed with the alginate, CMC and pectin. Above 0.75% G' and G" increased in a concentration dependent manner. The viscoelastic profile showed that the addition of carrageenan to xanthan changes the overall properties form a weak-gel system to a concentrated solution (Steffe 1996) which would typically be demonstrated by a lambda carrageenan solution. Figure 4.12 shows that although the clearly defined strands seen with the xanthan/alginate mixture cannot be seen, there is still a strong birefringence, suggesting the presence of separation.

This evidence suggests that the phase separation in xanthan mixtures can be generalised to anionic polysaccharides, not simply those with carboxylate moieties. As a result of the separation observed in the mixtures containing pectin and carrageenan, it would suggest that the interactions with xanthan are non-specific.

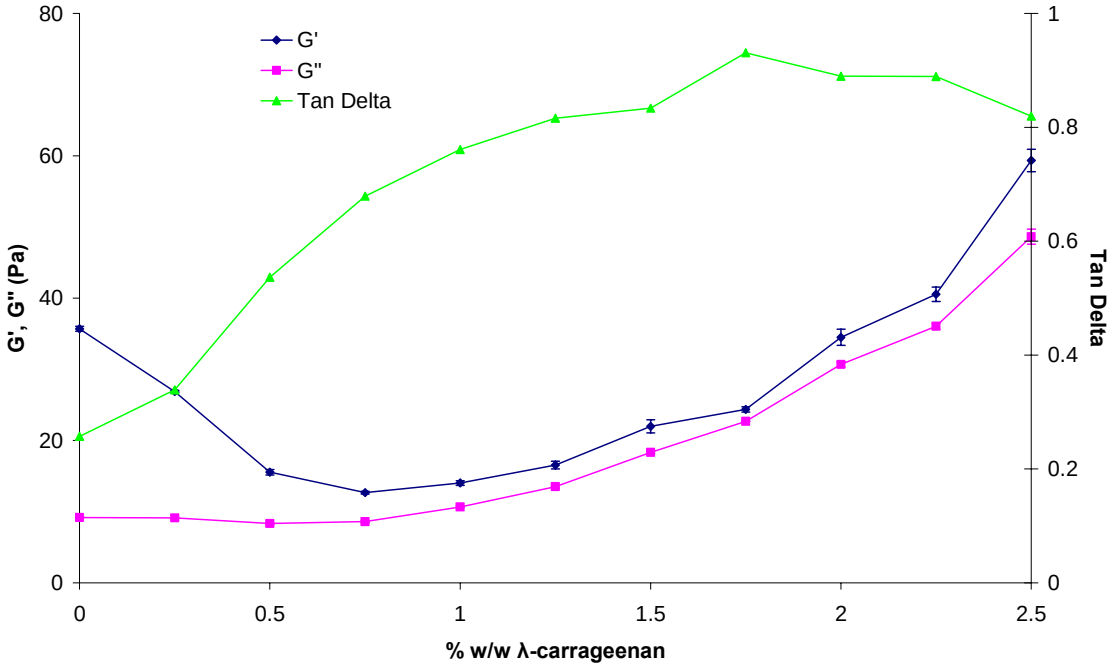

Figure 4.10. The effect of increasing concentrations of carrageenan on the viscoelastic properties of 1% xanthan gum.
The carrageenan used in this experiment was a lambda carrageenan.
Frequency = 1.02Hz Geometry = CP 4°/40mm. Temperature = 25 ± 0.1°C. Mean ± SD, n=3

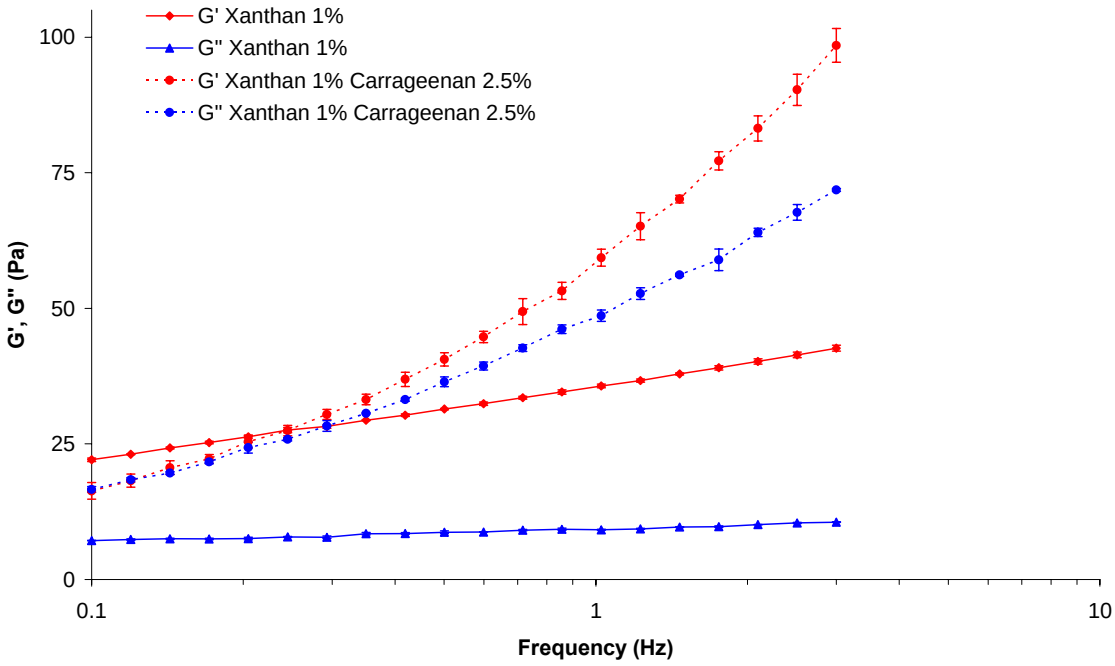

Figure 4.11. The effect of carrageenan on the overall viscoelastic properties of xanthan gum.
The carrageenan used in this experiment was a lambda carrageenan.
Geometry = CP 4°/40mm. Temperature = 25 ± 0.1°C. Mean ± SD, n=3.

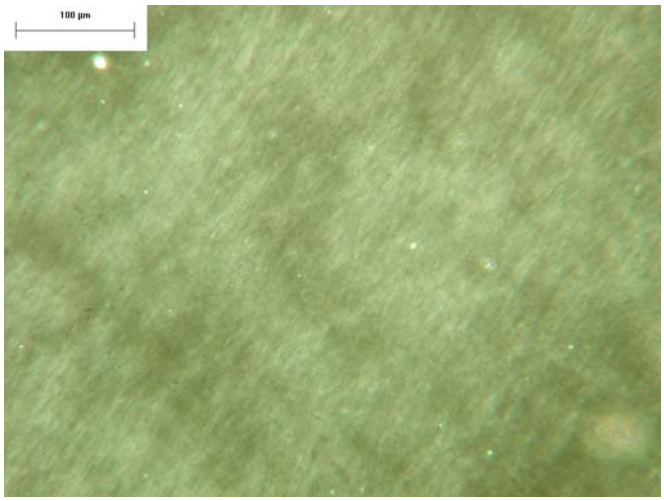

Figure 4.12. A light microscope image taken between crossed polarising lenses of a mixture of 2.5% λ-carrageenan with 1% xanthan.

4.4.4 Mixtures of maltodextrin and xanthan

To establish the necessity of an anionic charge, neutral polysaccharides were mixed with xanthan gum to see if phase separation occurred.

The rheological properties of mixtures of maltodextrin and xanthan gum are shown in Figure 4.13 and Figure 4.14. They indicate that maltodextrin at concentrations up to 25% had little effect on the rheological properties of xanthan. A small change is evident in Figure 4.14; however, this can be explained by the reduction in overall water content by 24%, effectively increasing the xanthan concentration from 1% to 1.32%. The lack of mesophase formation when viewed microscopically further supports the evidence that separation in this system did not occur.

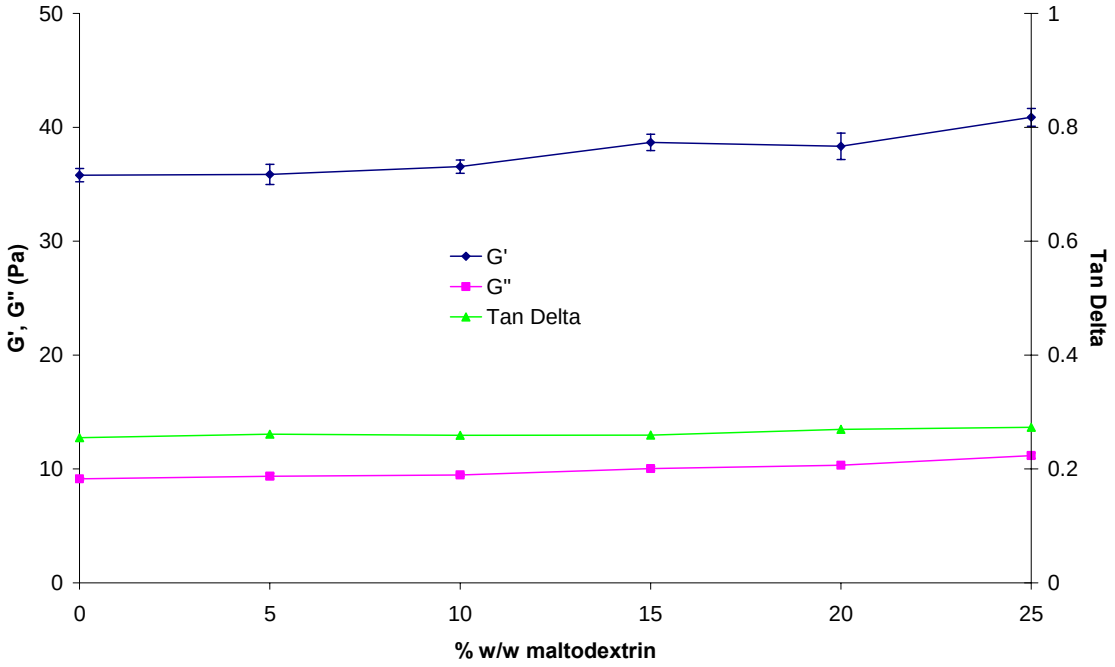

Figure 4.13. The effect of increasing concentrations of maltodextrin on the viscoelastic properties of 1% xanthan gum.
The maltodextrin used in this experiment had a dextrose equivalent (DE) value of 18.
Frequency = 1.02Hz Geometry = CP 4°/40mm. Temperature = 25 ± 0.1°C. Mean ± SD, n=3

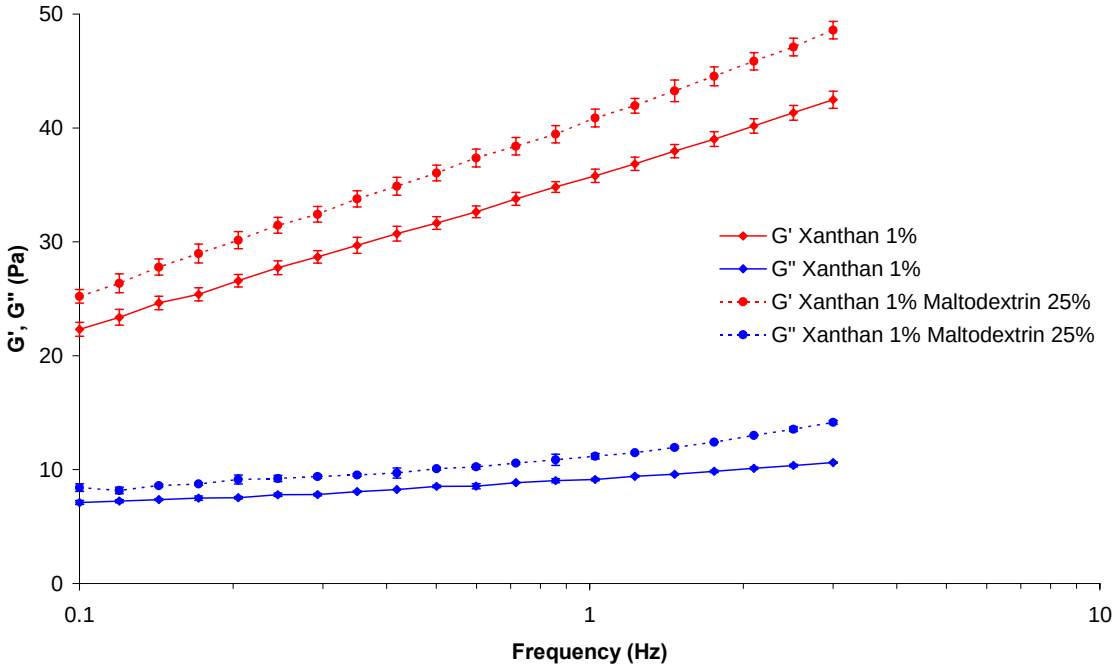

Figure 4.14. The effect of maltodextrin on the overall viscoelastic properties of xanthan gum.
The maltodextrin used in this experiment had a dextrose equivalent (DE) value of 18.
Geometry = CP 4°/40mm. Temperature = 25 ± 0.1°C. Mean ± SD, n=3.

4.4.5 Mixtures of methylcellulose and xanthan

Figure 4.15 and Figure 4.16 show how methylcellulose has a similar rheological profile to xanthan gum and exhibits weak gel-like properties in solution. The mixture exhibits viscoelastic moduli much higher than the individual polysaccharides suggesting the interact co-operatively. The lack of mesophase formation when viewed under the microscope confirms separation has not occurred.

The results from these neutral polysaccharides would strongly suggest that a charge is necessary for the xanthan mesophases formation to occur. It is likely that the charge must also be anionic in nature as a cationic polysaccharide would form attractive electrostatic interactions with the xanthan gum side chains preventing a segregative separation.

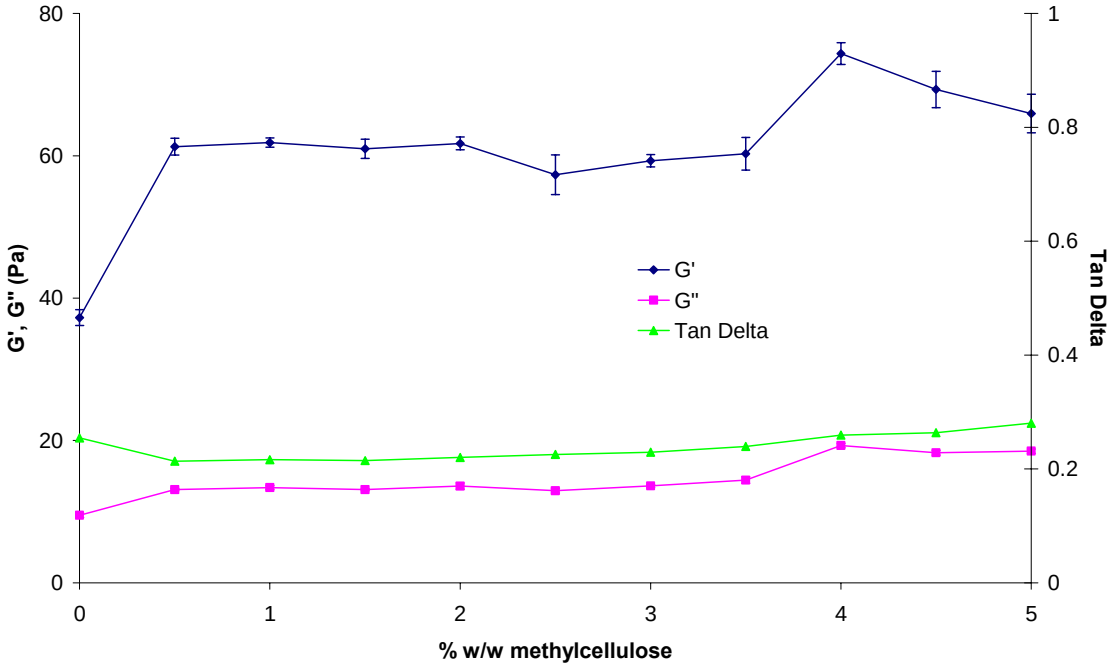

Figure 4.15. The effect of increasing concentrations of methylcellulose on the viscoelastic properties of 1% xanthan gum.
The methylcellulose in this experiment was Methocel A15LV, a low viscosity grade methylcellulose. Frequency = 1.02Hz Geometry = CP 4°/40mm. Temperature = 25 ± 0.1°C. Mean ± SD, n=3

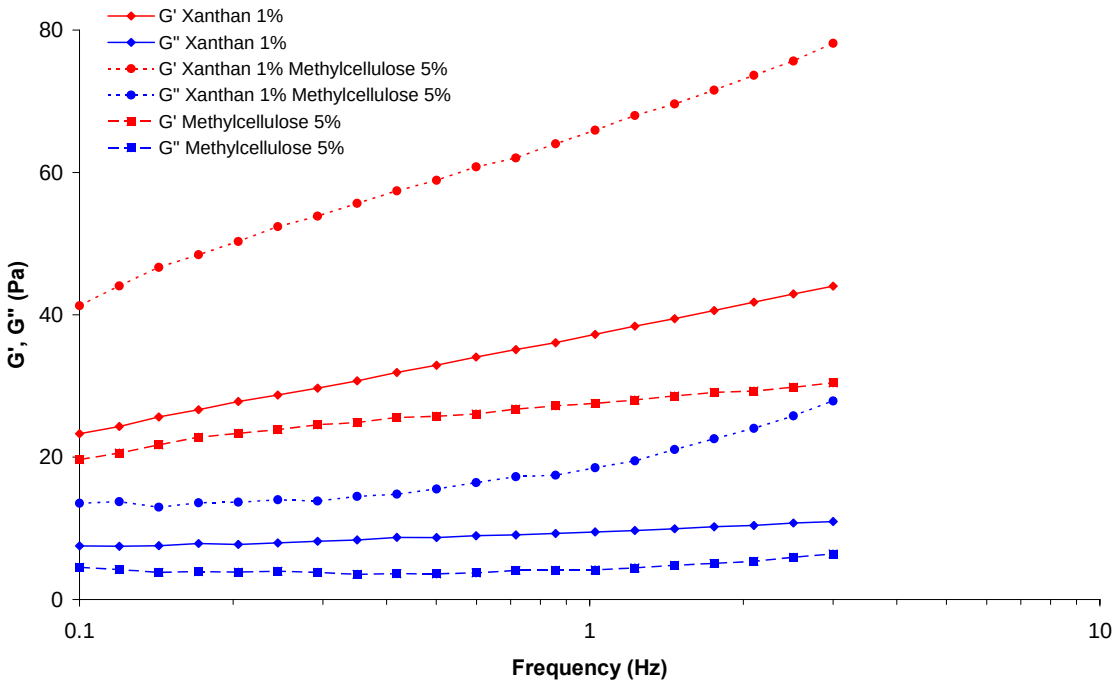

Figure 4.16. The effect of methylcellulose on the overall viscoelastic properties of xanthan gum.
The methylcellulose in this experiment was Methocel A15LV, a low viscosity grade methylcellulose. Geometry = CP 4°/40mm. Temperature = 25 ± 0.1°C. Mean ± SD, n=3.

4.4.6 Mixtures of polyacrylic acid and xanthan

Sodium polyacrylate was chosen as a model non-polysaccharide polymer. It has regular repeating linear hydrocarbon backbone with a carboxylate group on every alternate backbone carbon. This highly charged polymer is used here as a model anionic non-polysaccharide macromolecule, to examine if the sugar ring of polysaccharides is necessary for phase separation.

The effect of sodium polyacrylate (8 kDa) concentration on the viscoelasticity of 1% xanthan gum is shown in Figure 4.17. At low concentrations, the elastic modulus increased, suggesting a strengthening of the weak-gel like state. It is probable that this may be a consequence of the raised sodium levels in the solution. At higher concentrations (> 5.75%) it can be seen that the elastic modulus decreases dramatically.

The effect of molecular weight was studied using three different molecular weight polyacrylates. Figure 4.18 shows the effect of these on viscoelasticity with respect to polyacrylate concentration. All three polyacrylates exhibited a drop in G', the concentration required to elicit this drop decreased with increasing molecular weight. This again agrees with the work shown previously in section 3.4.12 where a number of different alginate samples were studied.

Figure 4.19 shows polarised light micrographs of a 1% xanthan:5% PAA (30 kDa) mixture. The images are of the same mixture but from differing areas on the slide. Mesophase formation can be observed however they differ in morphology and size from those previously observed. They are significantly bigger (5 - 150μm) and in Figure 4.19b clear striations can be seen. The origin of these striations is unknown but it is possible that the mesophases could be adopting a helical conformation such as a xanthan 'super-helix'. It is also possible that the striations could be derived from the many individual xanthan helices within the mesophases packing in such a way that causes this appearance as a result of light diffraction, perhaps similar to that exhibited by collagen (Lin and Goh 2002).

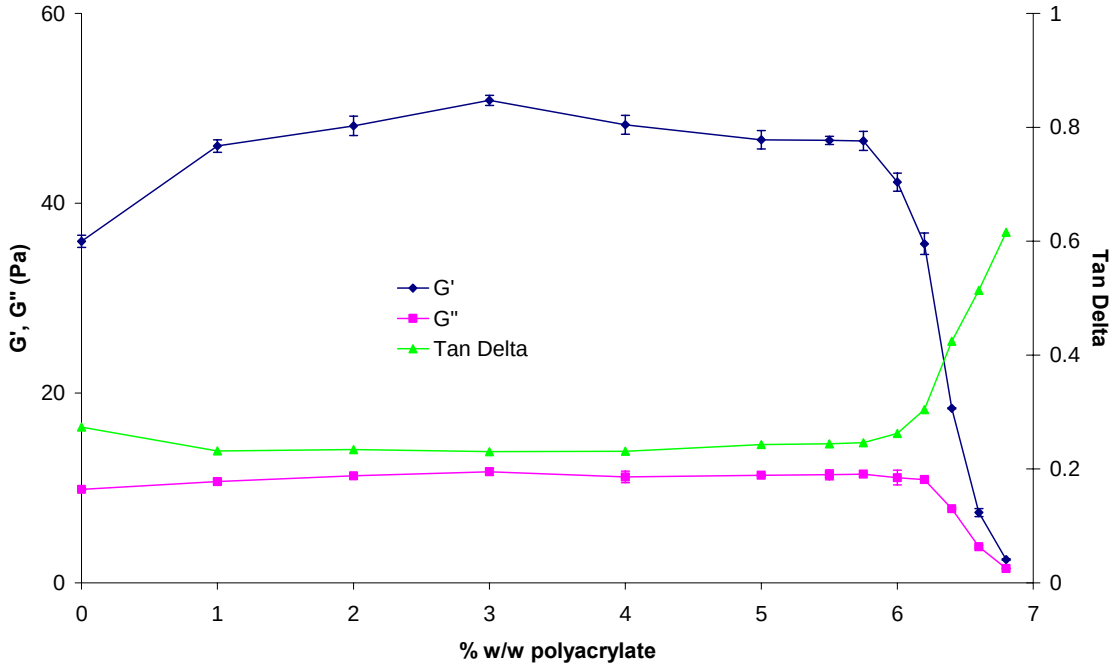

Figure 4.17. The effect of increasing concentrations of sodium polyacrylate on the viscoelastic properties of 1% xanthan gum.
Mw = 8 kDa. Frequency = 1.02Hz Geometry = CP 4°/40mm. Temperature = 25 ± 0.1°C. Mean ± SD, n=3

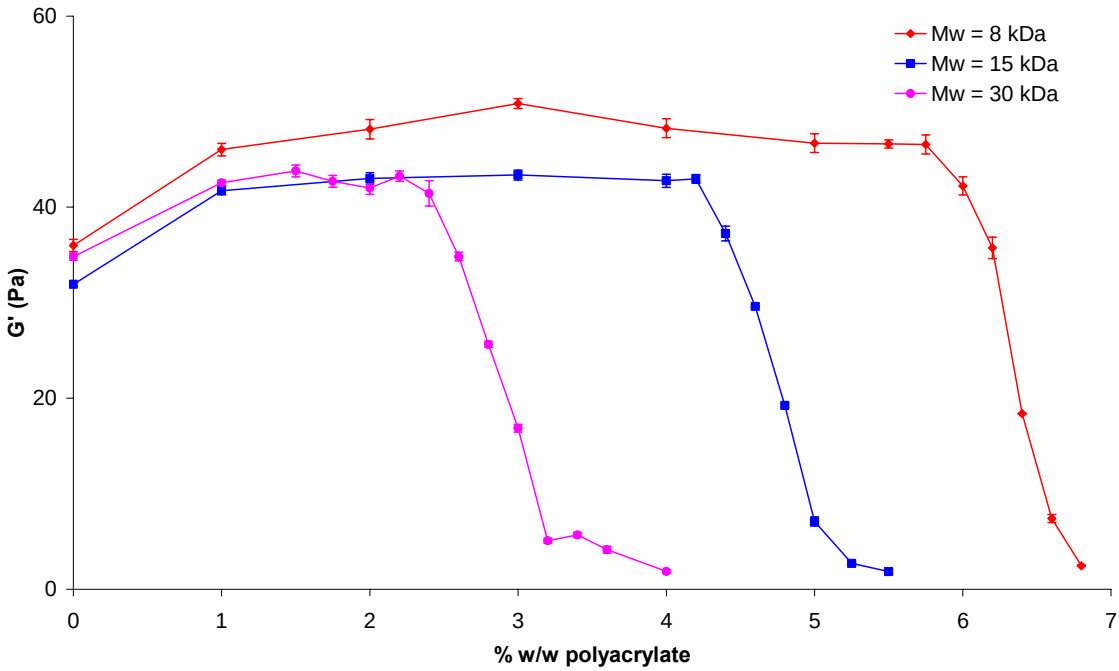

Figure 4.18. The effect of varying molecular weight sodium polyacrylates on the viscoelasticity of 1% xanthan gum.
Frequency = 1.02Hz Geometry = CP 4°/40mm. Temperature = 25 ± 0.1°C. Mean ± SD, n=3

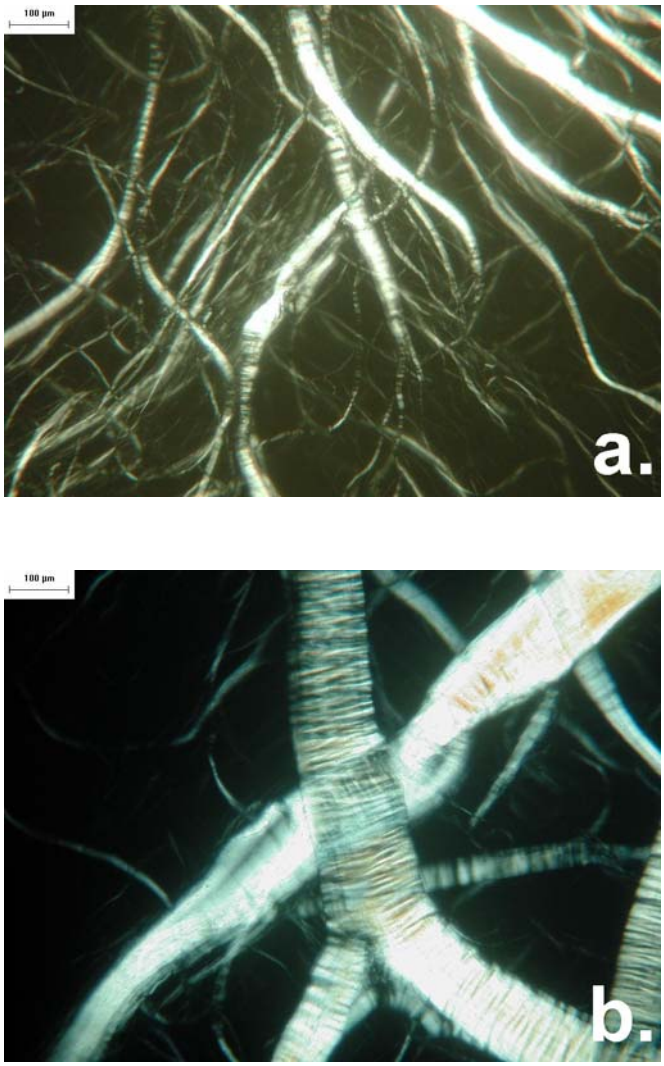

Figure 4.19. A light microscope image taken between crossed polarising lenses of a mixture of 5% PAA with 1% xanthan.
Mw = 30 kDa. Images (a) and (b) are images taken from the same sample but at different locations on the slide.

4.4.7 Mixtures of scleroglucan and alginate

Scleroglucan is a polysaccharide that adopts a stiff rod-like conformation in solution but has neutral rather than charged side chains. It has also been reported to form birefringent mesophases at high concentration (Yanaki, Norisuye et al. 1984). In this experiment it is used to investigate whether the charged nature of xanthan is a controlling factor in phase separation and whether it could be used in place of xanthan.

In Figure 4.20 and Figure 4.21 it can be seen that alginate has no significant effect on the viscoelastic properties of scleroglucan, even at high concentrations. The 1% scleroglucan: 5% alginate mixture showed no evidence of birefringence under crossed polarized microscopy. These results would suggest that phase separation in xanthan:alginate mixtures requires the presence of the charged side chain moiety in the xanthan structure.

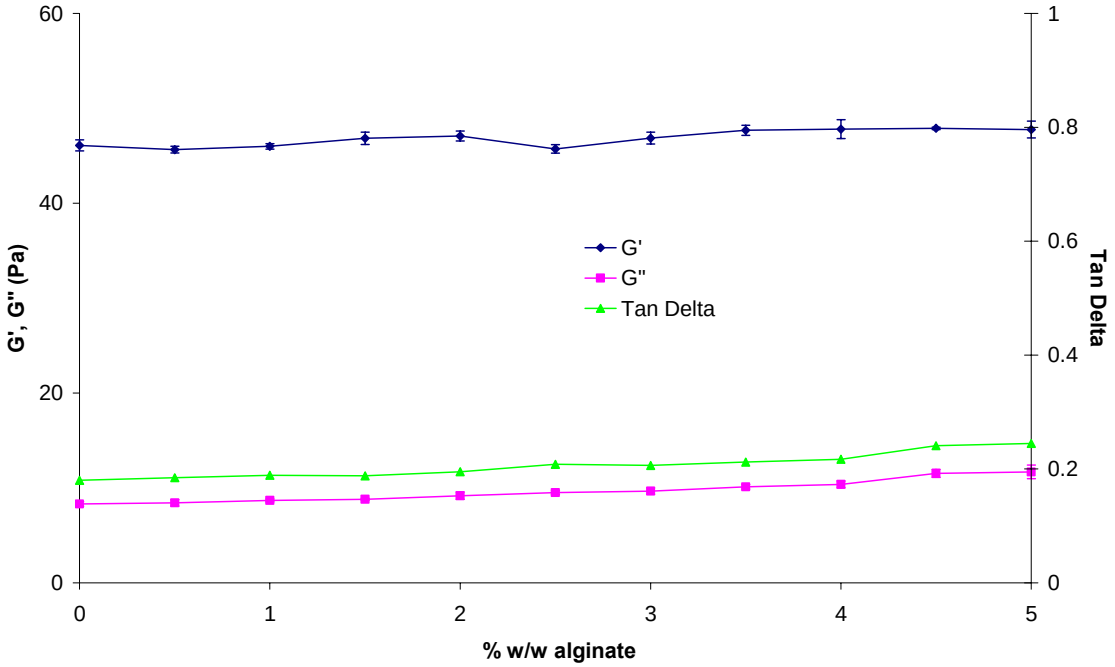

Figure 4.20. The effects of increasing concentrations of sodium alginate on the viscoelastic properties of 1% scleroglucan.
The alginate used in this experiment was Protanal LFR 5/60.
Frequency = 1.02Hz Geometry = CP 4°/40mm. Temperature = 25 ± 0.1°C. Mean ± SD, n=3

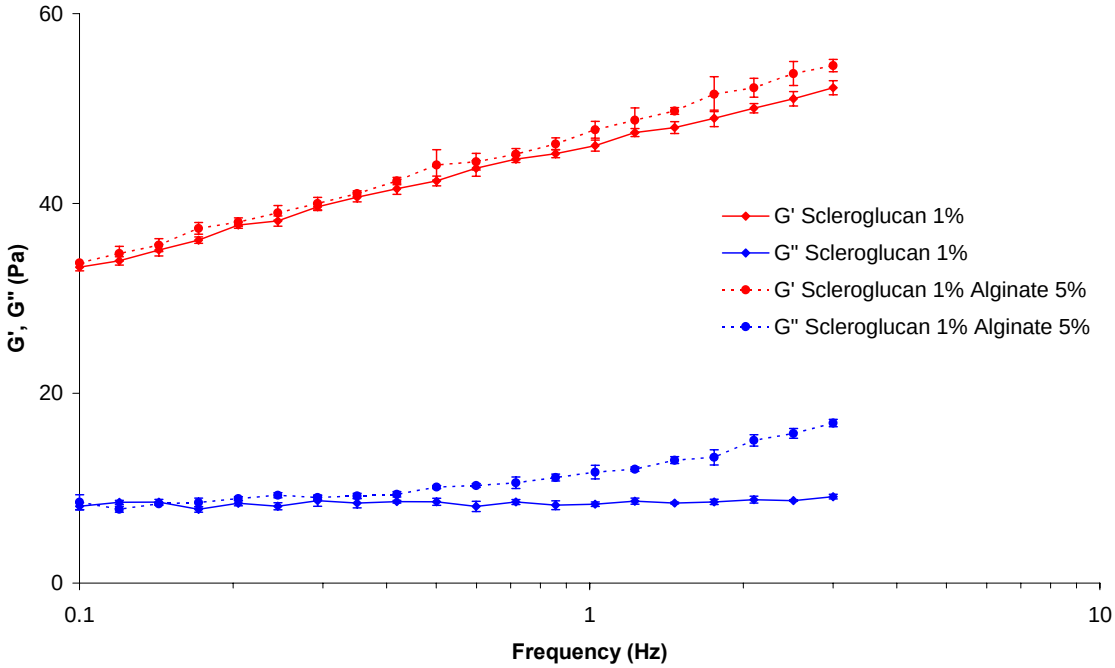

Figure 4.21. The effects of sodium alginate on the overall viscoelastic properties of Scleroglucan.
The alginate used in this experiment was Protanal LFR 5/60.
Geometry = CP 4°/40mm. Temperature = 25 ± 0.1°C. Mean ± SD, n=3.

4.4.8 Mixtures of xanthan and highly charged small molecules

The sodium salt of ethylenediamine tetra-acetic acid (EDTA) is a highly charged molecule with a molecular weight of 380 Da. It was used here to investigate whether a a highly charged small molecule can be substituted for a lower charge density polymer.

No birefringence was seen in a mixture of 1% xanthan and 50% EDTA. This suggests that the xanthan in solution is not concentrating into strands. This would imply that the polymeric nature of the second component is important to phase separation.

4.4.9 Scanning electron microscopy of a xanthan:polyacrylate blend

To further investigate the striated appearance of the strands in Figure 4.19b, scanning electron microscopy (SEM) was used to examine strand structure and surface topography at a higher resolution than light microscopy. The principal drawback with respect to our samples is the volume changes and solvent removal artifacts as a result of sample preparation and imaging under vacuum. Nevertheless micrographs may provide some confirmatory evidence of bundle morphology.

SEM images of a mixture of 1% xanthan gum and 5% PAA (30 kDa), at different magnifications, are shown in Figure 4.22. The images clearly show the strand-like nature of the sample. The images suggest that the large strands observed are made by deposition of a number of smaller strands to create a larger one. Although there is evidence of a slight twisting pattern in Figure 4.22b none of the images show a truly helical deposition that could correspond to the striations shown in Figure 4.19 suggesting the striations are more likely to be as a result of a complex light diffraction pattern. This pattern could also be a result of changes in diffraction due to internal differences in composite strand size; it may also be possible that the smaller strands making up the larger ones may not be packing uniformly, creating voids in the structure and allowing light to pass through more easily in some places than in others.

Figure 4.22f shows that by using SEM, strands of the size of a single micron can be seen, much smaller than that observed using light microscopy. Despite the solvent having been driven off, there is evidence that a bi-continuous network may have been present with the xanthan rich phase (Figure 4.22c) forming a continuous network interspersed throughout the alginate continuous phase, as opposed to a true disperse phase in a continuous phase.

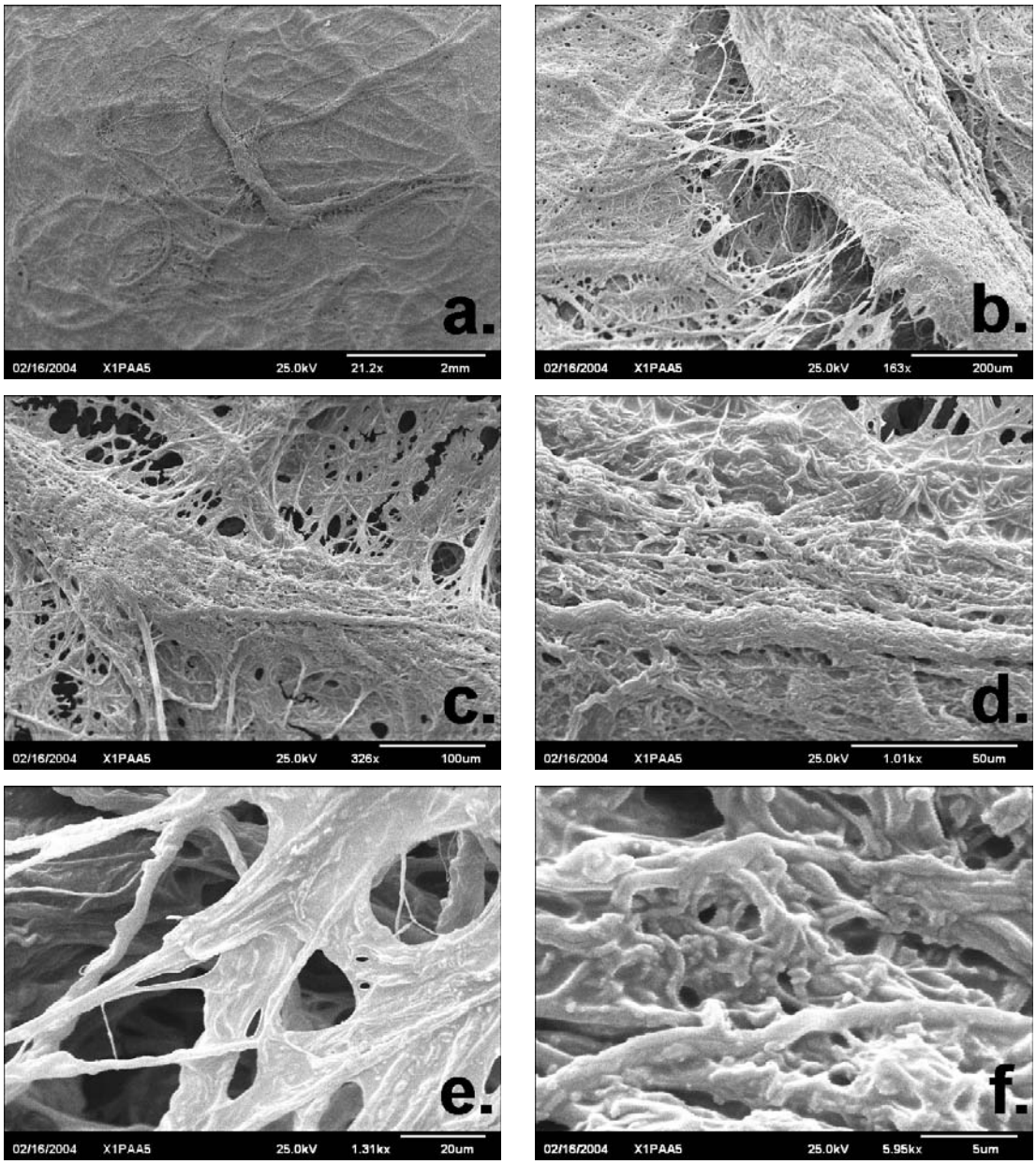

Figure 4.22. Scanning electron micrograph images of a dried film 1% xanthan with 5% polyacrylate.
The images are increasing magnifications of the same sample (a) 21.2x magnification, (b) 163x magnification, (c) 326x magnification, (d) 1010x magnification, (e) 1310x magnification and (f) 5950x magnification (Mw = 30 kDa).

4.5 Conclusions

This chapter has investigated a number of key factors involved in the phase separation of xanthan mixtures. It has clearly been shown that separation is not restricted to sodium alginate, but can be generalised to that of an anionic polymer which can derive its anionic charge from carboxylate or sulphate groups. It has also been shown that this effect is not exclusive to polysaccharides. The phase composition analysis of the xanthan:CMC mixtures showed that the disperse phase was predominantly xanthan in a similar way to that shown with alginate, providing an explanation for the loss of weak gel-like properties on separation. The decrease in the threshold concentration for separation with increasing polyacrylate molecular weight was in agreement with the work on alginate molecular weight in chapter 3.

Phase separation is often perceived as a problem that is a hindrance to pharmaceutical formulators and food technologists alike as it can cause instability. However, the use of phase separation as a tool for modulating properties is becoming more widespread. The key to this is that systems are understood and exploited accordingly (Tolstoguzov 2003).

This wide range of choices for the second polymer provides many different mixture properties as the continuous phase dominates the overall behaviour. The use of pectins and carrageenans raises ideas of how xanthan may potentially modify gel structure and textures in food products. The use of CMC creates potential ideas for use in household products. The use of PAA opens a wide range of potential in non-food and pharmaceutical areas.

Chapter 5

Modulating the phase separation phenomenon

5.1 Introduction

In the preceding chapters the factors affecting phase separation between xanthan and anionic polymers have been investigated. The focus has been principally on the solution property changes that occur when moving from the homogenous regions of the phase diagram to the heterogeneous, phase separated region. Phase separation is often viewed as a significant hindrance in the formulation of food and pharmaceutical products. This chapter examines the effect of moving from the phase separated region to the homogenous region to investigate whether this could provide anything useful for exploitation.

There are two principal approaches which may be used to investigate this transition. The first would be to change the composition of the system such that the mixture moves directly from the heterogeneous to homogenous state. This could be a simple dilution, or removal of either of the components, for example by chemical chelation or a pH related solubility change. The second is to maintain the system composition and move the phase separation boundary (the binodal line). This could be achieved by altering the

thermodynamic state of the mixture. The two strategies are illustrated diagrammatically in Figure 5.1.

5.2 Aims

This chapter examines some of the possible ramifications and applications of the work outlined in chapters 3 and 4, and in particular it will address:

1. The consequences of traversing the phase boundary from separated to non-separated by the addition of water.
2. If these mixtures were to be used as a pharmaceutical or food product, then what would be the effect of traversing the boundary in a Gastric pH environment?
3. Can ionic species be used to enhance or modify any dilution effects?
4. What role does temperature have on the dilution effects?
5. Can the method of the mixture preparation be altered to yield further advantages?
6. Can the xanthan gum/locust bean gum interaction be used to enhance the system further?

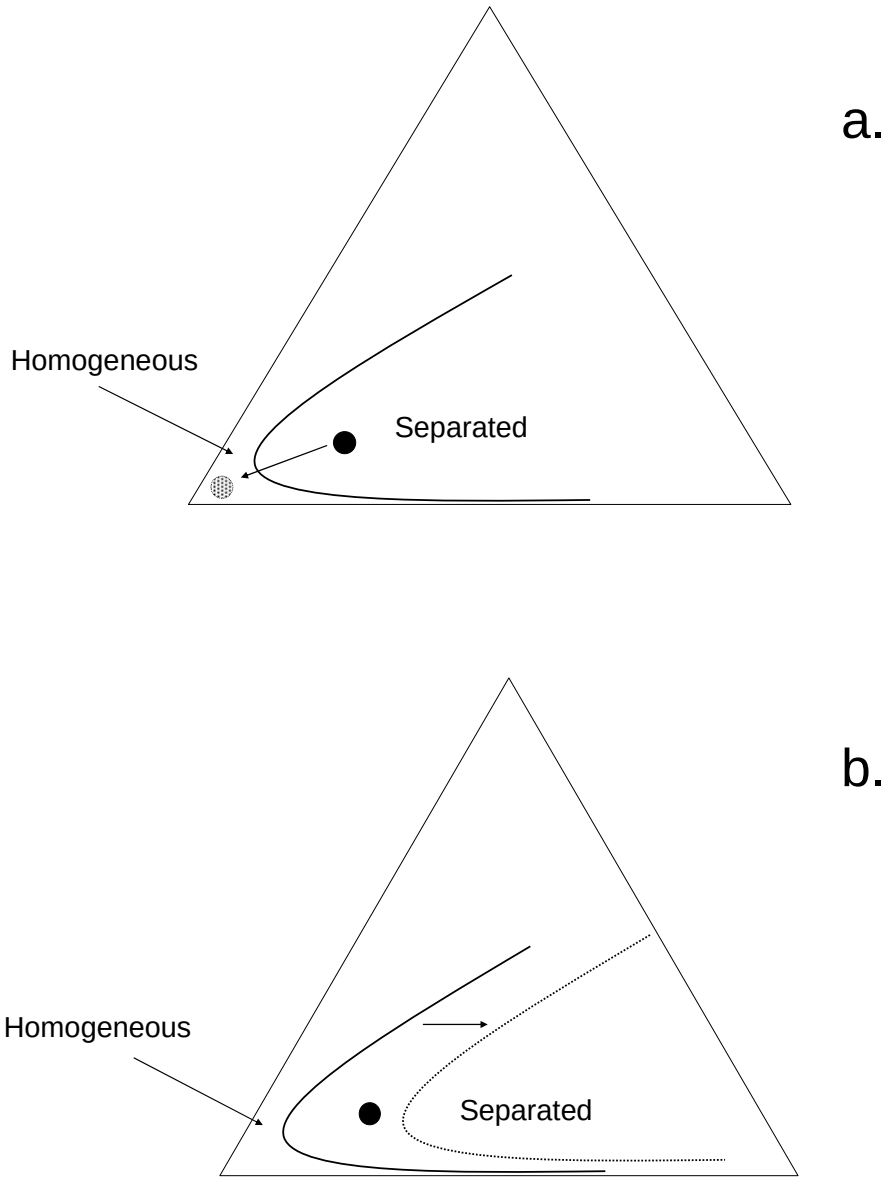

Figure 5.1. Strategies for investigating the transition from separated to homogeneous system. Transition can occur by altering (a) the concentration of the mixture to take it outside of the phase separated region or (b) the phase boundary can be shifted, without changing the overall composition of the mixture.

5.3 Materials and methods

5.3.1 Materials

The details of all the materials used are listed in Appendix 1. Protanal LFR 5/60 (35kDa) was the alginate used for all of the experiments in this chapter.

5.3.2 Preparation of concentrated polysaccharide solutions

Solutions were prepared by dispersion of the requisite amount of powder in water. A large surface area vortex was created using an Ika-Werke Eurostar Digital (Staufen, Germany) overhead stirrer using a Jiffy® stirrer blade. The powder was added down the side of the created vortex. All powders were analysed for moisture content as described in section 2.2.1, and weighings were made on a dry weight basis. Xanthan gum was dispersed at 1000 rpm for 45 minutes, sodium alginate at 500 rpm for 20 minutes.

Locust bean gum was dispersed at 80^{o}C for 30 minutes at 1000 rpm using the water bath described in figure 4.2.

5.3.3 Preparation of concentrated polyacrylate solutions

The polyacrylate sodium samples were purchased as highly concentrated solutions. Using the accurately determined moisture content values (see section 2.2.1 for method, appendix 1 for values), concentrated stock solutions were prepared by dilution with water, and stirred at 500 rpm for 10 minutes.

5.3.4 Preparation of mixtures by combining stock solutions

Mixtures were prepared by combining concentrated stock solutions to achieve the desired concentrations, adding water as necessary. These were then stirred at 1000 rpm for 5 minutes to effect mixing.

5.3.5 Preparation of mixtures by direct addition

Sodium alginate was dispersed into an appropriate quantity of water at 500 rpm for 20 minutes using an Ika-Werke Eurostar Digital Power Control-Visc (Staufen, Germany) overhead stirrer. Xanthan gum powder was added directly into this solution at 1000 rpm and stirred for 45 minutes.

5.3.6 Preparation of ternary polysaccharide mixtures

Mixtures containing xanthan gum, locust bean gum (LBG) and sodium alginate were prepared by combining concentrated stock solutions in a similar way to those previously described. A xanthan/alginate mixture was prepared by mixing the stock solutions of xanthan and alginate. The LBG stock solution was then added into this mixture and stirred for 10 minutes at 1000 rpm. A schematic representation is given in Figure 5.2.

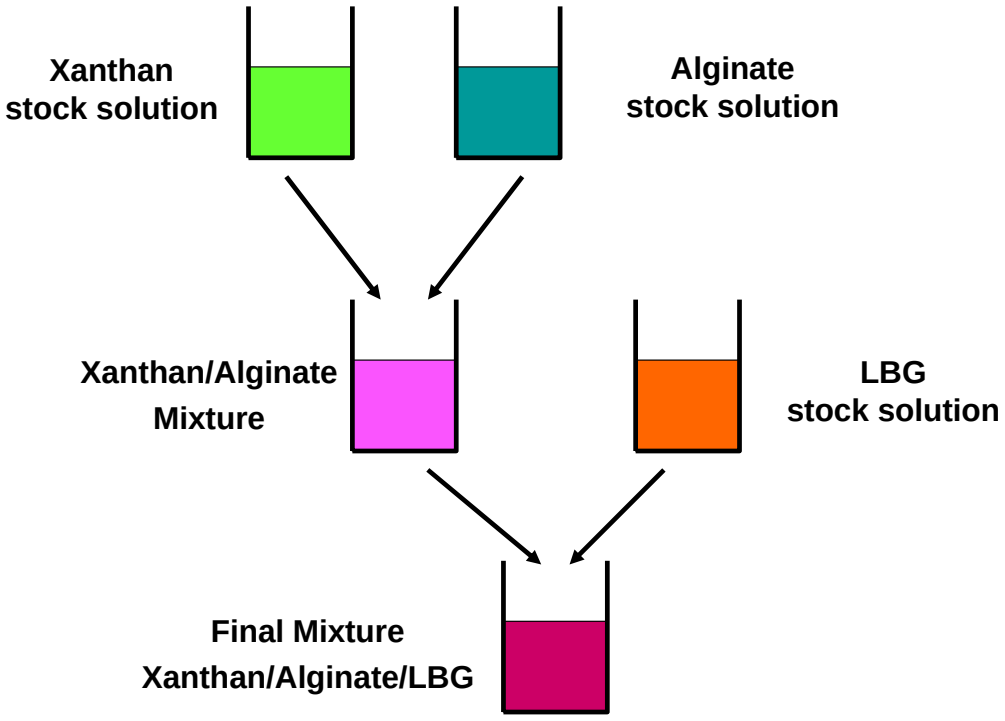

Figure 5.2. A schematic representation of the preparation of ternary mixtures containing xanthan gum, locust bean gum (LBG) and sodium alginate.

5.3.7 Preparation of simulated gastric fluid

Simulated gastric fluid (SGF) was prepared according to the United States Pharmacoepia (USP) (2005) with the purified pepsin component omitted.

5.3.8 Rheological analysis – Continuous shear viscometry

The continuous shear properties of the mixtures were measured using the method described in section 2.2.3 using a 4^{o}/40mm cone and plate geometry at 25 ± 0.1^{o}C.

5.3.9 Rheological analysis – Dynamic oscillation

Viscoelastic properties were examined as described in section 2.2.3 using a 4^{o}/40mm cone and plate geometry at 25 ± 0.1^{o}C.

5.3.10 Measuring the effect of dilution

5.3.10.a Viscosity development with time

The effect of dilution was examined using a Rapid Visco-analyser (RVA, Newport Scientific, supplied by Calibre Control International Ltd., Warrington, UK). This instrument combines the action of mixing with "real time" viscosity measurements.

An appropriate portion of the mixture (Table 5.1) was placed in a measuring canister, followed by the requisite amount of water taking care not to mix the components. Each sample for measurement had a total weight of 30.0g and experiments were undertaken at 25 ± 0.5^{o}C unless otherwise stated. Prior to each measurement, the paddle was

zeroed. Samples were mixed at 200 rpm and the viscosity measured every 4 seconds for 10 minutes unless otherwise stated.

Control mixtures were prepared, to establish if phase separation had any permanent effects on the hydrocolloid properties. The controls were prepared from the concentrated stock solutions and mixed; however the composition was at no point in the phase separated region of the phase diagram. For example, a 0.5% xanthan:1% alginate mixture was prepared by mixing 37.5g of 2% xanthan, 37.5g of 4% alginate and 75.0g of water.

% dilution	Mass of mixture	Mass of diluent	Final concentration % w/w
50%	15g	15g	0.5%
75%	7.5g	22.5g	0.25%
80%	6g	24g	0.2%

Table 5.1. The quantities used for examining the effect of dilution using the RVA

5.3.10.b The effect of varying the level of dilution

Pre-prepared dilutions were prepared by diluting the desired mixture and stirring at 1000 rpm for 5 minutes. These mixtures were analysed using continuous shear and viscoelastic rheology. The percentage dilution quoted is the percentage of added water relative to the quantity of sample, i.e. a 10% dilution is 10% water and 90% mixture; a 20% dilution is 20% water 80% sample etc (see definitions section for further examples).

5.3.11 Microscopy

Crossed polarised light microscope images were obtained using the method described in section 2.2.6 at room temperature.

5.4 Results and discussion

5.4.1 Transition across the xanthan/alginate phase boundary by dilution with water

5.4.1.a The effect of dilution

The effect of dilution across the phase boundary was investigated using the Rapid Visco-Analyser (RVA). Figure 5.3 shows the effect of diluting a mixture of 1% xanthan and 5% alginate across the phase boundary in comparison to a control mixture. The control mixture (see section 5.3.10.a for preparation details) was used to examine if the phase separation had any permanent effects and was prepared without going into the phase separated region. A concentration of 5% alginate was chosen as this is the concentration of alginate commonly used in anti-reflux medicines such as Gaviscon™ (Anon. 2004). The viscosity of the undiluted mixture was approximately 200 mPa.s, and following an 80% dilution, sufficient to cross the phase boundary, the viscosity decreased to approximately 100 mPa.s. The addition of water therefore reduced the viscosity as would be expected when any polysaccharide solution is diluted. The control mixture showed little difference from the diluted system suggesting separation did not permanently affect the system and that separation was fully reversible.

The effect of diluting a mixture significantly closer to the phase boundary, 1% xanthan:2% alginate, relative to a control mixture prepared without entering the phase separated region, is shown in Figure 5.4. The viscosity of the undiluted mixture was 100 mPa.s, but dilution to 50% crossing the phase boundary resulted in a viscosity increase to 200 mPa.s. The viscosity increase started immediately and was complete within 3 minutes. It is probable that this is a combination of both a mixing effect and an effect of time as a result of further hydration of the polysaccharides. The unseparated control showed no difference from the diluted mixture. Dilution of polysaccharide solutions

normally results in significant decreases in viscosity, however dilution of this xanthan:alginate mixture showed the opposite.

The effect of diluting a 2% xanthan:2% alginate mixture, a separated mixture of similar distance from the phase boundary to 1% xanthan:2% alginate, was investigated. Figure 5.5 shows that the viscosity increase previously observed with the 1% xanthan mixture is repeated. The undiluted and diluted viscosities of the 2% mixture were both twice the magnitude of that with the 1% mixture.

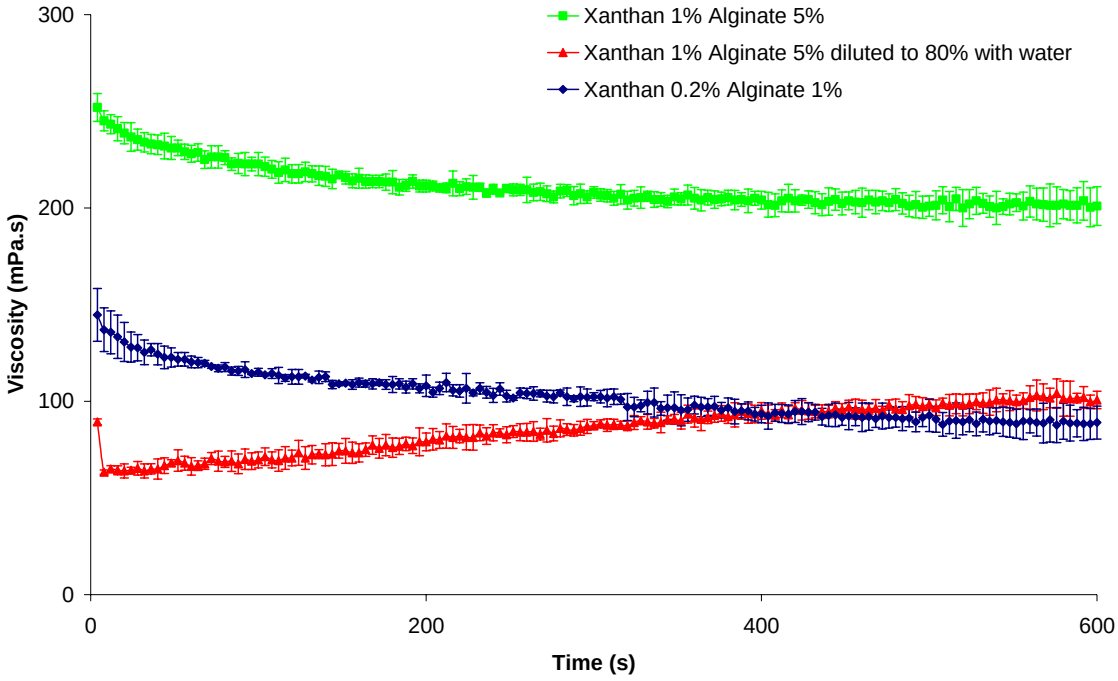

Figure 5.3. An RVA dilution profile showing the effect of diluting a 1% xanthan:5% alginate mixture with water.
The 0.2% xanthan:1% alginate mixture was prepared such that it had not previously undergone separation Sodium Alginate: Protanal LFR5/60. Paddle speed 200rpm. 25 ± 0.5°C. Mean ± SD, n=3

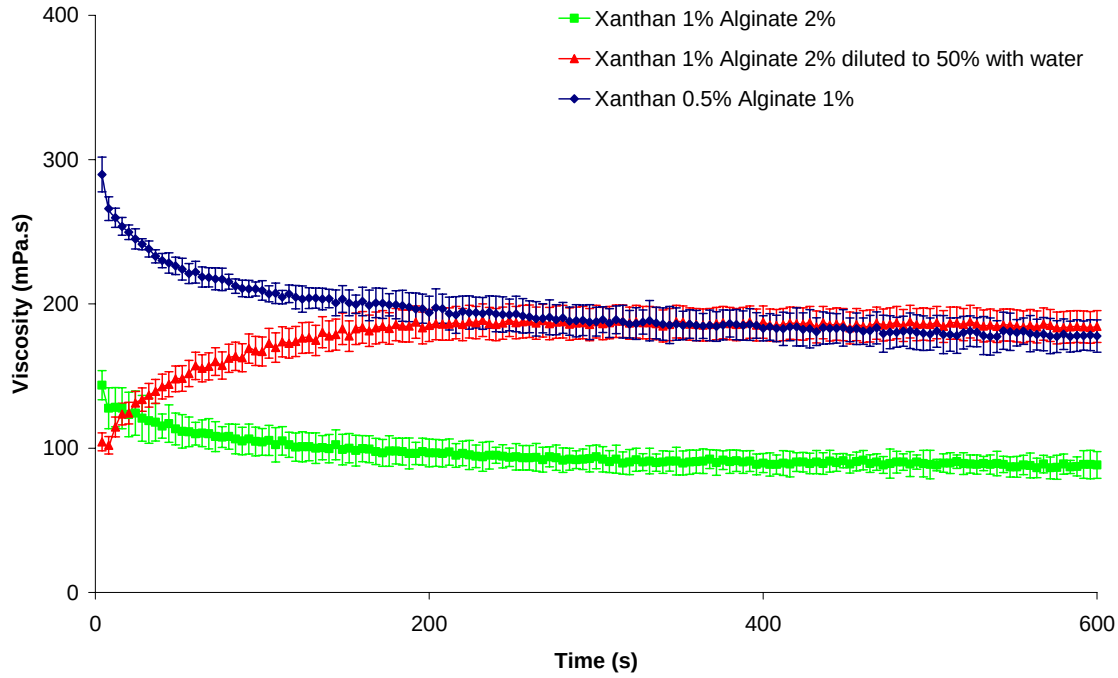

Figure 5.4. An RVA dilution profile showing the effect of diluting a 1% xanthan:2% alginate mixture with water.
The xanthan 0.5% alginate 1% mixture was prepared such that it had not previously undergone separation Sodium Alginate: Protanal LFR5/60. Paddle speed 200rpm. 25 ± 0.5°C. Mean ± SD, n=3

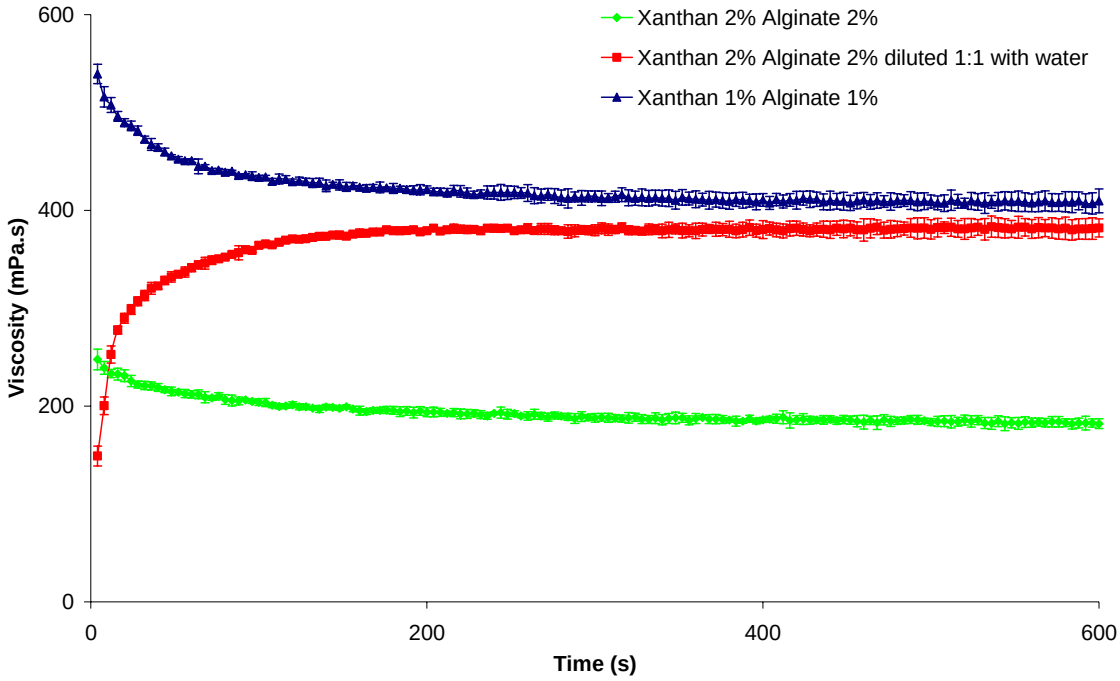

Figure 5.5. An RVA dilution profile showing the effect of diluting a 2% xanthan:2% alginate mixture with water.
The xanthan 1% alginate 1% mixture was prepared such that it had not previously undergone separation Sodium Alginate: Protanal LFR5/60. Paddle speed 200rpm. 25 ± 0.5°C. Mean ± SD, n=3

The RVA provides empirical viscosity data and as a consequence can only provide data comparative with itself. The continuous shear behaviour of the fully mixed dilution and the undiluted mixtures was measured over a wide range of shear rates. Figure 5.6 shows the viscosity changes on dilution of a 1% xanthan:5% alginate mixture. There was no difference between the diluted mixture and a mixture that had not been previously separated (control). At low shear rates ($< 1s^{-1}$) dilution increased the viscosity, but at higher shear rates ($> 10s^{-1}$) dilution reduced viscosity. The dynamic viscoelastic properties of this system are shown in Figure 5.7. The undiluted mixture exhibited low magnitude, viscous-dominated properties, with G" > G' at most frequencies. In contrast the diluted system showed low magnitude, elastic dominated properties, showing that dilution had significantly changed the properties of the mixture.

Figure 5.8 and Figure 5.9 show the changes in continuous shear and viscoelastic properties that occurred on dilution of a 1% xanthan:2% alginate mixture. The continuous shear profile showed that at shear rates below $400s^{-1}$ a viscosity increase on dilution was observed. At a shear rate of $0.1s^{-1}$ the viscosity increase was in excess of an order of magnitude. On dilution, the viscoelastic properties were observed to change from an essentially non-viscous system to that of a weak gel-like system. Both figures suggest that the separation is fully reversible as there was no significant variation between the diluted mixture and the control.

Figure 5.10 and Figure 5.11 examine the effect of diluting the 2% xanthan:2% alginate mixture. The continuous shear profile showed a viscosity increase at shear rates below $300s^{-1}$; it is interesting to note that the viscosity increase at $0.1s^{-1}$ is not as substantial as that with the 1% xanthan mixture, but the diluted mixture produced a viscosity greater than that of the 1% mixture. The viscoelastic data shows that the undiluted mixture has very weak elastic like properties which are greatly enhanced on dilution.

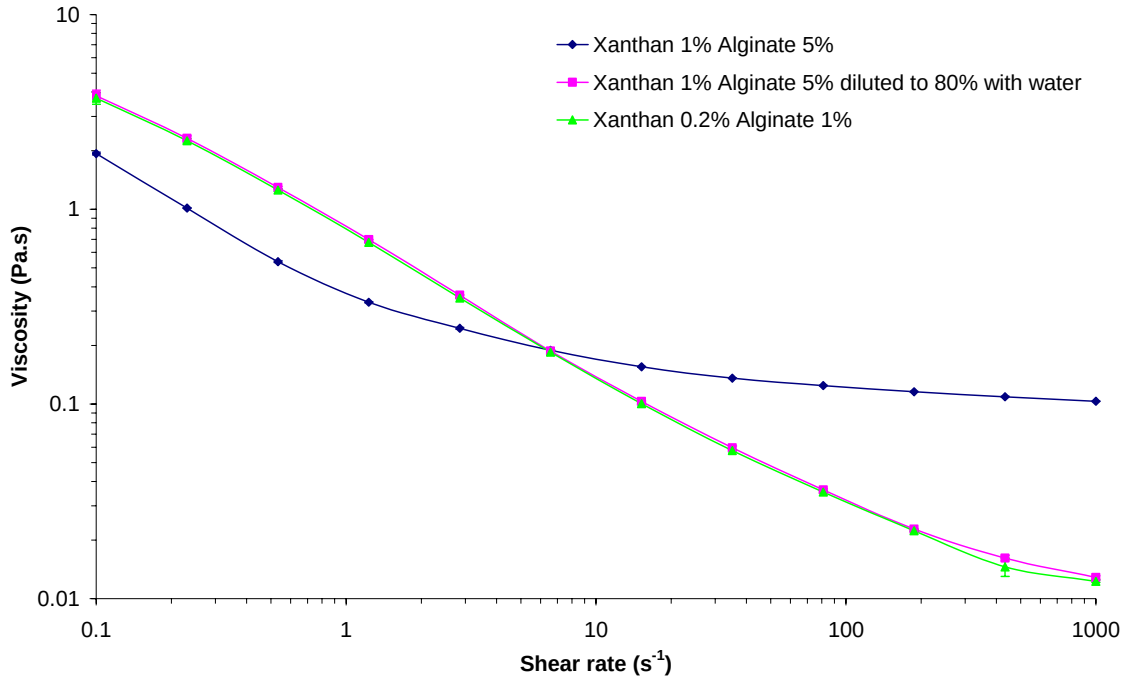

Figure 5.6. The continuous shear profiles of a 1% xanthan:5% alginate mixture, undiluted and diluted to 80% with water, and a previously unseparated control.
The diluted mixture was thoroughly mixed prior to measurement. The 0.2% xanthan:1% alginate mixture was prepared such that it had not previously undergone separation. Geometry CP 4°/40mm 25 ± 0.1°C. Mean ± SD, n=3.

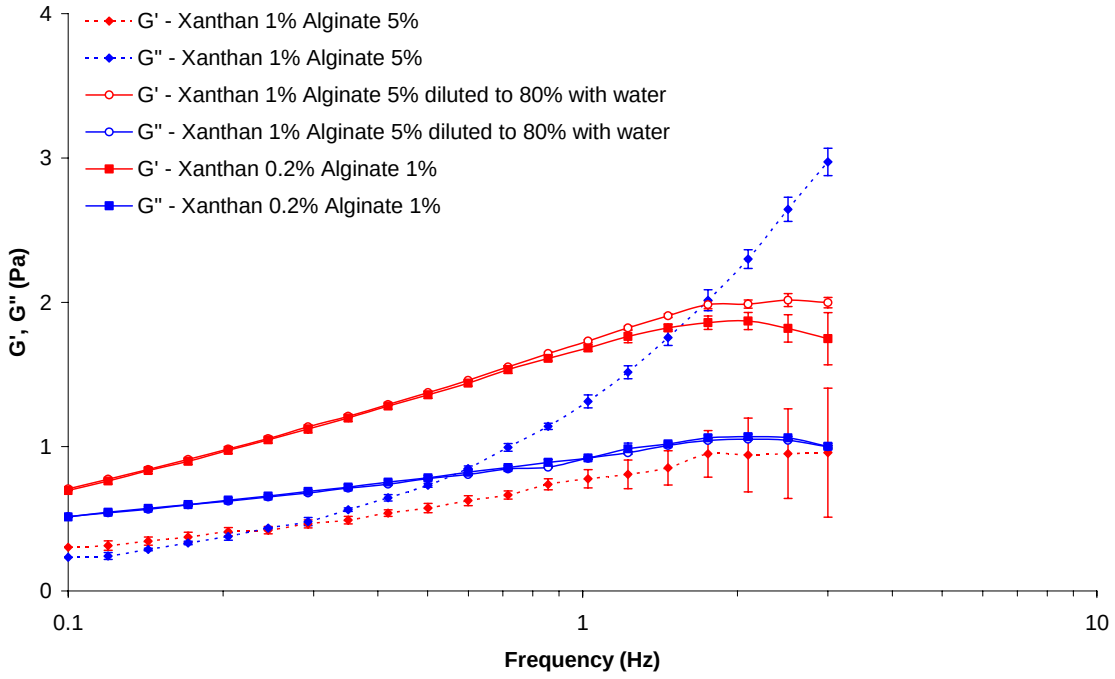

Figure 5.7. The dynamic viscoelastic properties of a 1% xanthan:5% alginate mixture, undiluted and diluted to 80% with water, and a previously unseparated control.
The diluted mixture was thoroughly mixed prior to measurement. The 0.2% xanthan:1% alginate mixture was prepared such that it had not previously undergone separation. Geometry CP 4°/40mm 25 ± 0.1°C. Mean ± SD, n=3.

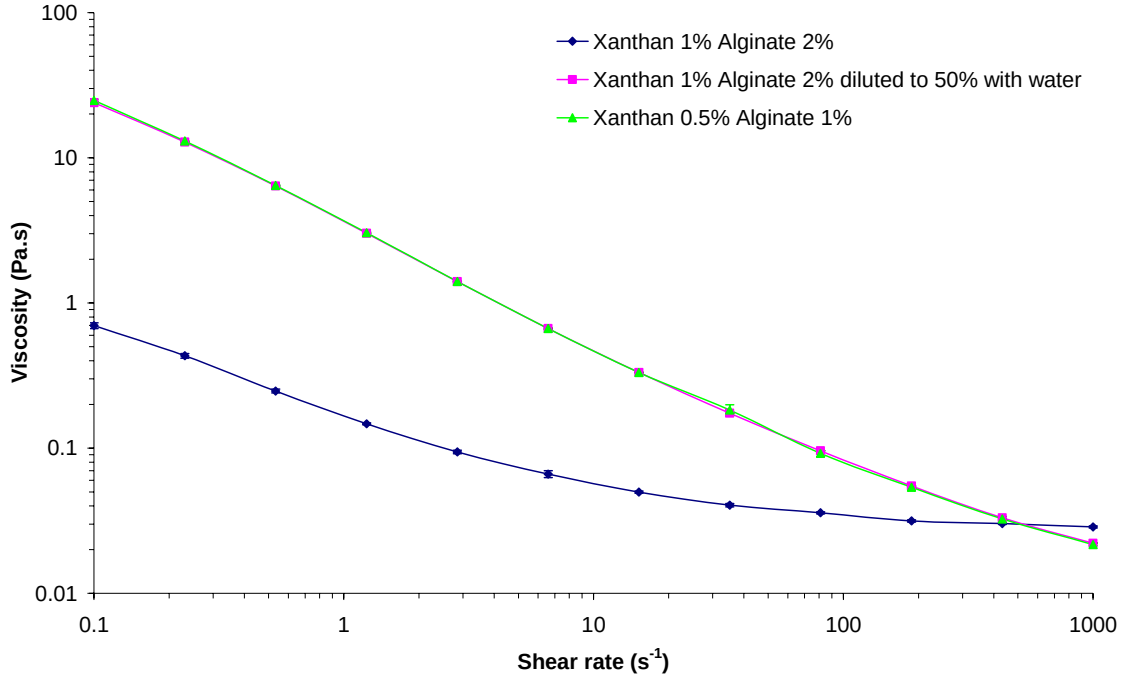

Figure 5.8. The continuous shear profiles of a 1% xanthan:2% alginate mixture, undiluted and diluted to 50% with water, and a previously unseparated control.
The diluted mixture was thoroughly mixed prior to measurement. The 0.5% xanthan:1% alginate mixture was prepared such that it had not previously undergone separation. Geometry CP 4°/40mm 25 ± 0.1°C. Mean ± SD, n=3.

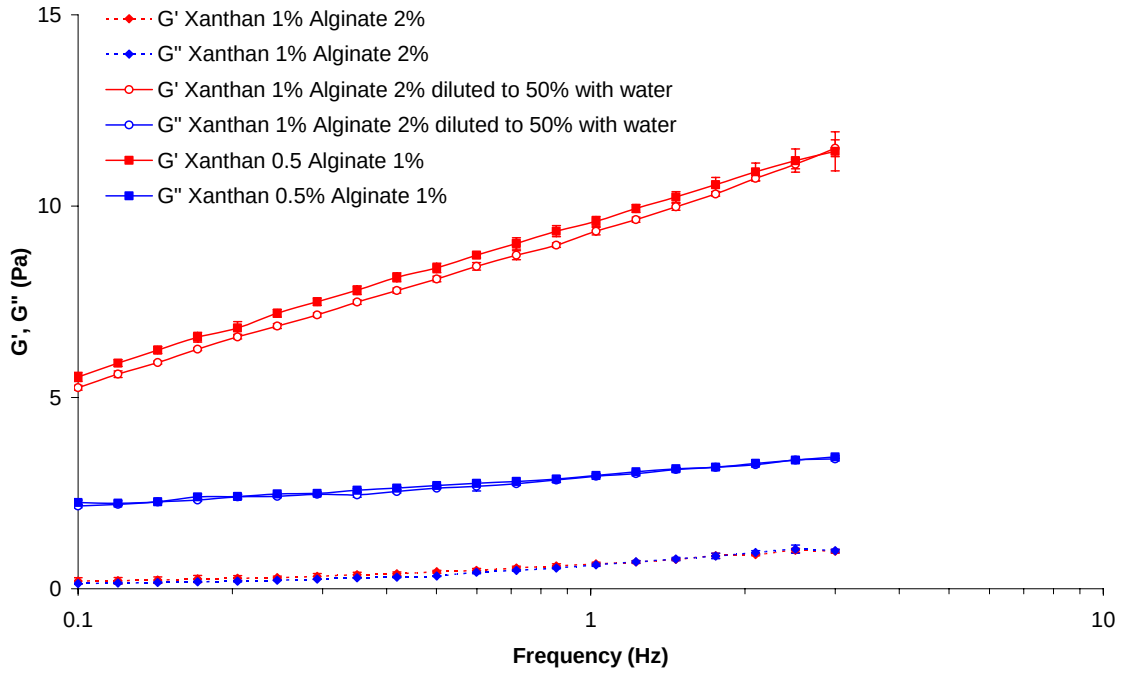

Figure 5.9. The dynamic viscoelastic properties of a 1% xanthan:2% alginate mixture, undiluted and diluted to 50% with water, and a previously unseparated control.
The diluted mixture was thoroughly mixed prior to measurement. The 0.5% xanthan:1% alginate mixture was prepared such that it had not previously undergone separation. Geometry CP 4°/40mm 25 ± 0.1°C. Mean ± SD, n=3.

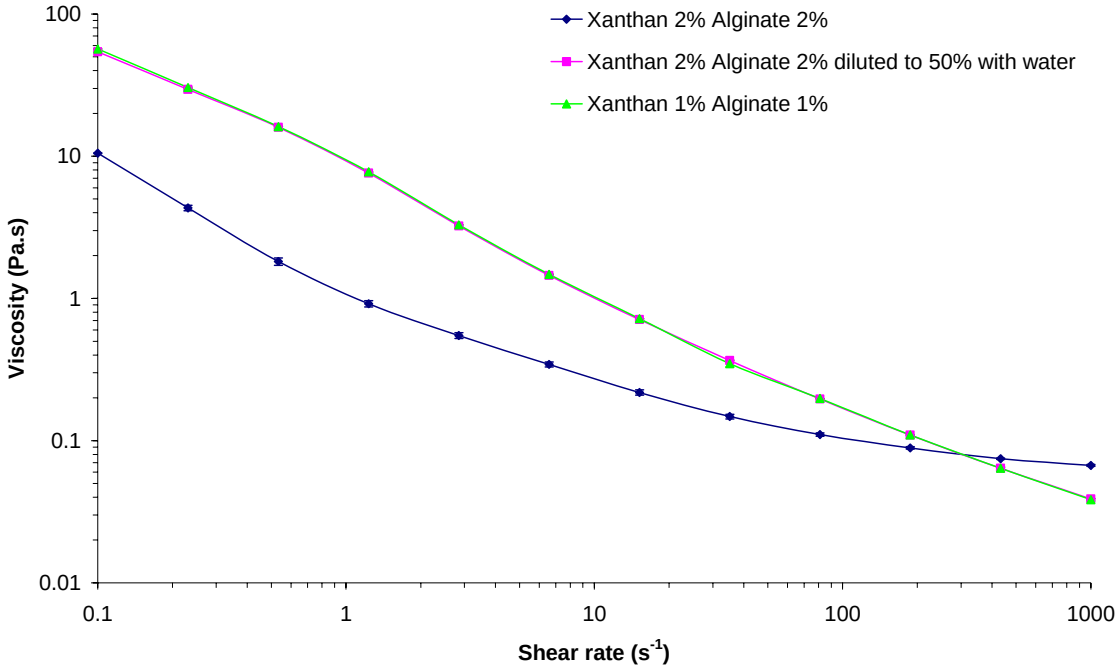

Figure 5.10. The continuous shear profiles of a 2% xanthan:2% alginate mixture, undiluted and diluted to 50% with water, and a previously unseparated control.
The diluted mixture was thoroughly mixed prior to measurement. The 1% xanthan:1% alginate mixture was prepared such that it had not previously undergone separation. Geometry CP 4°/40mm 25 ± 0.1°C. Mean ± SD, n=3.

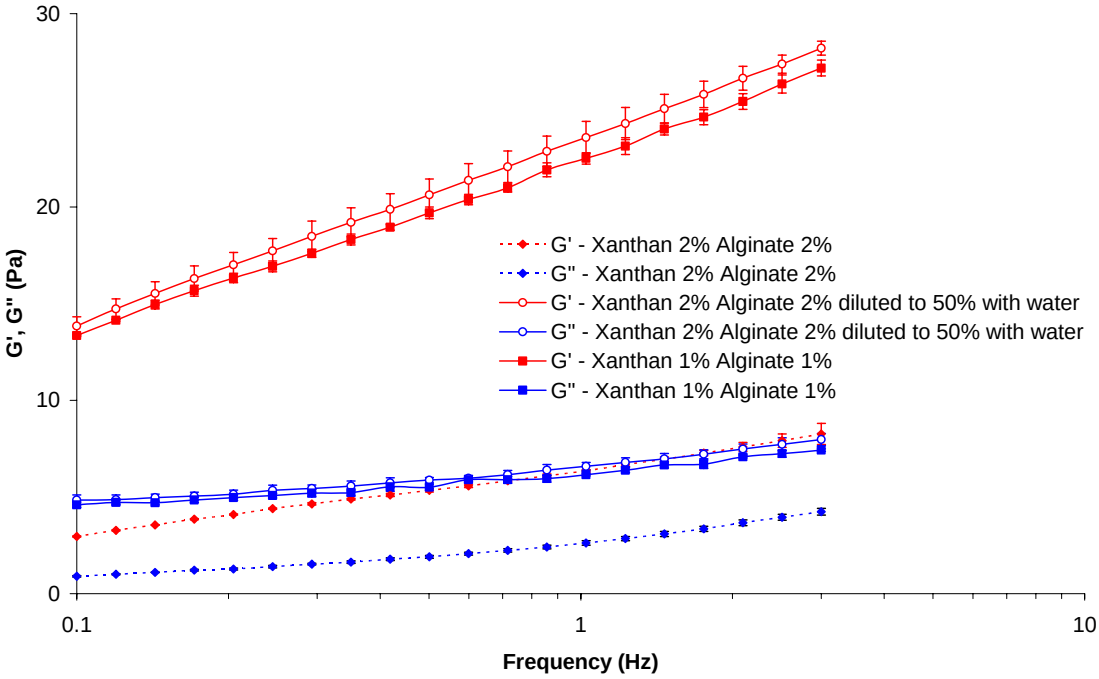

Figure 5.11. The dynamic viscoelastic properties of a 2% xanthan:2% alginate mixture, undiluted and diluted to 50% with water, and a previously unseparated control.
The diluted mixture was thoroughly mixed prior to measurement. The 1% xanthan:1% alginate mixture was prepared such that it had not previously undergone separation. Geometry CP 4°/40mm 25 ± 0.1°C. Mean ± SD, n=3.

5.4.1.b Effect of varying the degree of dilution

The effect of varying the degree of dilution were studied by diluting a 1% xanthan:2% alginate mixture, and mixing thoroughly prior to analysis. Figure 5.12 examines the viscosity change as a function of the amount of dilution. The addition of 20% w/w water resulted in a very slight viscosity decrease, whereas addition of further quantities of water up to 50% dilution resulted in a viscosity increase to greater than an order of magnitude. Dilution beyond 50% resulted in a gradual decrease in viscosity. The shape of the curve would suggest that transition across the phase boundary is not at a single concentration, but occurs over a concentration range of 20% to 50% dilution. This further supports the hypothesis that the mixture is polydisperse as discussed in chapter 3. Figure 5.13 shows the corresponding changes in elastic modulus on dilution. The graph appears very similar in shape to the continuous shear data.

Figure 5.14 shows crossed polarised light microscope images taken at different dilutions. Birefringent mesophases can be seen in samples diluted up to 40%, with the number and density of the strands being less with each dilution. The 50% dilution shows no birefringence. This suggests that maximal viscosity is not achieved until complete reversal of the separation has occurred. The change in the density and number of visible strands corresponds with the shape of the curves for both continuous shear and viscoelastic changes as they demonstrate a gradual change from separated to homogenous.

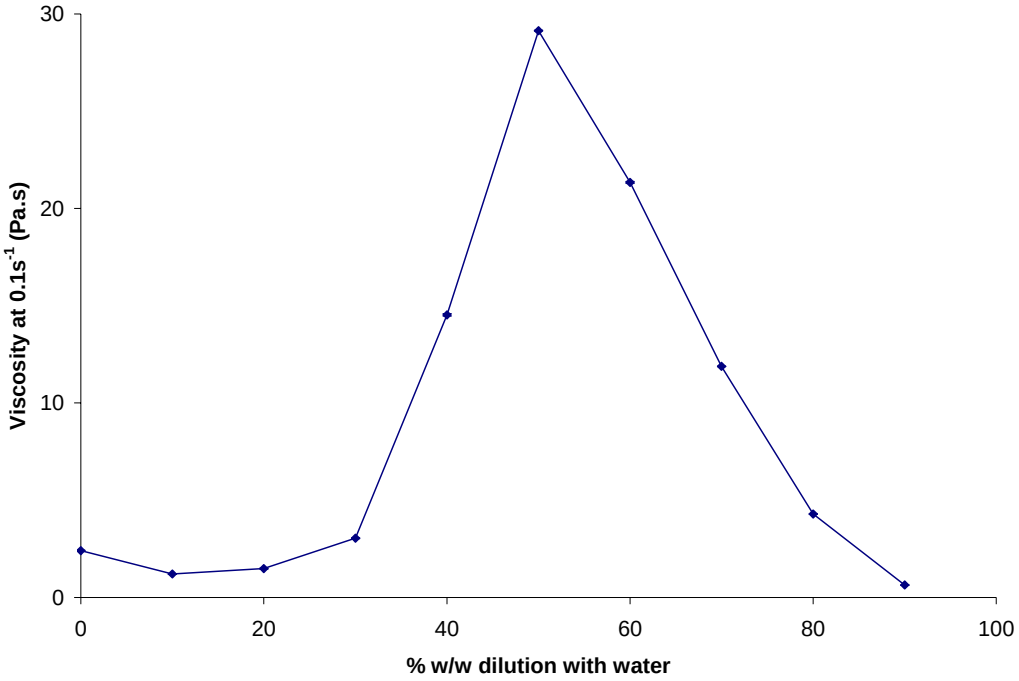

Figure 5.12. The continuous shear viscosity at 0.1s^{-1} of a 1% xanthan:2% alginate mixture when diluted with water.
Samples were mixed prior to measurement. Geometry CP 4°/40mm 25 ± 0.1°C. Mean ± SD, n=3.

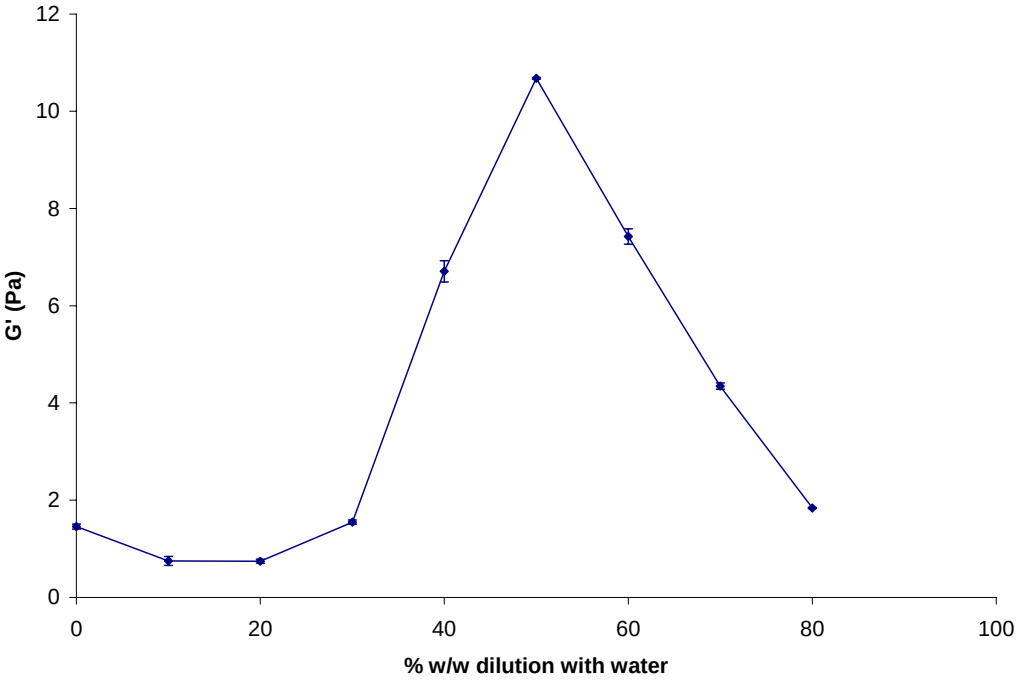

Figure 5.13. The effect of dilution on the elastic modulus of a 1% xanthan:2% alginate mixture.
Samples were mixed prior to measurement. Geometry CP 4°/40mm 25 ± 0.1°C. Frequency = 1.02Hz. Mean ± SD, n=3.

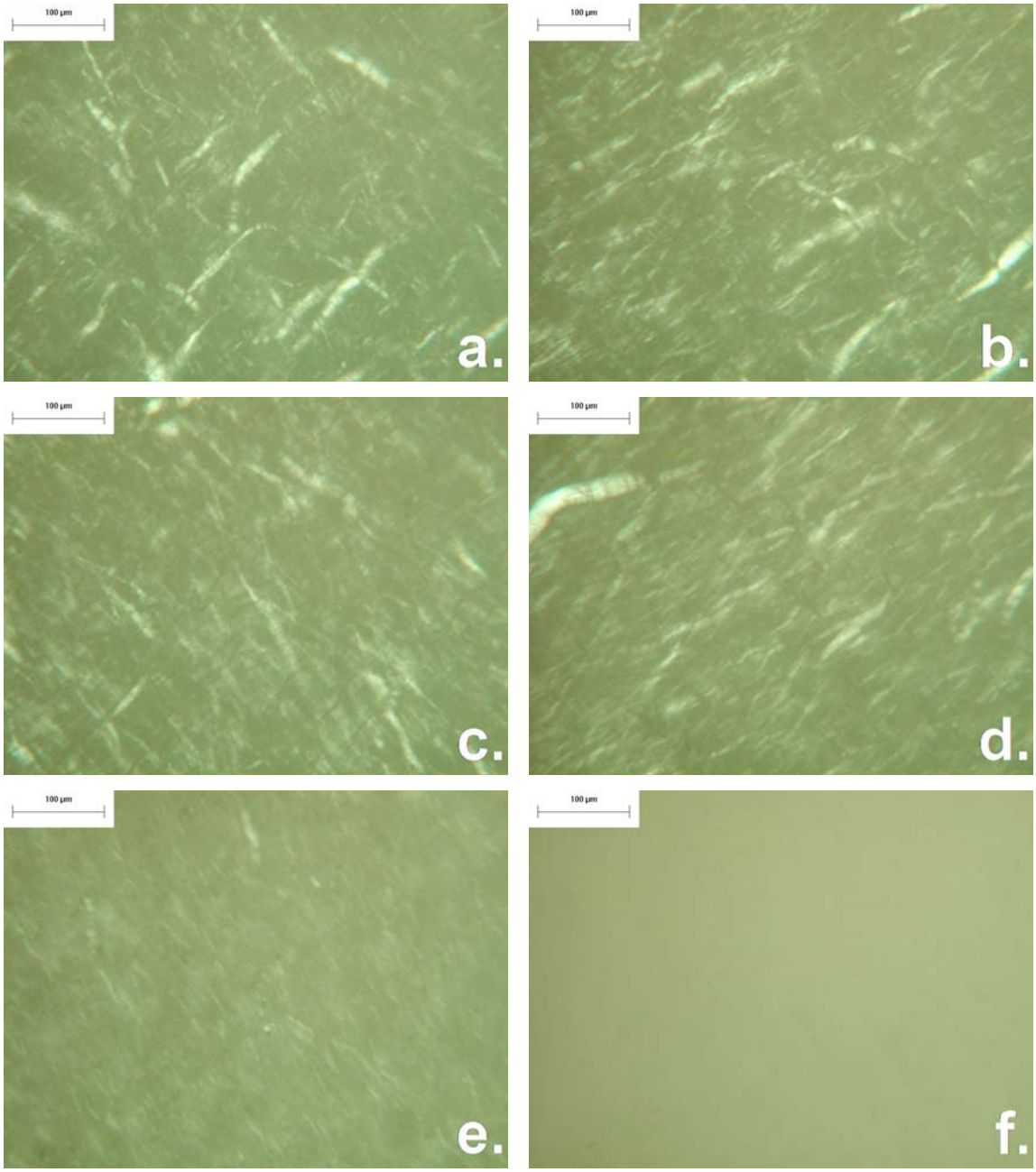

Figure 5.14. Microscope images taken between crossed polarizing lenses of a 1% xanthan:2% alginate mixture when diluted to varying degrees with water.
(a) 0% dilution, (b) 10% dilution, (c) 20% dilution, (d) 30% dilution, (e) 40% dilution, (f) 50% dilution.

5.4.2 Transition across the xanthan/alginate phase boundary on dilution with simulated gastric fluid (SGF)

This next section examines the possible implications if a system comprised of xanthan and alginate was taken into a gastric environment. To model this, the diluent was changed from deionised water to USP simulated gastric fluid (without enzymes). SGF is principally composed of hydrochloric acid and has a typical pH of 1.2; it also contains 0.2% sodium chloride. At low pH sodium alginate is normally converted to alginic acid, which can precipitate.

The effect of diluting a 1% xanthan:5% alginate mixture with water or SGF is compared in Figure 5.15. The undiluted mixture and the mixture diluted with water had a viscosity of 200 mPa.s and 100 mPa.s (at 600s) respectively. The mixture diluted with SGF showed a rapid increase in viscosity to approximately 350 mPa.s, which then decreased slightly to approximately 200 mPa.s after 600s. This pattern suggests that more than one phenomenon may be occurring. The mixture diluted with SGF showed wide variability in viscosity as shown by the size of the error bars, suggesting that dilution with SGF is more complex than dilution with water.

Figure 5.16 and Figure 5.17 show the RVA dilution profile of mixtures containing 2% alginate and 1% or 2% xanthan with SGF. Both figures showed an almost instantaneous increase in viscosity with maximal viscosity being achieved after 20 to 30 seconds. After the 600s period, dilution with water had increased the viscosity two fold whereas the dilution with SGF increased the viscosity seven fold.

To establish the origin of these viscosity increases, individual solutions of xanthan and alginate were diluted with water and SGF to understand exactly which components may be contributing to the viscosity changes. Figure 5.18 and Figure 5.19 show the dilution of a 1% and 2% xanthan solution respectively. Both figures show similar profiles, but the magnitude is different as a result of the concentration effect. The undiluted xanthan

showed high viscosity that remained constant over the time course of the study. When diluted with water, the xanthan solutions increased in viscosity over 60 to 80 seconds. This is not a true increase in viscosity but a result of the time taken for the xanthan solution and the water to fully mix. The dilution profile using SGF was distinctly different. The solution of xanthan diluted with SGF took 480 to 540 seconds to reach its maximal viscosity. At 600s the viscosity was identical in value to that of the solution diluted with water, suggesting that xanthan on its own does not mix efficiently with SGF, but mixes effectively with water. These results indicate that the viscosity increase observed in the xanthan:alginate mixtures is unlikely to be as a result of the dilution of the xanthan component.

The effect of diluting alginate solutions with SGF was also investigated. Figure 5.20 shows the effect of dilution on a 5% alginate solution. Dilution with water reduced the viscosity from 100 mPa.s to 35 mPa.s and mixing was complete in a few seconds. Dilution with SGF caused an increase in viscosity, and as indicated by the large error bars, the increase was highly variable in magnitude. This is most likely as a result of the conversion of sodium alginate to an alginic acid gel as a result of low pH conditions (Draget, Skjåk-Bræk et al. 2005/6). Figure 5.21 shows the dilution of a 2% alginate solution. Dilution with water reduced viscosity as expected, but the dilution profile with SGF was remarkably similar to that shown in Figure 5.15. A rapid increase in viscosity to approximately 275 mPa.s occurred during the first few seconds following dilution, this was then followed by a decrease to a maintenance viscosity of 175 mPa.s. The error bars would suggest that unlike the 5% solution, SGF had only viscosified the alginate solution, as opposed to forming an acid gel.

These experiments suggest that the viscosity increases seen on diluting the xanthan:alginate mixtures with SGF are of dual origin and the effect of traversing the phase boundary is greatly enhanced by the viscosification of the alginate as a result of the pH decrease. This provides a potentially useful system for a gastric medicine whereby a low viscosity mixture can be delivered, which on contact with the gastric fluid can greatly enhance viscosity and possibly improve gastric retention times.

The viscoelastic changes that occurred when a 1% xanthan:2% alginate mixture was diluted with SGF are shown in Figure 5.22. It can be seen that on dilution a weak gel was formed, with G' greater than G" at all frequencies and both moduli increased in a frequency dependent manner.

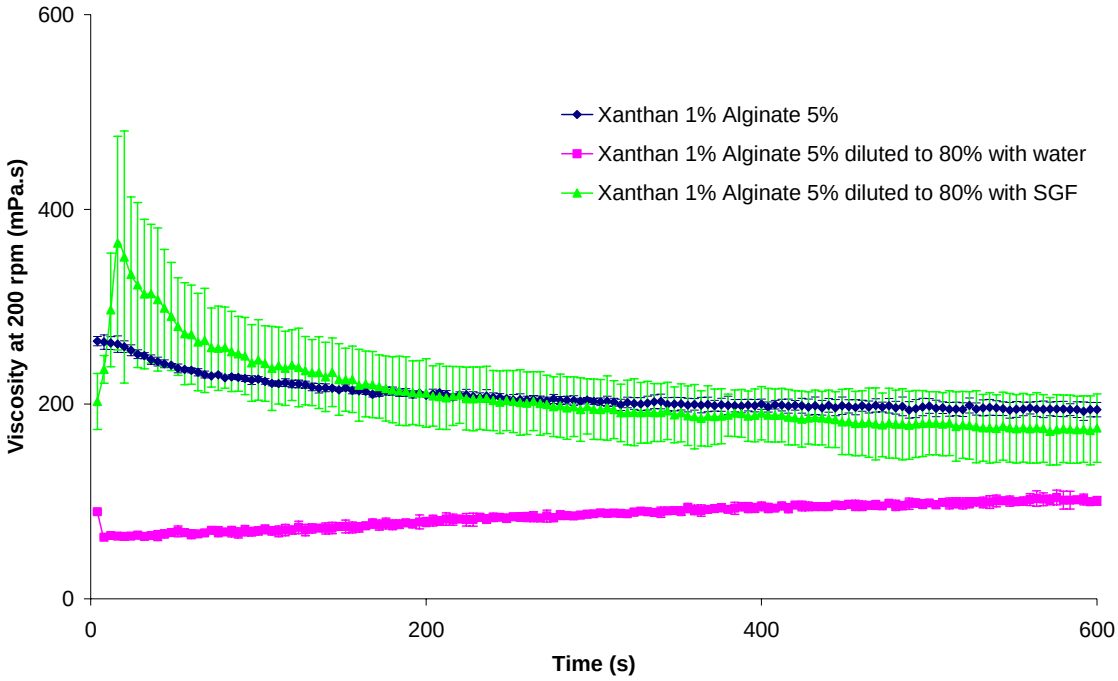

Figure 5.15. An RVA dilution profile of a 1% xanthan:5% alginate mixture undiluted, and diluted to 80% with water or simulated gastric fluid USP.
Paddle speed 200rpm. 25 ± 0.5°C. (Mean ± SD, n=3)

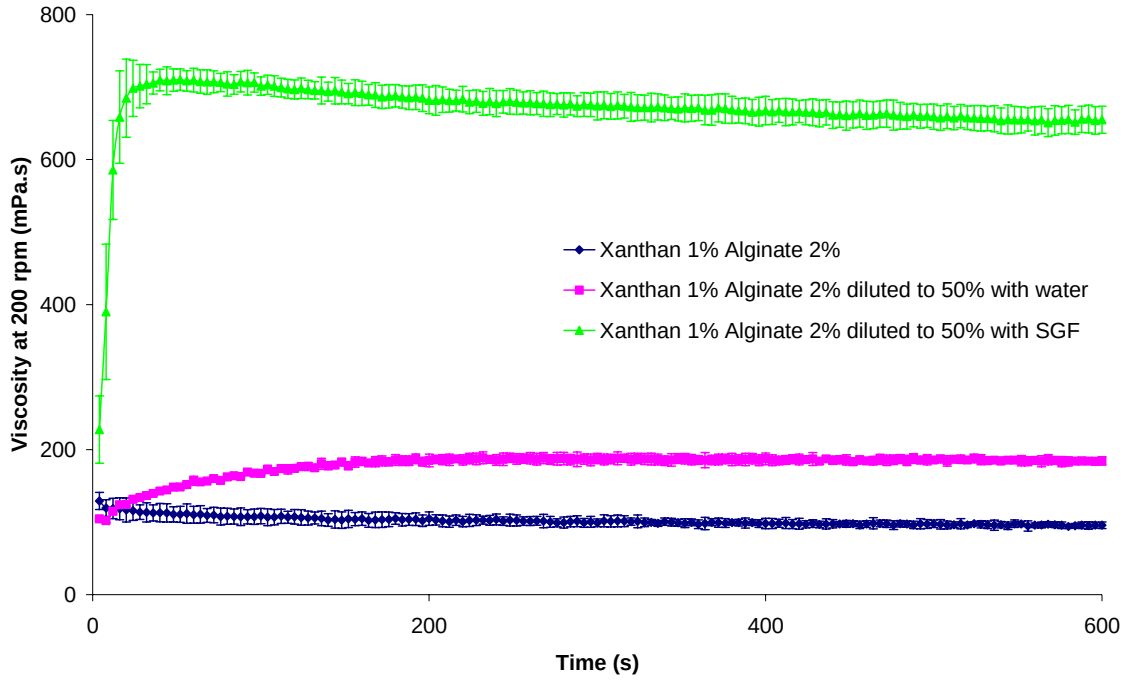

Figure 5.16. An RVA dilution profile of a 1% xanthan:2% alginate mixture undiluted, and diluted to 50% with water or simulated gastric fluid USP.
Paddle speed 200rpm. 25 ± 0.5°C. (Mean ± SD, n=3)

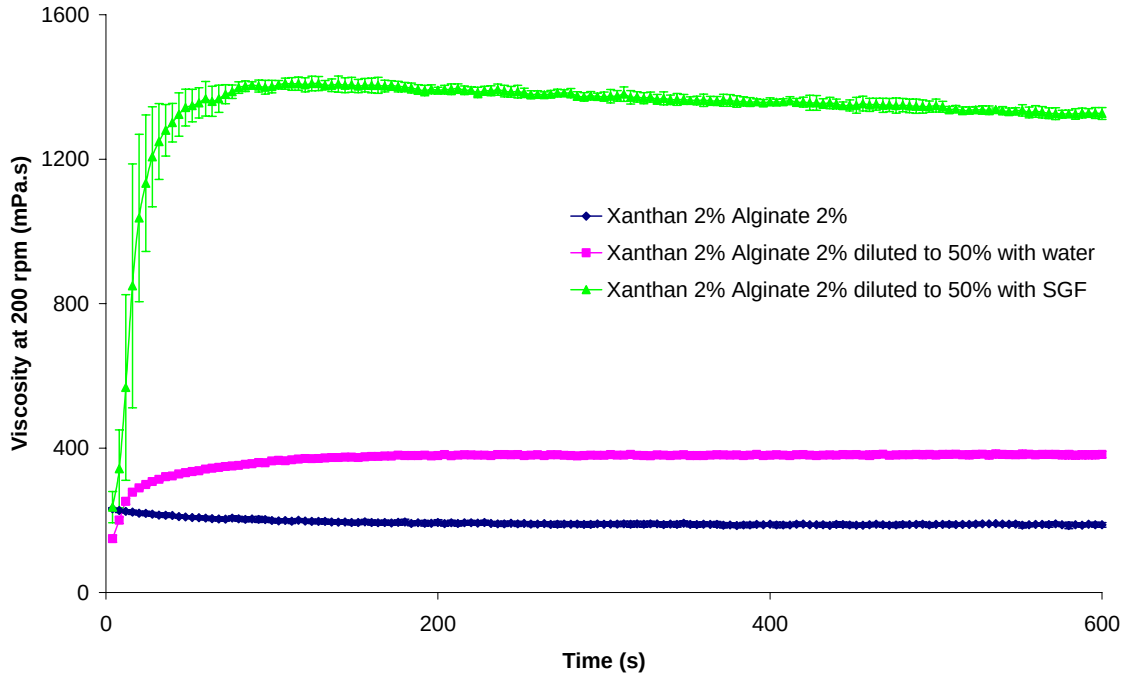

Figure 5.17. An RVA dilution profile of a 2% xanthan:2% alginate mixture undiluted, and diluted to 50% with water or simulated gastric fluid USP.
Paddle speed 200rpm. 25 ± 0.5°C. (Mean ± SD, n=3)

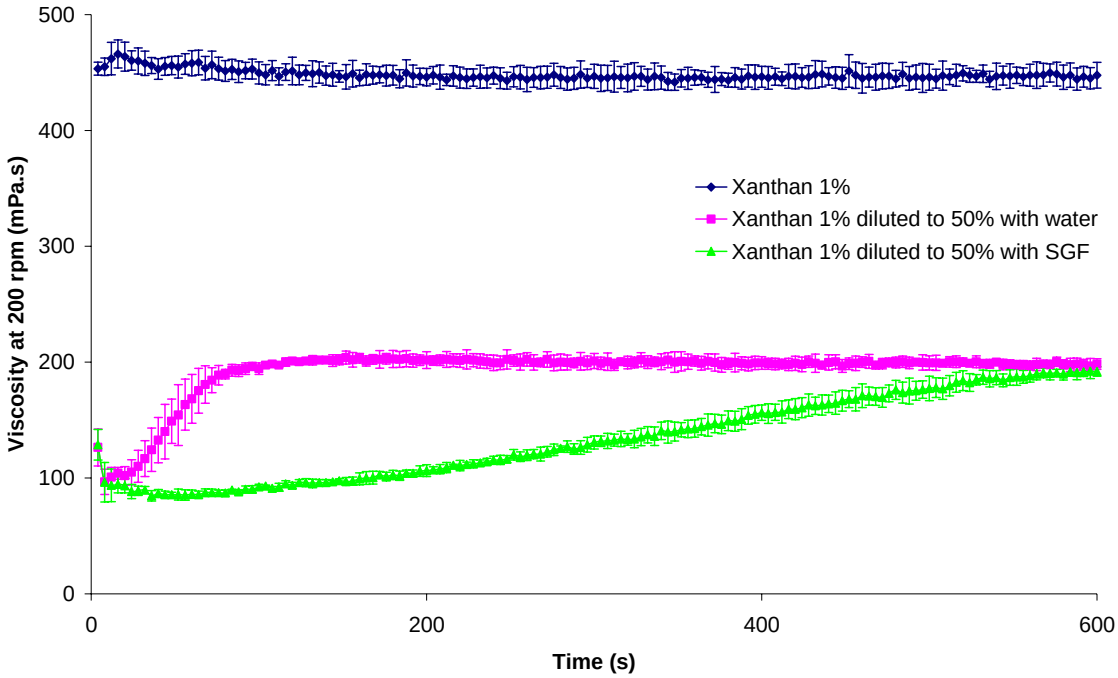

Figure 5.18. An RVA dilution profile of a 1% xanthan solution and a 1% xanthan solution diluted to 50% with water or simulated gastric fluid USP.
Paddle speed 200rpm. 25 ± 0.5°C. Mean ± SD, n=3

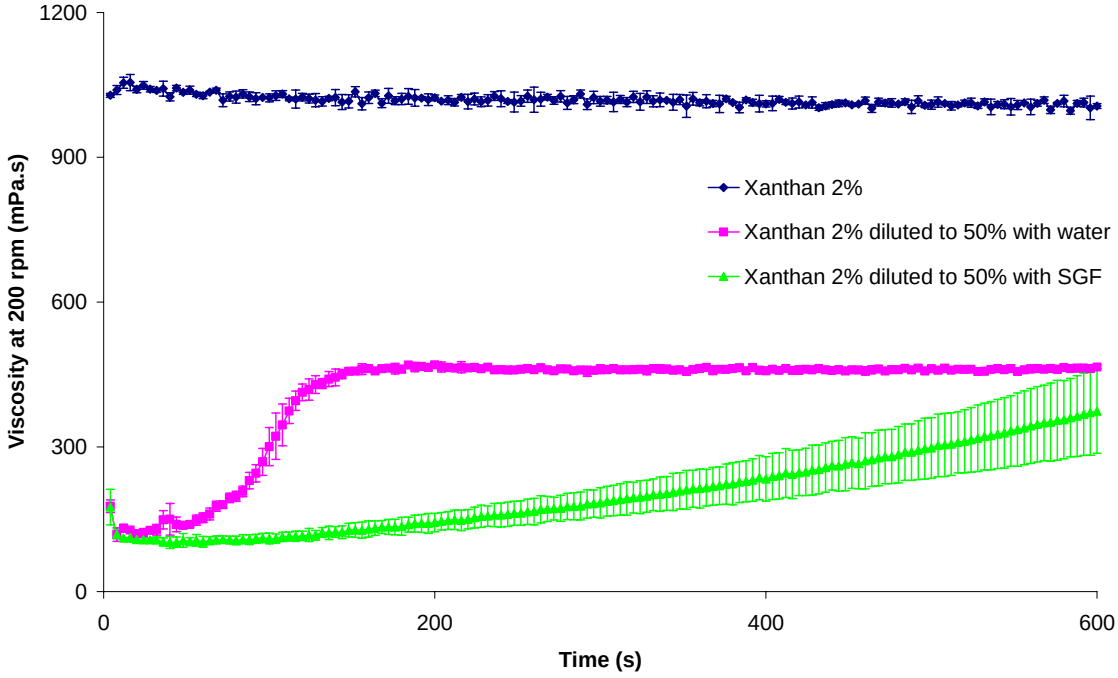

Figure 5.19. An RVA dilution profile of a 2% xanthan solution and a 2% xanthan solution diluted to 50% with water or simulated gastric fluid USP.
Paddle speed 200rpm. 25 ± 0.5°C. (Mean ± SD, n=3)

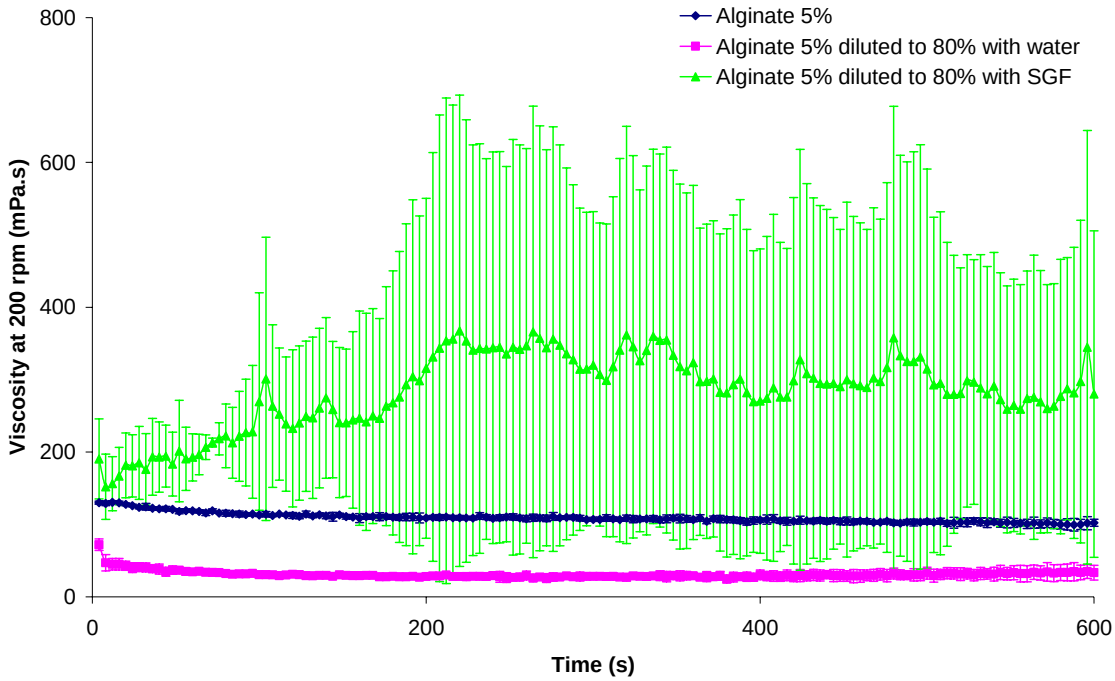

Figure 5.20. An RVA dilution profile of a 5% alginate solution and a 5% alginate solution diluted to 80% with water or simulated gastric fluid USP.
Paddle speed 200rpm. 25 ± 0.5°C. (Mean ± SD, n=3)

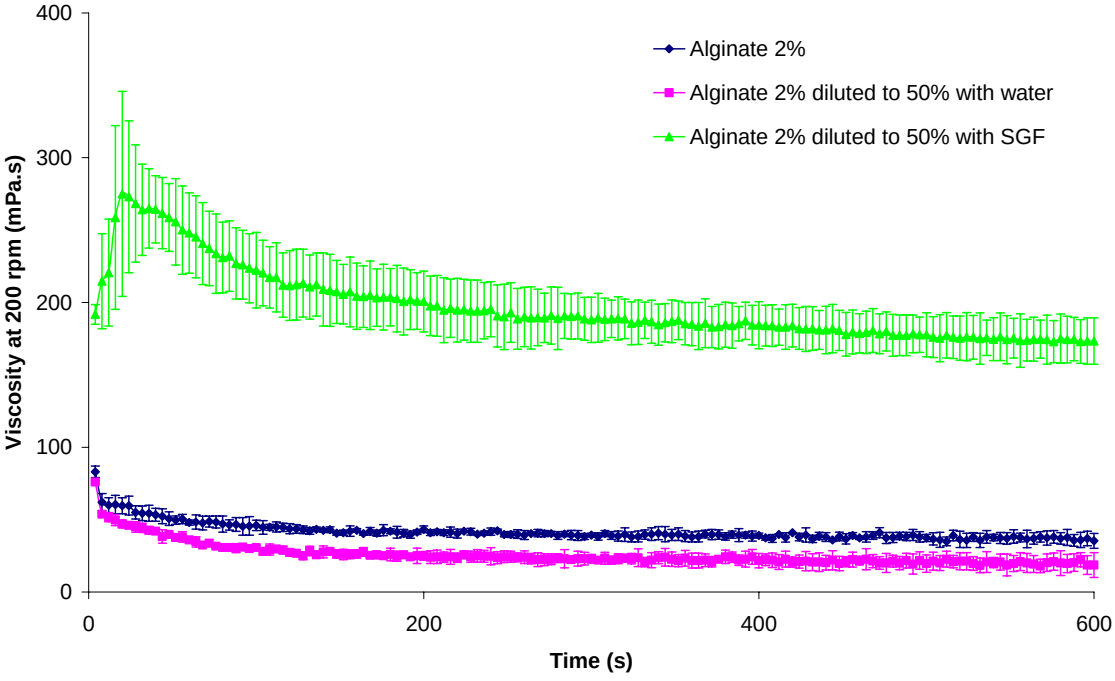

Figure 5.21. An RVA dilution profile of a 2% alginate solution and a 2% alginate solution diluted to 50% with water or simulated gastric fluid USP.
Paddle speed 200rpm. 25 ± 0.5°C . (Mean ± SD, n=3)

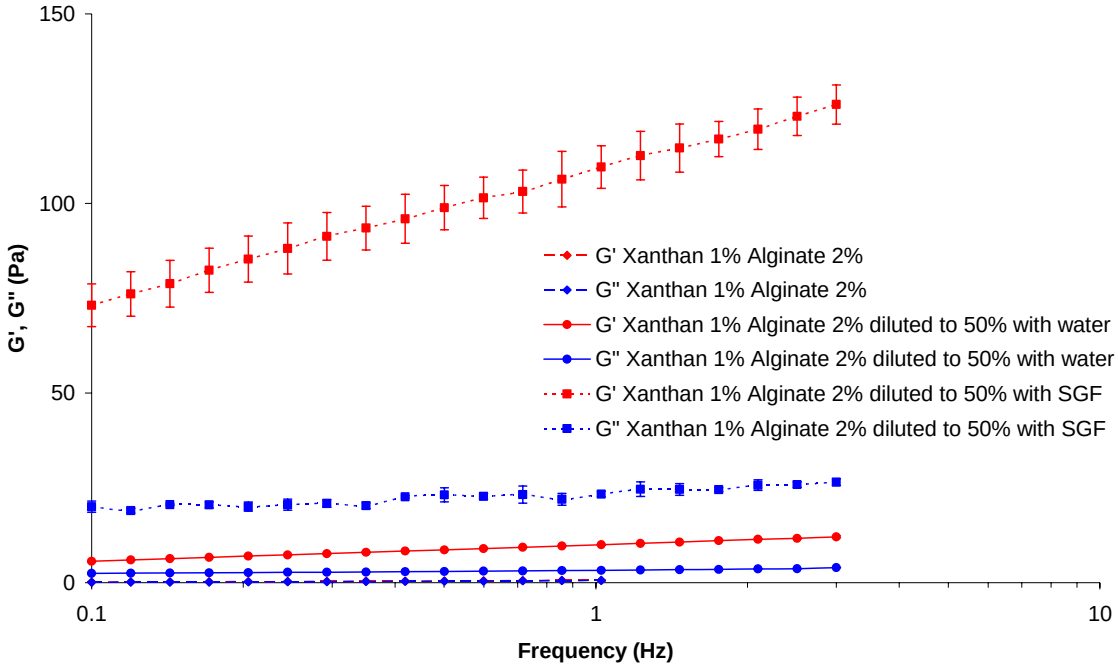

Figure 5.22. The dynamic viscoelastic profile of a 1% xanthan:2% alginate mixture compared with a 1% xanthan:2%alginate mixture diluted to 50% with water or simulated gastric fluid USP.
Geometry CP 4°/40mm 25 ± 0.1°C. Mean ± SD, n=3

5.4.3 Modifying the dilution profile by altering proximity to the phase boundary

The effect of modifying the position within the phase separated region has been touched on in section 5.4.1. In this section, the effect of choosing a composition closer to the binodal will be investigated.

Figure 5.23 compares the dilution profile of two mixtures both containing 1% xanthan and 1.5% or 2% alginate. The 1% xanthan:1.5% alginate mixture is closer to the binodal than the 1% xanthan:2% alginate mixture. Both mixtures show similar shaped dilution profiles. The reduction in alginate concentration caused the dilution curve to shift upwards and to the left. The undiluted 2% alginate mixture had a viscosity of 2 to 3 Pa.s at $0.1s^{-1}$ which increased to a maximum of 29 Pa.s on dilution. The mixture containing 1.5% alginate had an undiluted viscosity of 8 Pa.s reaching a maximum on dilution, of 45 Pa.s. The onset of the viscosity increase started at 10% dilution for the 1.5% mixture, whereas the viscosity increase in the 2% mixture did not start until 20% dilution. These results showed that by choosing a mixture closer to the phase boundary it is possible to achieve a higher maximum viscosity. The quantity of water required to trigger the viscosity increase can also be modulated. The superimposition of the viscosity curves suggests that following complete reversal of the separation the normal effect of dilution takes over.

The viscoelastic changes following dilution are shown in Figure 5.24. Both mixtures showed a slight decrease in G' on initial dilution, and a corresponding increase in tan delta. This suggests changes in property towards a viscous system, as would be expected on dilution. The decrease in G' was then followed by an increase to 18 Pa and 11 Pa for the dilution of the 1.5% and 2% mixtures respectively. Accompanying the increase in G' there is a corresponding decrease in tan delta, indicating the transition to a more elastic gel-like system. After reaching a maximum, G' decreased with increasing

dilution such that at 90% dilution the viscoelastic properties were beyond the measuring limits of the rheometer.

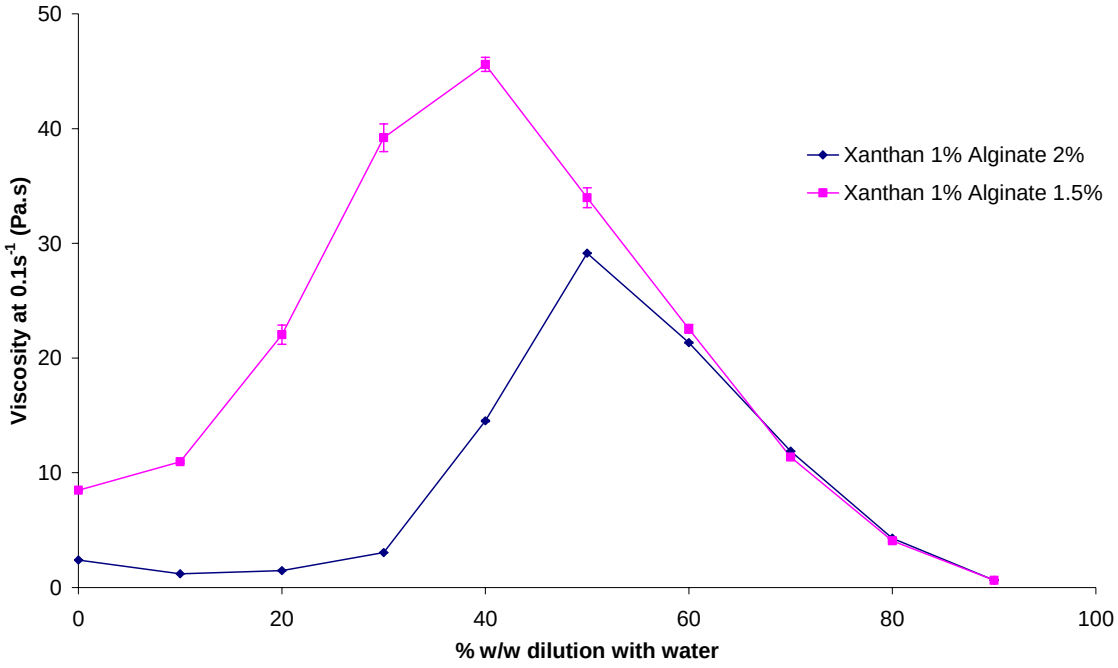

Figure 5.23. The continuous shear viscosity at 0.1s^{-1} of a 1% xanthan:2% alginate mixture and 1% xanthan:1.5% alginate mixture when diluted to varying degrees with water.
Percentage dilution refers to final composition e.g. 20% dilution refers to 20% water and 80% mixture. Samples were mixed prior to measurement. Geometry CP 4°/40mm 25 ± 0.1°C. Mean ± SD, n=3

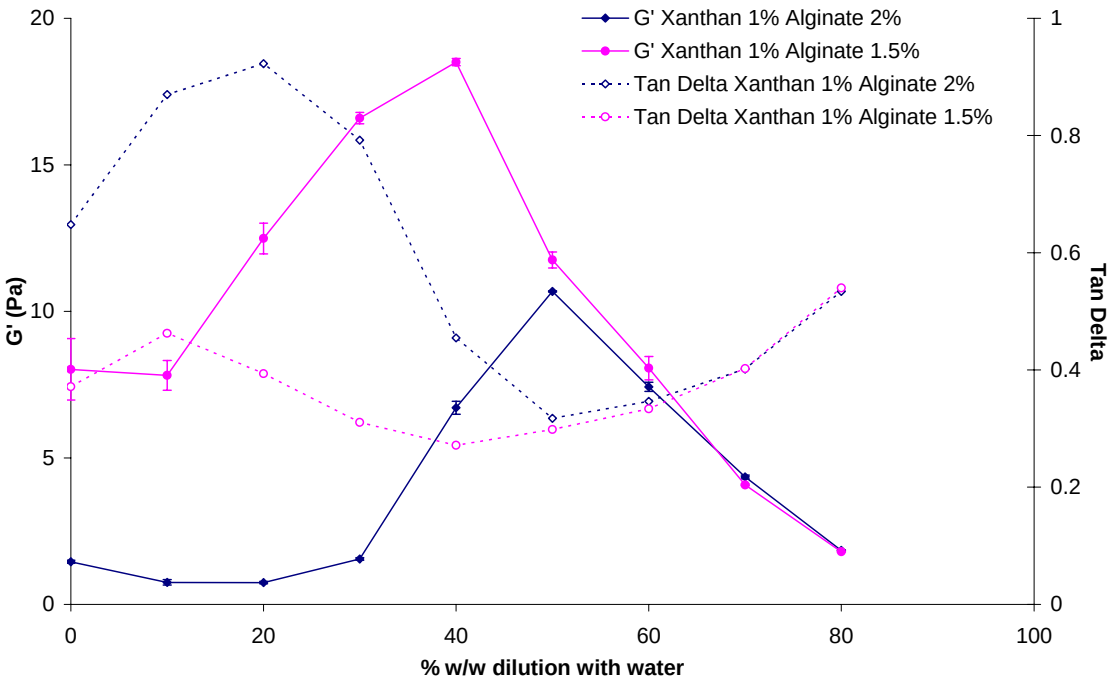

Figure 5.24 The dynamic viscoelastic properties of a 1% xanthan:2% alginate mixture and 1% xanthan:1.5% alginate mixture when diluted to varying degrees with water.
Percentage dilution refers to final composition e.g. 20% dilution refers to 20% water and 80% mixture. Samples were mixed prior to measurement. Geometry CP 4°/40mm 25 ± 0.1°C. Mean ± SD, n=3

5.4.4 Modifying the dilution profile by altering the position of the phase boundary

The work in section 3.4.11 demonstrated clearly that the phase boundary can be shifted by the addition of salts. The aim of this work was to investigate if the use of salt to shift the phase boundary to a higher alginate concentration could improve the dilution profile. The use of a higher alginate concentration to trigger phase separation would mean that a lower percentage of water would be needed to traverse the phase boundary. This is because the concentration range over which separation occurs does not appear to change with concentration. As a consequence, if a reduction in alginate concentration of 1% is required to reverse separation, a 1% reduction from 2% is a 50% decrease whereas a 1% reduction from 4% is a 25% decrease. This therefore affects the final mixture composition such that the xanthan concentration, if a 1% mixture were diluted, would be 0.5% or 0.75% respectively, and hence the latter would show a higher viscosity.

Figure 5.25 shows the effect of adding 2% NaCl to the xanthan:alginate mixtures (the lower concentrations of NaCl are also shown for comparison). The addition of 2% salt shifts the phase boundary to between 3% and 4% alginate, significantly higher than with no salt present.

Figure 5.26 shows the RVA dilution profile of a 1% xanthan:4% alginate mixture that also contains 2% NaCl. The dilution to 25% (3:1) showed a slight increase in viscosity, whilst dilution to 50% (1:1) showed a decrease in viscosity. When compared with Figure 5.3 and Figure 5.4, both without salt, it can be seen that the viscosity of the undiluted mixture with salt present is significantly higher. This higher undiluted viscosity prevents the viscosity increase on dilution occurring by effectively shifting the baseline. This would suggest that the use of salt does not enhance the dilution effect as desired.

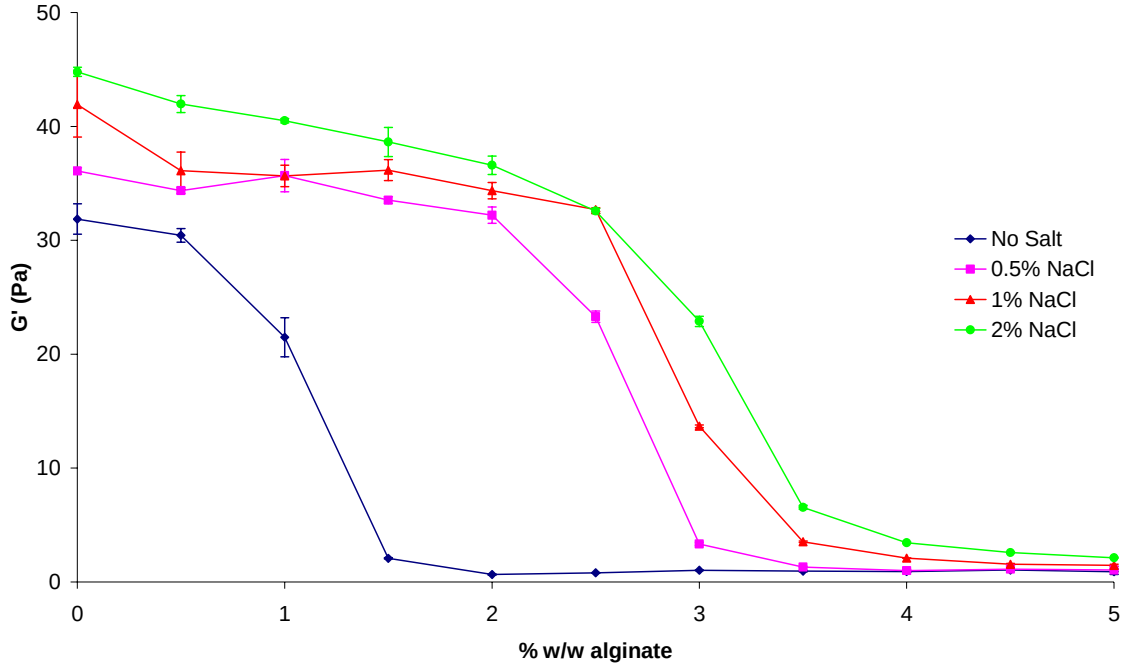

Figure 5.25. The dynamic viscoelastic properties of mixtures of 1% xanthan and alginate in the presence of varying concentrations of sodium chloride (NaCl).
Geometry CP 4°/40mm 25 ± 0.1°C. Mean ± SD, n=3

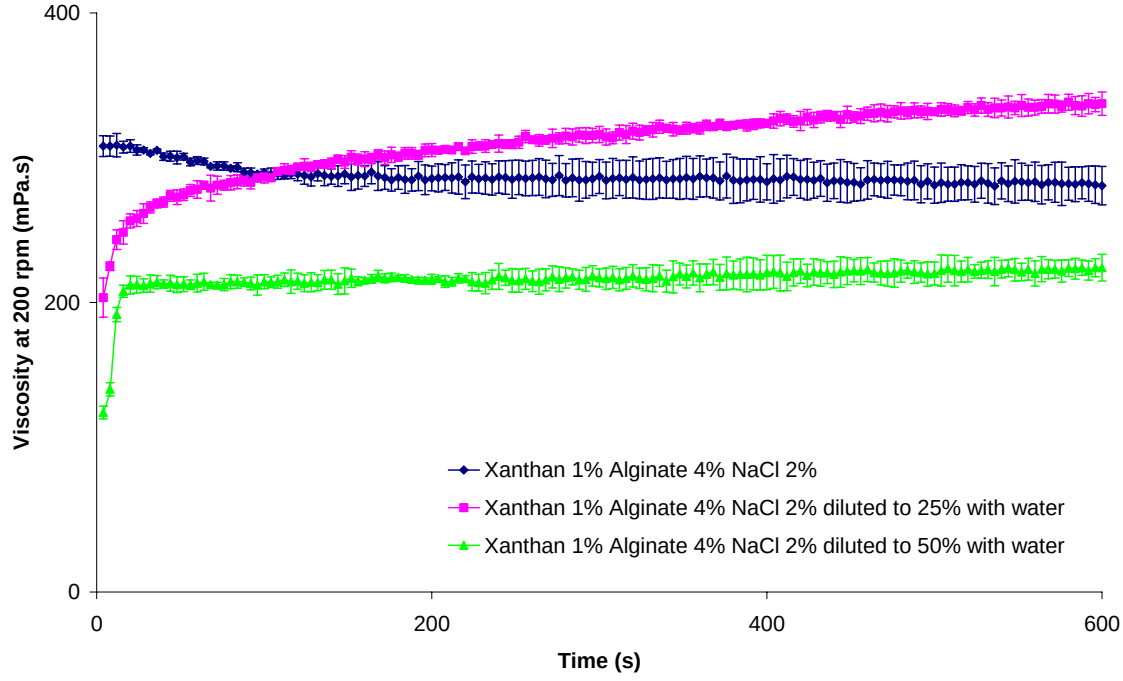

Figure 5.26. An RVA dilution profile of a 1% xanthan:4% alginate:2% sodium chloride (NaCl) mixture undiluted and when diluted to 25% and 50% with water.
Paddle speed 200rpm. 25 ± 0.5°C. Mean ± SD, n=3

5.4.5 The effect of dilution on xanthan:carboxymethylcellulose mixtures

This section examines mixtures of xanthan gum and CMC to investigate whether the effects observed on dilution of xanthan:alginate mixtures can be reproduced with dilution of xanthan:CMC mixtures.

The RVA dilution profile of a 1% xanthan:1.5% CMC mixture is shown in Figure 5.27. Dilution of the mixture by 50% with water showed a viscosity increase from 125 mPa.s to 180 mPa.s. When SGF was used as the diluent, the viscosity increased to 200 mPa.s. This shows that the effects observed with the xanthan:alginate mixtures are reproducible with xanthan:CMC mixtures. Figure 5.28 shows the effect of dilution on a solution of 1.5% CMC. Dilution with both water and SGF resulted in little change in viscosity. It is reported in the literature that the viscosity of CMC normally increases at pH's below 4 (Feddersen and Thorp 1993; Anon. 1999), which may explain the viscosity increase observed on the addition of SGF to the mixture; however the decrease in viscosity on dilution of the 1.5% CMC solution with SGF is inconsistent with this, and may be as a result of the viscosity being at the lower end of the measuring range of the RVA.

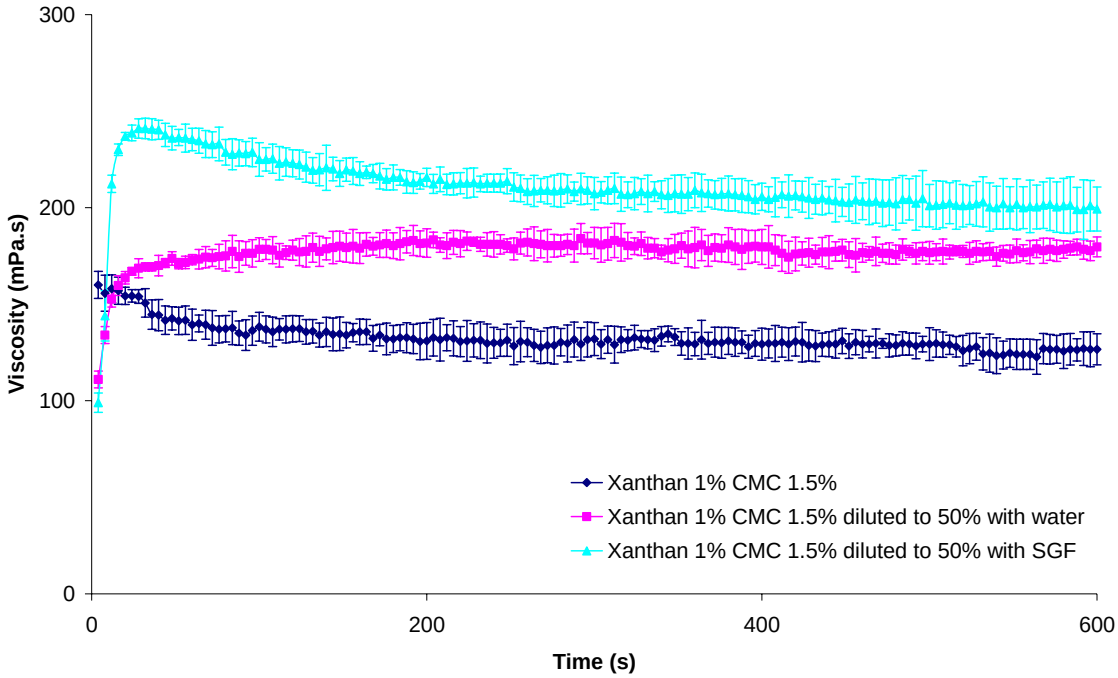

Figure 5.27. An RVA dilution profile of a 1% xanthan:1.5% CMC mixture undiluted, and diluted to 50% with water or simulated gastric fluid USP.
Paddle speed 200rpm. 25 ± 0.5°C. Mean ± SD, n=3

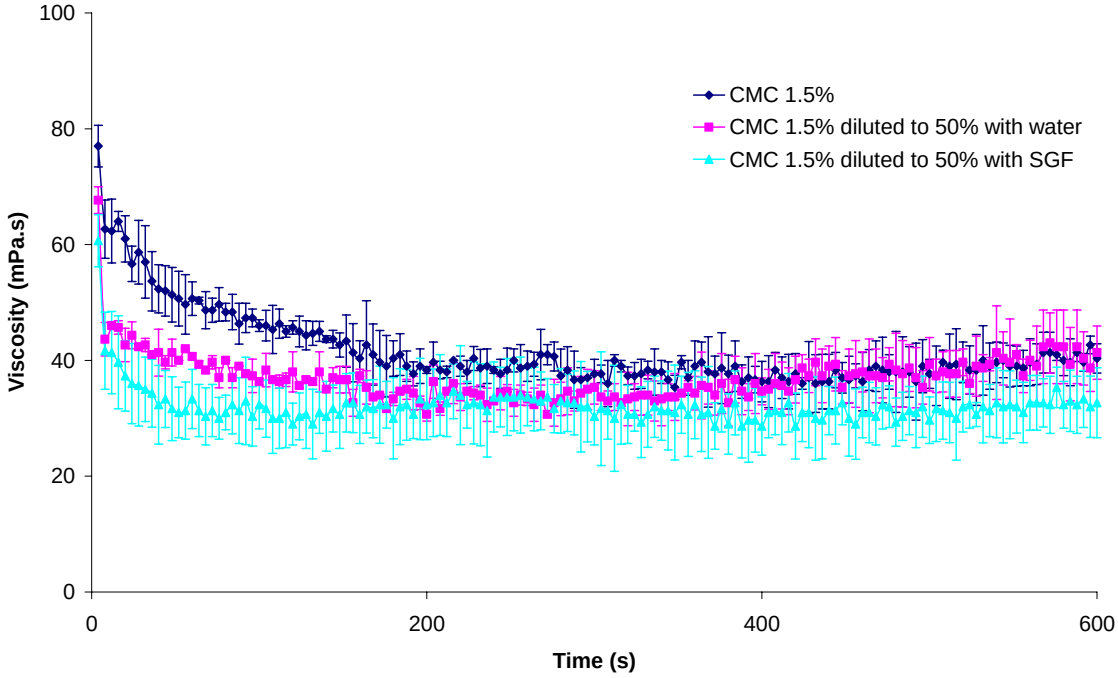

Figure 5.28. An RVA dilution profile of a 1.5% CMC solution undiluted, and diluted to 50% with water or simulated gastric fluid USP.
Paddle speed 200rpm. 25 ± 0.5°C. Mean ± SD, n=3

5.4.6 The effect of dilution on xanthan:polyacrylate mixtures

It has been shown that a viscosity increase on dilution is possible in both xanthan:alginate and xanthan:CMC mixtures. Both of these substances are based on natural products, which are subject to natural variation. This section examines whether dilution of xanthan:PAA mixtures can also produce similar effects. PAA is produced synthetically so has the potential to be more highly defined, such as lower degrees of polydispersity.

Figure 5.29 shows the RVA dilution profile with water and SGF, of a 1% xanthan:5.25% PAA (15 kDa) mixture. On dilution with either diluent, there is a rapid increase in viscosity from 100 mPa.s to 170 mPa.s, with mixing being almost complete in 10 to 15 seconds. Unlike the profiles observed with the dilution of the xanthan:alginate and xanthan:CMC mixtures, the use of SGF had no significant difference on the dilution profile over that with water. This would suggest that the PAA system is insensitive to low pH.

Figure 5.30 compares the dilution profile of mixtures of 1% xanthan with each of the different molecular weight polyacrylates (8kDa, 15kDa, 30 kDa). The concentration of PAA chosen was made based on figure 4.18. The concentration of PAA chosen was the concentration which reduced the value of G' to 10% of that of a 1% xanthan solution (4% for the 30 kDa; 5.25% for the 15 kDa and 6.8% for the 8 kDa). All three PAA samples showed similar dilution profiles, and each showed an increase in viscosity on dilution with water. It is noteworthy however that with decreasing molecular weight the quantity of water required before the onset of the viscosity increase, decreased also. The dilution profile of the mixture containing the 8 kDa PAA indicated that if the mixture was an oral product, a 10ml dose would only require 1.1ml of water to observe a significant viscosity increase. Figure 5.31 looks closer at the early stage of dilution of the 8kDa mixture and shows the viscosity increase starts at levels as low as 2.5% which has significant implications for oral products.

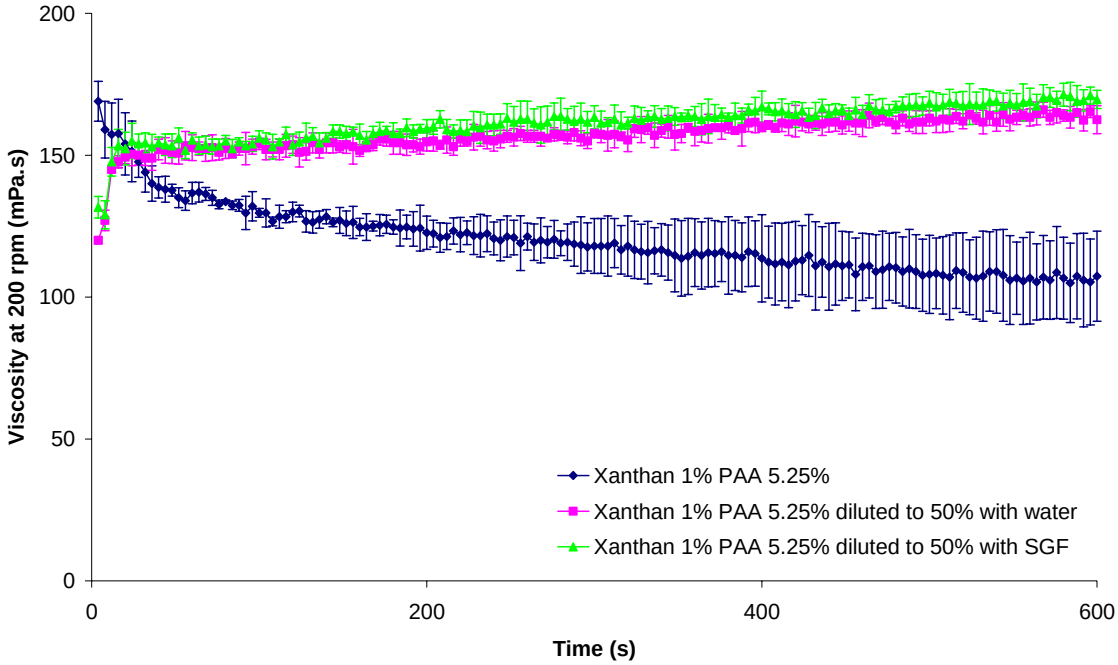

Figure 5.29. An RVA dilution profile of a 1% xanthan:5.25% sodium polyacrylate mixture and a 1% xanthan:5.25% sodium polyacrylate mixture diluted to 50% with water or simulated gastric fluid USP.
PAA Mw = 15 kDa. Paddle speed 200rpm. 25 ± 0.5°C. Mean ± SD, n=3

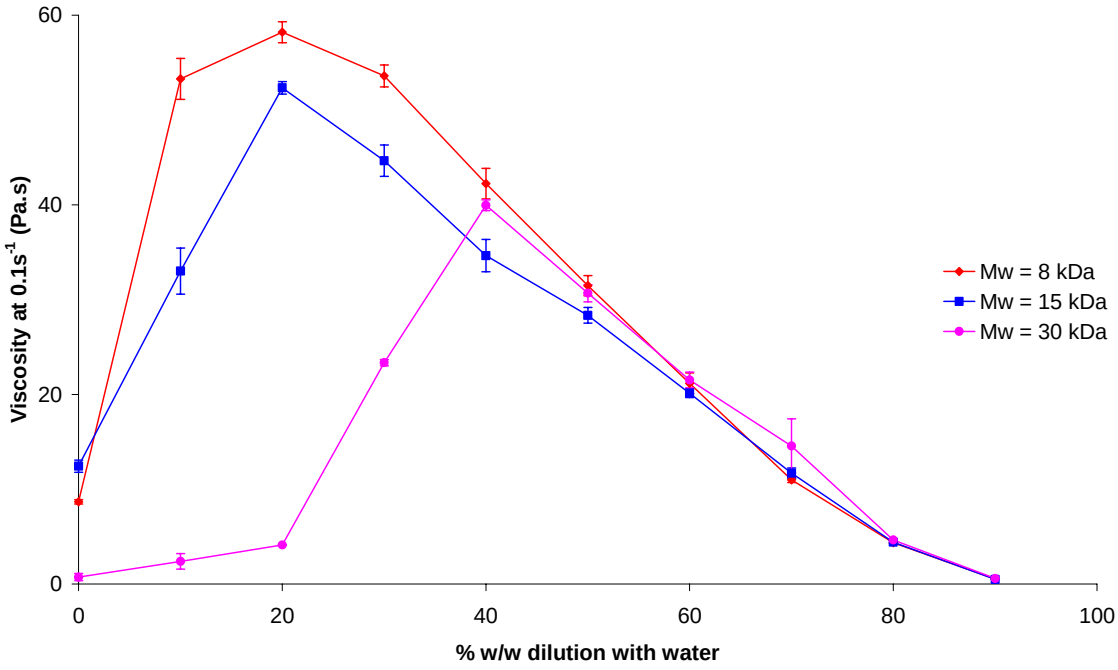

Figure 5.30. The continuous shear viscosity of mixtures of 1% xanthan and varying molecular weight polyacrylates when diluted with water.
Concentration of PAA used : 4% Mw = 30 kDa; 5.25% Mw = 15 kDa; 6.8% Mw = 8 kDa.
Geometry CP 4°/40mm 25 ± 0.1°C. Shear rate = $0.1s^{-1}$.Mean ± SD, n=3

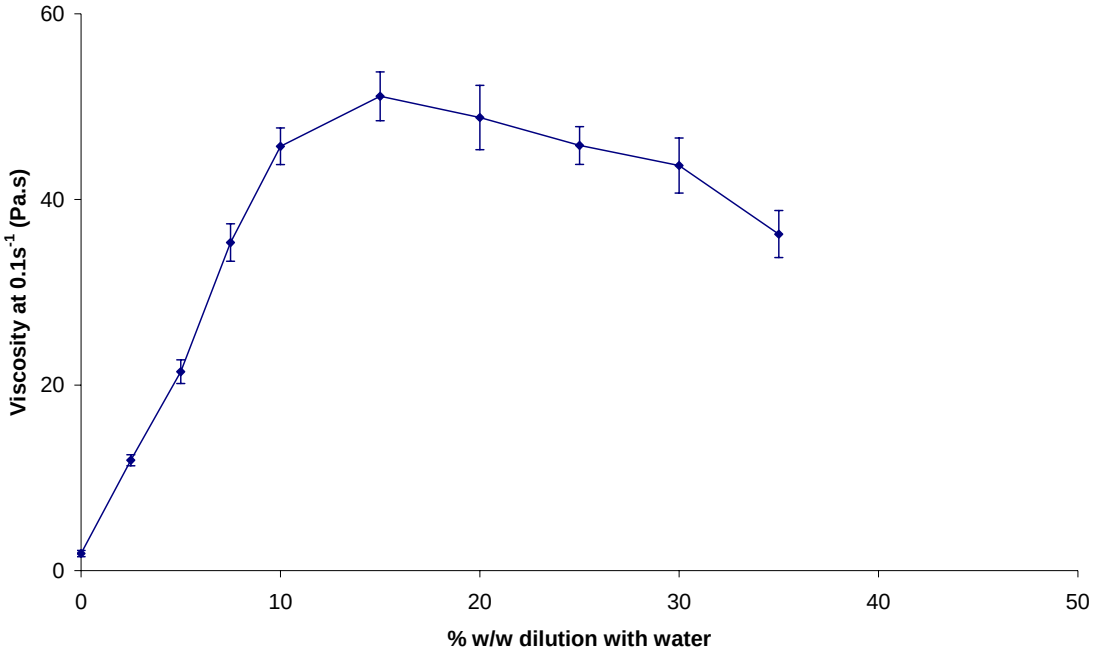

Figure 5.31. The continuous shear viscosity at 0.1s^{-1} of a 1% xanthan:6.8% PAA mixture when diluted with water.
PAA Mw = 8 kDa Geometry CP 4°/40mm 25 ± 0.1°C. Mean ± SD, n=3

5.4.7 The use of temperature to shift the phase boundary

5.4.7.a Moderate temperatures (10 - 50^{o}C)

It is common for phase separation to be reversed at higher temperatures (Sperling 2001). In chapter 3, DSC was employed to see if separation could be reversed using thermal methods and the results appeared to suggest that temperature could not reverse the separation. This section will examine the rheological changes that occur as a function of temperature to see if this agrees with the earlier DSC work.

Figure 5.32, Figure 5.33, Figure 5.34 and Figure 5.35 show the RVA dilution profiles for a 2% xanthan:2% alginate mixture at 10^{o}C, 25^{o}C, 37^{o}C, and 50^{o}C respectively. 2% xanthan was chosen to magnify any changes that might occur with temperature. All of the dilution profiles show a similarity in shape. It was evident that at each increase in temperature, the viscosity increase on dilution was enhanced. This would appear to be as a result of the viscosity of the undiluted mixture decreasing with higher temperatures, and the viscosity of the diluted mixture increasing with elevated temperatures. It was also evident that the viscosity of the diluted xanthan solution and the diluted mixture was not the same at the end of each experiment, the magnitude of the difference decreased with each increased temperature. The difference in viscosity would suggest that reversal of the phase separation was incomplete. The change in magnitude of the viscosity difference suggests that the phase boundary may have shifted as a result of the change in temperature.

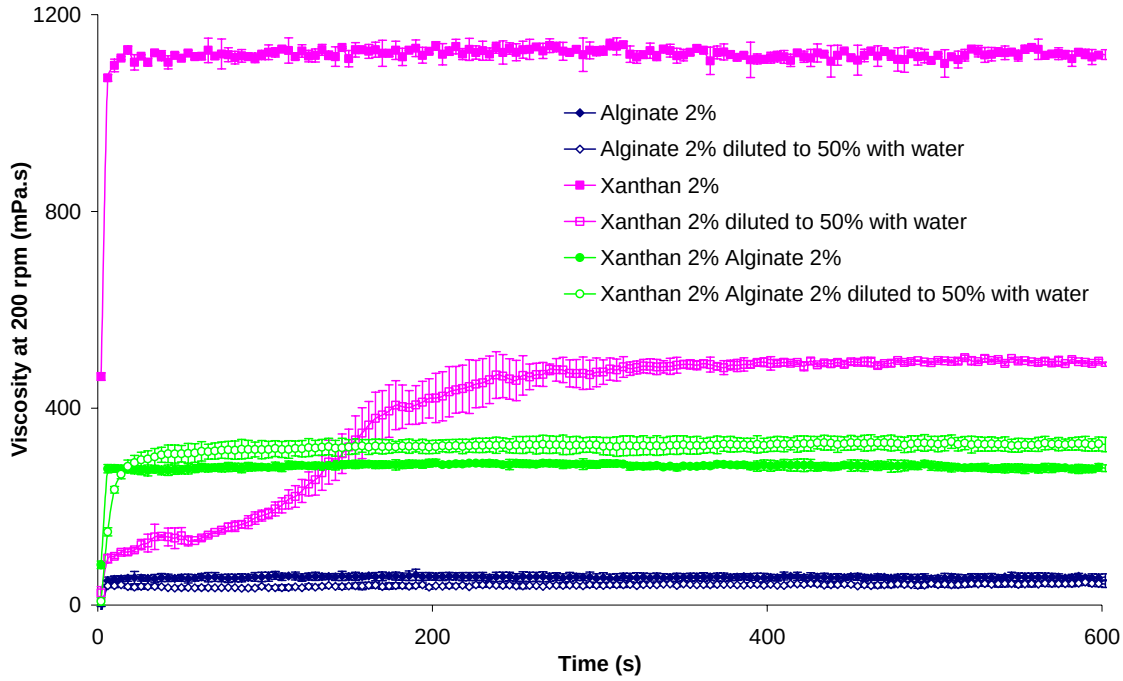

Figure 5.32. An RVA dilution profile of a 2% xanthan:2% alginate mixture diluted with water at 10°C compared to the dilution of the individual biopolymer solutions at the same concentrations.
Paddle speed 200rpm. 10 ± 0.5°C 30s thermal equilibrium. Mean ± SD, n=3

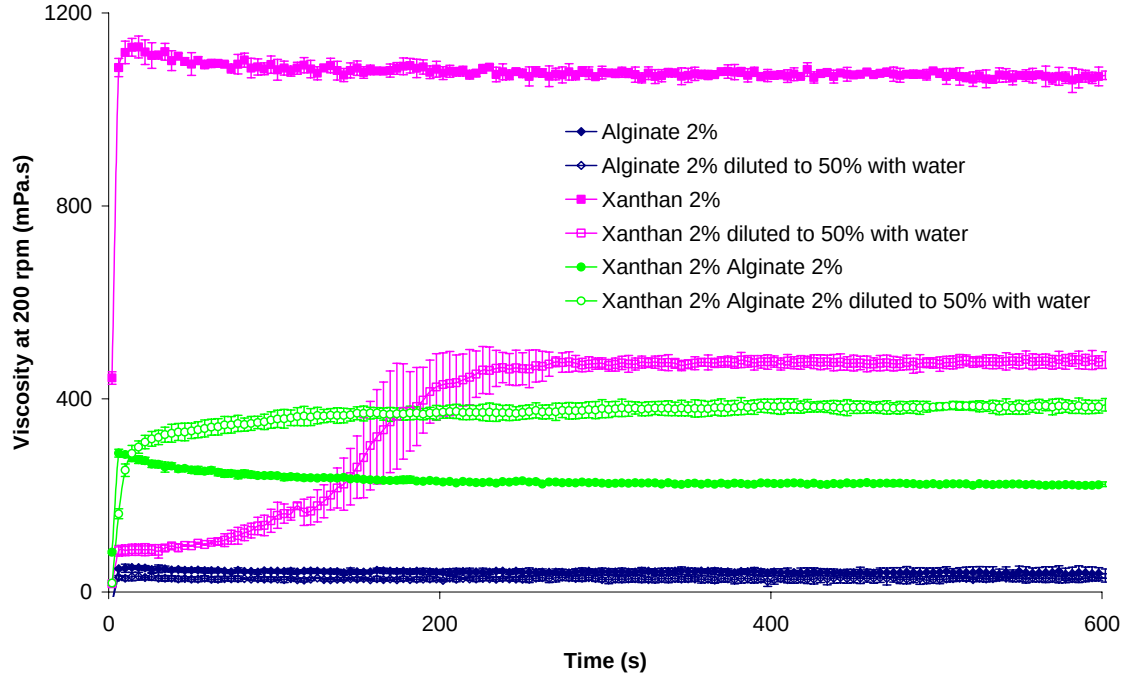

Figure 5.33. An RVA dilution profile of a 2% xanthan:2% alginate mixture diluted with water at 25°C compared to the dilution of the individual biopolymer solutions at the same concentrations.
Paddle speed 200rpm. 25 ± 0.5°C 30s thermal equilibrium. Mean ± SD, n=3

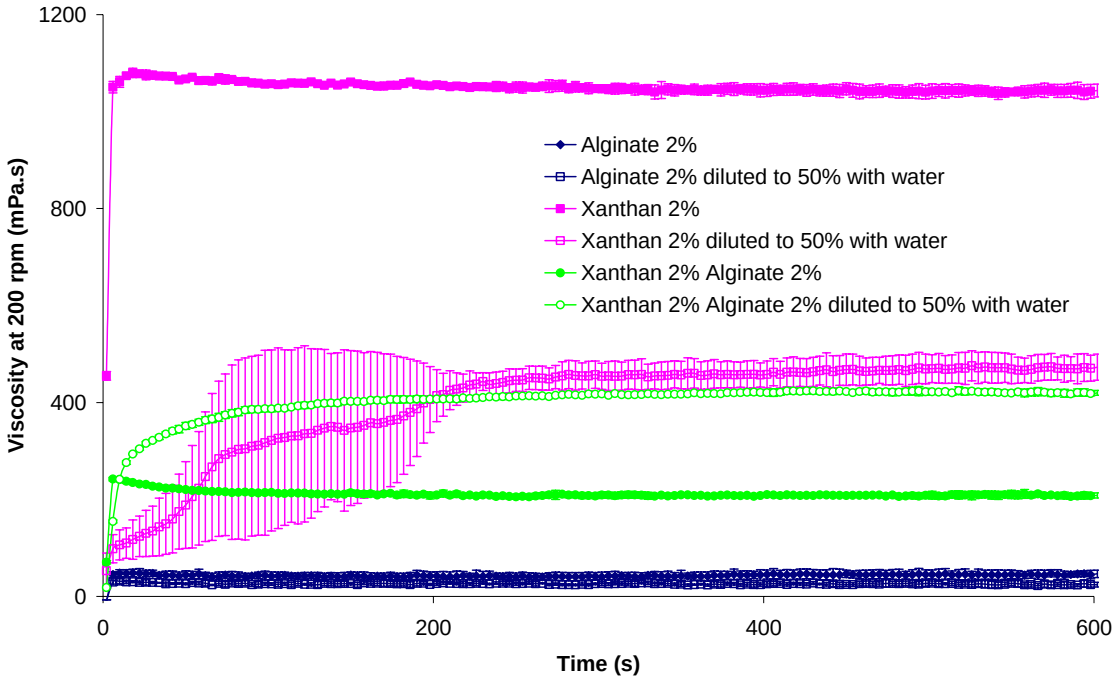

Figure 5.34. An RVA dilution profile of a 2% xanthan:2% alginate mixture diluted with water at 37°C compared to the dilution of the individual biopolymer solutions at the same concentrations.
Paddle speed 200rpm. 37 ± 0.5°C 30s thermal equilibrium. Mean ± SD, n=3

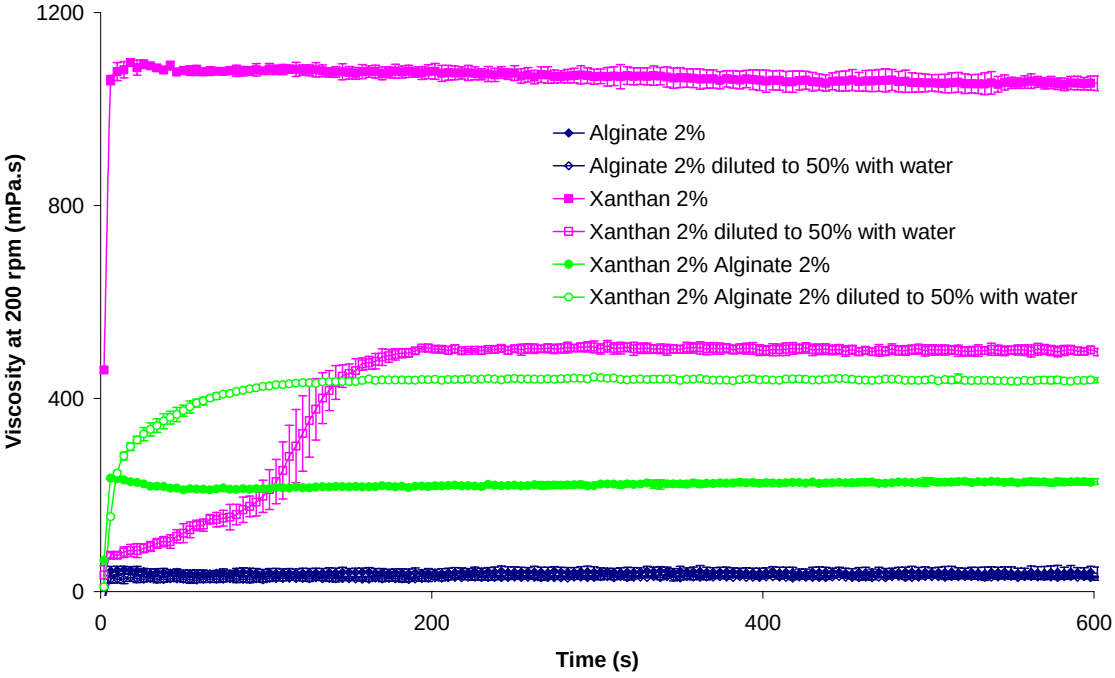

Figure 5.35. An RVA dilution profile of a 2% xanthan:2% alginate mixture diluted with water at 50°C compared to the dilution of the individual biopolymer solutions at the same concentrations.
Paddle speed 200rpm. 50 ± 0.5°C 30s thermal equilibrium. Mean ± SD, n=3

The effect of temperature on the continuous shear behaviour of both the undiluted and diluted systems are shown in Figure 5.36. It is apparent that with increasing temperature, the viscosity of the undiluted mixture decreased, whilst the diluted mixture increased in viscosity with increasing temperature. Linear regression of the data points provides equations describing the viscosity changes with temperature. For the undiluted mixture, the viscosity at $1s^{-1}$ at each given temperature is described by equation 5.1 where η_{undil} is viscosity and T is temperature in ^{o}C.

$$\eta_{undil} = -0.0227T + 2.9602 \quad (5.1)$$

The viscosity of the same mixture pre-diluted to 50% is described by equation 5.2, where η_{dil} is the viscosity of the premixed diluted mixture.

$$\eta_{dil} = 0.1522T + 9.579 \quad (5.2)$$

Combining equations 5.1 and 5.2 yields equation 5.3 which describes the viscosity increase expected at any given temperature between $10^{o}C$ and $50^{o}C$.

$$\eta_{inc} = 0.1749T + 6.6188 \quad (5.3)$$

The enhanced viscosity change with increasing temperature can be partially explained by studying the effect of temperature on the individual components. Figure 5.37 and Figure 5.38 show the effect of temperature on xanthan and alginate respectively. With increased temperature, the viscosity of xanthan is marginally raised. In comparison, the viscosity of the alginate significantly decreased with a temperature increase. Thus when the mixture is undiluted and is dominated by alginate properties, the viscosity decreases with increased temperature, in the diluted mixture where xanthan properties dominate, the viscosity increases with temperature.

Figure 5.39 examines the viscoelastic changes that occur with xanthan as a function of temperature. It shows that with increasing temperature, G' was decreased suggesting that at higher temperatures the elasticity of the xanthan solution is reduced.

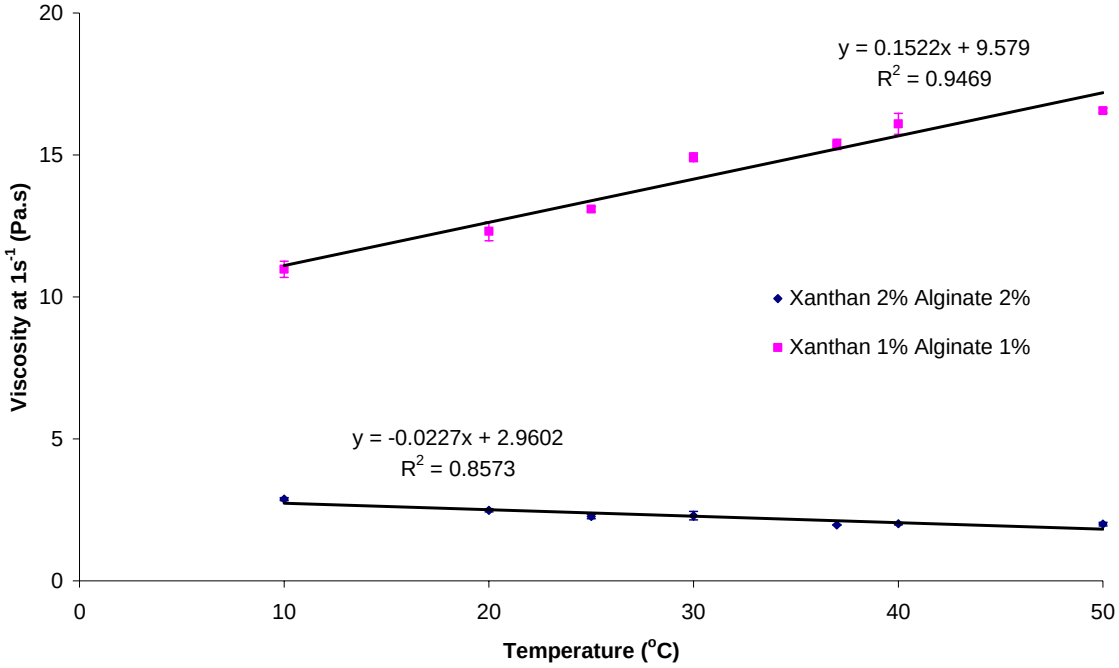

Figure 5.36. The effects of temperature on the continuous shear viscosity at $1s^{-1}$ of a 2% xanthan:2% alginate mixture undiluted and when diluted 1:1 with water.
The diluted mixture was thoroughly mixed prior to measurement. Geometry CP 4°/40mm. Temperature ± 0.1°C. Mean ± SD, n=3

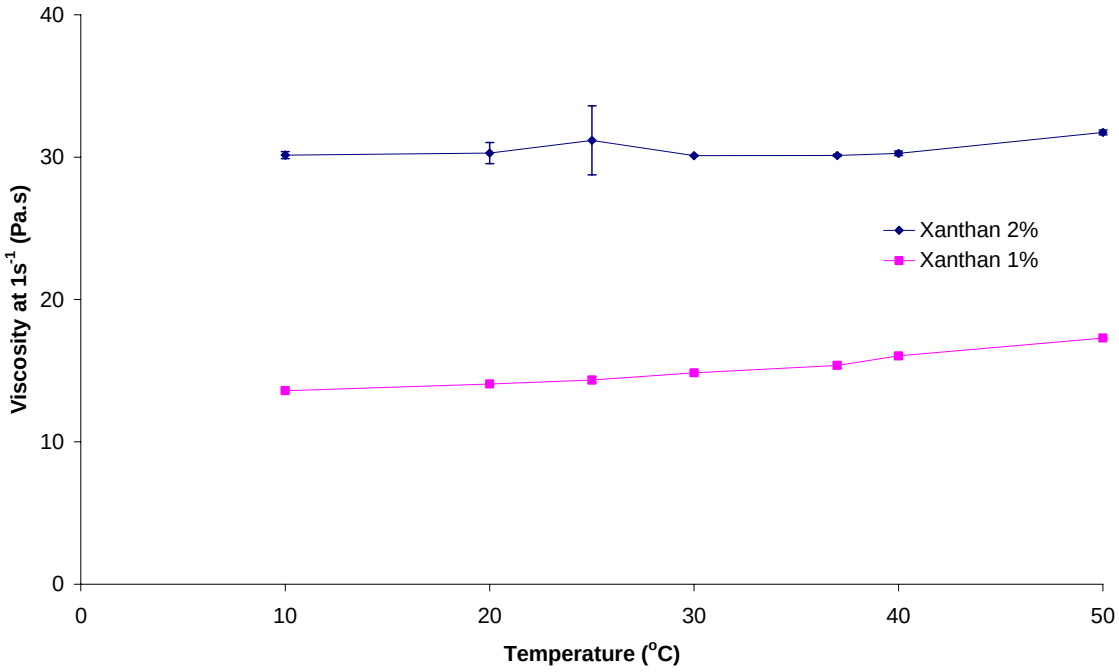

Figure 5.37. The effects of temperature on the continuous shear viscosity at $1s^{-1}$ of a 2% xanthan solution undiluted and when diluted 1:1 with water.
The diluted mixture was thoroughly mixed prior to measurement. Geometry CP 4°/40mm. Temperature ± 0.1°C. Mean ± SD, n=3

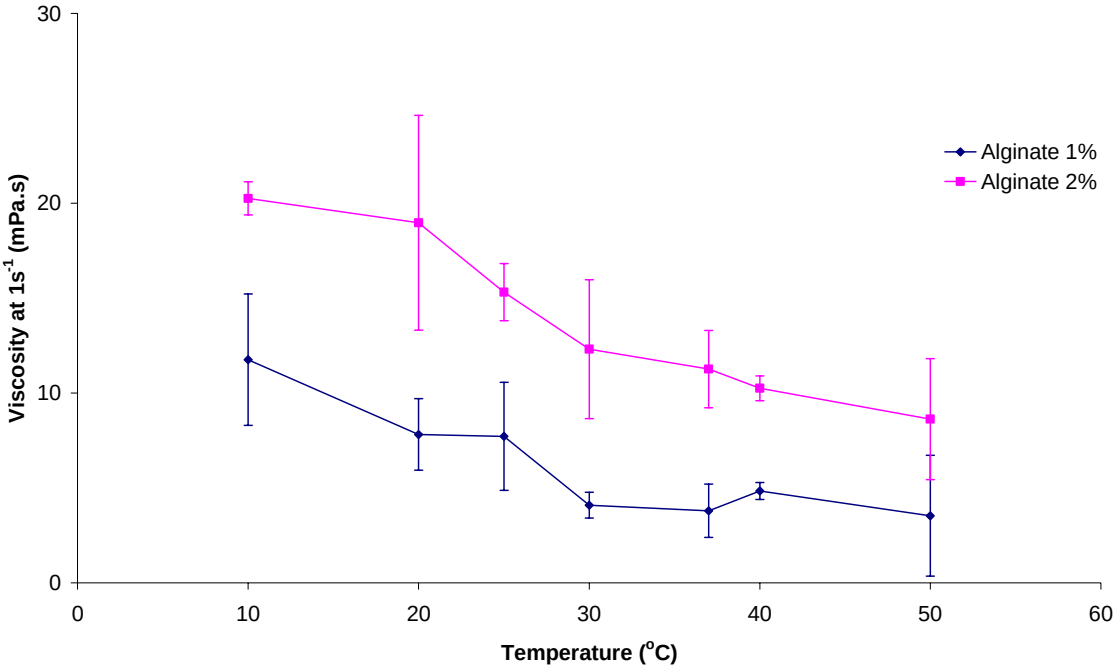

Figure 5.38. The effects of temperature on the continuous shear viscosity at $1s^{-1}$ of a 2% alginate solution undiluted and when diluted 1:1 with water.
The diluted mixture was thoroughly mixed prior to measurement. Geometry CP 4°/40mm. Temperature ± 0.1°C. Mean ± SD, n=3, Note the different units for this figure compared to Figure 5.36 and Figure 5.37.

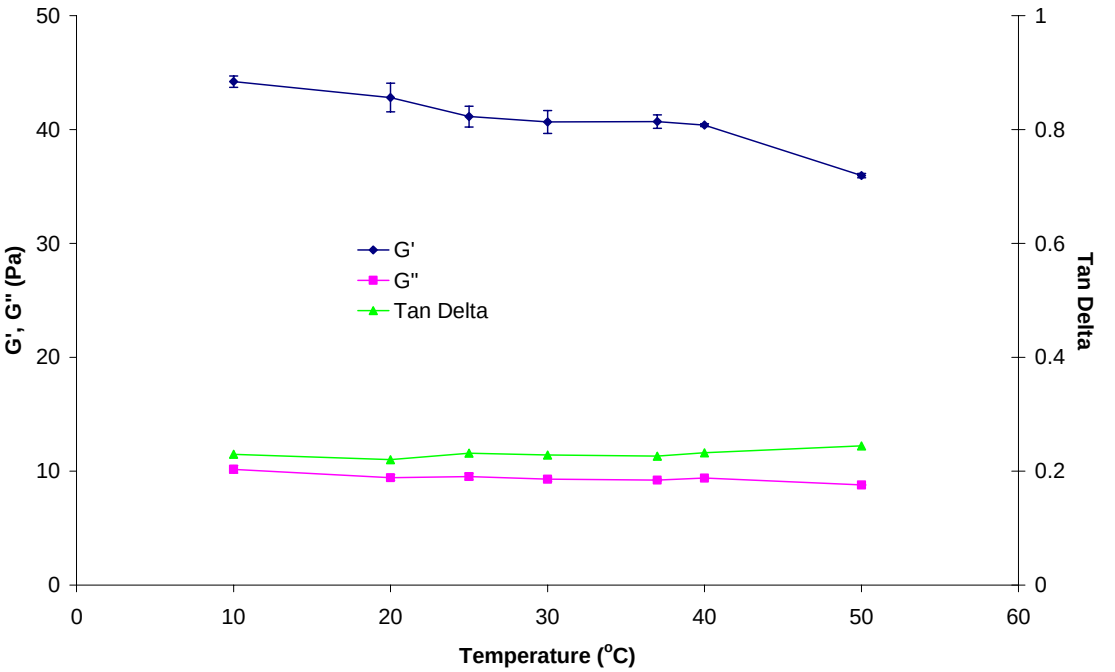

Figure 5.39. The effects of temperature on dynamic viscoelastic properties of a 1% xanthan solution.
Geometry CP 4°/40mm, Frequency = 1.02Hz, Temperature ± 0.1°C. Mean ± SD, n=3

5.4.7.b High temperature (80°C)

Figure 5.40 shows the RVA profile of a 2% xanthan:2% alginate mixture at 80°C. The dilution of the mixture at 80°C shows a similar profile to the other mixtures above 25°C. The profile of the undiluted mixture is significantly different. It can be seen that throughout the duration of the experiment the undiluted mixture increased in viscosity, to the extent that at after 10 minutes the viscosity of the undiluted mixture was greater than that of the diluted mixture.

Figure 5.42 shows the effect of heating a 1% xanthan:2% alginate mixture to 85°C for different lengths of time to investigate (a) the effect of high temperature on viscosity and (b) if prolonged elevated temperatures have any deleterious effects on mixture properties. A schematic flow chart of the method is provided in Figure 5.41. Samples were held at 25 °C for 15 minutes with no rotational motion to thermally equilibrate; the viscosity was then monitored at 25°C for 10 minutes. The samples were then heated to 85°C for 20 minutes with a slow rotation of 10 rpm to allow thermal equilibration. After this time the viscosity of the mixture was measured for 10 minutes, 20 minutes or 60 minutes before cooling to 25°C for 30 minutes followed by measurement at 25°C for a final 10 minutes. The results show that when heated and equilibrated to 85°C the mixture greatly increased in viscosity to 350 mPa.s a figure 3.5 times greater than the undiluted mixture. It also shows that maintaining the mixture at high temperature had no overall detrimental effect on the viscosity at 25°C suggesting that the elevated temperature had not irreparably damaged the mixture.

These results would suggest that the phase boundary can be shifted by the use of higher temperatures. The viscosity increase with temperature alone offers another potential trigger for use with the viscosity increase phenomenon. This however would be unlikely to be of use in a biological environment due to the high temperatures required.

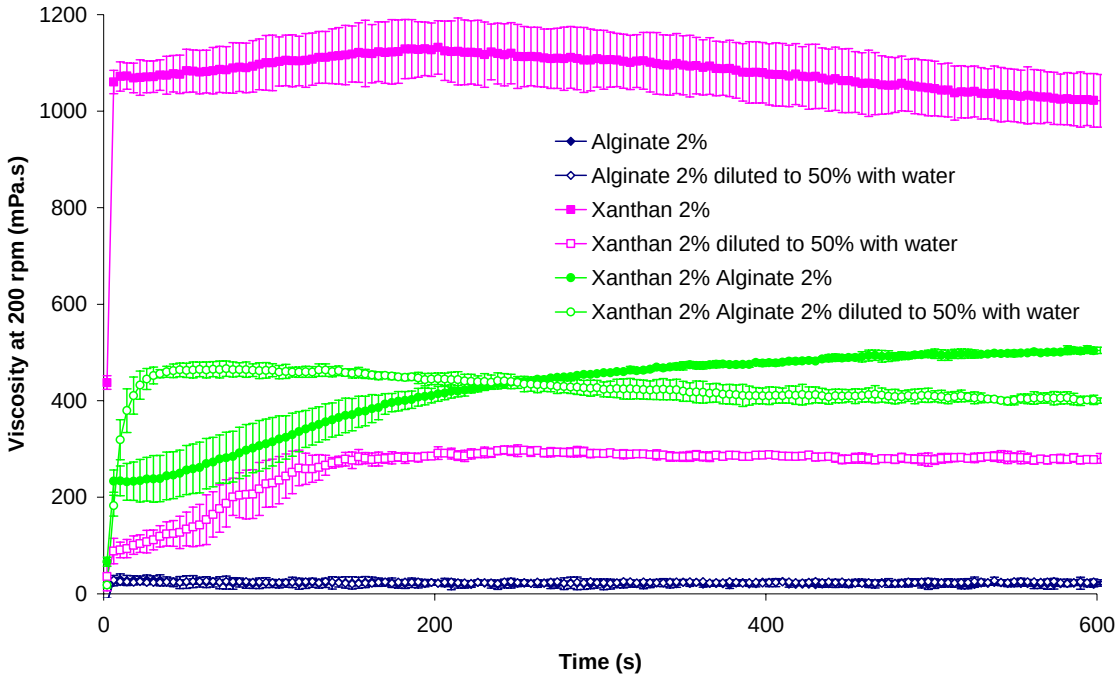

Figure 5.40. An RVA dilution profile of a 2% xanthan:2% alginate mixture diluted with water at 80°C compared to the dilution of the individual biopolymer solutions at the same concentrations.
Paddle speed 200rpm. 80 ± 0.5°C 30s thermal equilibrium. Mean ± SD, n=3

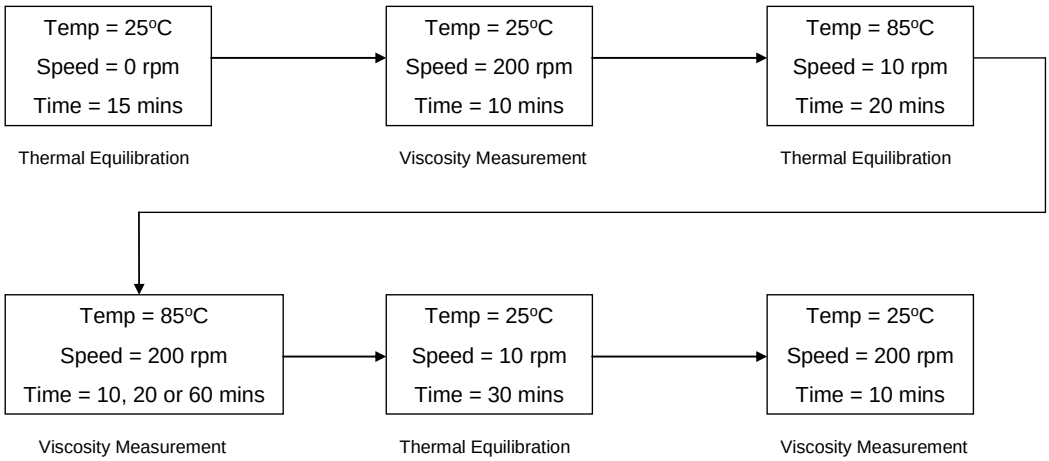

Figure 5.41. A diagrammatic representation of the RVA methodology used for studying the effects of prolonged elevated temperatures on the viscosity of xanthan:alginate mixtures.
Temperature refers to the temperature of the circulating water jacket, not a measured temperature of the mixture.

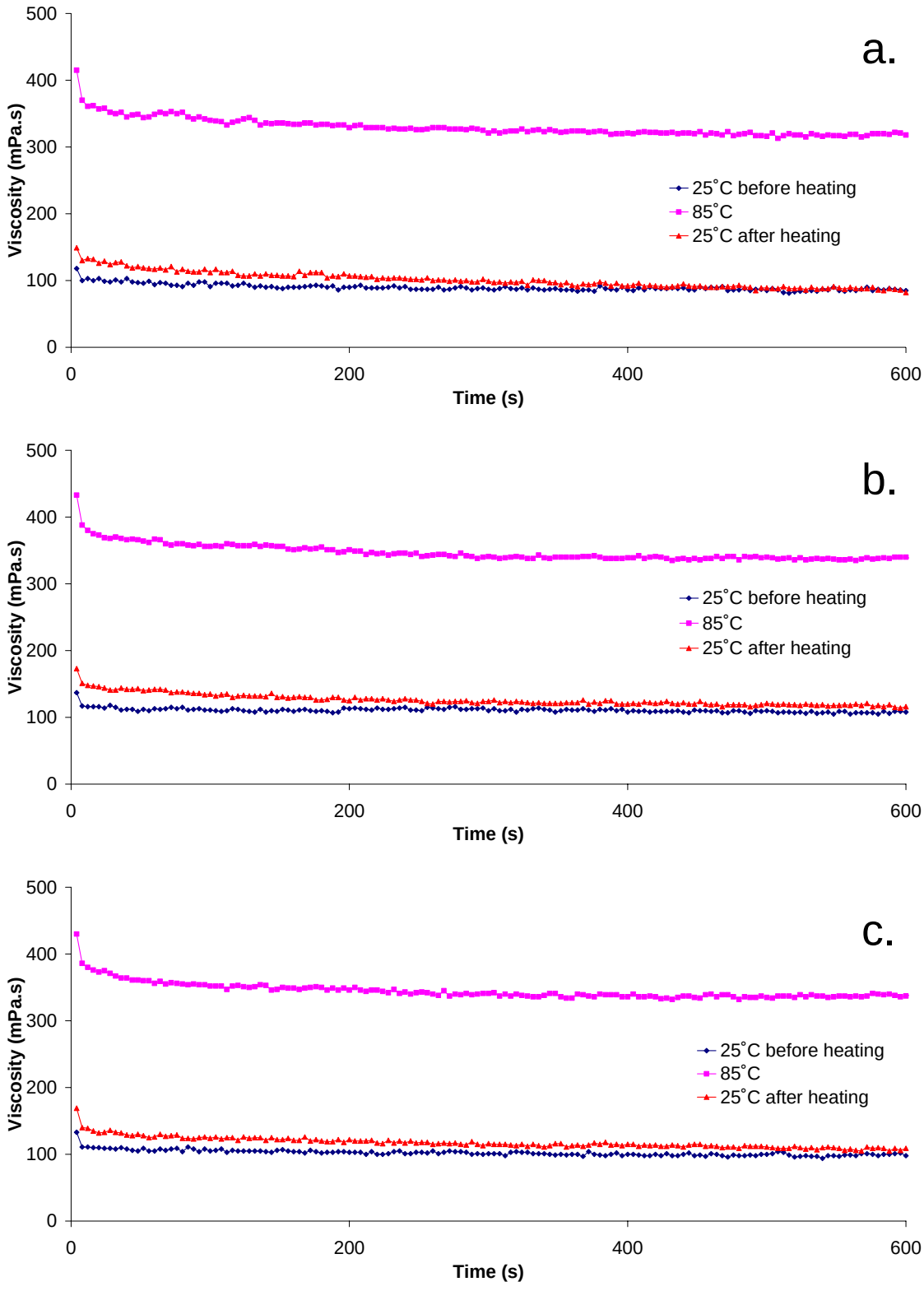

Figure 5.42. RVA profiles of 1% xanthan:2% alginate mixtures when subjected to differing temperature conditions.
Samples were held at 85°C for (a) 10 minutes (b) 20 minutes or (c) 60 minutes prior to cooling to 25°C. For the experimental protocol refer to Figure 5.41.

5.4.8 Preparation methods for xanthan/alginate mixtures

Throughout this project, mixtures have been prepared by combining concentrated stock solutions of each biopolymer. This section investigates whether it is possible to use the alginate solution as a solvent for the xanthan powder. The aim of this section is to see if preparing solutions by this 'direct addition' method yields solutions similar to those prepared by the combination of concentrated stock solutions.

Figure 5.43 investigates the continuous shear properties of 1% xanthan:2% alginate mixtures prepared by the two different methods. Both profiles show a small degree of pseudoplasticity, however the low shear viscosity of the mixture prepared by the combination of the stock solutions is significantly lower than that of the mixture prepared by direct addition. At high shear rates there is little difference in viscosity. Figure 5.44 compares the viscoelastic properties. Both mixtures exhibit very low overall viscoelastic behaviour; however, the mixture prepared by direct addition shows moduli significantly greater than by the stock combination method. Figure 5.45 shows microscope images of the two different mixtures. Both images show the presence of birefringent strands; however the mixture prepared by combination of concentrated stock solutions shows significantly larger strands than that prepared by the direct addition technique.

These results would suggest that the mixtures can be prepared using a method of direct addition. However, although the overall compositions are the same it would not be correct to say that these solutions show identical solution properties. It is possible that these differences arise as a result of the differing hydration levels of the xanthan. In the stock solution method xanthan has an opportunity to hydrate independently of alginate. In the direct addition technique xanthan has to compete with the water already being utilised by the alginate, thereby behaving in a manner similar to that of a suspension. In this case only a small percentage of the added xanthan may have dissolved, which is insufficient to traverse the phase boundary. This would result in xanthan in the continuous phase thereby increasing the viscosity and viscoelastic properties.

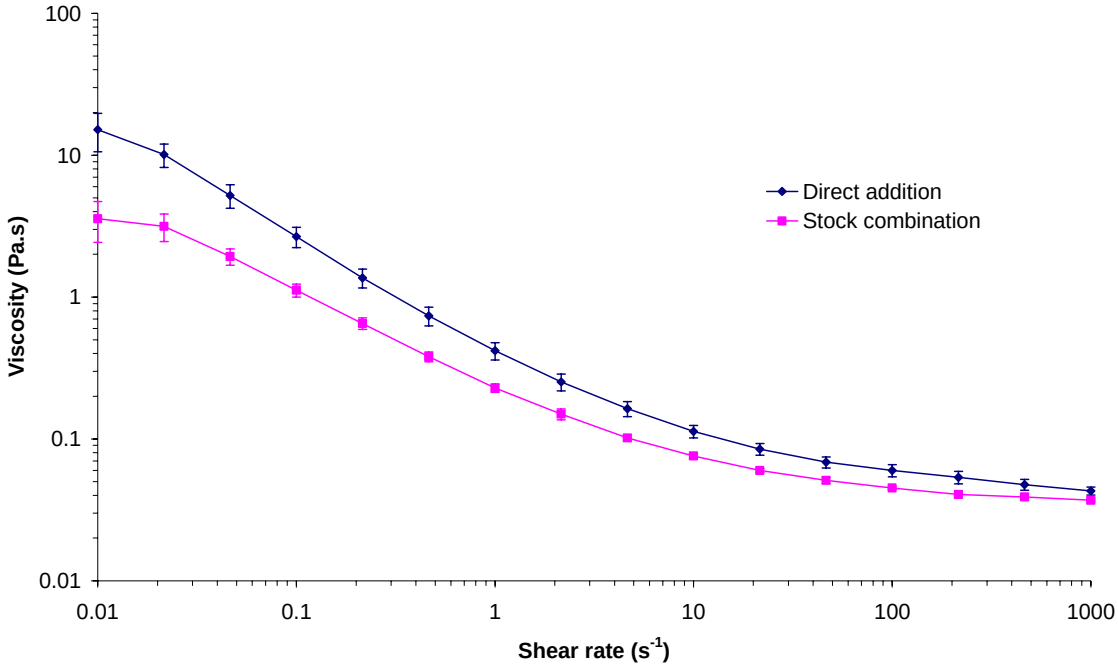

Figure 5.43. Continuous shear profiles of 1% xanthan:2% alginate mixtures prepared by different methods.
Stock combination: Individual concentrated biopolymer solutions are prepared and then mixed following hydration. Direct addition: Alginate is dispersed in water. Following hydration the xanthan is then dispersed directly into the alginate solution. Geometry CP 4°/40mm 25 ± 0.1°C. Mean ± SD, n=3

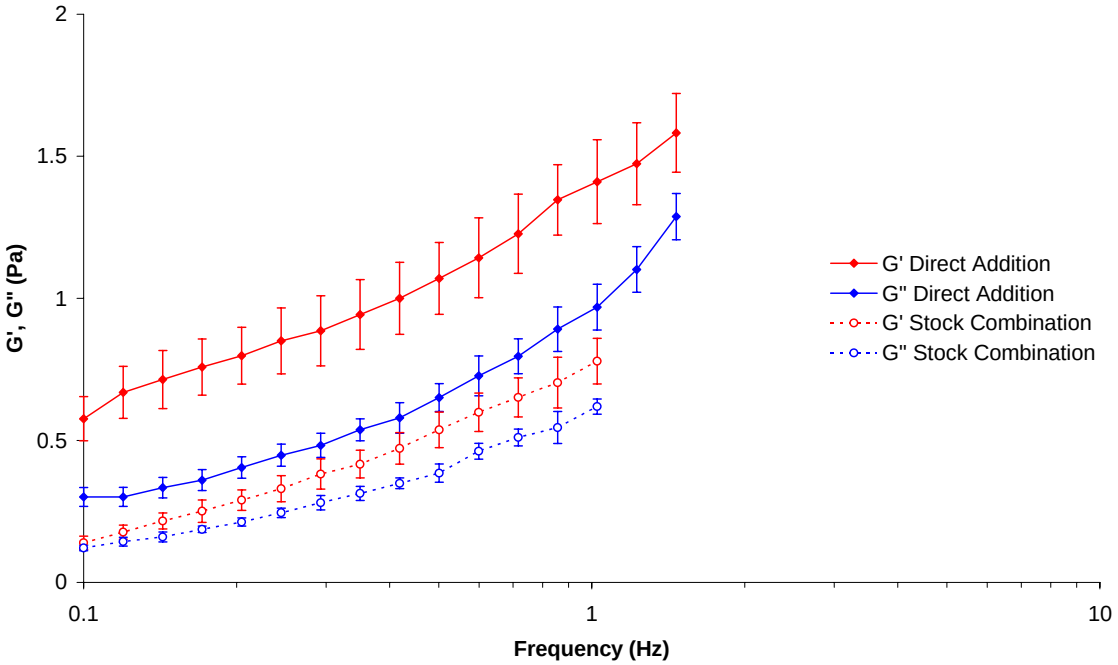

Figure 5.44. The dynamic viscoelastic profiles of 1% xanthan:2% alginate mixtures prepared by combination of concentrated stock solutions and by direct addition of powders.
Geometry CP 4°/40mm 25 ± 0.1°C. Mean ± SD, n=3

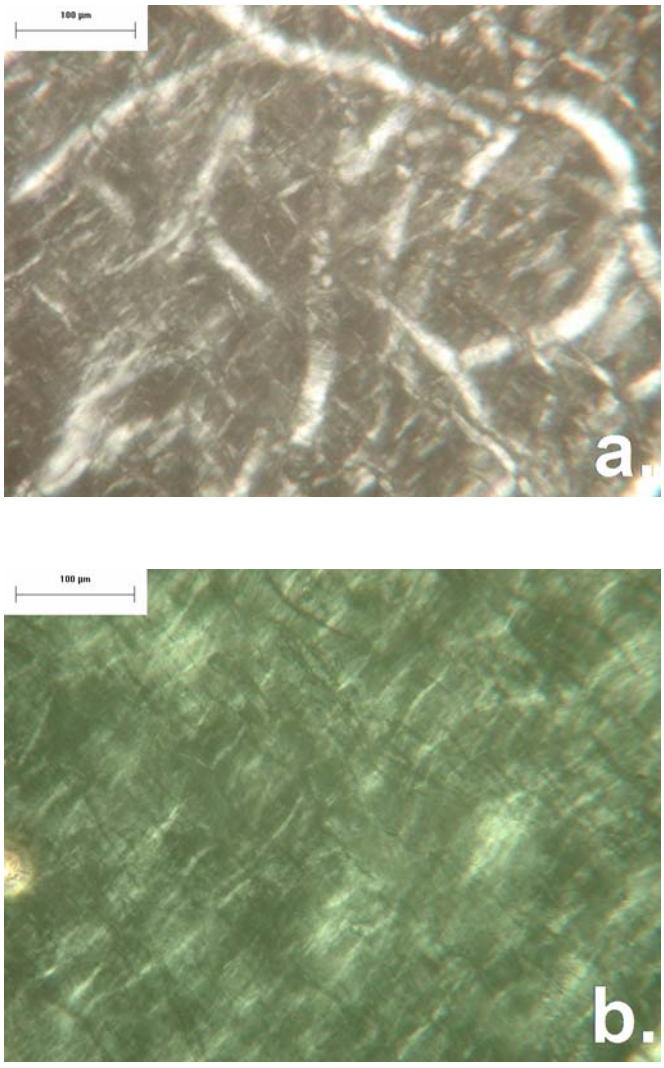

Figure 5.45. Crossed polarized light microscope images of 1% xanthan:2% alginate mixtures prepared by (a) the combination of concentrated stock solutions and (b) direct addition.

5.4.9 Direct addition as a means of achieving high concentration xanthan systems

The previous section showed that xanthan:alginate mixtures can be produced without preparing highly concentrated stock solutions which can be time consuming and difficult to prepare. This section investigates whether mixtures containing xanthan above 2% can be prepared, and examines the properties of the resulting mixture.

Figure 5.46 examines the viscoelastic properties of mixtures of 2% alginate and increasing concentrations of xanthan. The 1% xanthan mixture showed low viscoelastic moduli and a relatively high value of tan delta, indicating properties of an essentially non-viscous system. With increasing concentrations of xanthan, G' and G" increased with a corresponding decrease in tan delta, indicating that the increased xanthan concentration although in the disperse phase, was imparting more elastic-like properties on the mixtures. Above 4% xanthan, tan delta values plateaued at approximately 0.2. This shows that high concentration xanthan mixtures can be produced, and these exhibit high moduli weak gel-like properties. It is important to note that when preparing the higher concentration mixtures particular care and attention was necessary as a result of the pronounced Weissenberg effect created by the increased elasticity of the liquid (Barnes, Hutton et al. 1989).

Figure 5.47 shows a microscope image of the 10% xanthan:2% alginate mixture. Birefringence is highly pronounced, but the strand-like appearance is not as clearly defined as that seen normally in the 1% xanthan:2% alginate mixtures. It is possible based on the images presented in section 3.4.12 that as a result of the higher viscosity of the mixture, the clearly defined strand structures were prevented from forming.

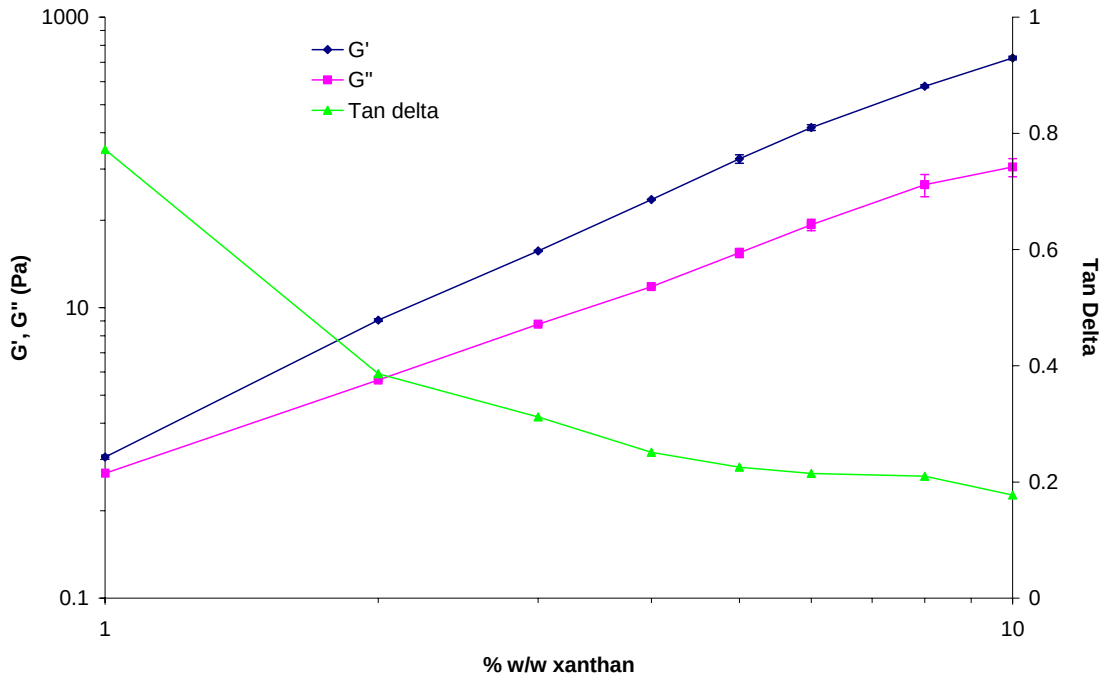

Figure 5.46. The effect on dynamic viscoelasticity of xanthan concentration on 2% alginate mixtures.
Mixtures were prepared by the direct addition method.
Geometry CP 4°/40mm, Frequency 1.02Hz, 25 ± 0.1°C. Mean ± SD, n=3
`

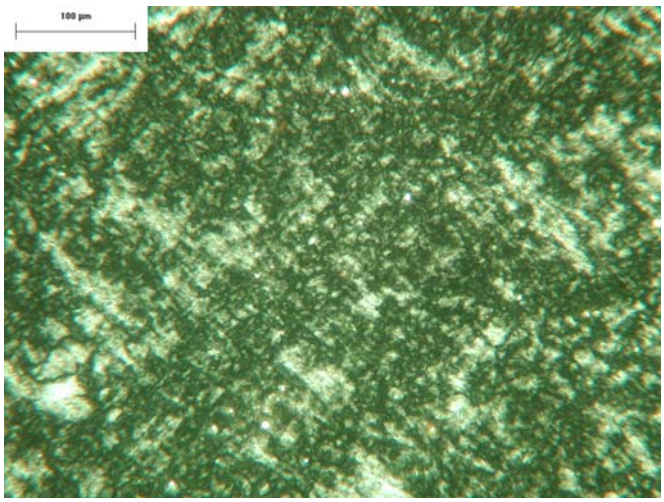

Figure 5.47. Crossed polarized light microscope image of a 10% xanthan:2% alginate mixture.
This mixture was prepared by the direct addition method.

5.4.10 Dilution of a high concentration xanthan mixture

The use of high concentration xanthan mixtures offers a wealth of possibilities for a number of common applications for xanthan. This next section investigates the dilution of a 4% xanthan:2% alginate mixture as an example of a high concentration xanthan system.

Figure 5.48 shows the viscoelastic changes observed with increasing levels of dilution. At low degrees of dilution (up to 30%), G' decreased significantly. Between 30% and 50% dilution G' values increased, as a result of reversal of the separation. At higher levels of dilution (>50%) G' decreases again with the effect of dilution.

Figure 5.49 shows the changes in viscosity on dilution of the 4% xanthan:2% alginate mixture. Dilution up to 30% shows no significant change in viscosity value. Further addition of water to 60% increased viscosity to twice the undiluted viscosity, subsequent dilution showed a decrease in viscosity. The dilution of the 4% xanthan:2% alginate mixture showed that viscosity was either maintained or increased at levels of up to at least 80% dilution i.e. a system where one part mixture can have 4 parts water added with no loss in viscosity. To further put this dilution effect into context, Figure 5.50 compares the dilution profiles of a 1% xanthan:2% alginate mixture with the 4% xanthan:2% alginate mixture. It shows that throughout the dilution range studied (up to 90%) the 4% xanthan mixture exhibits significantly higher viscosities.

The use of the higher concentration xanthan mixtures offers a number of potentially useful applications, not least as an easier method for making low concentration xanthan solutions.

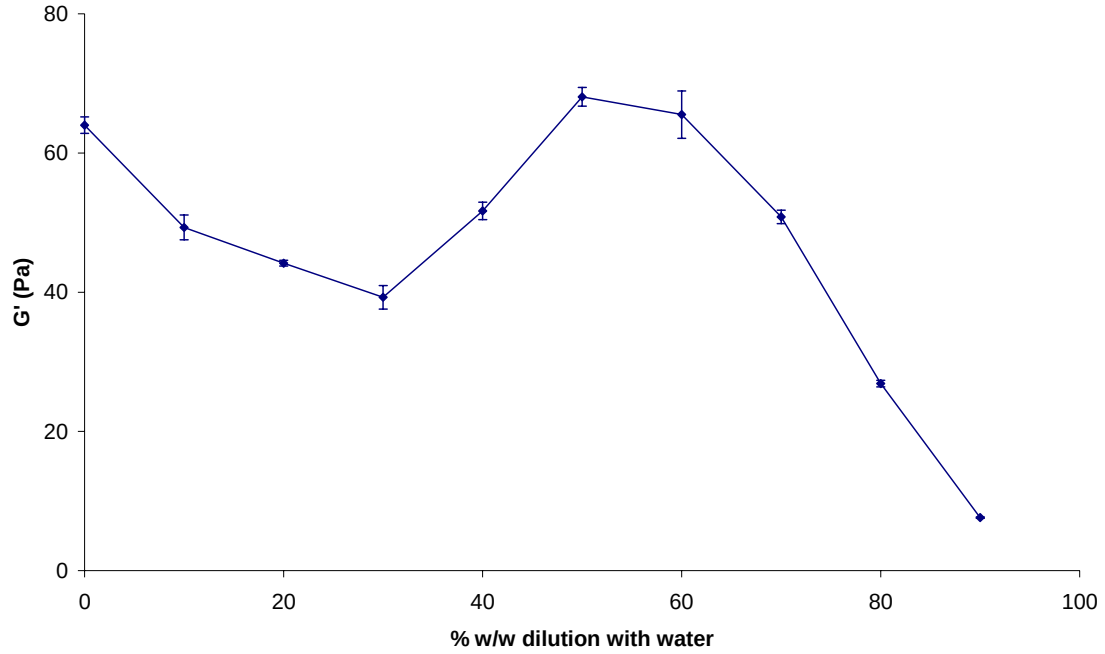

Figure 5.48. The effect of dilution on the dynamic viscoelastic properties of a 4% xanthan gum:2% alginate mixture prepared by direct addition.
Geometry CP 4°/40mm 25 ± 0.1°C. Frequency 1.02Hz Mean ± SD, n=3

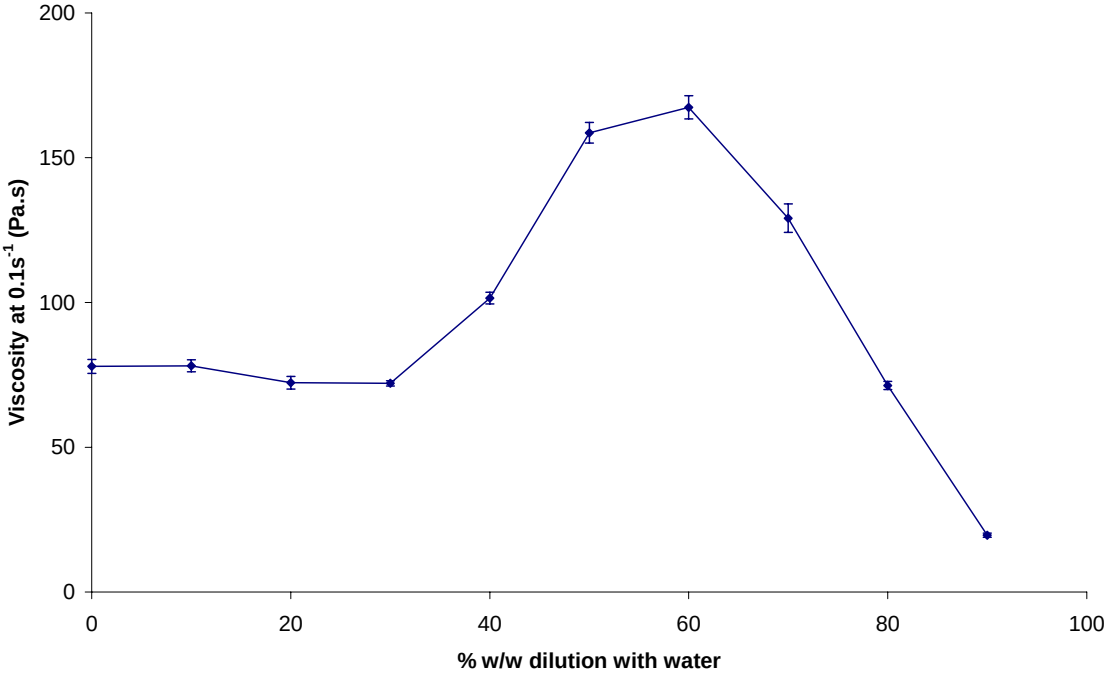

Figure 5.49. The effect of dilution on the continuous shear viscosity at $0.1s^{-1}$ of a 4% xanthan:2% alginate mixture prepared by direct addition.
Geometry CP 4°/40mm 25 ± 0.1°C. Mean ± SD, n=3

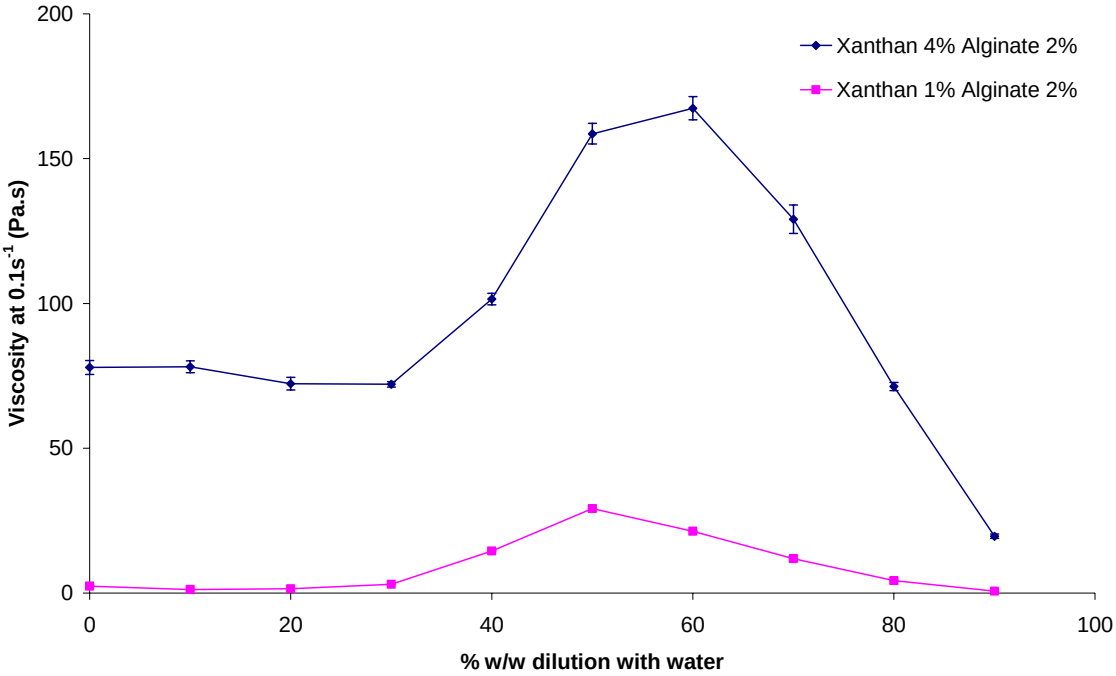

Figure 5.50. A comparison of the effect of dilution on viscosity at $0.1s^{-1}$ of a 4% xanthan:2% alginate mixture and a 1% xanthan:2% alginate mixture.
Geometry CP 4^{o}/40mm 25 ± 0.1^{o}C. Mean ± SD, n=3

5.4.11 Ternary mixtures utilising the xanthan/locust bean gum interaction

The previous sections have shown how dilution has pronounced effects on the rheological properties of the xanthan:alginate mixture. The work in chapter 3 showed how in sufficiently high concentration xanthan:alginate mixtures, xanthan forms distinct strand-like mesophases. This section examines whether these strands are a truly distinct phase and can be exploited for use with the well known xanthan/LBG synergistic gelling interaction (Figure 5.51).

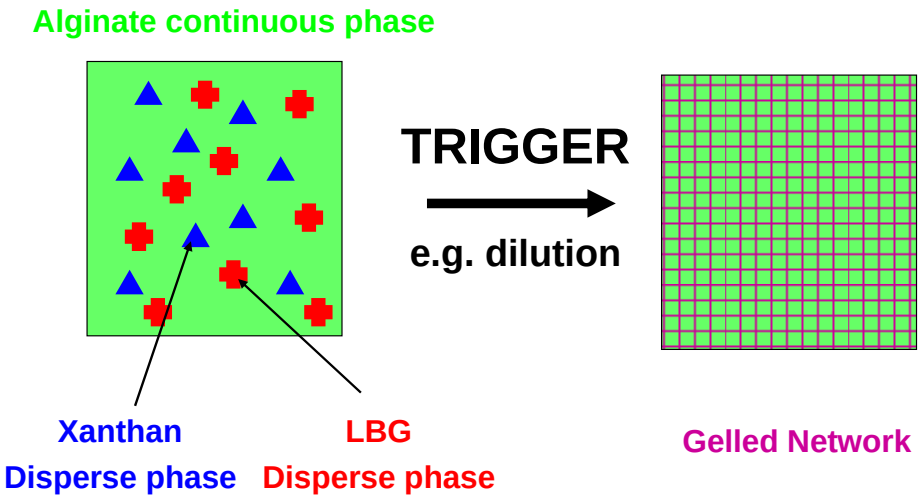

Figure 5.51. A schematic representation of the desired effect required on the dilution of a xanthan/alginate/LBG mixture.

5.4.11.a Miscibility of locust bean gum with alginate in solution

To understand the rheology of mixtures of LBG and alginate it is necessary to have an understanding of the rheological properties of LBG as an individual hydrocolloid solution. The viscoelastic profile of a 1% LBG solution is shown in Figure 5.52. G" is greater than G' at most frequencies studied; however at higher frequencies G' starts to converge on G". This profile is generally indicative of a concentrated solution (Steffe 1996).

For the hypothesis for the quaternary mixture to be successful it would be desirable for the LBG and alginate to also phase separate; creating a disperse LBG phase as well as a disperse xanthan phase. To study the compatibility of LBG and alginate a number of mixtures were prepared and their rheological properties measured. Figure 5.53 examines the viscoelastic properties of mixtures of 1% LBG with 0 – 5% alginate. 1% LBG shows viscous dominated properties with G" > G'. Increasing concentrations of alginate caused a concentration dependent change in properties which led to G' being greater then G" in the mixture with 5% alginate.

Figure 5.54 examines the addition of LBG to 5% alginate. A 5% alginate solution has viscoelastic parameters beyond the lower limits of the instrument. With increased concentrations of LBG the mixtures appeared to change from a non-viscous mixture to a mixture with weak gel-like properties suggesting that there may even be a weak synergistic effect between LBG and alginate. Figure 5.55 however shows the overall viscoelastic profile of the 1% LBG:5% alginate mixture. This would indicate that the mixture exhibits properties typical of a concentrated solution not a weak-gel. The G"/G' crossover point was shifted to a lower frequency giving the false impression in the previous figures that a weak-gel had formed.

Mixtures containing 1% LBG and either 5% or 10% alginate were prepared. These were centrifuged as previously described at 4000 rpm for one hour and neither mixture exhibited separation. Although the LBG:alginate mixtures did not exhibit separation,

provided that the xanthan does not interact with the LBG, the dilution effects could still occur as desired.

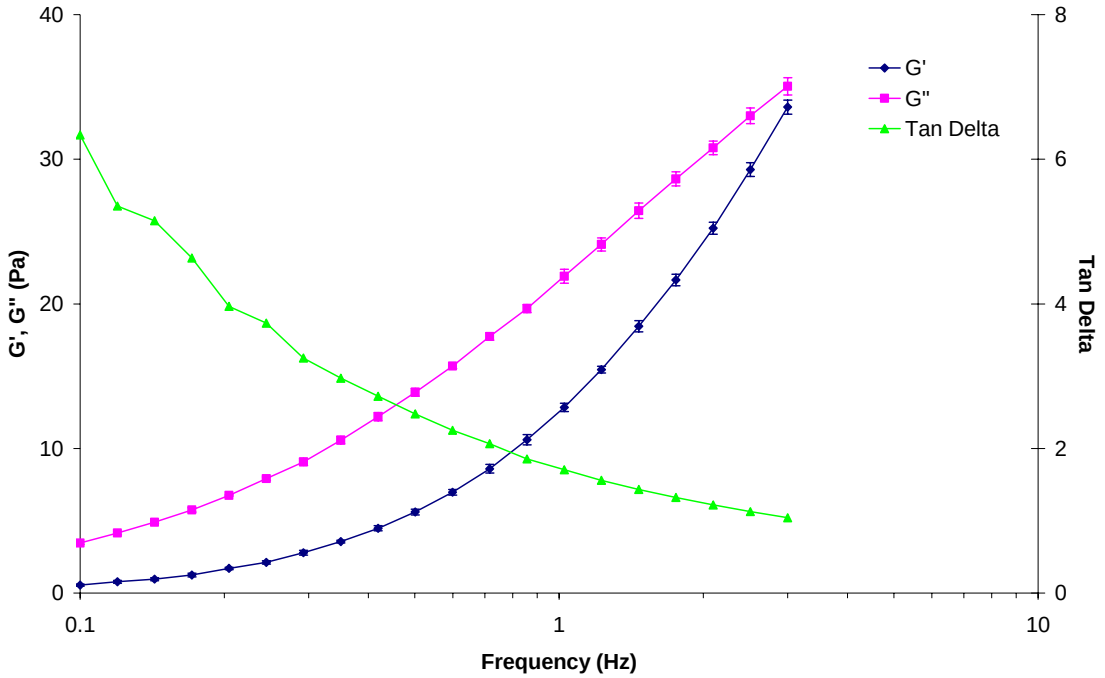

Figure 5.52. The dynamic viscoelastic properties of a 1% LBG solution.
Geometry CP 4°/40mm 25 ± 0.1°C. Mean ± SD, n=3

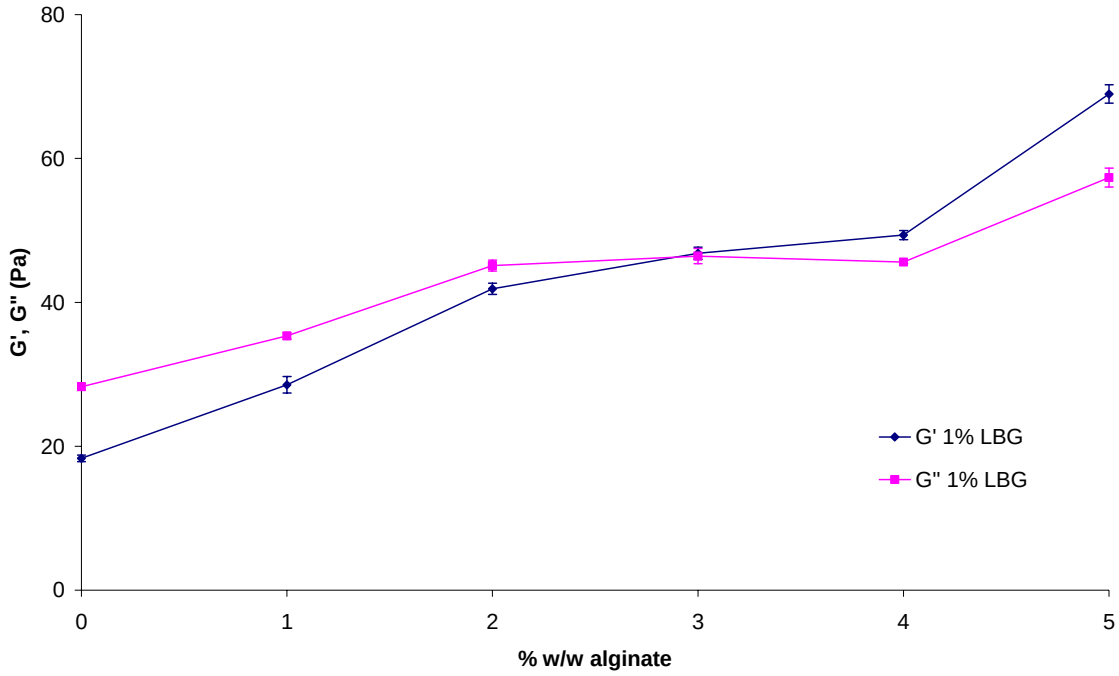

Figure 5.53. The effect on dynamic viscoelasticity of alginate concentration on 1% LBG mixtures. Geometry CP 4°/40mm 25 ± 0.1°C. Frequency 1.02Hz. Mean ± SD, n=3

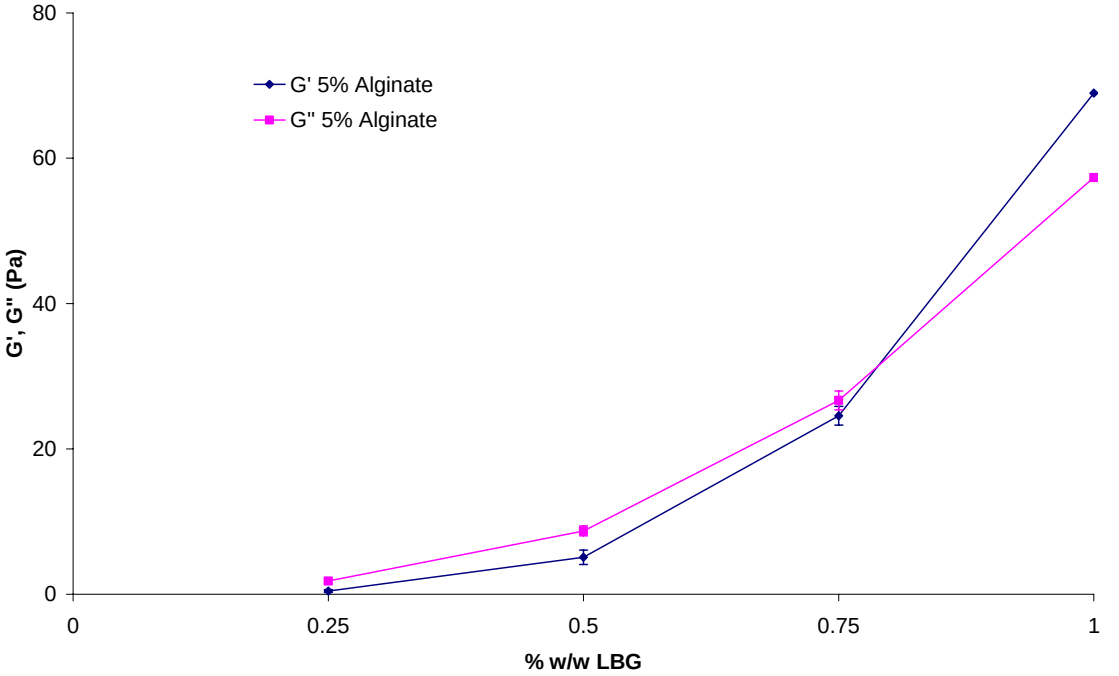

Figure 5.54. The effect on dynamic viscoelasticity of LBG concentration on 5% alginate mixtures. Geometry CP 4°/40mm 25 ± 0.1°C. Frequency 1.02Hz. Mean ± SD, n=3

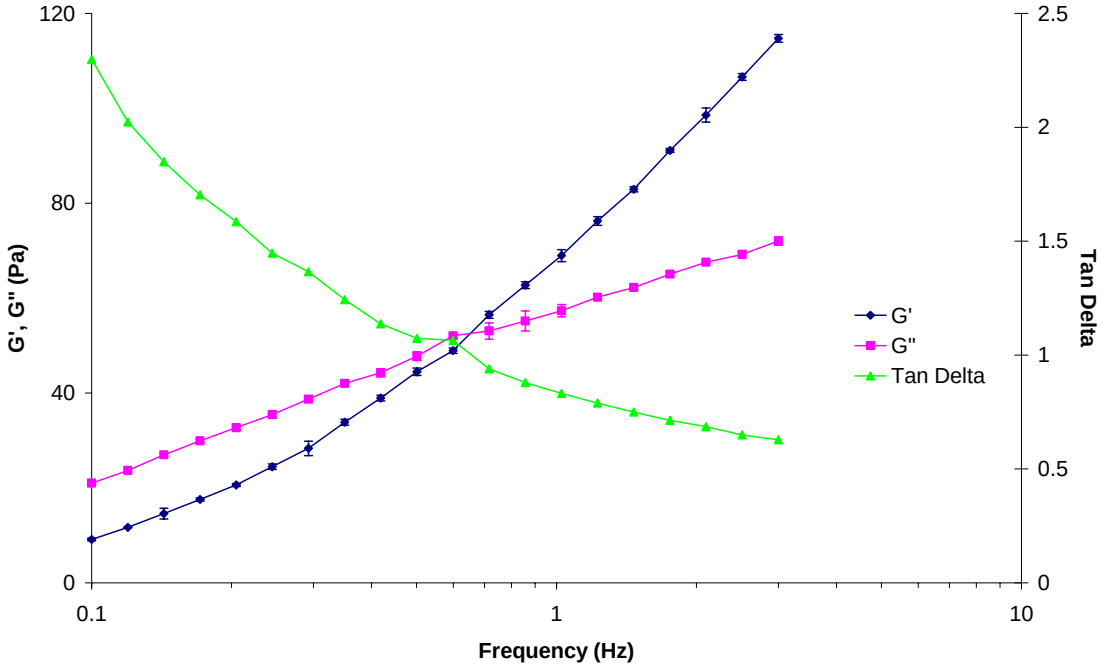

Figure 5.55. The dynamic viscoelastic profile of a 1% locust bean gum:5% alginate mixture. Geometry CP 4°/40mm 25 ± 0.1°C. Mean ± SD, n=3

5.4.11.b The rheology of xanthan/alginate/LBG mixtures

Ternary mixtures of 0.5% xanthan, 0.5% LBG, and increasing amounts of alginate were prepared by the method described in section 5.3.6. The viscoelastic properties of these mixtures are shown in Figure 5.56. It can be seen that with no alginate present the xanthan and LBG exhibited relatively high modulus gel-like properties with G' significantly greater than G". The addition of alginate up to 1.25% reduces the value of G' from 170 Pa to 25 Pa. Above 1.25% alginate G" was greater than G' indicating viscous dominated properties; these mixtures also showed birefringent strands under crossed polarised lenses. This data would suggest that the alginate was still interacting with the xanthan component, and hence preventing it from forming the usual synergistic gel system. It would also suggest that even with 2% added alginate there is still however some residual interaction between the xanthan and LBG as the moduli values are significantly higher than a 1% xanthan:2% alginate mixture without LBG present.

To ensure that the effect observed was not an ionic effect as a result of the presence of sodium ions from the sodium alginate, sodium chloride was added at concentrations which provide identical amounts of sodium ions. Figure 5.57 compares the viscoelastic properties of xanthan:LBG mixtures containing sodium from sodium alginate or sodium chloride. It can be see that the profiles are distinctly different, with sodium chloride increasing the value of G' compared with that of the mixture with no sodium present.

To further understand the interactions within the mixtures, each sample was heated to 90^{o}C for 1 hour and then cooled back to 25^{o}C. Once cooled the viscoelastic properties were measured. 90^{o}C is known to be above the melting point for most xanthan:LBG gels, thereby allowing all of the components to interact without interference of any potential xanthan:LBG gelled areas in the solution. Figure 5.58 shows the effect of the heating on these mixtures. Most of the mixtures exhibited higher moduli values as a result of heating. It was also apparent that in the mixtures containing sodium alginate, the mixture showed steady G' values at approximately 200 Pa up to 1.25% alginate

(~0.145% Na^+), the concentration where xanthan and alginate usually demonstrate clear separation. At concentrations of alginate greater than 1.25%, G' decreased significantly.

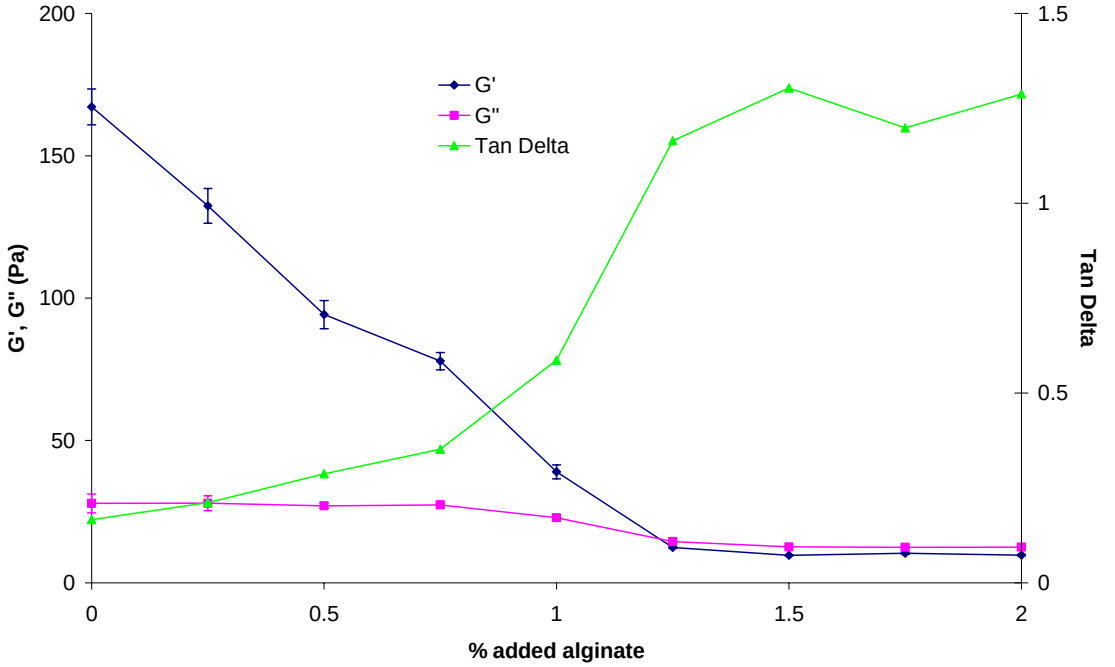

Figure 5.56. The effect on dynamic viscoelasticity of alginate concentration on 0.5% xanthan:0.5% LBG mixtures.
Geometry CP 4°/40mm 25 ± 0.1°C. Frequency 1.02Hz. Mean ± SD, n=3.

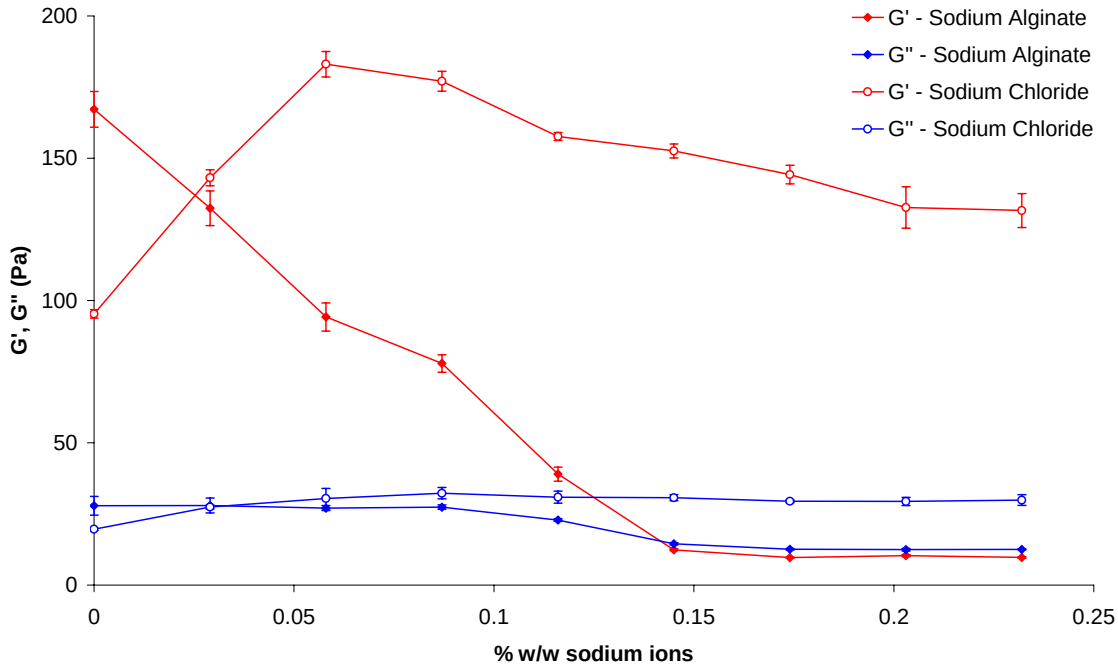

Figure 5.57. The effect on dynamic viscoelasticity of sodium concentration (from sodium alginate and sodium chloride) 0.5% xanthan:0.5% LBG mixtures.
Geometry CP 4°/40mm 25 ± 0.1°C. Frequency 1.02Hz. Mean ± SD, n=3.

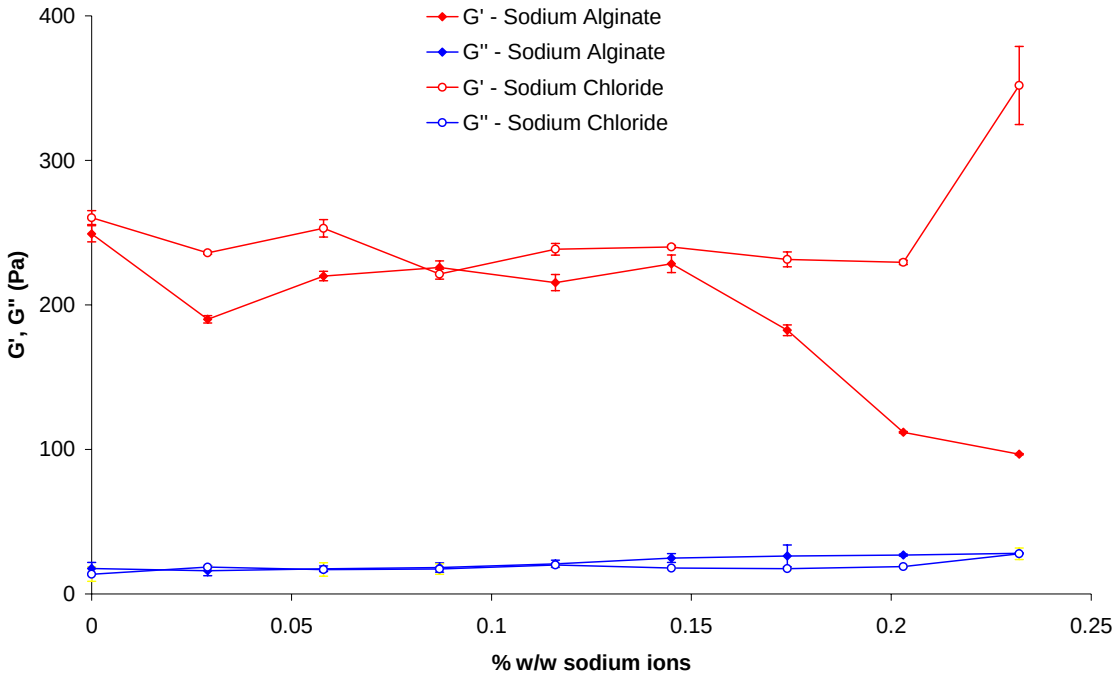

Figure 5.58. The effect on dynamic viscoelasticity of sodium concentration (from sodium alginate and sodium chloride) 0.5% xanthan:0.5% LBG mixtures after being heated at 90°C for 1 hour. Geometry CP 4°/40mm 25 ± 0.1°C. Frequency 1.02Hz Mean ± SD, n=3

5.4.11.c Dilution of a xanthan/alginate/LBG mixture

The aim of the use of the ternary mixture was to investigate if it could enhance the dilution effect seen with xanthan:alginate mixtures by forming a xanthan:LBG gel on dilution. Figure 5.59 examines the effect of dilution on a 1% xanthan:1% LBG:2% alginate mixture. With increased levels of dilution both G' and G" decreased in a concentration dependent manner, with a corresponding increase in tan delta. This dilution profile is very different from that exhibited by xanthan:alginate mixtures on dilution. This data would suggest that the addition of water had diluted the system without reversal of the phase separation and the desired gelation effect had not occurred.

Figure 5.60 shows the viscoelastic profiles of the diluted mixtures following heating at 90^{o}C for 1 hour. The heated mixtures showed a very different profile. The predicted profile on dilution was observed with the viscoelastic properties increasing at dilutions of 20% and above.

Figure 5.61 shows microscope images of the undiluted mixture, the 50% dilution, and the 50% dilution heated to 90^{o}C and cooled. Birefringence can be clearly seen in the unheated samples; however birefringence is not present in the heated sample.

All of the above experiments would strongly suggest that although xanthan forms strands as a result of the interaction with alginate, the formation of strands does not prevent the xanthan from interacting with the LBG at the strand surface. As a result, the dilution that would normally cross the phase boundary cannot occur as the xanthan is effectively 'locked' into the strand state and so dilution simply reduces the viscoelastic properties. The effect of heat melts out any gelation at the strand surface allowing the true effect of dilution to occur, and so on cooling the desired gel-like state is formed.

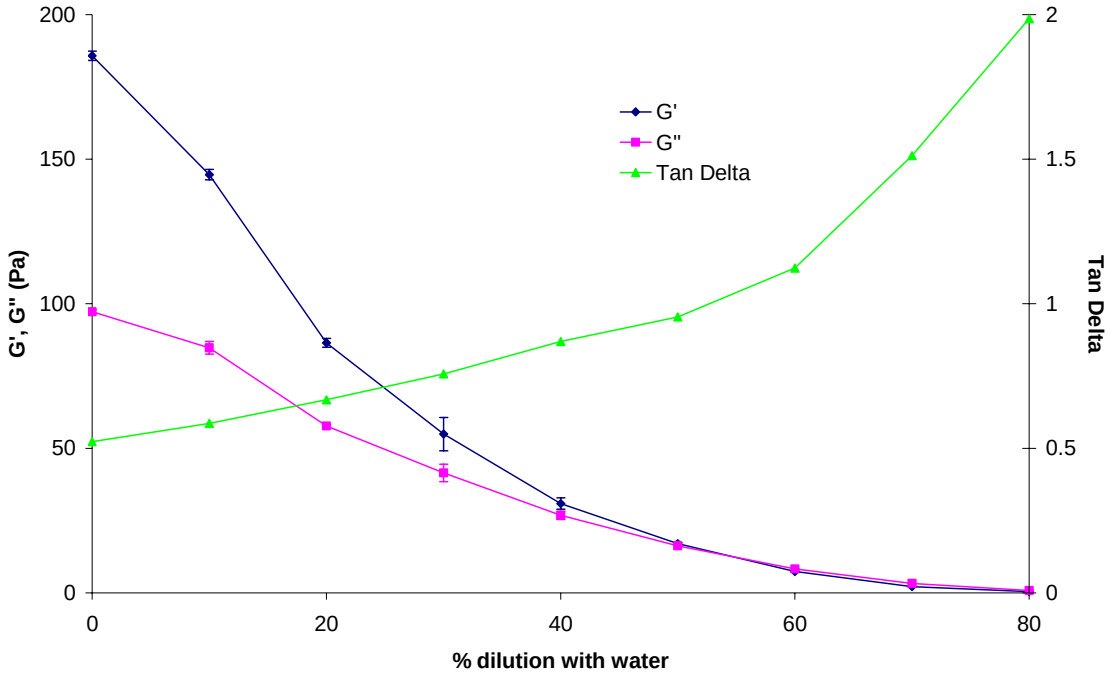

Figure 5.59. The effect of dilution on the dynamic viscoelastic properties of a 1% xanthan:1% LBG:2% alginate mixture.
Geometry CP 4°/40mm 25 ± 0.1°C. Frequency 1.02Hz Mean ± SD, n=3

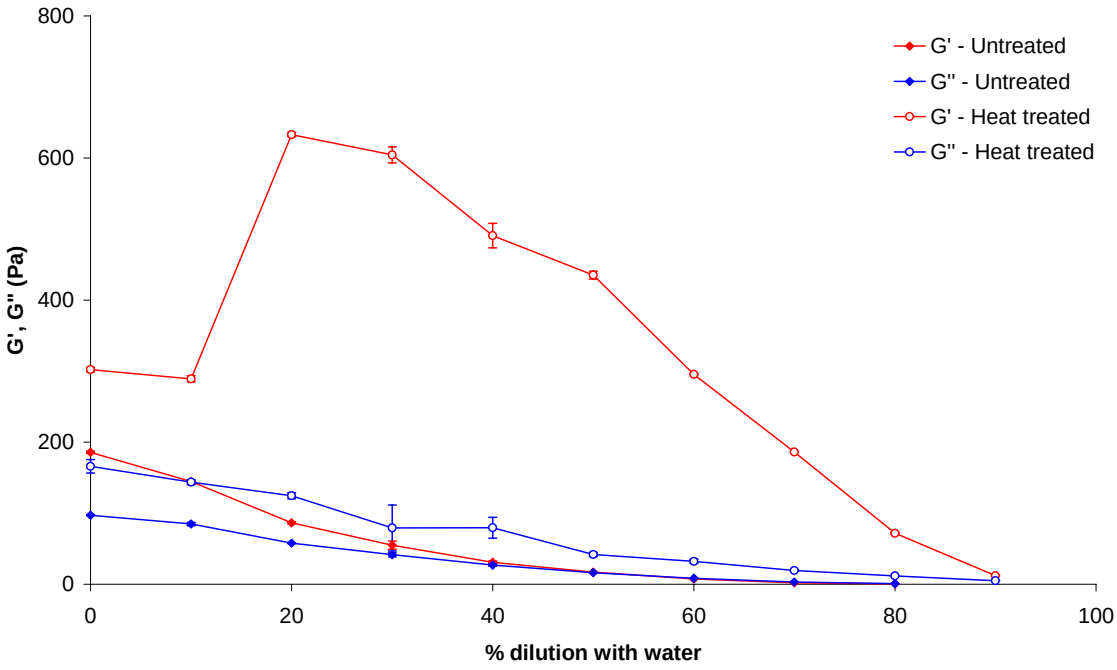

Figure 5.60. The effect of dilution on the dynamic viscoelastic properties of a 1% xanthan:1% LBG:2% alginate mixture before and after heat treatment of 90°C for 1 hour.
Geometry CP 4°/40mm 25 ± 0.1°C. Frequency 1.02Hz Mean ± SD, n=3

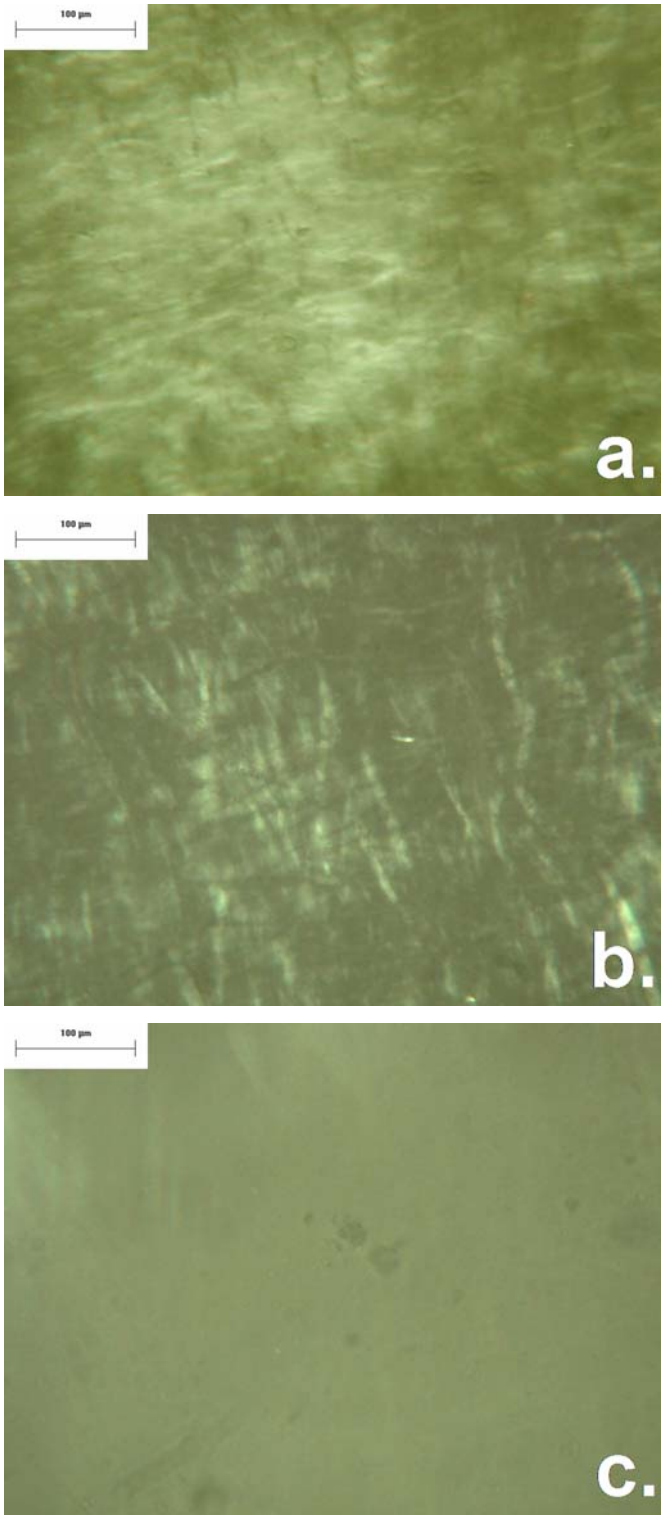

Figure 5.61. 1% Crossed polarized light micrographs of a 1% xanthan:1% LBG:2% alginate mixture.
(a) 0% dilution (b) 50% dilution with water (c) 50% dilution followed by heating to 90^{o}C for 1 hour and cooled.

5.5 Conclusions

This chapter has examined the effects of traversing the phase boundary from the separated to homogenous regions via a number of different routes. The addition of water to mixtures has been investigated and has been shown to trigger a significant viscosity increase on crossing the phase boundary. The increase observed is dependent on the starting composition of the mixture and proximity to the phase boundary. The effect of dilution in a simulated gastric environment was studied by the use of SGF and viscosity was shown to increase on dilution. The magnitude of the increase was significantly greater with SGF compared to that of water as a result of acidification of the alginate and hence gelation.

The effect of temperature on the viscosity increase on dilution were also investigated. It was shown that in higher temperature environments (40 - 50^{o}C) the viscosity increase observed was greater, whereas in colder environments (10^{o}C) the viscosity increase was noticeably reduced. In very high temperature environments (80^{o}C) the separation could be reversed yielding a viscosity increase.

The preparation technique for the mixtures was also investigated as a tool for creating more diverse mixtures. It was shown that mixtures containing much higher concentrations of xanthan than would normally be practical could be prepared by a technique using the second polysaccharide solution as the solvent. Dilution of these high concentration xanthan mixtures showed that a high viscosity could be maintained despite the addition of significant quantities of water.

Finally the xanthan:LBG interaction was probed as another potential method for improving the dilutions profiles observed. LBG was shown to be compatible with alginate in solution. However, the desired effect was not achieved at room temperature as a result of the interaction of LBG with the surface of the strand-like xanthan disperse

phase. The use of high temperature was able to reverse this to achieve the desired effect; however would be impractical in a biological environment.

Chapter 6

Discussion and conclusions

6.1 Summary

The work presented in this thesis has resulted in a number of key conclusions. These are:

- The addition of alginate to xanthan solutions above a critical threshold concentration results in a significant decrease in viscosity. At the same critical concentration, the weak gel-like properties normally observed with xanthan are abolished resulting in an essentially non-viscous system.

- These changes are associated with a strand-like phase separation. The continuous phase is exclusively composed of alginate whereas the strand phase is rich in xanthan with residual amounts of alginate.

- The alginate concentration required to promote phase separation decreases with alginate molecular weight over the range 1.5 kDa to 404 kDa. The separation threshold concentration increases with increasing salt concentration from 0 to

2% sodium chloride. Alginate M:G ratio appears to have little effect up to molecular weights of 404 kDa.

- The strand-like phase separation is not unique to xanthan:alginate mixtures. It would appear that alginate can be substituted for any water soluble anionic polyelectrolyte.

- Scleroglucan was investigated as a possible alternative for xanthan; however this was shown not to separate when mixed with alginate.

- Transition across the phase boundary by dilution has been shown to fully reverse the separation and a significant viscosity increase is observed. In the case of mixtures containing sodium alginate, the use of SGF enhances this further.

- The careful control of the mixture composition in relation to the phase boundary, and the extent of dilution provide a tool for controlling the viscosity increase. Mixtures close to the phase boundary require less dilution before onset of the viscosity increase compared with those further from the phase boundary. The viscosity of the mixture varies with the extent of dilution therefore viscosity can be modulated if dilution is controlled.

- The use of elevated temperatures has also been shown to increase the viscosity by shifting the position of the phase boundary.

The origins of these conclusions will now be discussed.

6.2 Origin of the phase separation

A solution of polymers will spontaneously phase separate only if there is a drop in the Gibbs' free energy of the system (Sperling 2001). The change in Gibbs' free energy (ΔG) is dependent on two factors, the change in enthalpy (ΔH) on mixing and also the change in entropy (ΔS) at a given absolute temperature (T). This is described in equation 6.1.

$$\Delta G = \Delta H - T\,\Delta S \tag{6.1}$$

Phase separation is well recognised in mixed biopolymer systems as a result of the low entropy gain on mixing. Work on the mechanisms of phase separation have been investigated extensively using the Flory-Huggins Lattice theory (Flory 1953). In this model, a lattice represents a solution where each lattice site contains either a solvent molecule, a small molecule or a segment of a polymer (Figure 6.1). The model assumes that a polymer is flexible and as a result a subsequent segment can occupy any space $k + 1$, around segment k with equal probability, with the exception of the space occupied by the preceding segment, $k - 1$.

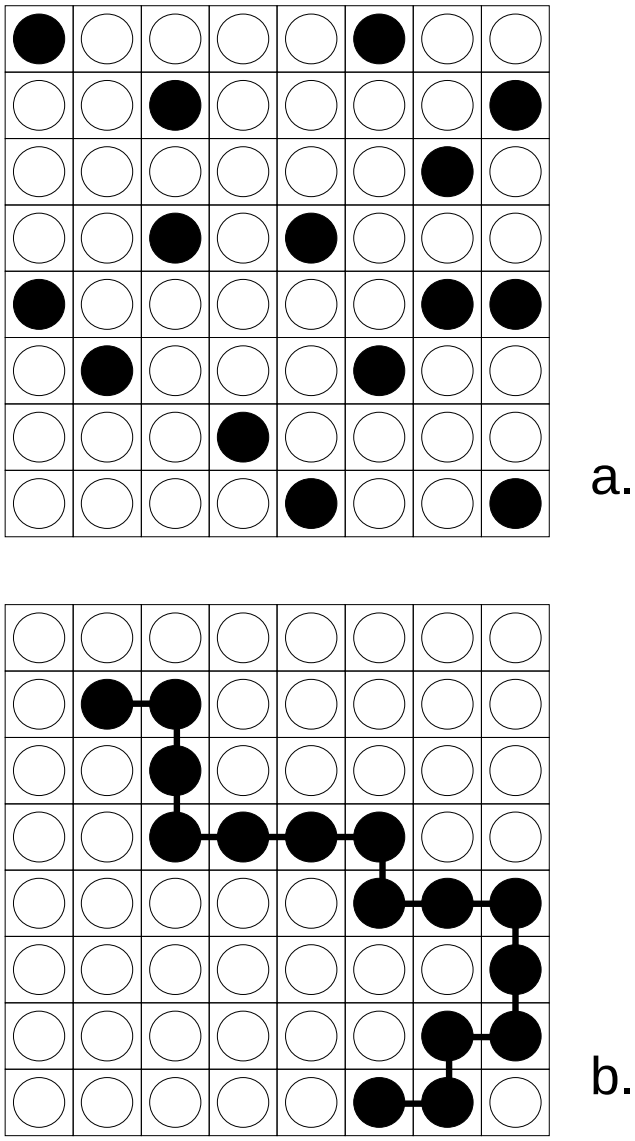

Figure 6.1. A diagrammatic representation of the Flory-Huggins Lattice theory.
The white circles represent solvent molecules, the black circles monomer units. (a) shows a small molecule dispersed in solvent (b) shows a polymer dispersed in solvent. (adapted from Flory 1953)

With respect to the entropy of mixing, the configurational involvement is provided by the number of distinct ways the molecules can be arranged into the lattice. This therefore assumes that all configurations are equally likely, irrespective of molecular interactions. When a binary mixture is obtained from components 1 and 2 the resulting entropy change on mixing is given by equation 6.2 (Flory 1953).

$$\Delta S_{mix} = -k\left[\frac{\Phi_1}{r_1}\ln\Phi_1 + \frac{\Phi_2}{r_2}\ln\Phi_2\right] \tag{6.2}$$

In this equation, k is the Boltzmann constant, Φ_1 is the volume fraction of component 1 and r_1 the number of segments per molecule. As can be seen from equation 6.2 when $r_1 = r_2 = 1$ in the case of small molecules, the ΔS term is relatively large. In the case of a polymer in water r_2 will be large and so the entropy term will be smaller. When considering large values for r_1 and r_2 the entropy change will be very small. Xanthan has a high molecular weight, and the polyelectrolytes studied can be considered to have high molecular weight with respect to that of small molecules, such as the solvent, hence the entropy change on mixing will be small and separation is likely to be favoured.

In the lattice model, short range interactions are restricted to adjacent neighbours. The interaction between two components i and j, is described by the dimensionless parameter, χ_{ij} shown in equation 6.3.

$$\chi_{ij} = \frac{z}{kT}\left(w_{ij} - \frac{w_{ii} + w_{jj}}{2}\right) \tag{6.3}$$

z is the number of nearest adjacent neighbours to any lattice site, and w_{ij} is the free energy of interaction between segments i and j when they are in adjacent sites within the lattice. The importance of this equation is that the differences are multiplied by the number of nearest neighbours and the expression in brackets describes the difference in

the pair interactions between unlike segments minus the average of the interactions between like segments $(w_{ii} + w_{jj})/2$. Attractive pair interactions are negative and therefore χ_{ij} becomes positive when like molecules prefer like. Conversely when χ_{ij} is less than 0 the pair interaction is repulsive (Piculell, Bergfeldt et al. 1995).

In very simple systems in which interactions are restricted to van der Waals forces, values of w_{ij} are effectively pure interaction energies. In solvents such as water this is not however the case. Other factors such as orientation and hydrogen bonding become important, and affect both energetic and entropic effects, making the interaction parameter far more complex.

A binary mixture containing two components 1 and 2 of limited miscibility will separate into two phases when the critical interaction parameter χ_{c12} exceeds a critical value as given by equation 6.4 (Scott 1949).

$$\chi_{c12} = \frac{\left(\sqrt{r_1} + \sqrt{r_2}\right)^2}{2r_1 r_2} \tag{6.4}$$

Equation 6.4 indicates that separation is determined by the relative molecular lengths of the components. The critical interaction parameter is a measure of how tolerant a mixture is to segment-segment repulsion before separation occurs. Typically for a monomeric mixture χ_{c12} will equal 2; for long polymers this approaches 0.5. When r_1 and r_2 tend to infinity χ_{c12} tends to zero. This offers an explanation with respect to the experiments looking at both alginate and polyacrylate molecular weight. As the molecular weights of the polymer increased, the value of χ_{c12} decreased thereby lowering the threshold concentration for separation to occur.

The separation observed in xanthan mixtures has been shown to require the presence of two polyelectrolytes. It is clear from the information presented above that the entropy of mixing is heavily influenced by the total number of molecules within the mixture. On dissolution, a polyelectrolyte dissociates into a polyion and numerous counterions, and

the entropy of mixing encourages the counter ions to distribute throughout the whole mixture. With respect to separation, the entropically favourable situation is where the counterions can still do this. In a separating system however, electroneutrality must also be preserved. This requires the counterions to remain in the phase containing the polyion, which is entropically unfavourable and promotes miscibility. This offers a potential explanation of why mixtures of xanthan and neutral polysaccharides did not phase separate. Had phase separation occurred, there would be a high concentration of counterions in the xanthan phase with respect to the neutral polysaccharide phase, creating an entropically unfavourable situation where the counterions could not distribute throughout the mixture. The presence of high salt concentrations can alter this entropically unfavourable state as a result of ion flooding thereby reducing the entropic imbalance. It is therefore possible that 'salting out' can occur (Piculell, Bergfeldt et al. 1995). The Flory-Huggins model allows for this counterion effect by treating the counterions as a separate component.

The effect of counterions can have significant bearing on separation properties. In chapter 3, salt was shown to raise the critical concentration of alginate required to elicit separation. On the basis of the above argument, salt would therefore be expected to promote phase separation; however it is possible that the presence of additional counterions could affect the separation by one or more mechanisms in addition to the entropic mechanism discussed above, including hydrodynamic volume effects, charge effects and conformational effects.

Since the entropy of mixing is always positive, phase separation must be driven by a decrease in ΔH, the change in enthalpy. An increase in ionic strength will reduce this electrostatic component as a result of charge screening. As a result of electrostatic repulsion between the two polyelectrolytes, there will be a driving force for phase separation which will not be seen in mixed systems containing a polyelectrolyte and a neutral polymer. Thus scleroglucan:polyelectrolyte mixtures do not phase separate nor do xanthan:maltodextrin or xanthan:methylcellulose blends. In addition phase separation requires higher concentrations of polyelectrolytes in a high salt environment,

thus the origin of the ionic effect can be found in equation 6.3 where the reduced electrostatic repulsion, as a result of charge screening, is described by the w_{ij} term.

A possible additional effect is the reduction in hydrodynamic volume as evidenced by the decrease in intrinsic viscosity in increasing salt concentrations (Zhanq, Wang et al. 2001). This would make the coils more compact and will reduce the overlap between the two macromolecules (Figure 6.2). Within this context it would be interesting to speculate on whether the addition of another polyelectrolyte alters the xanthan order-disorder transition, as it is well know that this is influenced by ionic strength (Morris 1977). This has been explained on the grounds of a reduction in repulsive interactions between the charged xanthan side-chains. The presence of another polyelectrolyte might be considered to drive xanthan into the ordered conformation and this would reduce unfavourable electrotostatic contact and raise the order-disorder transition temperature. Further calorimetric work would be necessary to investigate this hypothesis.

The final possible explanation for the ionic effect on the phase separation boundary is that the presence of additional salt affects the xanthan molecule such that it becomes more resistant to phase separation. It was shown in chapter 3 that sodium chloride increases the elastic modulus of a 1% xanthan solution suggesting a strengthening of the internal structure. This explanation however is unlikely as xanthan does not form true gels.

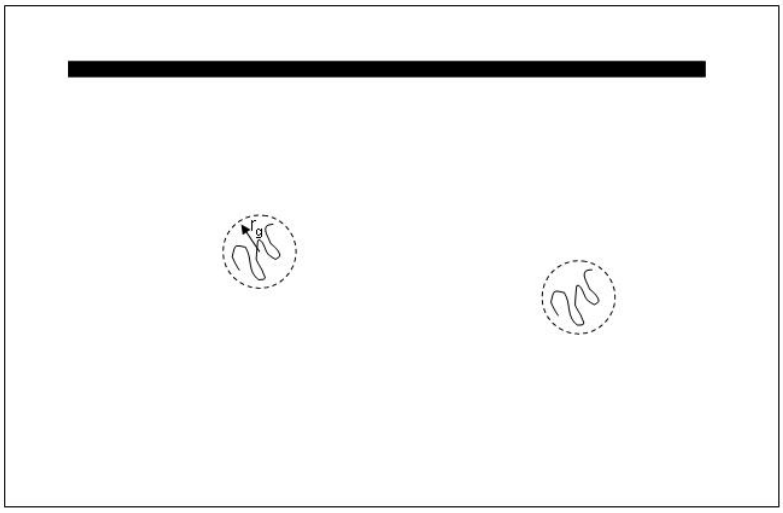

a.

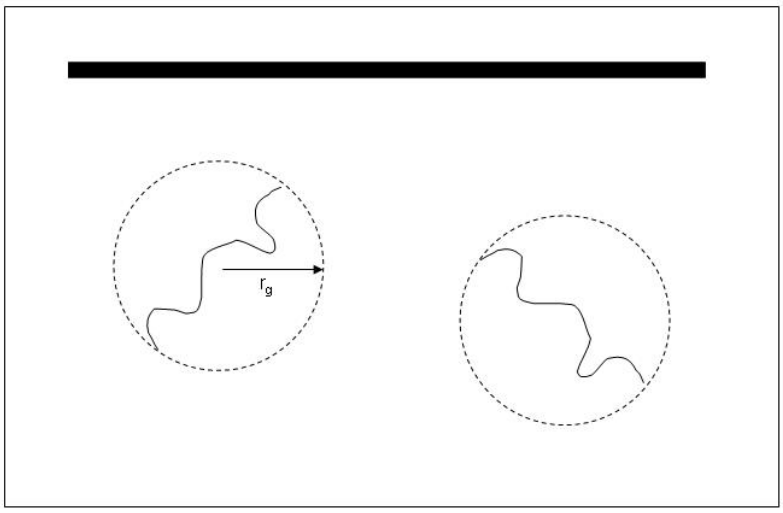

b.

Figure 6.2. The effect of salt on the hydrodynamic volume and radius of gyration (r_g) of a random coil polyelectrolyte interacting with a rigid rod-like molecule.
(a) low ionic strength environment (b) high ionic strength environment. The rod like molecule is represented by the straight line. The random coil by the wavy line. The addition of salt reduces the hydrodynamic volume and also the radius of gyration. As a result, the contact area between macromolecules is reduced and the probability of steric interaction is also less.

6.3 Origin of the strand morphology

In the absence of flow and gelation, the structure of phase separated systems most commonly consists of spherical droplets of one phase dispersed within another phase as this morphology provides the lowest interfacial tension and hence the lowest free energy.

Xanthan is very unusual in that it has an extremely high persistence length typically of the order of 120 nm. This is typically 10 times that of CMC and of a similar magnitude to that of DNA (Ross-Murphy, Morris et al. 1983; Tinland and Rinaudo 1989). It has been shown that the threshold for the formation of lyotropic liquid crystalline phases is inversely proportional to the persistence length (Ciferri 1982; Flory 1982).

The lattice theory, when applied to rod-shaped molecules, predicts that a liquid crystalline phase should result when a certain volume fraction V^* of a polymer (which corresponds to a critical concentration C^*) is achieved. The volume fraction is linked to the aspect ratio (the length-diameter ratio, p), of rigid rods, such that where $p \geq 10$ equation 6.5 applies (Flory 1956).

$$V^* = \frac{8}{p}\left(1 - \frac{2}{p}\right) \tag{6.5}$$

This equation shows that with increasing values of p the volume fraction required for the formation of the anisotropic phase decreases. Above C^* an anisotropic phase is produced within the isotropic continuous phase and at higher concentrations the volume fraction of the anisotropic phase also increases. This process is driven by the release in entropy. At a further critical concentration C^{**} corresponding to a volume fraction V^{**} the solution becomes completely anisotropic. For large axial ratios this is defined by equation 6.6 (Flory and Ronca 1979; Flory and Ronca 1979).

$$V^{**} = \frac{11.6}{p} \tag{6.6}$$

If p is known then V^* and V^{**} can be calculated. From these values it is possible, using equation 6.7 (Lapasin and Pricl 1999), to calculate the corresponding values for C^* and C^{**}

$$C = \frac{100V/\rho_s}{V(1/\rho_s - 1/\rho_p) + 1/\rho_p} \tag{6.7}$$

where ρ_s and ρ_p are the densities of the solvent and polymer respectively.

Xanthan, in the ordered form, has a mass per unit length of 1000 - 2000 Da/nm, and an aspect ratio of 250 - 500, as a result the molecular rod is 1000 nm in length and 2-4 nm in diameter (Holzwarth 1978; Whitcomb 1978; Lim, Uhl et al. 1984; Kojima and Berry 1988) and through equations 6.5, 6.6 and 6.7 this provides values of C^* and C^{**}. It has recently been shown by Carnali that the onset of anisotropy (C^*) can be as low as 0.8% (Carnali 1991), whilst studies of viscosity and birefringence as a function of xanthan concentration by Allain et al. (1988) have shown the onset to be at 0.7%. This is in contrast with the predicted onset given using Florys theory, which would suggest that the onset would be at 2.9% (Flory 1956). It has been proposed that this overestimation is as a result of aggravating factors such as polydispersity and other attractive interactions (Carnali 1991). Allain et al. (1988) suggest that the xanthan liquid crystals formed, were of the nematic type as a result of the small decrease in viscosity following the viscosity maximum.

The lattice theory is not the only model for studying the formation of anisotropic phases. Onsager (1949) produced a well known theory based on analysis of the second virial coefficient for very long rod-like particles. This theory was the first to show that long rod-like molecules form two-phase systems, one anisotropic the other fully

isotropic, with the anisotropic phase being more concentrated than the other. This method however is less appropriate at evaluating high virial coefficients for highly asymmetric particles and from the non-convergence of the virial series at concentrations necessary for formation of stable mesophases (Flory 1956; Flory and Ronca 1979). The lattice theory is therefore generally used in preference.

6.4 Other issues of importance in the phase separation phenomenon

The phase composition diagram for mixtures of xanthan and alginate is presented in Figure 3.17. The disperse phase had a xanthan concentration in excess of 3% xanthan. As a result, anisotropic regions formed and birefringence was observed between crossed polarising lenses. Moreover it might be expected that the unseparated mixtures containing xanthan gum (i.e. at low alginate concentrations) should also exhibit birefringence as these are above the C^* concentration of 0.7% suggested by Allain et al. (1988). As the volume fraction of the anisotropic phase increases with concentration, at concentrations near 1% the volume fraction is low and birefringence is probably undetectable by human observation; however it could perhaps have been detected using a diode array spectrophotometer as used by Carnali (1991).

Regarding the composition of the continuous phase, it was found that this contained no xanthan. On general thermodynamic grounds it is recognised that for a continuous phase rich in component 1, as the molecular weight of component 2 increases, the amount of component 2 present in the continuous phase will decrease (Donald, Durrani et al. 1995). Thus when the high molecular weight of xanthan is considered, little xanthan would be expected in the continuous phase. An additional factor that may be important is the rod like conformation of xanthan. Flory (1978) has further shown that extension of the lattice theory to mixtures of rod-like molecules and flexible coils is possible. He showed that when the phase diagram is calculated the isotropic phase should tolerate a

significant amount of the rod-like component, but beyond a threshold concentration, the quantity of the rod-like component becomes negligibly small (Flory 1984) as was shown in Figure 3.17.

It was observed in Figure 3.29 that the strand morphology varied between different mixtures as a function of polysaccharide type and, in the case of polyacrylate, molecular weight. Figure 3.30 showed how the complex viscosities of the same mixtures was inversely proportional to the strand morphology. We believe that this is likely to be kinetic in origin and can be regarded as analogous to a crystallisation process, where the rate is dependent on the rates of nucleation and growth. At a given nucleation rate, crystal size will increase with growth rate. In a viscous polysaccharide solution, the ability of molecules to assemble will depend on their ability to move in the bulk solution, i.e. on the viscosity. In this context therefore the rate of growth of the xanthan liquid crystal will be inversely proportional to viscosity. Thus the largest strands would be observed in the lowest viscosity system. This is exemplified in the xanthan:polyacrylate mixtures where viscosity was very low resulting in a large strand size.

6.5 Implications of the rheological changes on traversing the phase boundary for future medicines

This project proposed to examine the use of phase separation as method of controlling rheological properties, with the eventual objective of producing a bioadhesive system that could be used to protect the oesophagus against reflux episodes. Whilst in the end this final objective was not tested we can draw conclusions from our data which may aid design of such a system in the future. In chapters 3 and 4 the rheological properties of mixtures containing varying levels of xanthan and other polyelectrolytes were explored and it was shown that low viscosity mixtures could be produced despite the fact that they contained a biopolymer that usually formed highly viscous systems. A low viscosity liquid would be an important pre-requisite for a liquid medicine, the majority

of which would need to reach the lower oesophagus on swallowing. Chapter 5 took these rheological changes and studied the effects of moving from a phase separated system to a homogenous system by dilution with water and simulated gastric fluid, and also altering the temperature.

Polysaccharide solutions and mixtures are, by their highly viscous nature, adhesive. The xanthan:polyelectrolyte mixtures are of a sufficiently low viscosity that they would be pourable and easy to swallow. Although not tested, it would not be unreasonable to predict that a small quantity of the undiluted mixture could be retained for a limited period on the oesophageal mucosa, the remainder carrying on forward into the stomach. On arrival the mixture would mix with the food contents in the fed state or with the residual gastric fluid in the fasted state environment with a pH anywhere between 1 and 3.5 (Aulton 1988), the pH being at the higher end of the range in the fed state. In an alginate based system this is below the pKa of the uronic acid residues, 3.38 and 3.65 for mannuronate and guluronate respectively (Clare 1993). As a result, the alginate is likely to precipitate and form an alginic acid gel, as was shown by the dilution of mixtures with SGF. Removal of sodium alginate from solution in this way would move the mixture from the separated to homogenous region of the phase diagram, resulting in a viscosity increase. A further approach might be to use an insoluble calcium salt. In the event of a reflux episode, a gelled mixture would be expected to be significantly less adherent than a viscous liquid. Tang and co-workers (2005a) have demonstrated how alginate solutions can significantly retard acid and pepsin diffusion. Therefore if these solutions could be viscosified with xanthan and the oesophageal retention time increased, it is likely that the acid and pepsin protection would be enhanced. We have also shown that careful choice of the type and concentration of the second polyelectrolyte can significantly modulate the viscosity increase. The 8 kDa polyacrylate mixture demonstrated that only 1.1 ml of diluent was necessary to significantly viscosify a 10ml dose. It may therefore be possible to ingest the mixture and by dilution with saliva alone without any additional water, a viscosity increase can be achieved.

As a result of their highly viscous nature, the high concentrations of xanthan used within this study (e.g. >1% xanthan) would be unpleasant for a person to consume as single biopolymer solutions. The use of the phase separated system overcomes this problem.

The enhanced viscosity in the stomach may also have a further advantage in delaying gastric emptying time (Marciani, Gowland et al. 2000; Xu, Brining et al. 2005) prolonging gastric retention to enhance the absorption of a weakly basic drug and perhaps providing an extended release profile.

The quaternary xanthan:alginate:LBG system did however show that the exploitation of the xanthan:LBG interaction is not a viable mechanism for achieving viscosity enhancement.

The viscosity increase that was observed at significantly elevated temperatures near 80^{o}C is clearly of little use in a pharmaceutical setting as the temperature is significantly higher than that present in normal physiological systems; however it may well have uses in non-pharmaceutical settings.

6.6 Future work

This thesis has investigated the phase behaviour of xanthan based hydrocolloid mixtures. The study has opened up numerous interesting ideas and in several respects has created many more questions than answers. With respect to where to go next there are a number of areas that merit further investigation. These could include:

- The ultimate aim of the thesis was to look at the phase changes in mixtures as a tool for producing a mixture with enhanced oesophageal protective properties. The phase changes within mixtures of xanthan and other polymers have been studied in terms of rheological and morphological changes; however the actual bioadhesive potential has not been modelled or investigated based on a tissue system.

- The mixtures studied were simple aqueous mixtures without some of the common excipients found in medicines for GORD. It is likely that other excipients would have beneficial effects on the mixtures such as calcium carbonate which is soluble in an acidic pH environment.

- The formation of the xanthan strands is unique and has not been reported before. Further investigation is required to study the exact molecular origins of these strands, and how the molecules aggregate. Techniques such as Atomic Force Microscopy may be useful.

References

21 CFR 172.620.

21 CFR 172.695.

21 CFR 173.73.

21 CFR 182.1480.

21 CFR 182.1745.

21 CFR 184.1444.

21 CFR 184.1588.

21 CFR 184.1724.

Albertsson, P. Å. (1986). Partition of Cell Particles and Macromolecules. 3rd Edition. New York, John Wiley & Sons, Inc.

Albertsson, P. Å. (1995). Aqueous polymer phase systems: Properties and applications in bioseparation. Biopolymer Mixtures. S. E. Harding, S. E. Hill and J. R. Mitchell. Nottingham, Nottingham University Press**:** 1-12.

Albertsson, P. Å. and F. Tjerneld (1994). Phase-Diagrams. Aqueous Two-Phase Systems. San Diego, Academic Press Inc. **228:** 3-13.

Allain, C., J. Lecourtier and G. Chauveteau (1988). "Mesophase formation in high molecular-weight xanthan solutions." Rheologica Acta **27**(3): 255-262.

Amenitsch, H., H. Edlund, A. Khan, E. F. Marques and C. La Mesa (2003). "Bile salts form lyotropic liquid crystals." Colloids and Surfaces A: Physicochemical and Engineering Aspects **213**(1): 79-92.

Andrew, T. R. (1977). Applications of xanthan gum in foods and related products. Extracellular microbial polysaccharides. P. A. Sandford and A. Laskin. Washington D.C., American Chemical Society. **45:** 231-241.

Anon. (1999). Aqualon. Sodium Carboxymethylcellulose - Physical and Chemical Properties. Wilmington, USA, Hercules Inc.

Anon. (2000). "FMC Alginates - General Technology." Product Literature.

Anon. (2004). Medicines Compendium. Espom, Datapharm Communications Ltd.

Aulton, M. E. (1988). Pharmaceutics - The science of dosage form design. Edinburgh, Churchill Livingstone.

Barnes, H. A., J. F. Hutton and K. Walters (1989). An Introduction to Rheology. Amsterdam, Elsevier.

Batchelor, H. K. (2005). "Bioadhesive dosage forms for esophageal drug delivery." Pharmaceutical Research **22**(2): 175-181.

Batchelor, H. K., D. Banning, P. W. Dettmar, F. C. Hampson, I. G. Jolliffe and D. Q. M. Craig (2002). "An in vitro mucosal model for prediction of the bioadhesion of alginate solutions to the oesophagus." International Journal of Pharmaceutics **238**(1-2): 123-132.

Batchelor, H. K., P. W. Dettmar, F. C. Hampson, I. G. Jolliffe and D. Craig (2004). "Microscopic techniques as potential tools to quantify the extent of bioadhesion of liquid systems." European Journal of Pharmaceutical Sciences **22**(5): 341-346.

Bergfeldt, K., L. Piculell and P. Linse (1996). "Segregation and association in mixed polymer solutions from Flory-Huggins model calculations." Journal of Physical Chemistry **100**(9): 3680-3687.

Bergfeldt, K., L. Piculell and F. Tjerneld (1995). "Phase-separation phenomena and viscosity enhancements in aqueous mixtures of poly(styrenesulfonate) with poly(acrylic acid) at different degrees of neutralization." Macromolecules **28**(9): 3360-3370.

Brigand, G. (1993). Scleroglucan. Industrial Gums - Polysaccharides and their derivatives. R. L. Whistler and J. N. BeMiller. 3rd Edition. London, Academic Press, Inc.

British National Formulary (2005). 49th Edition. London, British Medical Association and Royal Pharmaceutical Society of Great Britain.

Bungenberg de Jong, H. G. (1949). Complex colloid systems. Colloid Science. H. R. Kruyt. New York, Elsevier. **2:** 335-384.

Bungenberg de Jong, H. G. (1949). Crystallisation-coacervation-flocculation. Colloid Science. H. R. Kruyt. New York, Elsevier. **2:** 232-258.

Butterfield, J., E. Summers, A. Holmes, J. Daintith, A. Issacs, J. Law and E. Martin, Eds. (2003). English Dictionary - Complete and Unabridged. Glasgow, Collins.

Callet, F., M. Milas and B. Tinland (1988). Role of xanthan structure on the rheological properties in aqueous solutions. Gums and Stabilisers for the Food Industry 4. G. O. Phillips, P. A. Williams and D. J. Wedlock. Oxford, IRL Press**:** 203-210.

Carico, R. D. (1976). "Suspension properties of polymer fluids used in drilling, workover, and completion operations." Society of Petroleum Engineers of AIME **SPE 5870**.

Carnali, J. O. (1991). "A dispersed anisotropic phase as the origin of the weak-gel properties of aqueous xanthan gum." Journal of Applied Polymer Science **43**(5): 929-941.

Casas, J. A. and F. Garcia-Ochoa (1999). "Viscosity of solutions of xanthan/locust bean gum mixtures." Journal of the Science of Food and Agriculture **79**(1): 25-31.

Castell, D. O., J. A. Murray, R. Tutuian, R. C. Orlando and R. Arnold (2004). "Review article: The pathophysiology of gastro-oesophageal reflux disease - oesophageal manifestations." Alimentary Pharmacology & Therapeutics **20**(Suppl 9): 14-25.

Cerestar. (2005). "Cerestar Pharmaceutical Excipients: Maltodextrin." Retrieved 19 July, 2005, from http://www.cerestarpharma.com/maltodextrin.html.

Challen, I. A. (1993). Xanthan gum: A multifunctional stabilser for food products. Food Hydrocolloids - Structures, Properties and Functions. K. Nishinari and E. Doi. New York, Plenum Press**:** 135-140.

Chronakis, I. S. (1998). "On the molecular characteristics, compositional properties, and structural-functional mechanisms of maltodextrins: A review." Critical Reviews in Food Science and Nutrition **38**(7): 599-637.

Ciferri, A. (1982). Rigid and semirigid chain polymeric mesogens. Polymer Liquid Crystals. A. Ciferri, W. R. Krigbaum and R. B. Meyer. New York, Academic Press**:** 63-102.

Clare, K. (1993). Algin. Industrial Gums - Polysaccharides and their derivatives. R. L. Whistler and J. N. BeMiller. 3rd Edition. London, Academic Press, Inc.

Collings, P. J. (1990). Liquid Crystals. 1st Edition. Bristol, IOP Publishing Ltd.

Colorcon. (2002). "How to prepare an aqueous solution of Methocel." Retrieved 1 July, 2005, from http://www.colorcon.com/pharma/mod_rel/methocel/literature/prep_aqueous.pdf.

Cottrell, I. W., K. S. Kang and P. Kovacs (1980). Xanthan Gum. Handbook of Water-Soluble Gums and Resins. R. L. Davidson. 1st Edition. New York, McGraw Hill**:** 24:1 - 24:30.

Cottrell, I. W. and K. Kovacs (1980). Alginates. Handbook of Water-Soluble Gums and Resins. R. L. Davidson. 1st Edition. New York, McGraw Hill**:** 2:1 - 2:42.

Coviello, T., A. Palleschi, M. Grassi, P. Matricardi, G. Bocchinfuso and F. Alhaique (2005). "Scleroglucan: A versatile polysaccharide for modified drug delivery." Molecules **10**(1): 6-33.

Cox, G. (1996). "Pectin Liquid Pharmaceutical Compositions." World Intellectual Property Organisation Patent: WO9629055.

Cox, G. (1996). "Pectin Pharmaceutical Compositions." World Intellectual Property Organisation Patent: WO9629054.

Cuvelier, G. and B. Launay (1986). "Concentration regimes in xanthan gum solutions deduced from flow and viscoelastic properties." Carbohydrate Polymers **6**(5): 321-333.

Davidson, M. W. and M. Abramowitz. (2004). "Optical Microscopy." Retrieved 7 June, 2004, from http://www.microscopy.fsu.edu/primer/pdfs/microscopy.pdf.

Dea, I. C. M. and E. R. Morris (1977). Synergistic xanthan gels. Extracellular Microbial Polysaccharides. P. A. Sandford and A. Laskin. Washington, D.C., American Chemical Society. **45:** 174-182.

Dea, I. C. M., E. R. Morris, D. A. Rees, E. J. Welsh, H. A. Barnes and J. Price (1977). "Associations of like and unlike polysaccharides: Mechanism and specificity in galactomannans, interacting bacterial polysaccharides, and related systems." Carbohydrate Research **57**: 249-272.

Dea, I. C. M. and A. Morrison (1975). "Chemistry and Interactions of Seed Galactomannans." Advances in Carbohydrate Chemistry and Biochemistry **31**: 241-312.

Degussa Texturant Systems Unipectine™ OG 903 CS. Product Data Sheet.

Dintzis, F. R., G. E. Babcock and R. Tobin (1970). "Studies on dilute solutions and dispersions of the polysaccharide from *Xanthomonas campestris* NRRL B-1459." Carbohydrate Research **13**: 257-267.

DiPalma, J. A. (2001). "Management of severe gastroesophageal reflux disease." Journal of Clinical Gastroenterology **32**(1): 19-26.

Doelker, E. (1993). "Cellulose Derivatives." Advances in Polymer Science **107**: 199-265.

Donald, A. M., C. M. Durrani, R. A. L. Jones, A. R. Rennie and R. H. Tromp (1995). Physical methods to study phase separation in protein-polysaccharide mixtures. Biopolymer Mixtures. S. Harding, S. E. Hill and J. Mitchell. Nottingham, Nottingham University Press.

Draget, K. I., G. Skjåk-Bræk and O. Smidsrød (1997). "Alginate based new materials." International journal of biological macromolecules **21**(1-2): 47-55.

Draget, K. I., G. Skjåk-Bræk and B. T. Stokke (2006). "Similarities and differences between alginic acid gels and ionically crosslinked alginate gels." Food Hydrocolloids **20**(2-3): 170-175.

Draget, K. I., G. S. Skjåk-Bræk and O. Smidsrød (1994). "Alginic acid gels - the effect of alginate chemical-composition and molecular-weight." Carbohydrate Polymers **25**(1): 31-38.

Draget, K. I., B. Strand, M. Hartmann, S. Valla, O. Smidsrød and G. Skjåk-Bræk (2000). "Ionic and acid gel formation of epimerised alginates; the effect of AlgE4." International Journal of Biological Macromolecules **27**(2): 117-122.

Eccleston, G. and R. Paterson (2003). "Gastric raft composition." World Intellectual Property Organisation Patent: WO03037300 (A1).

Eckel, J. R. (1968). "How mud and hydraulics affect drill rate." Oil and Gas Journal **66**(25): 69-73.

Feddersen, R. L. and S. N. Thorp (1993). Sodium Carboxymethylcellulose. Industrial Gums - Polysaccharides and their derivatives. R. L. Whistler and J. N. BeMiller. 3rd Edition. London, Academic Press, Inc.

Ferry, J. D. (1980). Viscoelastic properties of polymers. 3rd Edition. New York, John Wiley & Sons.

Fitzgerald, R. C. (2005). "Barrett's oesophagus and oesophageal adenocarcinoma: how does acid interfere with cell proliferation and differentiation?" Gut **54**(Suppl 1): i21-i26.

Fléjou, J.-F. (2005). "Barrett's oesophagus: from metaplasia to dyspepsia and cancer." Gut **54**(Suppl 1): i6-i12.

Florence, A. T. and D. Attwood (1988). Physicochemical Principles of Pharmacy. 2nd Edition. London, The MacMillan Press, Ltd.

Flory, P. J. (1953). Principles of Polymer Chemistry. New York, Cornell University Press.

Flory, P. J. (1956). "Phase equilibria in solutions of rod-like particles." Proceedings of the Royal Society of London Series A - Mathematical and Physical Sciences **234**: 73-89.

Flory, P. J. (1978). "Statistical thermodynamics of mixtures of rodlike particles 5. Mixtures with random coils." Macromolecules **11**(6): 1138 - 1141.

Flory, P. J. (1982). Molecular theories of liquid crystals. Polymer Liquid Crystals. A. Ciferri, W. R. Krigbaum and R. B. Meyer. New York, Academic Press Inc.**:** 103-113.

Flory, P. J. (1984). "Molecular theory of liquid-crystals." Advances in Polymer Science **59**: 1-36.

Flory, P. J. and G. Ronca (1979). "Theory of Systems of Rodlike Particles 1. Athermal Systems." Molecular Crystals and Liquid Crystals **54**(3-4): 289-309.

Flory, P. J. and G. Ronca (1979). "Theory of systems of rodlike particles 2. Thermotropic systems with orientation-dependent interactions." Molecular Crystals and Liquid Crystals **54**(3-4): 311-330.

Food Standards Agency. (2005). "List of current European Union-approved additives and their E Numbers." Retrieved 15 July, 2005, from http://www.food.gov.uk/safereating/additivesbranch/enumberlist.

Gacesa, P. (1988). "Alginates." Carbohydrate Polymers **8**(3): 161-182.

Gamini, A. and M. Mandel (1994). "Physicochemical properties of aqueous xanthan solutions - Static light-scattering." Biopolymers **34**(6): 783-797.

Garcia-Ochoa, F., V. E. Santos, J. A. Casas and E. Gomez (2000). "Xanthan gum: production, recovery, and properties." Biotechnology Advances **18**(7): 549-579.

Ghannam, M. T. and M. N. Esmail (1997). "Rheological properties of carboxymethyl cellulose." Journal of Applied Polymer Science **64**(2): 289-301.

Grant, G., E. Morris, D. Rees, P. Smith and D. Thom (1973). "Biological interactions between polysaccharides and divalent cations: The egg-box model." Febs Lett. **32**(1): 195-198.

Grassi, M., R. Lapasin and S. Pricl (1996). "A study of the rheological behavior of scleroglucan weak gel systems." Carbohydrate Polymers **29**(2): 169-181.

Grover, J. (1993). Methylcellulose and its derivatives. Industrial Gums - Polysaccharides and their derivatives. R. L. Whistler and J. N. BeMiller. 3rd Edition. London, Academic Press, Inc.

Guo, J. H., G. W. Skinner, W. W. Harcum and P. E. Barnum (1998). "Pharmaceutical applications of naturally occurring water-soluble polymers." Pharmaceutical Science & Technology Today **1**(6): 254-261.

Halleck, F. E. (1970). "Animal food products containing polysaccharides." Chemical Abstracts **73**: 34028n.

Halleck, F. E. (1970). "Food Products." UK Patent: 1187614.

Haque, A. and E. R. Morris (1993). "Thermogelation of Methylcellulose. Part I: molecular structures and processes." Carbohydrate Polymers **22**: 161-173.

Haque, A., R. K. Richardson and E. R. Morris (1993). "Thermogelation of Methylcellulose. Part II: effect of hydroxypropyl substituents." Carbohydrate Polymers **22**: 175-186.

Hatakeyama T., Nakamura K., Yoshida H. and Hatakeyama H. (1989). "Mesomorphic properties of highly concentrated aqueous solutions of polyelectrolytes from saccharides." Food Hydrocolloids **3**(4): 301-311.

Haug, A., B. Larsen and O. Smidsrod (1966). "A study of the constitution of alginic acid by partial acid hydrolysis." Acta Chemica Scandinavica **20**: 183-190.

Hodsdon, A. C., Mitchell, J.R., Davies, M.C., and Melia, C.D. (1995). "Structure and behaviour in hydrophilic matrix sustained release dosage forms: 3. The influence of pH on the sustained-release performance and internal gel structure of sodium alginate matrices." Journal of Controlled Release **33**: 143-152.

Holzwarth, G. (1976). "Conformation of the extracellular polysaccharide of *Xanthomonas campestris*." Biochemistry **15**(19): 4333-4339.

Holzwarth, G. (1978). "Molecular weight of xanthan polysaccharide." Carbohydrate Research **66**: 173-186.

Holzwarth, G. and E. B. Prestridge (1977). "Multistranded helix in xanthan polysaccharide." Science **197**: 757-759.

Holzwarth, G. M. (1981). Is xanthan a wormlike chain or a rigid rod? Solution Properties of Polysaccharides. D. A. Brant. Washington D.C., American Chemical Society. **150:** 15-23.

Imeson, A. (1990). Applications of alginates. Gums and Stabilisers for the Food Industry 5. G. O. Phillips, D. J. Wedlock and P. A. Williams. Oxford, Oxford University Press**:** 553-561.

Inatomi, S., Y. Jinbo, T. Sato and A. Teramoto (1992). "Isotropic liquid-crystal phase-equilibrium in semiflexible polymer-solutions - Effects of molecular-weight and ionic-strength in polyelectrolyte solutions." Macromolecules **25**(19): 5013-5019.

Jansson, P.-E., L. Kenne and B. Lindberg (1975). "Structure of the extracellular polysaccharide from *Xanthomonas campestris*." Carbohydrate Research **45**: 275-282.

Jeanes, A. (1973). Extracellular microbial polysaccharides: New hydrocolloids having both fundamental and practical importance. Water-Soluble Polymers. N. M. Bikales. New York, Plenum Press. **2:** 227-242.

Jeanes, A., J. E. Pittsley and F. R. Senti (1961). "Polysaccharide B-1459: New hydrocolloid polyelectrolyte produced from glucose by bacterial fermentation." Journal of Applied Polymer Science **5**(17): 519-526.

Kang, K. S. and D. J. Pettitt (1993). Xanthan, gellan, welan, and rhamsan. Industrial Gums - Polysaccharides and their derivatives. R. L. Whistler and J. N. BeMiller. 3rd Edition. London, Academic Press, Inc.

Karabinos, J. V. and M. Hindert (1954). Carboxymethylcellulose. Advances in Carbohydrate Chemistry. M. L. Wolfrom. New York, Academic Press Inc. **9:** 285-302.

Kennedy, J. F. and I. J. Bradshaw (1984). "Production, properties, and applications of xanthan." Progress in Industrial Microbiology **19**: 319-371.

Kitamura, S., T. Kuge and B. T. Stokke (1990). A differential scanning calorimetric study of the conformational transition of xanthan in aqueous NaCl. Gums and Stabilisers for the Food Industry 5. G. O. Phillips, D. J. Wedlock and P. A. Williams. Oxford, Oxford University Press**:** 329-332.

Kojima, T. and G. C. Berry (1988). "Solution properties of xanthan - Light-scattering and viscometry on dilute and moderately concentrated-solutions." Polymer **29**(12): 2249-2260.

Komatsu, N., S. Kikumoto, K. Kimura, S. Sakai, T. Kamasuka, Y. Momoki, T. Yamamoto, S. Takada and J. Sugayama (1970). "Polysaccharides with antitumor activity." Chemical Abstracts **72**: 41748e.

Kuo, C. K. and P. X. Ma (2001). "Ionically crosslinked alginate hydrogels as scaffolds for tissue engineering: Part 1. Structure, gelation rate and mechanical properties." Biomaterials **22**(6): 511-521.

Lagergren, J. (2005). "Adenocarcinoma of oesophagus: what exactly is the size of the porblem and who is at risk?" Gut **54**(Suppl 1): i1-i5.

Lapasin, R. and S. Pricl (1999). Rheology of Industrial Polysaccharides - Theory and Applications. Gaithersburg, Maryland, Aspen Publishers Inc.

Lee, H. C. and D. A. Brant (1999). "Rheological properties of concentrated scleroglucan solutions." Abstracts of Papers of the American Chemical Society **217**: 032-BTEC.

Lee, H. C. and D. A. Brant (2002). "Rheology of concentrated isotropic and anisotropic xanthan solutions. 1. A rodlike low molecular weight sample." Macromolecules **35**(6): 2212-2222.

Lee, H. C. and D. A. Brant (2002). "Rheology of concentrated isotropic and anisotropic xanthan solutions. 2. A semiflexible wormlike intermediate molecular weight sample." Macromolecules **35**(6): 2223-2234.

Li, L., P. M. Thangamathesvaran, C. Y. Yue, K. C. Tam, X. Hu and Y. C. Lam (2001). "Gel network structure of methylcellulose in water." Langmuir **17**(26): 8062-8068.

Lim, T., J. T. Uhl and R. K. Prudhomme (1984). "Rheology of self-associating concentrated xanthan solutions." Journal of Rheology **28**(4): 367-379.

Lin, A. C. and M. C. Goh (2002). "Investigating the ultrastructure of fibrous long spacing collagen by parallel atomic force and transmission electron microscopy." Proteins: Structure, Function and Genetics **49**: 378-384.

Livolant, F. and Y. Bouligand (1986). "Liquid-crystalline phases given by helical biological polymers (DNA, Pblg and Xanthan) - Columnar textures." Journal De Physique **47**(10): 1813-1827.

Locke, G. R., N. J. Talley, S. L. Fett, A. R. Zinsmeister and L. J. Melton (1997). "Prevalence and clinical spectrum of gastroesophageal reflux: A population-based study in Olmstead County, Minnesota." Gastroenterology **112**: 1448-1456.

Locke, G. R., N. J. Talley, S. L. Fett, A. R. Zinsmeister and L. J. Melton (1999). "Risk Factors Associated with Symptoms of Gastroesophageal Reflux." The American Journal of Medicine **106**(6): 642-649.

MacWilliams, D. C., J. H. Rogers and T. J. West (1973). Water-soluble polymers in petroleum recovery. Water-Soluble Polymers. N. M. Bikales. New York, Plenum Press. **2:** 105-126.

Maier, H., M. Anderson, C. Karl, K. Magnuson and R. L. Whistler (1993). Guar, Locust Bean, Tara and Fenugreek Gums. Industrial Gums - Polysaccharides and their derivatives. R. L. Whistler and J. N. BeMiller. 3rd Edition. London, Academic Press, Inc.

Mandel, K. G., B. P. Daggy, D. A. Brodie and H. I. Jacoby (2000). "Review article: alginate-raft formulations in the treatment of heartburn and acid reflux." Alimentary Pharmacology & Therapeutics **14**(6): 669-690.

Mannion, R. O., C. D. Melia, B. Launay, G. Cuvelier, S. E. Hill, S. E. Harding and J. R. Mitchell (1992). "Xanthan locust bean gum interactions at room-temperature." Carbohydrate Polymers **19**(2): 91-97.

Marciani, L., P. A. Gowland, R. C. Spiller, P. Manoj, R. J. Moore, P. Young, S. Al-Sahab, D. Bush, J. Wright and A. J. Fillery-Travis (2000). "Gastric response to

increased meal viscosity assessed by echo-planar magnetic resonance imaging in humans." Journal of Nutrition **130**(1): 122-127.

Marciani, L., S. L. Little, J. Snee, N. S. Coleman, D. J. Tyler, J. Sykes, I. G. Jolliffe, P. W. Dettmar, R. C. Spiller and P. A. Gowland (2002). "Echo-planar magnetic resonance imaging of Gaviscon alginate rafts in-vivo." Journal of Pharmacy and Pharmacology **54**(10): 1351-1356.

Maret, G., M. Milas and M. Rinaudo (1981). "Cholesteric order in aqueous-solutions of the polysaccharide xanthan." Polymer Bulletin **4**(5): 291-297.

Marijnissen, W., G. van Osch, J. Aigner, S. W. van der Veen, A. P. Hollander, H. L. Verwoerd-Verhoef and J. A. N. Verhaar (2002). "Alginate as a chondrocyte-delivery substance in combination with a non-woven scaffold for cartilage tissue engineering." Biomaterials **23**(6): 1511-1517.

Matheson, R. R. (1980). "Viscosity of solutions of rigid rodlike macromolecules." Macromolecules **13**: 643-648.

McDowell, R. H. (1977). Properties of Alginates. Fourth. London, Alginate Industries Limited.

Melton, L. D., L. Mindt, D. A. Rees and G. R. Sanderson (1976). "Covalent structure of the extracellular polysaccharide from *Xanthomonas campestris*: Evidence from partial hydrolysis studies." Carbohydrate Research **46**: 245-257.

Merchant, K. and R. L. Rill (1994). "Isotropic to anisotropic phase-transition of extremely long DNA in an aqueous saline solution." Macromolecules **27**(9): 2365-2370.

Merchant, K. and R. L. Rill (1997). "DNA length and concentration dependencies of anisotropic phase transitions of DNA solutions." Biophysical Journal **73**(6): 3154-3163.

Milas, M. and M. Rinaudo (1979). "Conformational investigation on the bacterial polysaccharide xanthan." Carbohydrate Research **76**: 189-196.

Milas, M. and M. Rinaudo (1983). "Properties of the concentrated xanthan gum solutions." Polymer Bulletin **10**(5-6): 271-273.

Milas, M., M. Rinaudo and B. Tinland (1985). "The viscosity dependence on concentration, molecular-weight and shear rate of xanthan solutions." Polymer Bulletin **14**(2): 157-164.

Moorhouse, R., M. D. Walkinshaw and S. Arnott (1977). Xanthan gum molecular conformation and interactions. Extracellular Microbial Polysaccharides. P. A. Sandford and A. Laskin. Washington, D.C., American Chemical Society. **45**.

Morris, E. R. (1977). Molecular origin of xanthan solution properties. Extracellular Microbial Polysaccharides. P. A. Sandford and A. Laskin. Washington, D.C., American Chemical Society. **45**.

Morris, E. R. (1984). Rheology of hydrocolloids. Gums and Stabilisers in the Food Industry 2 - Applications of Hydrocolloids. G. O. Phillips, D. J. Wedlock and P. A. Williams. Oxford, Pergammon Press**:** 57-78.

Morris, E. R. (1986). "Molecular-interactions in polysaccharide gelation." British Polymer Journal **18**(1): 14-21.

Morris, E. R. (1990). Comparison of the properties and function of alginates and carrageenans. Gums and Stabilisers for the Food Industry 5. G. O. Phillips, D. J. Wedlock and P. A. Williams. Oxford, Oxford University Press**:** 483-496.

Morris, E. R., D. A. Rees, G. Young, M. D. Walkinshaw and A. Darke (1977). "Order-disorder transition for a bacterial polysaccharide in solution. A role for polysaccharide conformation in recognition between *Xanthomonas* pathogen and its plant host." Journal of Molecular Biology **1977**(110): 1-16.

Nandurkar, S. and N. J. Talley (2000). "Epidemiology and natural history of reflux disease." Baillière's Best Practice & Research. Clinical Gastroenterology **14**(5): 743-757.

Norton, I. T., D. M. Goodall, S. A. Frangou, E. R. Morris and D. A. Rees (1984). "Mechanism and dynamics of conformational ordering in xanthan polysaccharide." Journal of Molecular Biology **175**(3): 371-394.

Oertel, R. and W. M. Kulicke (1991). "Viscoelastic properties of liquid-crystals of aqueous biopolymer solutions." Rheologica Acta **30**(2): 140-150.

Onogi, S. and T. Asada (1980). Rheology and rheo-optics of polymer liquid crystals. Rheology - Volume 1:Principles. G. Astarita, G. Marrucci and L. Nicolais. New York, Plenum Press**:** 127-147.

Onsager, L. (1949). "The effects of shape on the interaction of colloidal particles." Annals New York Academy of Sciences **51**: 627-659.

Paoletti, S., A. Cesaro and F. Delben (1983). "Thermally induced conformational transition of xanthan polyelectrolyte." Carbohydrate Research **123**(1): 173-178.

Paradossi, G. and D. A. Brant (1982). "Light-scattering study of a series of xanthan fractions in aqueous-solution." Macromolecules **15**(3): 874-879.

Pelletier, E., C. Viebke, J. Meadows and P. A. Williams (2001). "A rheological study of the order-disorder conformational transition of xanthan gum." Biopolymers **59**(5): 339-346.

Piculell, L., K. Bergfeldt and S. Nilsson (1995). Factors determining phase behaviour of multi component polymer systems. Biopolymer Mixtures. S. E. Harding, S. E. Hill and J. R. Mitchell. Nottingham, Nottingham University Press.

Piculell, L. and B. Lindman (1992). "Association and segregation in aqueous polymer/polymer, polymer surfactant, and surfactant surfactant mixtures - similarities and differences." Advances in Colloid and Interface Science **41**: 149-178.

Pope, C. E. (1997). "The esophagus for the nonesophagologist." American Journal of Medicine **103**(5A (Supplement)): 19S-22S.

Potts, A. M., C. G. Wilson, H. N. E. Stevens, D. J. Dobrozsi, N. Washington, M. Frier and A. C. Perkins (2000). "Oesophageal bandaging: a new opportunity for thermosetting polymers." STP Pharmaceutical Sciences **10**(4): 293-301.

Racciato, J. S. (1976). "Better gum for carpet printing." American Dyestuff Reporter **65**(11): 51, 69.

Rees, D. A. (1972). "Shapely polysaccharides." Biochemical Journal **126**(2): 257-273.

Rees, D. A. and J. W. B. Samuel (1967). "The structure of alginic acid. Part VI. Minor features and structural variations." Journal of the Chemical Society C - Organic: 2295-2298.

Richardson, J. C., P. W. Dettmar, F. C. Hampson and C. D. Melia (2004). "Oesophageal bioadhesion of sodium alginate suspensions: particle swelling and mucosal retention." European Journal of Pharmaceutical Sciences **23**(1): 49-56.

Richardson, J. C., P. W. Dettmar, F. C. Hampson and C. D. Melia (2005). "Oesophageal bioadhesion of sodium alginate suspensions 2. Suspension behaviour on oesophageal mucosa." European Journal of Pharmaceutical Sciences **24**(1): 107-114.

Richardson, R. K. and S. B. Ross-Murphy (1987). "Non-linear viscoelasticity of polysaccharide solutions.2. Xanthan polysaccharide solutions." International Journal of Biological Macromolecules **9**(5): 257-264.

Rinaudo, M. (2001). "Relation between the molecular structure of some polysaccharides and original properties in sol and gel states." Food Hydrocolloids **15**: 433-440.

Rinaudo, M. and M. Milas (1982). "Xanthan properties in aqueous solution." Carbohydrate Polymers **2**: 264-269.

Rolin, C. (1993). Pectin. Industrial Gums - Polysaccharides and their derivatives. R. L. Whistler and J. N. BeMiller. 3rd Edition. London, Academic Press, Inc.

Ross-Murphy, S. B. (1988). Small deformation measurements. Food Structure - Its creation and evaluation. J. M. V. Blanshard and J. R. Mitchell. London, Butterworths**:** 387-400.

Ross-Murphy, S. B. (1995). "Structure-property relationships in food biopolymer gels and solutions." Journal of Rheology **39**(6): 1451-1463.

Ross-Murphy, S. B., V. J. Morris and E. R. Morris (1983). "Molecular viscoelasticity of xanthan polysaccharide." Faraday Symposia of the Chemical Society **18**: 115-129.

Rossi, S., M. C. Bonferoni, F. Ferrari and C. Caramella (1999). "Drug release and washability of mucoadhesive gels based on sodium carboxymethylcellulose and polyacrylic acid." Pharmaceutical Development and Technology **4**(1): 55-63.

Sakai, T., T. Sakamoto, J. Hallaert and E. J. Vandamme (1993). Pectin, pectinase, and protopectinase - Production, properties, and applications. Advances in Applied Microbiology, Vol 39. San Diego, Academic Press Inc. **39:** 213-294.

Sandford, P. A., J. E. Pittsley, C. A. Knutson, P. R. Watson, M. C. Cadmus and A. Jeanes (1977). Variation in *Xanthomonas campestris* NRRL B-1459: Characterisation of xanthan products of differing pyruvic acid content. Extracellular Microbial Polysaccharides. P. A. Sandford and A. Laskin. Washington, D.C., American Chemical Society. **45:** 192-210.

Sandvik, E. I. and J. M. Maerker (1977). Application of xanthan gum for enhanced oil recovery. Extracellular microbial polysaccharides. P. A. Sandford and A. Laskin. Washington D.C., American Chemical Society. **45:** 242-264.

Sato, T., T. Kakihara, S. Inatomi and A. Teramoto (1990). "Phase-equilibrium in polymer liquid-crystals - Xanthan, a stiff polyelectrolyte." Abstracts of Papers of the American Chemical Society **200**: 165-POLY.

Sato, T., T. Kakihara and A. Teramoto (1990). "Isotropic liquid-crystal phase-equilibrium in semiflexible polymer-solutions - Xanthan, a rigid polyelectrolyte." Polymer **31**(5): 824-828.

Sato, T., T. Norisuye and H. Fujita (1984). "Double-stranded helix of xanthan - Dimensional and hydrodynamic properties in 0.1M aqueous sodium-chloride." Macromolecules **17**(12): 2696-2700.

Sato, T. and A. Teramoto (1991). "Perturbation-theory of isotropic-liquid-crystal phase-equilibria in polyelectrolyte solutions." Physica A **176**(1): 72-86.

Sato, T. and A. Teramoto (1996). Concentrated solutions of liquid-crystalline polymers. Biopolymers Liquid Crystalline Polymers Phase Emulsion. Berlin 33, Springer-Verlag Berlin. **126:** 85-161.

Schultz, G. S., R. G. Sibbald, V. Falanga, E. A. Ayello, C. Dowsett, K. Harding, M. Romanelli, M. C. Stacey, L. Teot and W. Vanscheidt (2003). "Wound bed preparation: a systematic approach to wound management." Wound Repair and Regeneration **11**(S1): S1-S28.

Scott, R. L. (1949). "The thermodynamics of high polymer solutions. V. Phase equilibria in the ternary system - polymer 1 - polymer 2 - solvent." Journal of Chemical Physics **17**(3): 279-284.

Sherwood, L. (1993). Human Physiology: From cells to systems. 2nd Edition. Minneapolis/St. Paul, West Publishing.

Singh, P. P. and R. L. Whistler (1974). "Scleroglucan, an antitumor polysaccharide from *Sclerotium glucanicum*." Carbohydrate Research **37**: 245-247.

Skaugrud, O., A. Hagen, B. Borgersen and M. Dornish (1999). Biomedical and pharmaceutical applications of alginate and chitosan. Biotechnology and Genetic Engineering Reviews, Vol 16. Andover, Intercept Ltd Scientific, Technical & Medical Publishers. **16:** 23-40.

Smidsrød, O. (1974). "Molecular basis for some physical properties of alginates in the gel state." Faraday Discussions of the Chemical Society **57**: 263-275.

Smidsrød, O. and K. Draget (1996). "Chemical and physical properties of alginates." Carbohydrates in Europe **14**: 6-13.

Soon-Shiong, P. (1999). "Treatment of type I diabetes using encapsulated islets." Advanced Drug Delivery Reviews **35**(2-3): 259-270.

Southwick, J. G., A. M. Jamieson and J. Blackwell (1982). "Conformation of xanthan dissolved in aqueous urea and sodium-chloride solutions." Carbohydrate Research **99**(2): 117-127.

Sperling, L. H. (2001). Introduction to physical polymer science. 3rd Edition. Toronto, Wiley.

Steffe, J. F. (1996). Rheological methods in food process engineering. 2nd Edition. East Lansing, MI, Freeman Press.

Stokke, B. T., A. Elgsaeter and O. Smidsrod (1986). "Electron-microscopic study of single-stranded and double-stranded xanthan." International Journal of Biological Macromolecules **8**(4): 217-225.

Stokke, B. T., O. Smidsrød, P. Bruheim and G. Skjåk-Bræk (1991). "Distribution of uronate residues in alginate chains in relation to alginate gelling properties." Macromolecules **24**(16): 4637-4645.

Strugala, V. (2003). Reckitt Benckiser. Test Method On File.

Sugden, K. and K. G. Hutchinson (1995). "Pharmaceutical product for treatment of reflux oesophagitis, gastritis or peptic ulceration." UK Patent: GB2283171.

Sutherland, I. W. (1993). Biosynthesis of extracellular polysaccharides (exopolysaccharides). Industrial Gums - Polysaccharides and their derivatives. R. L. Whistler and J. N. BeMiller. 3rd Edition. London, Academic Press, Inc.

Sutherland, I. W. (1994). "Structure-function-relationships in microbial exopolysaccharides." Biotechnology Advances **12**(2): 393-448.

Sutherland, I. W. (1995). "Polysaccharide Lyases." Fems Microbiology Reviews **16**(4): 323-347.

Sutherland, I. W. (2001). "Microbial polysaccharides from Gram-negative bacteria." International Dairy Journal **11**(9): 663-674.

Sworn, G. (2004). Hydrocolloid thickeners and their applications. Gums and Stabilisers for the Food Industry 12. P. A. Williams and G. O. Philips. Cambridge, Royal Society of Chemistry**:** 13-22.

Tabilo-Munizaga, G. and G. V. Barbosa-Canovas (2005). "Rheology for the food industry." Journal of Food Engineering **67**: 147–156.

Tako, M., A. Asato and S. Nakamura (1984). "Rheological aspects of the intermolecular interaction between xanthan and locust bean gum in aqueous-media." Agricultural and Biological Chemistry **48**(12): 2995-3000.

Talukdar, M. M. and R. Kinget (1995). "Swelling and drug release behaviour of xanthan gum matrix tablets." International Journal of Pharmaceutics **120**: 63-72.

Tang, M., P. W. Dettmar and H. Batchelor (2005). "Bioadhesive oesophageal bandages:protection against acid and pepsin injury." International Journal of Pharmaceutics **292**: 169-177.

Tang, M., P. W. Dettmar and H. K. Batchelor (2005). "An in vitro examination of adhesive alginate solution as oesophageal protectants." Gut **54**(Suppl 2): A54.

Tang, M., P. W. Dettmar and H. K. Batchelor (2005). "Oesophageal adhesive solutions of alginate protect against damage caused by gastric reflux." Gut **54**(Suppl 2): A54.

Teramoto, A., K. Yoshiba, N. Nakamura, J. Nakamura and T. Sato (2001). "Cholesteric structure and order-disorder transition in aqueous solutions of schizophyllan, a triple-helical polysaccharide." Molecular Crystals and Liquid Crystals **365**: 1329-1336.

Thakur, B. R., R. K. Singh and A. K. Handa (1997). "Chemistry and uses of pectin - A review." Critical Reviews in Food Science and Nutrition **37**(1): 47-73.

The United States Pharmacopeia (2005). Rockville, USA, United States Pharmacopeial Convention Inc.

Therkelsen, G. (1993). Carrageenan. Industrial Gums - Polysaccharides and their derivatives. R. L. Whistler and J. N. BeMiller. 3rd Edition. London, Academic Press, Inc.

Tinland, B. and M. Rinaudo (1989). "Dependence of the stiffness of the xanthan chain on the external salt concentration." Macromolecules **22**: 1863-1865.

Tolstoguzov, V. (2003). "Some thermodynamic considerations in food formulation." Food Hydrocolloids **17**(1): 1-23.

Tompa, H. (1956). Polymer Solutions. London, Butterworths Scientific Publications.

Tonnesen, H. H. and J. Karlsen (2002). "Alginate in drug delivery systems." Drug Development and Industrial Pharmacy **28**(6): 621-630.

Van, K., T. Norisuye and A. Teramoto (1981). "Liquid-crystal formation in aqueous-solutions of a polysaccharide schizophyllan." Molecular Crystals and Liquid Crystals **78**(1-4): 123-134.

Vernhet, A., P. Pellerin, C. Prieur, J. Osmianski and M. Moutounet (1996). "Charge properties of some grape and wine polysaccharide and polyphenolic fractions." American Journal of Enology and Viticulture **47**(1): 25-30.

Vivian, E. M. and M. A. Thompson (2000). "Pharmacologic Strategies for treating gastroesophageal reflux disease." Clinical Therapeutics **22**(6): 654-672.

Waugh, A. and A. Grant (2001). Ross and Wilson: Anatomy and physiology in health and illness. 9th Edition. Edinburgh, Churchill Livingstone.

Whistler, R. L., A. A. Bushway, P. P. Singh, N. Waro and R. Tokuzen (1976). "Noncytotoxic, antitumor polysaccharides." Advances in Carbohydrate Chemistry and Biochemistry **32**: 235-275.

Whitcomb, P. J. (1978). "Rheology of Xanthan Gum." Journal of Rheology **22**(5): 493-505.

Whitcomb, P. J., B. J. Ek and C. W. Macosko (1977). Rheology of xanthan gum solutions. Extracellular Microbial Polysaccharides. P. A. Sandford and A. Laskin. Washington, D.C., American Chemical Society. **45:** 160-173.

Wissbrun, K. F. (1981). "Rheology of rod-like polymers in the liquid-crystalline state." Journal of Rheology **25**(6): 619-662.

Xu, X., D. Brining, A. Rafiq, J. Hayes and J. Chen (2005). "Effects of enhanced viscosity on canine gastric and intestinal motility." Journal of Gastroenterology and Hepatology **20**(3): 387.

Yanaki, T., T. Norisuye and A. Teramoto (1984). "Cholesteric mesophase in aqueous-solutions of a triple helical polysaccharide scleroglucan." Polymer Journal **16**(2): 165-173.

Young, S. L., M. Martino, C. Kienzlesterzer and J. A. Torres (1994). "Potentiometric titration studies on xanthan solutions." Journal of the Science of Food and Agriculture **64**(1): 121-127.

Zhan, D. F., M. J. Ridout, G. J. Brownsey and V. J. Morris (1993). "Xanthan locust bean gum interactions and gelation." Carbohydrate Polymers **21**(1): 53-58.

Zhanq, H. C., H. Q. Wang, J. J. Wang, R. F. Guo and Q. Z. Zhan (2001). "The effect of ionic strength on the viscosity of sodium alginate solution." Polymers for Advanced Technologies **12**(11-12): 740-745.

Appendix 1 - Materials

All of the materials, suppliers and batch numbers used in this project are detailed below.

A number of the items used were supplied as a gift from various sources to all of which we are most grateful. The xanthan gum was a gift from Reckitt Benckiser (Healthcare) UK Ltd. The alginate samples, locust bean gum and carrageenan were supplied by FMC Biopolymer (Norway). The pectin and scleroglucan were supplied by Degussa Texturants. The methylcellulose was supplied by Colorcon UK and the maltodextrin by Cerestar (UK).

All of the other items were purchased from the suppliers indicated.

Polysaccharides and polymers

Material	Grade/Brand name	Supplier	Batch number
Xanthan Gum	Rhodigel® 80	Caldic (UK) Ltd. Chesterfield, UK	9929002
Sodium Alginate	Protanal® LFR 5/60	FMC Biopolymer, Drammen, Norway	S13081
	Protanal® LF10L	FMC Biopolymer, Drammen, Norway	840017
	Protanal® LF120L	FMC Biopolymer, Drammen, Norway	907788
	Protanal® SF120	FMC Biopolymer, Drammen, Norway	907114
	Protanal® SF200	FMC Biopolymer, Drammen, Norway	910152
	Protanal® H120L	FMC Biopolymer, Drammen, Norway	240304
	Oligo-alginate Research Grade	FMC Biopolymer, Drammen, Norway	080799

Material	Grade/Brand name	Supplier	Batch number
Sodium Carboxymethylcellulose	Low Viscosity	Sigma-Aldrich Chemical Company, Dorset, UK	32K0007
Low Methoxyl Amidated Pectin	Unipectine® OG903GS	Degussa Texturant Systems, Newbury, UK	20741401/1
Lambda Carrageenan	Viscarin® GP109F	FMC Biopolymer, Philadelphia, USA	50502110
Methylcellulose	Methocel® A15LV	Colorcon, Dartford, UK	PI15012N22
Maltodextrin	C*Dry® MD 01915	Cerestar, Manchester, UK	AX1350
Sodium Polyacrylate	Mw = 30 kDa 40% w/w solution in water[*1]	Sigma-Aldrich Chemical Company, Dorset, UK	03323DO
	Mw = 15 kDa 35% w/w solution in water[*2]	Sigma-Aldrich Chemical Company, Dorset, UK	05206CA
	Mw = 8 kDa 45% w/w solution in water[*3]	Sigma-Aldrich Chemical Company, Dorset, UK	032224KF
Scleroglucan	Actigum® CS11	Degussa Texturant Systems, Boulogne-Billancourt, France	2003-0740
Locust Bean Gum	-	FMC Biopolymer, Drammen, Norway	2459

[*1] Accurately determined as 43.57% solids in water.
[*2] Accurately determined as 36.13% solids in water.
[*3] Accurately determined as 47.45% solids in water.

Other excipients and reagents

Material	Grade/Brand name	Supplier	Batch number
Sodium Chloride	Sigma Ultra	Sigma-Aldrich Chemical Company Dorset, UK	028K0135
Potassium Chloride	Sigma Ultra	Sigma-Aldrich Chemical Company, Dorset, UK	121K0146
Magnesium Chloride	Sigma Ultra	Sigma-Aldrich Chemical Company, Dorset, UK	072K0063
Sucrose	Sigma Ultra	Sigma-Aldrich Chemical Company, Dorset, UK	22K0065
Sorbitol	Sigma Ultra	Sigma-Aldrich Chemical Company, Dorset, UK	051K0005
Glycerol	Sigma Ultra	Sigma-Aldrich Chemical Company, Dorset, UK	121K0021
EDTA Tetrasodium salt	Sigma Ultra	Sigma-Aldrich Chemical Company, Dorset, UK	01TK0312
Poly-DADMAC	-	Carisbrooke Instrument Services Ltd. Woking, Surrey, UK	-
Concentrated Hydrochloric Acid	ACS Reagent Grade	Sigma-Aldrich Chemical Company, Dorset, UK	052K3481

Material	Grade/Brand name	Supplier	Batch number
Phosphorous Pentoxide	-	Fisher Scientific, Loughborough, UK	0258497
Sodium Hydroxide	Sigma Ultra	Sigma-Aldrich Chemical Company, Dorset, UK	063K0047
Hydrochloric Acid	0.1N Volumetric Standard	Sigma-Aldrich Chemical Company, Dorset, UK	04905AC
Dimethylformamide	-	Sigma-Aldrich Chemical Company, Dorset, UK	519006-463
Fluoresceinamine	Isomer I	Sigma-Aldrich Chemical Company, Dorset, UK	063K5314
1-ethyl-3-(3-dimethylaminopropyl) carbodiimide (EDAC)	-	Sigma-Aldrich Chemical Company, Dorset, UK	033K12261